THE FINITE-ELEMENT METHOD

FOR

WAVEGUIDE PROBLEMS

বাংলাদেশ প্রকৌশল বিশ্ববিদ্যালয়
নং 39550
তাং 23/3/77
লাইব্রেরী, ঢাকা

by

SHAMSUDDIN AHMED, B.Sc., M.S.

A Thesis submitted for the degree of Doctor of Philosophy in the Department of Electrical and Electronic Engineering, the University of Leeds.

September, 1969.

IN THE NAME OF GOD,

THE MOST GRACIOUS, THE DISPENSER OF GRACE

"ALL PRAISE BELONGS TO GOD,

THE SUSTAINER OF ALL THE WORLDS."

AMEN.

বাংলাদেশ প্রকৌশল বিশ্ববিদ্যালয়
নং 39550
তাং 23.3.77
লাইব্রেরী, ঢাকা

Acknowledgements

The author wishes to thank the following people and organisations who have assisted this research in their various ways: Dr. C.D. Hannaford, who supervised the work at its initial stages; Dr. P. Daly, who supervised the work in the final stage and was a constant source of encouragement; the Government of Pakistan, for providing the financial assistance under the auspices of the Colombo-plan Overseas Training Program; the staff of the British Council for extending their warm hospitality and for the management of financial affairs; Professor G.W. Carter, for permission to undertake the research and to make use of the facilities in the Department of Electrical and Electronic Engineering; the Electronic Computing Laboratory of the University of Leeds, for use of the KDF9 Computer. Finally, the author wishes to thank his wife, who exercised considerable patience and sympathy during the period of the research.

Parts of this thesis have been or are scheduled to be published as follows:

1) "Finite-Element Method for Waveguide Problems", by S. Ahmed.
Electronics Letter, Vol. 4, No. 18, 6th September, 1968.

2) "Finite-Element Methods for Waveguide Problems", by S. Ahmed and P. Daly.
The Radio and Electronic Engineer (to be published)

3) "Finite-Element Methods for Inhomogeneous Waveguides", by S. Ahmed and P. Daly.
Proc. I.E.E. (to be published)

Summary

Wave-equations and a scalar variational formulation are developed for electromagnetic wave propagation in a waveguide having continuously variable permeability and permittivity. Particular forms of the variational expressions for other types of dielectric loaded waveguides are deduced therefrom.

A finite-element method for solving all types of waveguide problems (isotropic) is introduced. This method is based on function minimisation techniques. In this method the actual field functions which are defined over the entire cross-section of a waveguide are approximated by a set of algebraic polynomials, each of which is defined only over a subregion or element of the whole cross-section. The actual field function in an appropriate extremum functional is then replaced by the above mentioned approximated fields. The extremum functional is then minimised with respect to the values of field at the vertices of the elements. This way of minimisation generates a set of linear algebraic eigenvalue equations. The solution for the lowest eigenvalue of the set of algebraic eigenvalue equations corresponds to the dominant mode wavenumber under consideration.

Numerical results from computations with the finite-element method are given which illustrates the principle discussed. Comparison of a few results obtained by the finite-

element method with the corresponding results given by the finite-difference method shows that in all cases the finite-element method gives at least as good a result as could be obtained by the finite-difference method. Extension of the finite-element method to isotropic Plasma Loaded Waveguide is discussed briefly.

List of Principal Symbols

ω	Angular frequency
μ_o	Permeability of free space
ϵ_o	Permittivity of free space
μ_r	Relative permeability
ϵ_r	Relative permittivity
c	Velocity of light in free space ($c = 1/\sqrt{\epsilon_o \mu_o}$)
λ_o	Free space wave length ($\lambda_o = \frac{2\pi c}{\omega}$)
β	Phase change co-efficient of waveguide propagation
$\bar{\beta}$	Normalised phase change co-efficient ($= \frac{\beta c}{\omega}$)
ψ	Normalised longitudinal component of electric field ($= \frac{\omega \epsilon_o}{\beta} E_z$)
ϕ	Longitudinal component of magnetic field
∇_t^2	Transverse Laplacian $\left(\frac{\partial^2}{x^2} + \frac{\partial^2}{y^2} \right)$
k_o^2	Free space wave number ($= \omega^2 \mu_o \epsilon_o - \beta^2$)
k_c^2	Wave number in a generalised medium ($= \omega^2 \mu \epsilon - \beta^2$)
t	Ratio of Wave numbers (k_o^2 / k_c^2)
P	Functions of t and ϵ_r ($= \bar{\beta}^2 t \epsilon_r$)
R	Functions of t and μ_r ($= t \mu_r$)
W	Function of t ($= \bar{\beta}^2 t$)

List of Principal Symbols (Continued)

$\underline{n}$	Unit outward normal to a Surface or Contour
$\underline{c}$	Unit vector tangential to a Contour
$\underline{L}$	Matrix Operator whose elements are differential operators
O	2 x 1 Vector containing ψ and ϕ
M	Diagonal Matrix operator
$\underline{A}$	Matrix operator equivalent to Integral operator $\int_S \lvert\nabla_t \phi\rvert^2 \, ds$
$\underline{B}$	Matrix operator equivalent to Integral operator $\int \phi^2 \, ds$
$\underline{S}^e$	Element Submatrices forming Matrix $\underline{A}$
$\underline{F}$	Element Submatrices forming Matrix $\underline{B}$
FE	Abbreviation for the Finite-Element
FD	Abbreviation for the Finite-Difference
SOR	Abbreviation for the Successive Over-Relaxation

Contents

		Page
	Acknowledgements	(ii)
	Summary	(iv)
	List of Principal Symbols	(vi)
Chapter 1.	INTRODUCTION	1
1.1.	Propagation Problems in Waveguides	1
1.2.	The Separation of Variables Techniques	3
1.3.	Approximate Methods	5
1.4.	The Finite-Difference Method	8
1.5.	The Finite-Element/Variational Method	11
1.6.	Content of the Thesis	14
	References	18
Chapter 2.	WAVE-EQUATIONS AND VARIATIONAL FORMULATION FOR WAVEGUIDES FILLED WITH GENERALISED ISOTROPIC MEDIA	22
2.1.	Mathematical Approach	22
2.1.1.	Basic Assumptions	22
2.1.2.	Wave Equations	23
2.1.3.	Wave Equations for Inhomogeneous Waveguides	28
2.2.	Variational Formulation	31
2.3.	Evaluation of the Variational Character	37
2.3.1.	Indirect Proof	37
2.3.2.	Direct Proof	40

Contents | Page

2.4. Restriction on the Variations of μ_r and ϵ_r 42

2.4.1. Discontinuous Variations of μ_r and ϵ_r 42

2.4.2. Sectionally Constant μ_r and ϵ_r 47

2.5. Operator Eigenvalue Problems 49

2.5.1. Wave-Equations Written in Matrix Form 49

2.5.2. Properties of the Matrix Operators 50

Appendix A2.

A2.1. Green's Theorem 54

A2.2. Stokes' Theorem 55

A2.3. Derivation of Equation (2.53) 57

A2.4. Derivation of Equation (2.101) 59

References 61

Chapter 3. THE FINITE-ELEMENT FORMULATION FOR WAVEGUIDE PROBLEMS 62

3.1. Formulation of a Problem Suitable for the Finite-Element Method 62

3.2. Development of the Finite-Element Equations for Triangular Elements 64

3.3. Evaluations of the Components of the Matrices $\underline{A}$ and $\underline{B}$ 72

3.4. Properties of the Matrix Operators $\underline{A}$ and $\underline{B}$ 76

3.5. Development of the Finite-Element Equations for Rectangular Elements 79

3.6. Evaluation of the Components of the Matrix Operators $\underline{A}'$ and $\underline{B}'$ 82

Contents

Page

Appendix A3. 86

A3.1. Evaluations of Some Important Surface Integrals for Triangular Elements 86

A3.2. Effect of the Change of the Origin of the Reference Co-ordinates on the Components of the Element Submatrices 88

A3.3. Effect of the Shape of the Triangular Element on the Components of the Element Submatrices 91

References 94

Chapter 4. APPLICATION OF FINITE-ELEMENT METHOD TO HOMOGENEOUS WAVE-GUIDES 95

4.1. Description of the Problem 95

4.2. Solving the Matrix Eigenvalue Problems 97

4.2.1. Description of the Successive Over-Relaxation Technique 99

4.2.2. Determination of the least Eigenvalues 101

4.3. Eigenvalue Extrapolation 102

4.4. Particular Solutions: 103

4.4.1. TE_{10}-Mode in a Rectangular Waveguide 103

4.4.2. Characteristics of FE and FD Representations of One Dimensional Wave Equations 105

4.4.3. Numerical Results for TE_{10}-Mode 107

4.4.4. TM_{11}-Mode in a Rectangular Waveguide 109

Contents

Page

4.5. Circular Waveguide 112

4.6. Boundary Matching 114

4.7. Singularities in Waveguides 121

4.7.1. Mathematical Approach to Singular points in Waveguide problems 121

4.7.2. Practical Treatment of Singular Points 123

4.7.3. L-Shaped Waveguide 126

4.7.4. Ridged Rectangular Waveguides 129

4.7.5. Channel Waveguide 132

4.8. Transmission Lines with Singularities 136

4.8.1. Determination of Capacitance 138

4.8.2. Numerical Results: 140

4.8.2a. Square Transmission Line 140

4.8.2b. Homogeneous Strip Line 142

4.9. Conclusions 145

References 147

Appendix A4. 152

Chapter 5. FINITE-ELEMENT METHOD FOR INHOMOGENEOUS WAVEGUIDES 162

5.1. Description of the Problem 162

5.2. Finite-Element Equations and the Matrix Formulation 165

5.2.1a. Matrix Formulation and Properties 165

5.2.1b. Properties of Matrices A and B 169

Contents | Page

5.2.2. Derivation of Descretised Equations for a general point 172

5.2.2a. Subregions in 1st and 3rd Quadrants 173

5.2.2b. Subregions in 2nd and 4th Quadrants 175

5.2.2c. General Discretised Equations 177

5.3. Special Cases: 180

5.3.1. Interior Vertices 180

5.3.2. Plane Boundary Vertices 181

5.3.3. $\pi/2$ Dielectric Corner 182

5.4. Applications: 183

5.4.1. A Rectangular Waveguide Partially Filled with a Full Height Dielectric Slab 184

5.4.2. A Slab Loaded Rectangular Waveguide with Slab Perpendicular to $\underset{\sim}{E}$ at Cut-Off 193

5.4.3. A Rectangular Waveguide Partially Filled with a Rectangular Dielectric Insert 201

5.5. Conclusions 210

References 213

Chapter 6. WAVEGUIDE LOADED WITH A GENERALISED ISOTROPIC DIELECTRIC 214

6.1. Introduction 214

6.2. Finite-Element Approach to Generalised Medium 215

6.2.1. Extension to Two-Dimensional Variations 222

Contents

Page

6.3. Rayleigh-Ritz Method 225

6.3.1. Practical Difficulties 226

6.3.2. Rayleigh-Ritz Method for Arbitrary Loading 230

References 233

Chapter 7 CONCLUSIONS AND RECOMMENDATIONS

7.1. Conclusions 234

7.2. Extension of the FE Method and Recommendation 237

References 239

CHAPTER 1

INTRODUCTION

1.1 Propagation Problems in Waveguides

The properties and behaviour of electromagnetic waves propagating in waveguides depend partly on the shape of the guide cross-section and partly on the medium filling the waveguide.. Depending on the nature of the medium inside the guide one can divide them into homogeneous, inhomogeneous and anisotropic waveguides. Each type has its practical utility in microwave engineering. In general the analysis of electromagnetic wave propagation in waveguides requires the determination of fields that are solutions to Maxwell's equations. For a uniform waveguide filled with isotropic dielectrics, the problem can be rewritten as one of finding solutions to a pair of second order differential equations called wave equations.

There are various analytic, semi-analytic and numerical methods that can be used for waveguide problems. In this thesis consideration is given to a new numerical approach called "The finite element approach" to the solution of wave equations for uniform homogeneous waveguides with arbitrary shaped cross-sections and also for waveguides with inhomogeneous and generalised isotropic dielectric fillings. Regular uniform homogeneous waveguides are normally used for microwave power transmission in this respect they are equivalent to uniform coaxial lines. Two main cylindrical geometries, usually

rectangular and circular waveguides are used for this prupose. However, for many modern engineering applications modifications of regular shaped waveguides may produce lower cutoff frequency, increased bandwidth, or increased power handling capacity etc.

The number of homogeneous waveguide problems capable of having exact solutions is limited to a few very simple shapes even when the common approximations of infinitely long and infinite conductivity of the bounding walls are assumed. Exact solutions in compact form are not obtainable for the modified waveguide problems and they require special considerations.

Inhomogeneously filled waveguides are used in the form of microwave components such as phase shifter, isolator etc. To get a clear understanding of the operation of these components, it is required to have a first-hand knowledge of the propagation characteristics of the corresponding ideal homogeneous waveguides.

Generalised waveguide medium as considered in this thesis is one where the permittivity is a function of transverse co-ordinates otherwise uniform along the axis of propagation. Wave equations for this type of problem in general become a set of two continuously coupled second order differential equations. This phenomenon may occur in plasma filled waveguide.

Before going into the finite-element method we will give here a short account of the methods currently available to solve waveguide problems and their range of applications.

1.2 The Separation of Variables Techniques

This method can be applied to those systems where the waveguide boundaries coincide with the constant co-ordinate surfaces in those co-ordinates in which the wave equation is separable, such as cartesian co-ordinates, cylindrical co-ordinates, spherical co-ordinates etc. For real propagation, a time dependence of the form exp(jwt) and a variation in the direction of propagation of the form $\exp(-j\beta Z)$ (for Z being considered as the axis of propagation) are assumed. The three dimensional field problem described by the vector wave equation is then written for any field component as a product of three partial factors each of which is dependent on one co-ordinate only. When the dependence with respect to Z- as assumed above is inserted and the resulting Z- dependence factor is separated out, a two-dimensional wave equation will result which when separated and solved for appropriate boundary conditions yields an infinite number of discrete solutions or modes, each having a characteristic set of fields and a phase change co-efficient associated with it.

Although the general vector field has three space components, it does not require to solve the corresponding wave equations individually for each of the components, normally, in most of the cases, it is necessary to consider the wave equation for the longitudinal components of the appropriate fields, since all other field components can be derived from

the longitudinal components. For a homogeneous waveguide, it is always possible to sustain a pure TE mode or TM mode, so consideration of the longitudinal component of electric field or magnetic field (as appropriate), would be sufficient to give the necessary information regarding the nature of other components and their propagation characteristics.)

For inhomogeneously filled waveguide problems, separation of variable technique can be used for those cases where propagating mode can be identified as the LSE mode or LSM mode. This is limited to a few special types of dielectric fillings. Propagating mode in inhomogeneous waveguide system is usually hybrid in nature, i.e. both the longitudinal components of electric field and magnetic field exist simultaneously to satisfy the boundary conditions at the vacuum/dielectric interface. Exceptions occur where there is no variation of fields along the dielectric interface, as in the case of TE_{10} mode in a rectangular waveguide loaded with a full height dielectric slab and TM_{01} mode in the circular waveguide containing a concentric dielectric rod. For these problems simple particular solutions are obtained from the general solutions. The presence of additional boundary conditions produce a transcendental equation to be solved for the phase change co-efficient. In all other configurations except those which can sustain LSE and LSM modes, the solution would require an infinite number of terms of the general solutions and would be intractable by

this method. Many waveguide structures which are of engineering interest and which belong to the above category, particularly those having rectangular outer boundaries require treatment by other approximate methods.

1.3 Approximate Methods

There are a number of approximate theoretical and numerical techniques that could be used to determine the useful characteristics of propagation in waveguides where the exact theoretical analysis is not possible. Among these, perturbation, variational and field matching techniques, the method of conformal transformations[1] and a point matching[2] and the finite-difference methods are often used.

Perturbation techniques are particularly useful[3] and can produce fairly good results if there exists a compact solution for the unperturbed waveguide and perturbation of the physical configuration is so small that the unperturbed fields are slightly disturbed.

When the perturbation term is large, the perturbation methods become tedious and the physical meaning of the results is clouded by the complexity of the expressions and normally in such a case use of the perturbation technique will be a relatively poor approximation.

Variational methods are becoming increasingly more important than other approximate methods. This method permits

the exploitation of any information bearing on the problem such as might be available from purely intuitional considerations. This is based on the philosophy that the integral of some functions typical of a system has a smaller value for the actual performance of the system than it would have for any other assumed performance which is subjected to some general requirements representing the characteristic feature of the problem under study. For waveguide problems it is usually more important to know the 'wavenumber' which relates w with β rather than the fields. In a variational method, the 'wavenumber' is expressed as a stationary integral of the fields. Thus a good estimate of the wavenumber can be obtained from a rough estimate of the fields. Variational integrals using vector fields suitable for use in solving waveguide problems have been developed by Rumsey,[4] Berk[5] and Eidsen[6].

Another important approximate method is the Rayleigh-Ritz method.[7] It is a scaler variational method and is a more powerful technique and potentially a more accurate variational method for loaded waveguides which have simple outer boundary shapes. The essential character of this method is based on the principle that any arbitrary field distribution in a loaded waveguide may be written by an infinite set of normal mode functions of the corresponding empty waveguide. In this respect it resembles the Fourier series approximation

of a periodic function. In practice the trial fields consisting of a finite sum of normal mode functions are substituted into a variational integral and their amplitudes are adjusted so as to produce the optimum results for the wavenumber. There are two main disadvantages in this method: (a) the normal mode functions are required to be known for the corresponding homogeneous waveguides, and this is not always possible; (b) it is often difficult to determine whether all the significant terms have been included in the normal mode series.

The transverse resonance method developed by Cohn,[8] is another important approach to approximate solutions. In this method the discontinuity problem in waveguide is solved by considering propagation in the transverse direction. A complicated cross-section is divided into a number of simple homogeneous subsections and in each of these subsections a solution to wave equation is written separately. These solutions are then combined so as to satisfy the boundary conditions and give a transverse resonance. This method has been used for ridged waveguide,[9] channel waveguide,[10] etc. Lavik and Unger[11] used this method to solve the problem of rectangular waveguide containing a rectangular dielectric insert. The disadvantage of this method is that it becomes progressively more unwieldy with the increase of complexity of the transverse cross-section.

1.4 The Finite-difference Method

It is clear from the above discussions that there are many waveguide configurations in both homogeneous and inhomogeneous types where it is not possible to obtain analytic solutions in simple form and also for which approximate methods outlined above are not suitable. For these complicated boundary value problems, one can profitably use the finite-difference method.

The basic idea behind the finite-difference formulation of a problem is the discretisation of the differential operator equations which represent the physical system by a set of difference equations. This means that the continuous point set G defined over the domain D and on its boundary B are replaced by discrete sets D_h and B_h where D_h is the discrete set of points defined within the domain D and B_h is the discrete set defined on the boundary B of D. In other words the given problem which is one in the field of differential equations will be replaced in the finite-difference method by an approximate problem which is one in the field of algebra. This is obtained by expanding the fields at a point in terms of its value and derivatives at a neighbouring point by Taylor series and suitably truncating this series.

Although the use of finite-difference techniques for

the solution of differential equations was well-established long before (see, for example, Southwell[12]), its application to homogeneous waveguides and cavity resonator problems was first reported by Motz[13] in 1946. Due to the limitation of the computer facilities at that time they could not advance the method any further. Subsequently, the advent of the high speed digital computer has made the method increasingly attractive to many workers in this field and it was used by Taylor and Kitching[14] in the design of linear accelerator. For homogeneous waveguides with arbitrary boundaries, recently, Davis and Muilwyk[15] have developed a computer program to find the wavenumber.)

For inhomogeneously loaded waveguide, to the best of the author's knowledge, the first work has been reported by Collins and Daly[16] and they derived the finite-difference equations for points at plane vacuum/dielectric interface as well as interior points and then solved the problem by direct matrix method. Recently, Muilwyk[17] and also Hannaford[18] investigated, independently, the inhomogeneously filled waveguide by the finite-element technique. They have used the SOR method[19] for calculating the wavenumber for the range of normalised propagation constant $\bar{\beta}$ less than unity. For the range of $\bar{\beta}$ greater than unity, the SOR method becomes uncertain and methods of conjugate gradient or Kackmarz which

are reported to be very slow in convergence are used in ref. (17).

The difficulties in using the finite-difference method are the following: (1) It cannot treat singular point very efficiently because normal derivatives at such points cannot be defined, such points often occur in strip transmission lines, ridged waveguides, channel waveguide, re-entrant cavities, etc., which have many engineering applications; (2) It is difficult to match the boundaries in the finite-difference method if the boundaries do not coincide with the constant co-ordinate surfaces; (3) For the inhomogeneously filled waveguides, if the interface boundaries do not coincide with the discretised mesh lines or their diagonals, rather represented by a non-linear curve, then it would be difficult to take into account the effect of such boundaries. It is mainly due to the fact that the differential operator wave equations are defined within the domain bounded by each of the regions and are not defined at the interface boundaries; (4) When a waveguide is filled with more than two distinct dielectrics and there exist points common to the boundaries of more than two dielectric regions, the finite-element equivalent of such a point is not yet available. The same is true for a generalised medium.

1.5 The Finite-element/Variational Method

The finite-element/variational method which is the subject matter of this thesis is developed as an alternative to the finite-difference method for propagation problems. As we shall see later, in this method, treatments of singular points or arbitrary boundaries in homogeneous and in inhomogeneous waveguides do not require any special consideration.

The finite-element method is based on the following principle. The differential operator equations which describe the physical problem are replaced by an appropriate extremum functional which is variational for the desired quantity and is written in Euler density form. A discretised set of linear algebraic equations is then derived from this variational expression. This is obtained by grading the entire cross-sectional area into a finite set of polygonal subregions called elements. In this scheme of grading, a number of vertices is generated and a set of field values are assigned to these vertices. Within the domain described by an element, the actual field function is approximated by a set of algebraic polynomials which are uniquely defined over the particular element under consideration and which are linearly dependent on the values of fields assigned to the vertices of the element and which are reduced to zero outside the element. Thus, in this method, the actual field over the entire domain

is approximated by a finite number of trial sets of algebraic functions which are uniquely defined and differentiable.

The sets of algebraic functions approximating the true fields are then substituted into the appropriate extremum functional which may be variational for the wavenumber in waveguides, or for the capacitance in transmission lines. When the integrations involved in the extremum functional are carried out over each element separately, the resulting expression becomes a function of the vertex values of the fields. This is then minimised with respect to the fields at each of the vertices so as to produce the optimum values for fields at the vertices. This type of minimisation generates a set of linear algebraic equations which can be written in matrix form as $A\phi = \lambda B\phi$ for waveguide problems and $A\phi = 0$ for transmission line problems. The solutions of the above matrix operator problems give approximate solutions to the original problems.

The variational functional which is used to develop the finite-element equations is in exactly the same form as used in the Rayleigh-Ritz method. The difference between the two methods lies in the range of sub-domain over which the set of trial functions are defined. The Rayleigh-Ritz method, as we have seen before, starts by approximating the true field functions with a set of normal mode functions defined

over the entire cross-sectional area of the waveguide whereas the finite-elements method starts with a set of algebraic functions as described in this section. In a braod sense, one can say that the finite-element method is a modification of the standard Rayleigh-Ritz method. Probably, for this reason, some authors[20],[21] working with the problem of neutron diffusion called this method the "Ritz-difference method".

The possibility of obtaining the difference equations from a variational formulation was first suggested by Courant[22] for problems with Dirichelet type boundary conditions and some work along this line has been reported by Friedriches and Keller.[23] In the field of Engineering Science, the finite-element method was originally developed as an intuitive discretisation approach to structural problems and Clough and his associates[24] used this method to calculate the stress-strain relations for complicated structures for which no known solution existed. Later works found its firm base in variational calculus. Now it has become the most general and one of the most powerful tools for the analysis of structures. The present position of this method in structural engineering is summarised in ref.(25). Solutions of Laplace's and Poisson's equations by this method are reported by Zienkiewiez[26] and Kellogg.[20] In the field of propagation in waveguides, to the best of the

author's knowledge, no works by this method have been reported earlier than the author's report LU/EE/68/03 written in March 1968. In two recent papers, (27), (28) numerical solutions of homogeneously filled waveguide problems by this method are reported. Our work in this thesis extended the applications of this method to inhomogeneous and generalised mediums as well.

1.6 Content of the Thesis

Chapter 2 describes the derivation of wave equations and the corresponding variational formulation for a wave-guide filled with a generalised isotropic medium. A generalised isotropic medium as considered in this thesis is one whose relative permittivity and permeability are scalar functions of space co-ordinates. This means that the electric field vector $\underline{E}$ and the magnetic field vector $\underline{H}$ at any point in space are related to their corresponding flux density vectors $\underline{D}$ and $\underline{B}$ by $\underline{D} = \epsilon \underline{E}$ and $\underline{B} = \mu \underline{H}$ where ϵ and μ are scalar functions of space. It is assumed that the variations of the relative dielectric constant ϵ_r and relative permeability μ_r are confined in a plane transverse to the direction of propagation. It can be shown that for a waveguide filled with such a medium, it is not always possible to sustain pure TE or TM modes. A propagating mode, in general, contains both the longitudinal components of the electric

and the magnetic fields. This type of mode function is called a hybrid mode. The variational formulation derived for the generalised medium is shown to be the general scalar variational form and all other special cases can be deduced therefrom. It is also shown that the operator eigen value problem for such a medium is self adjoint in nature. This self adjointness of the differential operator is an equivalent condition for the symmetry of the corresponding discretised matrix eigen value problems.

In chapter 3, derivation of finite-element equations based on triangular and rectangular mesh discretisations of homogeneous waveguides are given. It is shown that for all arbitrary shaped triangular and rectangular elements, the corresponding matrix eigen-value operators remain symmetric, sparse, positive, definite and band type. Associated with chapter 3 is appendix A3-1 where a few important integrals which are used for triangular mesh are given and in appendix A3-2 the invarient property of the matrix components to a change of co-ordinates is demonstrated.

Chapter 4 deals with the applications of the finite-element method for calculating the fields, wavenumbers and characteristic impedance for a few typical homogeneous waveguides and transmission lines. These problems are chosen to demonstrate the relative rate of convergence, and to show

the versatility of the finite-element method in dealing with the singular points and in matching any arbitrary curved boundary without introducing asymmetry in the resultant equations.

Chapter 5 deals with inhomogeneously filled waveguides. A variational expression for this type of waveguide is deduced from the general variational expression developed in chapter 2 for a generalised medium by giving μ_r and ϵ_r sectionally constant values. A discretised finite-element equation is derived for a point surrounded by four $\pi/2$ dielectric corners and special cases are deduced. Properties of the matrix eigen-value problem, which for inhomogeneous waveguides become a function of frequency, are discussed for various ranges of normalised propagation constants. Numerical results obtained by the finite-element method are presented for a number of inhomogeneous waveguides. Also, results of other available methods are presented for comparison and assessment of their relative merits.

In chapter 6, the application of the finite-element method is extended to solve the propagation constant of a rectangular waveguide filled with linearly varying dielectrics. In this chapter also are shown the relative difficulties that one would face if one is to use the normal mode functions approximation in the Rayleigh-Ritz method.

In chapter 7, discussions of the results obtained in previous chapters, together with the conclusion regarding the use and scope of the method described in the thesis, are summarised. Although the methods developed in the thesis are quite general, particular emphasis is placed in all numerical calculations for rectilinear boundaries, partly due to the convenience of working in cartesian co-ordinates and partly because of the practical importance of such structures in the design of waveguide components. Since the main object of the thesis is to establish the hypothesis of the finite-element method for waveguide problems, no attempt was made to develop a general computer program or to optimise the computer program used.

Chapter 1 References

1. Meinke, H.H., Lange, K.P. and Ruger, J.F.: "TE and TM-Waves in Waveguides of Very General Cross-Section", Proc. IEEE, Vol.51, pp. 1436-1443, November 1963.

2. Yee, H.Y. and Audeh, N.F.: "Uniform Waveguides with Arbitrary Cross-section considered by the Point Matching Method", IEEE Trans. on Microwave Theory and Techniques, Vol.MIT-13, pp. 847-851, November 1965.

3. Morse, P. and Feshbach, H.: "Methods of Theoretical Physics", McGraw-Hill, 1953. Chapter 9.

4. Rumsey, V.H.: "Reaction Concept in Electromagnetic Theory", Phys. Rev. Vol.94, pp. 1483-1491, June 1954, and Vol.95, p. 1705, September 1954.

5. Berk, A.D.: "Variational Principles for Electromagnetic Resonators and Waveguides", Proc. IRE. Trans. A p.4, p.104, 1956.

6. Eidsen, J.C.: "Variational Principles for Systems Containing Lossy Gyromagnetic Media", M.L. Report No.1195, Microwave Laboratory, W.W. Hensen Laboratories of Physics, Stanford University, California, U.S.A., July 1964.

7. Collin, R.E.: "Field Theory of Guided Waves", McGraw-Hill Book Co., New York, 1960.

8. Cohn, S.B.: "Properties of Ridged Waveguides", Proc.IRE, Vol.35, pp. 783-788, August 1947.

9. Hopfer, S.: "The Design of Ridged Waveguides", IRE Trans. on Microwave Theory and Techniques, Vol.MTT-3, pp. 20-29, October 1955.

10. Roth, J.P. and Ishii, K.: "The Cut-Off Characteristics of the Channel Waveguides", IEEE Trans. on Microwave Theory and Techniques, Vol.MTT-12, pp. 245-247, March 1964.

11. Lavik, A. and Unger, H.: "Der Richteckhohlleiler mit der Electrischen Ubertragung, 18 Heft 1, p. 25, 1964.

12. Southwell, R.V.: "Relaxation Method in Engineering Science", Oxford Engineering Science Series, Clarendon Press, 1940.

13. Motz, H.: "Calculation of the Electromagnetic Field, Frequencies and Circuit Parameters of High Frequency Resonator Cavities", Journal IEE, Vol. 93, Part III, pp. 333-343, September 1946.

14. Taylor, R. and Kitching, P.: "Finite-Difference Compulation of Parameters of Electromagnetic Resonant Cavities relevant to Proton Linear Accelerators", Rutherford High Energy Laboratories, Harwell, Report NIRL/M/37, July 1962.

15. Davis, J.B. and Muilwyk, C.A.: "Numerical Solution of Hollow Waveguides with Boundaries of Arbitrary Shapes", Proc. IEE, Vol.113, No.2, P. 285, February, 1966.

16. Collins, J.H. and Daly, P.: "Calculations for Guided Electromagnetic Waves using Finite-Difference Method" J. Electronics and Control, Vol.14, p. 361, 1963.

17. Muilwyk, C.A.: "The Finite-Difference Solution of Arbitrary Shaped Waveguide with Arbitrary Filling". Ph.D. Thesis, The University of Sheffield, May, 1967.

18. Hannaford, C.D.: "The Finite-Difference/Variational Method for Inhomogeneous Isotropic or Anisotropic Waveguides," Ph.D. Thesis, The University of Leeds.

19. Fox, L.: "Numerical Solution of Ordinary and Partial Differential Equations", Pergamon Press, 1962.

20. Kellog, R.B.: "A Ritz-Finite Difference Approximation to the Neutron Diffusion Equation", Bettis Technical Review; WAPD-BT-31, 1964.

21. Bramble, J.H.: "Numerical Solution of Partial Differential Equations", Academic Press, 1966.

22. Courant, R.: "Variational Methods for the Solution of Problems of Equilibrium and Vibrations", Bull. Amer. Math. Soc., Vol. 49, pp. 1-23, 1943.

23. Friedrichs, K.O. and Keller, H.B.: "A Finite Difference Scheme for Generalised Neumann Problems", Chapter 1 of Ref.21.

24. Turner, M.J., Colough, R.W., Martin, H.C. and Topp, L.J.: "Stiffness and Deflection Analysis of Complex Structures", Journal Aeron. Science, Vol.23, No.9, 1956.

25. Zienkiewicz, O.C. and Cheung, Y.K.: "Finite-Elements Method in Structural and Continuous Mechanics", McGraw-Hill, 1967.

26. Zienkiewicz, O.C. and Cheung, Y.K.: "The Finite-Element in the Solution of Field Problems", The Engineers, pp. 507-510, September 1965.

27. Silvester, P.: "Finite-element Solution of Homogeneous Waveguide Problems", U.R.S.I. Symposium on Electromagnetic Waves, Stresa, Italy, 24th June, 1968.

28. Arlett, P.L., Bahrani, A.K. and Zienkiewicz, O.C.: "Application of Finite Elements to the Solution of Helmholtz's Equation", Proc. of IEE, December 1968, pp. 1762-1766.

CHAPTER 2

WAVE EQUATIONS AND VARIATIONAL FORMULATION FOR WAVE-GUIDES FILLED WITH GENERALISED ISOTROPIC MEDIA

2.1 Mathematical Formulation

2.1.1 Basic Assumptions

The geometry of a waveguide considered in this chapter is illustrated in Fig.(2.1) which is a cylindrical guide of arbitrary cross-section. The guide is assumed to be uniform along the longitudinal direction and also assumed to be infinitely long. It is considered that the dielectric filling is lossless and the waveguide wall is made of perfectly conducting material. It is assumed that the variations of the field components with respect to time is of the form exp(jwt). Under these conditions, for propagating mode, variations of all the field components along the Z-axis (direction of propagation) will be of the form $\exp(-\gamma Z)$, where γ is the propagation constant of the wave transmission and the boundary conditions which must be satisfied are simply that the longitudinal component of electric field vector $\underline{E}$ and the normal component of magnetic field vector $\underline{H}$ must vanish on the guide wall. Finally, the permeability μ and the permittivity ϵ are considered to be functions of the transverse co-ordinates X

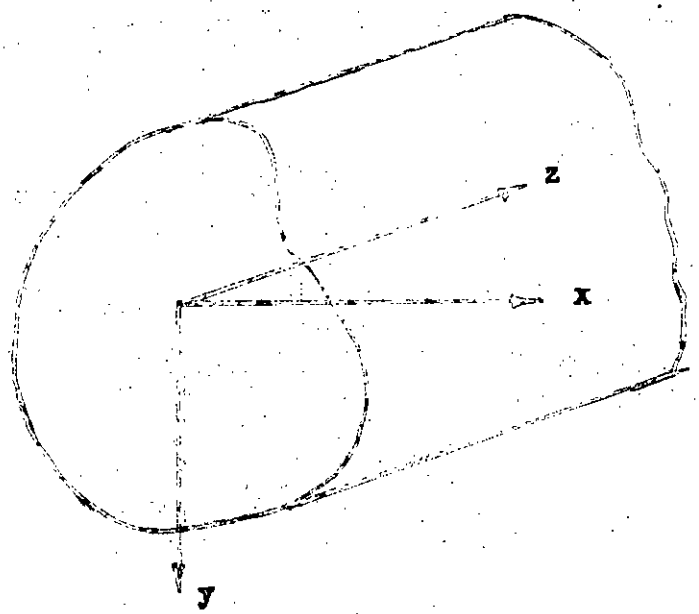

Figure (2.1)
Uniform cylindrical waveguide of arbitrary cross-section

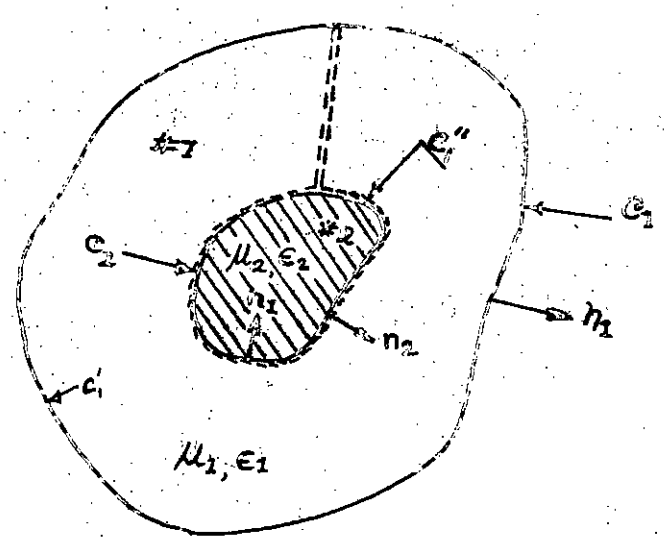

Figure (2.2)
Cross-section of an arbitrary waveguide, with arbitrary shaped filling.

and y, otherwise uniform along the axis of propagation.

2.1.2 Wave Equations

Under the above assumptions, the electric field vector $\underline{E}$ and the magnetic field vector $\underline{H}$ are related by Maxwell's equations[1] as follows:

$$\nabla \times \underset{\sim}{E} = -j\omega\mu \underset{\sim}{H} \tag{2-1}$$

$$\nabla \times \underset{\sim}{H} = j\omega\epsilon \underset{\sim}{E} \tag{2-2}$$

$$\nabla \cdot \underset{\sim}{D} = 0 \tag{2-3}$$

$$\nabla \cdot \underset{\sim}{B} = 0 \tag{2-4}$$

After expansion of equations (2-1) and (2-2) in terms of components, we obtain:

$$\frac{\partial E_z}{\partial y} - \frac{\partial E_y}{\partial z} = -j\omega\mu H_x \tag{2-5}$$

$$\frac{\partial E_x}{\partial z} - \frac{\partial E_z}{\partial x} = -j\omega\mu H_y \tag{2-6}$$

$$\frac{\partial E_y}{\partial x} - \frac{\partial E_x}{\partial y} = -j\omega\mu H_z \tag{2-7}$$

$$\frac{\partial H_z}{\partial y} - \frac{\partial H_y}{\partial z} = j\omega\epsilon E_x \tag{2-8}$$

$$\frac{\partial H_x}{\partial z} - \frac{\partial H_z}{\partial x} = j\omega\epsilon E_y \tag{2-9}$$

and $$\frac{\partial H_y}{\partial x} - \frac{\partial H_x}{\partial y} = j\omega\epsilon E_z \tag{2.10}$$

where suffixes x, y, and z indicate the corresponding components of the field vectors $\underset{\sim}{E}$ and $\underset{\sim}{H}$ respectively.

Substituting $-\gamma$ for $\frac{\partial}{\partial z}$, E_x, E_y, H_x and H_y can be written in terms of E_z and H_z as follows:

$$E_x = -\frac{1}{k_c^2}\left[-\gamma\frac{\partial E_z}{\partial x} + j\omega\mu\frac{\partial H_z}{\partial y}\right] \tag{2.11}$$

$$E_y = -\frac{1}{k_c^2}\left[-\gamma\frac{\partial E_z}{\partial y} - j\omega\mu\frac{\partial H_z}{\partial x}\right] \tag{2.12}$$

$$H_x = -\frac{1}{k_c^2}\left[-j\omega\epsilon\frac{\partial E_z}{\partial y} + \gamma\frac{\partial H_z}{\partial x}\right] \tag{2.13}$$

$$H_y = -\frac{1}{k_c^2}\left[j\omega\epsilon\frac{\partial E_z}{\partial x} + \gamma\frac{\partial H_z}{\partial y}\right] \tag{2.14}$$

where $k_c^2 = \omega^2\mu\epsilon + \gamma^2$, and is commonly referred to as the cut-off wave number. For a homogeneous waveguide, a knowledge of the cut-off wavenumber k_c^2 gives all the information regarding the propagation characteristics of the waveguide under consideration but for a generalised medium, the functional dependence of μ and ϵ makes it difficult to visualize the propagating behaviour from a study of k_c^2.

In vector notations equations (2.11) through (2.14) can be rewritten in a simple form as

$$\underline{E}_t = -\frac{\gamma}{k_c^2}\nabla_t E_z + \frac{j\omega\mu}{k_c^2}\,\underline{a}_z \times \nabla_t H_z \tag{2.15}$$

$$\underline{H}_t = -\frac{j\omega\epsilon}{k_c^2}\,\underline{a}_z \times \nabla_t E_z - \frac{\gamma}{k_c^2}\nabla_t H_z \tag{2.16}$$

where ∇_t indicates the transverse gradient and $\underline{a}_z$ indicates a unit vector along the z-direction; $\underline{E}_t$ and $\underline{H}_t$ indicate vector transverse components of $\underline{E}$ and $\underline{H}$ respectively.

Equations (2.3) and (2.4) can be rewritten as

$$\nabla\cdot\underline{D} = \nabla\cdot(\epsilon\underline{E}) = \epsilon\nabla\cdot\underline{E} + \nabla\epsilon\cdot\underline{E} = 0 \tag{2.17}$$

$$\nabla\cdot\underline{B} = \nabla\cdot(\mu\underline{H}) = \mu\nabla\cdot\underline{H} + \nabla\mu\cdot\underline{H} = 0 \tag{2.18}$$

Equations (2.17) and (2.18) show that for a generalised medium the div. of the electric field $\underline{E}$ and the magnetic field $\underline{H}$ are not zero.

Taking the curl of both sides of equation (2.1) and after expansion, we obtain

$$\nabla\times\nabla\times\underline{E} = \nabla(\nabla\cdot\underline{E}) - \nabla^2\underline{E} = -j\,\nabla\times(\mu\underline{H})$$
$$= -j\omega\mu\,\nabla\times\underline{H} - j\omega\,\nabla\mu\times\underline{H} \tag{2.19}$$

Now, substituting the values of $\nabla\cdot\underline{E}$ from equation (2.17) and $\nabla\times\underline{H}$ from equation (2.2) into equation (2.19), we get

$$-\nabla\left(\frac{1}{\epsilon}\nabla\epsilon\cdot\underline{E}\right) - \nabla^2\underline{E} = \omega^2\mu\epsilon\underline{E} - j\omega(\nabla\mu\times\underline{H}) \tag{2.20}$$

Similarly, performing the curl operation on both sides of equation (2.2) and substituting the values of $\nabla\cdot \underline{H}$ and $\nabla\times \underline{E}$ from equations (2.18) and (2.1) we get

$$-\nabla\left(\frac{1}{\mu}\nabla\mu\cdot H\right)-\nabla^2\underline{H}=\omega^2\mu\epsilon\,\underline{H}+j\omega(\nabla\epsilon\times\underline{E}) \quad (2.21)$$

Equations (2.20) and (2.21) are three dimensional vector wave equations. Separating into the transverse and the longitudinal components, the above vector wave equations can be rewritten as

$$-\nabla_t\left(\frac{1}{\epsilon}\nabla_t\epsilon\cdot\underline{E}_t\right)-\nabla^2\underline{E}_t-\omega^2\mu\epsilon\,\underline{E}_t+j\omega(\nabla_t\mu\times\underline{a}_z H_z)=0 \quad (2.22)$$

and

$$-\nabla_t\left(\frac{1}{\mu}\nabla_t\mu\cdot\underline{H}_t\right)-\nabla^2\underline{H}_t-\omega^2\mu\epsilon\,\underline{H}_t-j\omega(\nabla_t\epsilon\times\underline{a}_z E_z)=0 \quad (2.23)$$

for the transverse components, and

$$-\underline{a}_z\cdot\nabla_z\left(\frac{1}{\epsilon}\nabla_t\epsilon\cdot\underline{E}_t\right)-\nabla^2 E_z-\omega^2\mu\epsilon E_z+j\omega(\nabla_t\mu\times\underline{H}_t)\cdot\underline{a}_z=0 \quad (2.24)$$

and

$$-a_z\cdot\nabla_z\left(\frac{1}{\mu}\nabla_t\mu\cdot\underline{H}_t\right)-\nabla^2 H_z-\omega^2\mu\epsilon H_z-j\omega(\nabla_t\epsilon\times\underline{E}_t)\cdot\underline{a}_z=0 \quad (2.25)$$

for the longitudinal components. (Since μ and ϵ are independent of z). ∇_t and ∇_z represent the transverse and

the longitudinal components of the operator ∇ .

A study of equations (2.24) and (2.25) shows that in a generalised medium TEM wave cannot propagate. If E_z and H_z are zero then equation (2.24) reduces to

$$-\underline{a}_z \cdot \nabla_z \left(\frac{1}{\epsilon} \nabla_t \epsilon \cdot \underline{E}_t \right) + j\omega \underline{a}_z \left(\nabla_t \mu \times \underline{H}_t \right) = 0 \tag{2.26}$$

Replacing $- a_z \cdot \nabla_z$ by γ , equation (2.26) can be written as follows:

$$\frac{\gamma}{\epsilon} \left(\nabla_t \epsilon \cdot \underline{E}_t \right) + j\omega \, \underline{a}_z \cdot \left(\nabla_t \mu \times \underline{H}_t \right) = 0 \tag{2.27}$$

But variations of $\epsilon(x,y)$ and $\mu(x,y)$ are arbitrary, in case, if $\nabla_t \mu = 0$ and $\nabla_t \epsilon \neq 0$, then equation (2.27) becomes

$$\frac{\gamma}{\epsilon} \left(\nabla_t \epsilon \cdot \underline{E}_t \right) = 0 \tag{2.28}$$

Since $\epsilon(x,y)$ is an arbitrary function of (x,y) equation (2.28) can be satisfied if $E_t = 0$; thus $E_z = 0$ and $H_z = 0$ reduce all other components to zero. Therefore TEM wave cannot propagate through a generalised medium.

Now, considering the waveguide mode, the transverse components $\underline{E}_t$ and $\underline{H}_t$ in equations (2.24) and (2.25) can be replaced by their corresponding values given in equations (2.15) and (2.16) and these substitutions result in the following wave equations:

$$\nabla_t^2 E_z + k_c^2 E_z - \frac{\beta^2}{k_c^2}(\nabla_t \epsilon \cdot \nabla_t E_z) - \frac{\omega^2 \epsilon}{k_c^2}(\nabla_t \mu \cdot \nabla_t E_z)$$

$$- a_z \cdot \frac{\omega\beta}{k_c^2}\left(\frac{\mu}{\epsilon}\nabla_t \epsilon \times \nabla_t H_z + \nabla_t \mu \times \nabla_t H_z\right) = 0 \qquad (2.29)$$

$$\nabla_t^2 H_z + k_c^2 H_z - \frac{\beta^2}{k_c^2}(\nabla_t \mu \cdot \nabla H_z) - \frac{\omega^2 \mu}{k_c^2}(\nabla_t \epsilon \cdot \nabla H_z)$$

$$+ a_z \cdot \frac{\omega\beta}{k_c^2}\left(\nabla_t \epsilon \times \nabla_t E_z + \frac{\epsilon}{\mu}\nabla_t \mu \times \nabla_t E_z\right) = 0 \qquad (2.30)$$

where $j\beta = \gamma$ (The phase change co-efficient). (2.31)

Equations (2.29) and (2.30) reveal the fact that for a waveguide filled with lossless isotropic material whose permeability and permittivity are functions of the transverse co-ordinates, a pure transverse electric mode or a pure transverse magnetic mode cannot exist. Propagating mode in such a waveguide would be, in general, a hybrid one i.e. a combination of TE and TM modes.

2.1.3 Wave Equations for Inhomogeneous Waveguides

For a homogeneous waveguide μ_r and ϵ_r are constant over the entire cross-section and equations (2.29) and (2.30) reduce to

$$\nabla_t^2 E_z + k_{c_i}^2 E_z = 0 \qquad (2.32)$$

$$\nabla_t^2 H_z + k_{c_i}^2 H_z = 0 \qquad (2.33)$$

A waveguide which is filled with two or more uniform dielectrics, each occupying a part of the waveguide, is called an inhomogeneous waveguide. Thus for an inhomogeneously filled waveguide, μ and ϵ are sectionally constants, and $\nabla_t \epsilon$ and $\nabla_t \mu$ are zero over each of the homogeneous subsections and therefore, over each subregion equations (2.32) and (2.33) become

$$\nabla_t^2 E_z + k_{c_i}^2 E_z = 0 \tag{2.32a}$$

$$\nabla_t^2 H_z + k_{c_i}^2 H_z = 0 \tag{2.33b}$$

where, $k_{c_i}^2 = \omega^2 \mu_i \epsilon_i - \beta^2$ (wavenumber for the i th subregion for which μ and ϵ take the values μ_i and ϵ_i respectively)

Thus for a waveguide medium having sectionally constant permittivity and permeability, the continuously coupled set of wave equations (2.29) and (2.30) degenerates into a set of decoupled wave equations as in (2.32a) and (2.33a). But in such a case, there is a finite jump in μ_r and ϵ_r at the interface boundaries between two distinct subregions. At the interface boundaries E_z and H_z must be continuous. Also, components of $\underline{E}$ and $\underline{H}$ tangential to the interface boundaries and components of $\underline{D}$ and $\underline{B}$ normal to the interface boundaries must be continuous.

Consider an inhomogeneous waveguide as shown in Fig.(2.2) which is bounded by perfect conductors. Let the relative permeability and permittivity of region 1 be μ_1 and ϵ_1 and of region 2 be μ_2 and ϵ_2 respectively. The boundary conditions to be satisfied are given by

$$\left.\begin{aligned} E_z = 0 \; ; \qquad \frac{\partial E_z}{\partial c} = 0 \; ; \\ \frac{\partial H_z}{\partial n} = 0 \; . \end{aligned}\right\} \tag{2.34}$$

on the outer conducting boundary of region 1. On the inner boundary of region 1 which is, actually, the same as the outer boundary of region 2, the continuity of the tangential component of electric field gives

$$\frac{\beta}{\omega\mu_1}\frac{\partial E_z}{\partial c} + \left(\frac{\partial H_z}{\partial n}\right)_1 = \tau\frac{\mu_2}{\mu_1}\left[\frac{\beta}{\omega\mu_2}\frac{\partial E_z}{\partial c} - \left(\frac{\partial H_z}{\partial n}\right)_2\right] \tag{2.35}$$

and the continuity of the normal component of the electric flux density vector $\underline{D}$ gives

$$\frac{\partial H_z}{\partial c} - \frac{\beta}{\omega\mu_1}\left(\frac{\partial E_z}{\partial n}\right)_1 = \tau\frac{\mu_2\epsilon_2}{\mu_1\epsilon_1}\left[\frac{\beta}{\omega\mu_2}\left(\frac{\partial E_z}{\partial n}\right)_2 + \frac{\partial H_z}{\partial c}\right] \tag{2.36}$$

where,

$$\tau = \frac{\omega^2\mu_1\epsilon_1 - \beta^2}{\omega^2\mu_2\epsilon_2 - \beta^2} \tag{2.37}$$

and $\frac{\partial}{\partial t}$ indicates the spatial differentiation tangential to the interface boundary, and $\left(\frac{\partial}{\partial n}\right)_i$ indicates the spatial differentiation in the direction of the outward normal to the boundary surrounding the region 'i'.

Thus, for an inhomogeneous waveguide, the longitudinal components of the field vectors must satisfy the wave equations (2.32a) and (2.33a), together with the boundary conditions given in equations (2.34) and (2.35) and (2.36). Though the wave equations for an inhomogeneous waveguide do not contain any coupling term but restrictions put on the field components by the continuity relations show that a propagating mode through such a system, in general, would also be hybrid in nature.

2.2 Variational Formulation

A variational expression for the hybrid mode problems, as discussed in the above section will contain terms involving E_z and H_z. In order to make all terms dimensionally consistent, let us replace E_z and H_z by two scalar potential functions ϕ and ψ such that

$$\psi = \frac{\omega \epsilon_0}{\beta} E_z \tag{2.38}$$

and

$$\phi = H_z \tag{2.39}$$

Since the weighting factor $\frac{\omega\epsilon_0}{\beta}$ has the dimension of admittance, the scalar potential functions ϕ and ψ will have the same dimensions. In terms of ϕ and ψ equations (2.29) and (2.30) can be rewritten

$$\nabla_t^2\psi + k_c^2\psi - \frac{\beta^2}{k_c^2\epsilon}\nabla_t\epsilon\cdot\nabla_t\psi - \frac{\omega^2\epsilon}{k_c^2}\nabla_t\mu\cdot\nabla\psi$$

$$- \underline{a}_z\cdot\frac{\omega^2\epsilon_0}{k_c^2}\left(\frac{\mu}{\epsilon}\nabla_t\epsilon\times\nabla_t\phi + \nabla_t\mu\times\nabla_t\phi\right) = 0 \quad (2.40a)$$

and

$$\nabla_t^2\phi + k_c^2\phi - \frac{\beta^2}{k_c^2\mu}\nabla_t\mu\cdot\nabla_t\phi - \frac{\omega^2\mu}{k_c^2}\nabla_t\epsilon\cdot\nabla_t\phi$$

$$+ \underline{a}_z\cdot\frac{\beta^2}{k_c^2\epsilon_0}\left(\nabla_t\epsilon\times\nabla_t\psi + \frac{\epsilon}{\mu}\nabla_t\mu\times\nabla_t\psi\right) = 0 \quad (2.41a)$$

Substituting $\mu_0\mu_r = \mu$ and $\epsilon_0\epsilon_r = \epsilon$ and $\beta^2 = \omega^2\mu_0\epsilon_0$ in equations (2.40a) and (2.41a), we obtain

$$\nabla_t^2\psi + k_c^2\psi - \frac{\beta^2}{k_c^2\epsilon_r}\nabla_t\epsilon_r\cdot\nabla_t\psi - \frac{\beta_0^2\epsilon_r}{k_c^2}\nabla_t\mu_r\cdot\nabla_t\psi$$

$$- \underline{a}_z\cdot\frac{\beta_0^2}{k_c^2}\left(\frac{\mu_r}{\epsilon_r}\nabla_t\epsilon_r\times\nabla_t\phi + \nabla_t\mu_r\times\nabla_t\phi\right) = 0 \quad (2.40b)$$

and

$$\nabla_t^2\phi + k_c^2\phi - \frac{\beta^2}{k_c^2\mu_r}\nabla_t\mu_r\cdot\nabla_t\phi - \frac{\beta_0^2\mu_r}{k_c^2}\nabla_t\epsilon_r\cdot\nabla_t\phi$$

$$+ \underline{a}_z\cdot\frac{\beta^2}{k_c^2}\left(\frac{\epsilon_r}{\mu_r}\nabla_t\mu_r\times\nabla_t\psi + \nabla_t\epsilon_r\times\nabla_t\psi\right) = 0 \quad (2.41b)$$

At this stage, let us define the following parameters which will be used to simplify equations (2.40) and (2.41)

(a) $\bar{\beta} \triangleq \dfrac{\beta}{\beta_o} = \dfrac{\text{Propagation constant of the guided wave}}{\text{Free space propagation constant}}$

(b) $\tau \triangleq \dfrac{k_o^2}{k_c^2} = \dfrac{\omega^2 \mu_o \epsilon_o - \beta^2}{\omega^2 \mu \epsilon - \beta^2} = \dfrac{1 - \bar{\beta}^2}{\epsilon_r \mu_r - \bar{\beta}^2}$

(c) $P \triangleq \bar{\beta}^2 \tau \epsilon_r$

(d) $R \triangleq \tau \mu_r$

(e) $W \triangleq \bar{\beta}^2 \tau$

Now equations (2.40b) and (2.41b) can be rewritten by using the above parameters as

$$P \nabla_t^2 \psi + \frac{P}{\tau} k_o^2 \psi - \frac{\bar{\beta}^4 \tau}{\mu_r \epsilon_r - \bar{\beta}^2} \nabla_t \epsilon_r \cdot \nabla_t \psi - \frac{\bar{\beta}^2 \epsilon_r^2 \tau}{\mu_r \epsilon_r - \bar{\beta}^2} \nabla_t \mu_r \cdot \nabla_t \psi$$
$$- \underline{a}_z \cdot \left(\frac{\bar{\beta}^2 \tau \epsilon_r}{\mu_r \epsilon_r - \bar{\beta}^2} \nabla_t \mu_r \times \nabla_t \phi + \frac{\bar{\beta}^2 \tau \mu_r}{\mu_r \epsilon_r - \bar{\beta}^2} \nabla_t \epsilon_r \times \nabla_t \phi \right) = 0 \quad (2.42)$$

$$R \nabla_t^2 \phi + \frac{R}{\tau} k_o^2 \phi - \frac{\bar{\beta}^2 \tau}{\mu_r \epsilon_r - \bar{\beta}^2} \nabla_t \mu_r \cdot \nabla_t \phi - \frac{\mu_r^2 \tau}{\mu_r \epsilon_r - \bar{\beta}^2} \nabla_t \epsilon_r \cdot \nabla_t \phi$$
$$- \underline{a}_z \cdot \left(\frac{\bar{\beta}^2 \tau \epsilon_r}{\mu_r \epsilon_r - \bar{\beta}^2} \nabla_t \mu_r \times \nabla_t \psi + \frac{\bar{\beta}^2 \tau \mu_r}{\mu_r \epsilon_r - \bar{\beta}^2} \nabla_t \epsilon_r \times \nabla_t \psi \right) = 0 \quad (2.43)$$

Apparently the introduction of new parameters P, R, τ, W and $\bar{\beta}$ make equations (2.42) and (2.43) structurally more complicated than equations (2.40b) and (2.41b). The advantage of these parameters can be seen by studying the transverse gradient of P. R, τ and W as follows:

$$\nabla_t P = \nabla_t \left(\bar{\beta}^2 \tau \epsilon_r \right) = \bar{\beta}^2 \nabla_t (\tau \epsilon_r) \tag{2.44}$$

since $\bar{\beta}$ is a constant.

Substituting the values of τ as defined previously into equation (2.44), we obtain

$$\nabla_t P = -\frac{\bar{\beta}^4 \tau}{\mu_r \epsilon_r - \bar{\beta}^2} \nabla_t \epsilon_r - \frac{\bar{\beta}^2 \epsilon_r^2 \tau}{\mu_r \epsilon_r - \bar{\beta}^2} \nabla_t \mu_r \tag{2.45}$$

and

$$\nabla_t R = \left(1 - \bar{\beta}^2\right) \nabla_t \left(\frac{\mu_r}{\mu_r \epsilon_r - \bar{\beta}^2} \right) \tag{2.46}$$

which on further simplification gives

$$\nabla_t R = -\frac{\tau \bar{\beta}^2}{\mu_r \epsilon_r - \bar{\beta}^2} \nabla_t \mu_r - \frac{\tau \mu_r^2}{\mu_r \epsilon_r - \bar{\beta}^2} \nabla_t \epsilon_r \tag{2.47}$$

Similarly,

$$\nabla_t W = \bar{\beta}^2 \nabla_t \tau = -\frac{\bar{\beta}^2 \tau \epsilon_r}{\mu_r \epsilon_r - \bar{\beta}^2} \nabla_t \mu_r - \frac{\bar{\beta}^2 \tau \mu_r}{\mu_r \epsilon_r - \bar{\beta}^2} \nabla_t \epsilon_r \tag{2.48}$$

Comparing the terms of $\nabla_t P$, $\nabla_t R$ and $\nabla_t W$ with those of equations (2.42) and (2.43), equations (2.42) and (2.43) can be rearranged in compact form as given below:

$$P\nabla_t^2\psi + \frac{P}{\tau}k_o^2\psi + \nabla_t P\cdot\nabla_t\psi + \underline{a}_z\cdot\nabla_t W\times\nabla_t\phi = 0 \qquad (2.49)$$

and

$$R\nabla_t^2\phi + \frac{R}{\tau}k_o^2\phi + \nabla_t R\cdot\nabla\phi - \underline{a}_z\cdot\nabla_t W\times\nabla\psi = 0 \qquad (2.50)$$

Multiplying equation (2.50) by ψ and (2.51) by ϕ and integrating over the entire cross-section, we obtain

$$\int_S \psi P\nabla_t^2\psi\, ds + \int_S \frac{P}{\tau}k_o^2\psi^2 ds + \int_S \psi\nabla_t P\cdot\nabla_t\psi\, ds - \underline{a}_z\cdot\int_S \psi(\nabla_t W\times\nabla_t\phi)\, ds = 0 \qquad (2.50a)$$

$$\int_S \phi R\nabla_t^2\phi\, ds + \int_S \frac{R}{\tau}k_o^2\phi^2 ds + \int_S \phi\nabla_t R\cdot\nabla_t\phi\, ds + \underline{a}_z\cdot\int_S \phi(\nabla_t W\times\nabla_t\psi)\, ds = 0 \qquad (2.51)$$

Adding equation (2.50a) with (2.51) and after suitable rearrangement of terms gives:

$$k_o^2 = \left[\int_S \psi(P\nabla_t^2\psi + \nabla_t P\cdot\nabla_t\psi)\, ds + \int_S \phi(R\nabla_t^2\phi + \nabla_t R\cdot\nabla_t\phi)\, ds + \int_S \underline{a}_z\cdot\psi(\nabla_t W\times\nabla_t\phi)\, ds - \int_S \underline{a}_z\cdot\phi(\nabla_t W\times\nabla_t\psi)\, ds\right] \Big/ \left[\int_S \frac{P}{\tau}\psi^2 ds + \int_S \frac{R}{\tau}\phi^2 ds\right] \qquad (2.52)$$

The expression for k_o^2 as given above is stationary for trial functions ϕ and ψ . Though k_o^2 itself is not the cut-off wavenumber of the waveguide under consideration, it relates the frequency with the phase change constant provided that the right hand side of equation (2.52) can be

evaluated for any set of trial fields ϕ and ψ. Since the expressions for P, R, and W contain the term $\bar{\beta}^2$, a solution for frequency ω can be obtained by considering $\bar{\beta}^2$ as a parameter. A different solution exists for each $\bar{\beta}^2$, therefore, to construct a dispersion curve, the problem must be solved several times, each time assuming a new value of $\bar{\beta}^2$. In the case of a homogeneous waveguide, the solution for the cut-off wavenumber is straightforward, because the expression for k_o^2 does not contain $\bar{\beta}^2$ as a parameter.

By suitable use of Stoke's and Green's theorems and also taking into account of the boundary conditions, equation (2.52) can be written in a simple form as given below:

$$k_o^2 = \frac{\int_s P|\nabla_t\psi|^2 ds + \int_s R|\nabla_t\phi|^2 ds + 2\int_s Q_2 W(\nabla_t\psi \cdot \nabla_t\phi) ds}{\int \frac{P}{\tau}\psi^2 ds + \int \frac{R}{\tau}\phi^2 ds} \quad (2.53)$$

Derivation of equation (2.53) is given in Appendix A2.3. The expression for k_o^2 as given in equation (2.53) is variational for k_o^2 provided the trial functions ϕ and ψ together with their first derivatives are continuous throughout the region where P, R, and W are continuous and on the boundary where P, R, and W are discontinuous, trial functions ϕ and ψ should be continuous.

2.3 Evaluation of the Variational Character of k_o^2

2.3.1 Indirect Proof

The variational expression for any quantity based on the physical concept that the integral of some functions typical of the system has a smaller value for the actual performance of the system than that it would have for any other assumed performance which is subjected to some general requirements representing the characteristic feature of the problem under study. Let L be such an integrand. It may be a function of several independent variables of the system and may also be a function of the derivatives of these variables with respect to the parameters of integration. If the variables are designated by $\phi_1, \phi_2, \ldots \phi_n$; the parameters by $x_1, x_2, \ldots x_m$ and the derivatives $\frac{\partial \phi_r}{\partial x_s}$ by ϕ_{rs}, then the integral which is to be minimised is given by (2)

$$J = \int_{\alpha_1}^{\beta_1}\int_{\alpha_2}^{\beta_2}\cdots\int_{\alpha_m}^{\beta_m} L\left(\phi, \frac{\partial\phi}{\partial x}, x\right) dx_1\, dx_2 \ldots dx_m \qquad (2.54)$$

The integrand L is normally called Lagrange density of the system. The requirement that the integrand L should satisfy, so as to make J an extremum function is given by (2)

$$\sum_{r=1}^{m} \frac{\partial}{\partial x_r}\left(\frac{\partial L}{\partial \phi_{c,r}}\right) = \frac{\partial L}{\partial \phi_c} \qquad \text{for } c = 1, 2, \ldots n \qquad (2.55)$$

These equations which serve to determine the optimum form of ϕ^s are called Euler equations in calculus of variations. Lagrange density function corresponding to the system described by equation (2.53) is

$$L = P|\nabla_t \psi|^2 + R|\nabla_t \phi|^2 + 2W\underline{a}_z \cdot (\nabla_t \psi \times \nabla_t \phi) - \frac{P}{\tau}\psi^2 - \frac{R}{\tau}\phi^2 \qquad (2.56)$$

The density function L depends on ϕ, ψ and their first derivatives. The parameters of integration are x and y. We will now show that the Euler equations corresponding to the density function (2.56) are exactly the same as the wave equations for the system.

Euler equations for ϕ and ψ for the density functions given in equation (2.56) are:

$$\frac{\partial L}{\partial \phi} - \frac{\partial}{\partial x}\left(\frac{\partial L}{\partial \phi_x}\right) - \frac{\partial}{\partial y}\left(\frac{\partial L}{\partial \phi_y}\right) = 0 \qquad (2.57)$$

and

$$\frac{\partial L}{\partial \psi} - \frac{\partial}{\partial x}\left(\frac{\partial L}{\partial \psi_x}\right) - \frac{\partial}{\partial y}\left(\frac{\partial L}{\partial \psi_y}\right) = 0 \qquad (2.58)$$

where

$$\left.\begin{aligned} \phi_x &= \frac{\partial \phi}{\partial x}\ ; \quad \phi_y = \frac{\partial \phi}{\partial y} \\ \psi_x &= \frac{\partial \psi}{\partial x}\ ; \quad \psi_y = \frac{\partial \psi}{\partial y} \end{aligned}\right\} \qquad (2.59)$$

From equation (2.56), we get

$$\frac{\partial L}{\partial \phi} = -2\frac{R}{\tau}\phi \qquad (2.60)$$

$$\frac{\partial L}{\partial \phi_x} = 2R\phi_x - 2W\psi_y \qquad (2.61)$$

$$\frac{\partial}{\partial x}\left(\frac{\partial L}{\partial \phi_x}\right) = 2R\phi_{xx} + 2\frac{\partial R}{\partial x}\phi_x - 2\frac{\partial W}{\partial x}\psi_y - 2W\psi_{xy} \tag{2.62}$$

$$\frac{\partial L}{\partial \phi_y} = 2R\phi_y + 2W\psi_x \tag{2.63}$$

$$\frac{\partial}{\partial y}\left(\frac{\partial L}{\partial \phi_y}\right) = 2R\phi_{yy} + 2\frac{\partial R}{\partial y}\phi_y + 2\frac{\partial W}{\partial y}\psi_x + 2W\psi_{xy} \tag{2.64}$$

where

$$\left.\begin{aligned} \phi_{xx} &= \frac{\partial^2\phi}{\partial x^2}\,; \quad \phi_{yy} = \frac{\partial^2\phi}{\partial y^2} \\ \psi_{xy} &= \frac{\partial^2\psi}{\partial x\,\partial y} \end{aligned}\right\} \tag{2.65}$$

Adding equations (2.62) and (2.64) and subtracting the result from equation (2.60), we get

$$\frac{\partial L}{\partial \phi} - \frac{\partial}{\partial x}\left(\frac{\partial L}{\partial \phi_x}\right) - \frac{\partial}{\partial y}\left(\frac{\partial L}{\partial \phi_y}\right) = 2\Big| -\frac{R}{\tau}k_0^2\phi - R(\phi_{xx} + \phi_{yy})$$
$$- \left(\frac{\partial R}{\partial x}\phi_x + \frac{\partial R}{\partial y}\phi_y\right) + \left(\frac{\partial W}{\partial x}\psi_y - \frac{\partial W}{\partial y}\psi_x\right) \tag{2.66}$$

But

$$\phi_{xx} + \phi_{yy} = \nabla_t^2\phi \tag{2.67}$$

$$\frac{\partial R}{\partial x}\phi_x + \frac{\partial R}{\partial y}\phi_y = \nabla_t R\cdot\nabla_t\phi \tag{2.68}$$

and

$$\frac{\partial W}{\partial x}\psi_y - \frac{\partial W}{\partial y}\psi_x = (\nabla_t W \times \nabla_t\psi)\cdot\underline{a}_z \tag{2.69}$$

Substituting the values of equations (2.67), (2.68) and (2.69) in equation (2.66) results

$$\frac{\partial L}{\partial \phi} - \frac{\partial}{\partial x}\left(\frac{\partial L}{\partial \phi_x}\right) - \frac{\partial L}{\partial y}\left(\frac{\partial L}{\partial \phi_y}\right) = -2\Big| R\nabla_t^2\phi + \frac{R}{\tau}k_0^2\phi$$
$$+ \nabla_t R\cdot\nabla_t\phi - \underline{a}_z\cdot(\nabla_t W \times \nabla_t\psi) = 0 \tag{2.70}$$

Similarly, for the variable ψ , the corresponding Euler equation becomes

$$\frac{\partial L}{\partial \psi} - \frac{\partial}{\partial x}\left(\frac{\partial L}{\partial \psi_x}\right) - \frac{\partial}{\partial y}\left(\frac{\partial L}{\partial \psi_y}\right) = -2\Big[P\nabla_t^2\psi + \frac{P}{\tau}k_0^2\psi + \nabla_t P\cdot\nabla_t\psi + \underline{a}_z\cdot(\nabla_t W\times\nabla_t\phi)\Big] = 0 \qquad (2.71)$$

The right hand sides of equations (2.70) and (2.71) are the same as the wave equations for a generalised medium. Therefore, the functional J is an extremum function. This indirectly proves that the expression for k_0^2 as given in equation (2.53) is variational in character.

2.3.2 Direct Proof

That the expression for k_0^2 as given in equation (2.53) is stationary will be proved if any first order change in the values of ϕ and ψ from their true values ϕ_0 and ψ_0 produces only second order change[3] in k_0^2 , i.e. if we substitute $\phi_0+\delta\phi$ for ϕ and $\psi_0+\delta\psi$ for ψ and $k_0^2+\delta(k_0^2)$ for k_0^2 , then neglecting all the second order effects we must obtain $\delta[k_0^2] = 0$.

By actual substitution, and after a little algebraic manipulation we obtain

$$\delta[k_0^2] = 2\Big[\int_S P(\nabla_t\delta\psi\cdot\nabla_t\psi_0)\,ds + \int_S R(\nabla_t\delta\phi\cdot\nabla_t\phi_0)\,ds + \int_S W(\nabla_t\delta\psi\times\nabla_t\phi_0 + \nabla_t\psi_0\times\nabla_t\delta\phi)\cdot\underline{a}_z\,ds - k_0^2\int_S\frac{P}{\tau}\delta\psi\psi_0\,ds - k_0^2\int_S\frac{R}{\tau}\phi_0\delta\phi\,ds\Big]\Big/\Big[\int_S\frac{R}{\tau}\phi_0^2\,ds + \int_S\frac{P}{\tau}\psi_0^2\,ds\Big] \qquad (2.72)$$

Considering the numerator of the right-hand side of equation (2.72) term by term and using the appropriate form of Stokes' and Green's Theorems as given in Appendix A2, we get

$$\int_S P(\nabla_t \delta\psi \cdot \nabla_t \psi_0)\, ds = \oint_{C} P\,\delta\psi \frac{\partial \psi_0}{\partial n}\, dl - \int_S \delta\psi\,(P \nabla_t^2 \psi_0 + \nabla_t P \cdot \nabla_t \psi_0)\, ds \qquad (2.73)$$

$$\int_S R(\nabla_t \delta\phi \cdot \nabla_t \phi_0)\, ds = \oint_{C} R\,\delta\phi \frac{\partial \phi_0}{\partial n}\, dl - \int \delta\phi\,(R \nabla_t^2 \phi_0 + \nabla_t R \cdot \nabla_t \phi_0)\, ds \qquad (2.74)$$

$$\int_S W\, \underline{a}_z \cdot (\nabla_t \delta\psi \times \nabla_t \phi_0 + \nabla_t \psi_0 \times \nabla_t \delta\phi)\, ds = \oint_{C} \left(W\,\delta\psi \frac{\partial \phi_0}{\partial c} - W\,\delta\phi \frac{\partial \psi_0}{\partial c}\right) dl$$

$$+ \int_S \delta\phi\, \underline{a}_z \cdot (\nabla_t W \times \nabla_t \psi)\, ds - \int_S \delta\psi\, \underline{a}_z \cdot (\nabla_t W \times \nabla_t \phi)\, ds \qquad (2.75)$$

Substitution of the results of equations (2.73), (2.74) and (2.75) in equation (2.72) and after a proper rearrangements of terms gives

$$I\,\delta|k_0^2| = 2\left[\oint_{C} P\,\delta\psi \frac{\partial \psi_0}{\partial n}\, dl + \oint_{C} R\,\delta\phi \frac{\partial \phi_0}{\partial n}\, dl + \oint_{C} \delta\psi\, W \frac{\partial \phi_0}{\partial c}\, dl - \oint_{C} W\,\delta\phi \frac{\partial \psi_0}{\partial c}\, dl\right] \qquad (2.76)$$

where I is denominator of equation (2.72).

In equation (2.76) all contour integrals are performed on the outer boundary of the guide which is assumed to be made of perfectly conducting material and on which ϕ_0 and ψ_0 satisfy the following relations

$$\frac{\partial \phi_0}{\partial c} = 0; \qquad \psi_0 = 0; \quad \text{and} \qquad \frac{\partial \psi_0}{\partial c} = 0$$

These boundary conditions when incorporated into equation (2.76) become

$$I\,\delta|k_0^2| = 2\left[\oint_c F\,\delta\psi\,\frac{\partial \psi_0}{\partial n}\,dl + \oint_c w\,\delta\psi\,\frac{\partial \phi_0}{\partial c}\,dl\right] \tag{2.77}$$

But on the conducting boundary $\frac{\partial \psi_0}{\partial n}$ and $\frac{\partial \phi_0}{\partial c}$ are not zero. The above contour integrals would reduce to zero if $\delta\psi = 0$ on the boundary. Equation (2.77) shows that for $I\,\delta|k_0^2|$ to become zero, it does not require the condition that $\frac{\partial}{\partial n}(\delta\psi) = 0$ on the boundary. Therefore we can conclude that the expression for k_0^2 given in equation (2.53) is stationary for all trial functions which satisfy the same boundary conditions as satisfied by the true field ψ_0 and for any arbitrary ϕ.

2.4 Restrictions on the Variations of μ_r and ϵ_r

2.4.1 Discontinuous Variations of μ_r and ϵ_r

In this section we will show that the variational expression derived for a generalised medium would be valid for all types of variations of μ_r and ϵ_r. An extremum case is one for which values of μ_r and ϵ_r have a finite jump. It will be shown in this section that for the variational expression as derived earlier to be valid for this type of discontinuity, it does not require the condition that the trial field

should satisfy the continuity conditions at the interface boundaries. To illustrate, let us consider the waveguide cross-section as shown in Fig. (2.2). Let us assume that the cross-section of the guide is made of two distinct regions; #1 and#2 respectively. The permeability and permittivity of each region are given by

$$\mu_1 = \mu_1 (x,y); \qquad \mu_2 = \mu_2 (x,y);$$

$$\epsilon_1 = \epsilon_1 (x,y); \qquad \epsilon_2 = \epsilon_2 (x,y). \tag{2.78}$$

Also assume that changes from ϵ_1 to ϵ_2 and μ_1 to μ_2 are not continuous. At the discontinuity interface, the tangential components of $\underline{E}$ and $\underline{H}$ are continuous. In terms of ϕ and ψ these are

$$\left.\begin{aligned} E_{\text{tangential}} &= -\frac{j\beta^2}{\omega\epsilon_0 k_{ci}^2}\left(\frac{\partial\psi}{\partial c}\right)_i + \frac{j\omega\mu_i}{k_{ci}^2}\left(\frac{\partial\phi}{\partial n}\right)_i \\ H_{\text{tangential}} &= -\frac{j\beta\epsilon_n}{k_{ci}^2}\left(\frac{\partial\psi}{\partial n}\right)_i - \frac{j\beta}{k_{ci}^2}\left(\frac{\partial\phi}{\partial c}\right)_i \end{aligned}\right\} \tag{2.79}$$

Let us also assume that contour C_1 and C_2 represent the boundary contours of region#1 and#2 respectively. Region #1 has two disjointed boundaries, namely, the outer conducting boundary and the inner interface boundary between the two regions. In order to make the boundary of region#1 a simple boundary, let us take a longitudinal branch cut which connects the inner boundary of region#1 with its outer boundary (shown in Fig. (2.2). Since the variations of fields across this

branch cut are continuous, any line integral of these continuous fields performed over the branch cut twice in opposite direction shall be zero. Keeping this in mind, let us examine the expression for $\delta|k_0^2|$ as given in equation (2.72). This can be written for the above case as

$$I\,\delta|k_0^2| = 2\Big[\int_{S_1+S_2} \nabla_t\cdot(P\,\delta\psi\,\nabla_t\psi_0)\,ds + \int_{S_1+S_2} \nabla_t\cdot(R\,\delta\phi\,\nabla_t\phi_0)\,ds$$

$$+ \int_{S_1+S_2} \underline{a}_z\cdot\nabla_t\times(\delta\psi\,\nabla_t\phi_0 - \delta\phi\,\nabla\psi_0)\,ds\Big] \qquad (2.80)$$

where S_1 and S_2 are the surfaces bounded by regions#1 and#2 respectively. Converting the surface integrals into appropriate line integrals, we obtain

$$I\,\delta[k_0^2] = 2\Big[\oint_{C_1} P_1\,\delta\psi\left(\frac{\partial\psi_0}{\partial n}\right)_1 dl + \oint_{C_1} R_1\,\delta\phi\left(\frac{\partial\phi_0}{\partial n}\right) dl + \oint_{C_1} W_1\,\delta\psi\left(\frac{\partial\phi_0}{\partial c}\right)_1 dl$$

$$- \oint_{C_1} W_1\,\delta\phi\left(\frac{\partial\psi_0}{\partial c}\right)_1 dl + \oint_{C_2} P_2\,\delta\psi\left(\frac{\partial\psi_0}{\partial n}\right)_2 dl + \oint_{C_2} R_2\,\delta\phi\left(\frac{\partial\phi_0}{\partial n}\right)_2 dl$$

$$+ \oint_{C_2} W_2\left(\delta\psi\left(\frac{\partial\phi_0}{\partial c}\right)_2 - \delta\phi\left(\frac{\partial\psi_0}{\partial c}\right)_2\right)\Big] \qquad (2.81)$$

We assumed the convention that $\underline{n}\times\underline{c} = \underline{a}_z$, where $\underline{n}$ is a unit vector normal to the boundary of each region and directed away from the region; $\underline{c}$ is the corresponding unit tangent to the contour surrounding each region (shown in Fig.(2.3))

Now the contour C_1 consists of the perfectly conducting outer boundary C_1' on which $\delta\psi = 0$; $\frac{\partial\phi_0}{\partial n} = 0$; and

$\frac{\partial \psi_0}{\partial n} = 0$. The contour C_1'' which is virtually the same as the boundary contour C_2 of region 2 and the two sides of the branch cut. The contribution to the line integral over the boundary C_1' is zero due to the boundary conditions, and the contribution by the branch cut is also zero. The net value of $I\delta|k_0^2|$ is, therefore, determined by the following contour integral.

$$I\delta|k_0^2|/2 = \oint_{C_1''} P_1 \delta\psi \left(\frac{\partial \psi}{\partial n_1}\right)\cdot \underline{c}_1\, dl + \oint_{C_1''} R_1 \delta\phi \left(\frac{\partial \phi}{\partial n_1}\right)\cdot c_1\, dl + \oint_{C_1''} W_1 \Big(\delta\psi \frac{\partial \phi_0}{\partial c_1} - \delta\phi \frac{\partial \psi_0}{\partial c_1}\Big)\cdot \underline{c}_1\, dl + \oint_{C_2} \Big(P_2\, \delta\psi \frac{\partial \psi_0}{\partial n_2} + R_2 \delta\phi \frac{\partial \phi_0}{\partial n_2}\Big)\cdot \underline{c}_2\, dl + \oint_{C_2} W_2 \Big(\delta\psi \frac{\partial \phi_0}{\partial c_2} - \delta\phi \frac{\partial \psi_0}{\partial c_2}\Big)\cdot \underline{c}_2\, dl \qquad (2.82)$$

The contour C_1'' is virtually the same as the contour C_2 but the unit outward normal $\underline{n}_1$ and the unit tangent $\underline{c}_1$ on contour C_1'' are 180° opposite to the unit outward normal $\underline{n}_2$ and the unit tangent vector $\underline{c}_2$ on contour C_2. If we replace contour C_1'' by C_2 and properly rearrange the terms, we get

$$I\delta|k_0^2| = 2\Big[\oint_{C_2} \delta\psi \Big(P_2 \frac{\partial \psi_{02}}{\partial n} - P_1 \frac{\partial \psi_{01}}{\partial n} + W_2 \frac{\partial \phi_{02}}{\partial c} - W_1 \frac{\partial \phi_{01}}{\partial c}\Big) dl + \oint_{C_2} \delta\phi \Big(R_2 \frac{\partial \phi_{02}}{\partial n} - R_1 \frac{\partial \phi_{01}}{\partial n} + W_1 \frac{\partial \phi_{01}}{\partial c} - W_2 \frac{\partial \phi_{02}}{\partial c}\Big) dl\Big] \qquad (2.83)$$

where suffixes 01 and 02 indicate the values of ϕ and ψ at the interface C_2 when approached from regions 1 and 2 respectively.

In order to keep a first order variation in k_0^2 ie. $\delta|k_0^2|$ to zero for any arbitrary $\delta\psi$ and $\delta\phi$, the integrands associated with $\delta\psi$ and $\delta\phi$ in the above equation (2.83) must separately go to zero. i.e.

$$P_2 \frac{\partial \psi_{02}}{\partial n} - P_1 \frac{\partial \psi_{01}}{\partial n} + W_2 \frac{\partial \phi_{02}}{\partial c} - W_1 \frac{\partial \phi_{01}}{\partial c} = 0 \tag{2.84}$$

and

$$R_2 \frac{\partial \phi_{02}}{\partial n} - R_1 \frac{\partial \phi_{01}}{\partial n} + W_1 \frac{\partial \psi_{01}}{\partial c} - W_2 \frac{\partial \psi_{02}}{\partial c} = 0 \tag{2.85}$$

On substituting the values of P_1, P_2, R_1, R_2, W_1 and W_2 into equations (2.84) and after suitable rearrangement of terms, we obtain

$$\tau_2 \epsilon_{r2} \frac{\partial \psi_{02}}{\partial n} + \tau_2 \frac{\partial \phi_{02}}{\partial c} = \tau_1 \epsilon_{r1} \frac{\partial \psi_{01}}{\partial n} + \tau_1 \frac{\partial \phi_{01}}{\partial c} \tag{2.86}$$

Equation (2.86) is the continuity equation for the tangential component of the magnetic field at the interface. Similar substitution into equation (2.85) gives

$$\tau_2 \mu_{r2} \frac{\partial \phi_{02}}{\partial n} - \bar{\beta}^2 \tau_2 \frac{\partial \psi_{02}}{\partial c} = \tau_1 \mu_{r1} \frac{\partial \phi_{01}}{\partial n} - \bar{\beta}^2 \tau_1 \frac{\partial \psi_{01}}{\partial c} \tag{2.87}$$

which is the continuity relation for the tangential component of the electric field at the interface of two regions. Since

ϕ_0 and ψ_0 are the true fields, equations (2.84) and (2.85) are automatically satisfied. Therefore, we conclude that the expression (2.53) is stationary for all trial fields which satisfy the boundary conditions only at the conducting boundary walls.

2.4.2 Sectionally constant μ_r and ϵ_r.

There is an important class of practical waveguide system in which the permittivity of the dielectric fillings assume sectionally constant values. This type of waveguide loading is called inhomogeneously loaded waveguide. A scalar variational expression for inhomogeneous waveguides is given in reference (3). We will show in this subsection that the variational expression reported in reference (3) is a particular case of the more general expression derived in this chapter. To show this, let the relative permeabilities of regions 1 and 2 (Fig.2) be unity and the relative permittivity of region 1 be unity and that of region 2 be ϵ_r. The values of P, R and W corresponding to each of the regions are given below

Region 1: $P_1 = \bar{\beta}^2$; $R_1 = 1$; $W_1 = \bar{\beta}^2$.

Region 2: $P_2 = \bar{\beta}^2 \tau \epsilon_r$; $R_2 = \tau$; $W_2 = \tau \bar{\beta}^2$.

Substituting the values of P, R, and W as given above into equation (2.53), we obtain

$$k_0^2 = \Big[\int_{S_1} |\nabla_t \phi|^2 ds + \int_{S_2} \tau |\nabla_t \phi|^2 ds + \bar{\beta}^2 \int_{S_1} |\nabla_t \psi|^2 ds +$$

$$\bar{\beta}^2 \tau \epsilon_r \int_{S_2} |\nabla_t \psi|^2 ds + 2\bar{\beta} \int_{S_1} \underline{a}_z \cdot (\nabla_t \psi \times \nabla_t \phi)\, ds + 2\bar{\beta}^2 \tau \cdot$$

$$\int_{S_2} \underline{a}_z \cdot (\nabla_t \psi \times \nabla_t \phi)\, ds \Big] \Big/ \Big[\int_{S_1+S_2} \phi^2 ds + \bar{\beta}^2 \int_{S_1} \psi^2 ds + \bar{\beta}^2 \epsilon_r \int_{S_2} \psi^2 ds \Big] \tag{2.88}$$

The last two terms of the numerator of the right-hand side of equation (2.88) can be simplified as follows:

$$2\bar{\beta}^2 \int_{S_1} \underline{a}_z \cdot (\nabla_t \psi \times \nabla_t \phi)\, ds + 2\bar{\beta}^2 \tau \int_{S_2} \underline{a}_z \cdot (\nabla_t \psi \times \nabla_t \phi)\, ds$$

$$= 2\bar{\beta}^2 \oint_{C_1''} \psi \frac{\partial \phi}{\partial C_1} \cdot \underline{c}_z\, dl + 2\bar{\beta}^2 \tau \oint_{C_2} \psi \frac{\partial \phi}{\partial C_2} \cdot \underline{c}_z\, dl$$

$$= 2\bar{\beta}^2 (\tau - 1) \oint_{C_2} \psi \frac{\partial \phi}{\partial C_2}\, dl \tag{2.89}$$

Transforming the contour integral (2.89) back into surface integral and using the relation

$$2\bar{\beta}^2 (\tau - 1) = 2(\tau \epsilon_r - 1) \tag{2.90}$$

we obtain,

$$2\bar{\beta}^2 (\tau - 1) \oint_{C_2} \psi \frac{\partial \phi}{\partial C_2}\, dl$$

$$= 2(\tau \epsilon_r - 1) \int_{S_2} \underline{a}_z \cdot (\nabla_t \psi \times \nabla_t \phi)\, ds \tag{2.91}$$

Replacing the last two terms of the numerator of equation (2.88) by the result of equation (2.91) gives

$$k_0^2 = \Big[\int_{S_1} |\nabla_t \phi|^2 ds + \tau \int_{S_2} |\nabla_t \phi|^2 ds + \bar{\beta}^2 \int_{S_1} |\nabla_t \psi|^2 ds +$$

$$\bar{\beta}^2 \tau \epsilon_r \int_{S_2} |\nabla_t \psi|^2 ds + 2(\tau\epsilon_r - 1) \int_{S_2} \underline{a}_z \cdot (\nabla_t \psi \times \nabla_t \phi) ds \Big] \Big/$$

$$\Big[\int_{S_1+S_2} \phi^2 ds + \bar{\beta}^2 \int_{S_1} \psi^2 ds + \bar{\beta}^2 \epsilon_r \int_{S_2} \psi^2 ds \Big] \qquad (2.92)$$

Equation (2.92) is exactly of the same form as reported in reference (3). Finally for homogeneous waveguide ϕ and ψ modes can exist separately without being coupled with each other and the corresponding variational functionals become:

$$k_o^2 = \int_S |\nabla_t \phi|^2 ds \Big/ \int_S \phi^2 ds \qquad \text{for H mode} \qquad (2.93)$$

and

$$k_o^2 = \int_S |\nabla_t \psi|^2 ds \Big/ \int_S \psi^2 ds \qquad \text{for E mode} \qquad (2.94)$$

2.5 Operator Eigenvalue Problems.

2.5.1 Wave Equations Written in Matrix Form

The simultaneous partial differential equations (2.49) and (2.50) can be written in matrix notation as follows:

$$L\Theta + k_o^2 M\Theta = 0 \qquad (2.95)$$

where L, M and Θ are given by

$$L = \begin{bmatrix} P\nabla_t^2 + \nabla_t P \cdot \nabla_t & \underline{a}_z \nabla_t W \times \nabla_t \\ -\underline{a}_z \nabla_t W \times \nabla_t & R\nabla_t^2 + \nabla_t R \cdot \nabla_t \end{bmatrix} \qquad (2.96)$$

$$M = \begin{bmatrix} \frac{\partial^2}{\partial t^2} & 0 \\ 0 & \frac{d^2}{dt^2} \end{bmatrix} \tag{2.97}$$

and

$$\theta = \begin{bmatrix} w \\ \phi \end{bmatrix} \tag{2.98}$$

It is assumed that solutions of equations (2.95) will give rise to discrete eigenvalues and their eigen-functions. This is true for all bounded problems, because, the general property of bounded problems is such that they cannot have continuous spectrum of eigenvalues. It is well known that in the domain of complex functions, if all the eigenvalues of an operator are real then the operator must be Hermitian in character or in the field of real functions the operator must be self adjoint to give real eigenvalues. An operator is called self-adjoint, if the adjoint operator together with the adjoint boundary conditions coincide with the original operator and the associated boundary conditions.

2.5.2 Properties of the Matrix Operators

In this subsection we will show that the operators M and L as given in equation (2.96) and (2.97) are self-adjoint operators. That the Operator M is self-adjoint is obvious. For operator L to be self-adjoint, it is necessary that the following relation hold (4)

$$\int_s \theta_b^T L \theta_a \, ds = \int_s \theta_a^T L \theta_b \, ds \tag{2.99}$$

where θ_b^T is the transposed of the column vector θ_b whose elements are ψ_b and ϕ_b. The functions ψ_b and ϕ_b are arbitrary except that they are defined over the same domain in which ψ_a and ϕ_a are defined and that they satisfy the boundary conditions adjoint to the boundary conditions satisfied by ψ_a and ϕ_a. If the integrands of equation (2.99) are expanded in terms of differential operators, we obtain

$$\theta_b^T L \theta_a - \theta_a^T L \theta_b = \psi_b P \nabla_t^2 \psi_a + \psi_b \nabla_t P \cdot \nabla_t \psi_a + \psi_b \underline{a}_z \cdot \nabla_t W \times \nabla_t \phi_a +$$

$$\phi_b R \nabla_t^2 \phi_a + \phi_b \nabla_t R \cdot \nabla_t \phi_a - \phi_b \underline{a}_z \cdot \nabla_t W \times \nabla_t \psi_a - (\psi_a \nabla_t^2 \psi_b + \psi_a \nabla_t P \cdot \nabla_t \psi_b$$

$$+ \psi_a \underline{a}_z \cdot \nabla_t W \times \nabla_t \phi_b + \phi_a R \nabla_t^2 \phi_b + \phi_a \nabla_t R \cdot \nabla_t \phi_b - \phi_a \underline{a}_z \cdot \nabla_t W \times \nabla_t \psi_b) \quad (2.100)$$

Equation (2.100) can be simplified into the following form:

$$\theta_b^T L \theta_a - \theta_a^T L \theta_b = \nabla_t \cdot (P \underline{N}) + \nabla_t \cdot (R \underline{Q}) + \underline{a}_z \cdot \nabla_t \times W [\nabla_t (\psi_b \phi_a - \phi_b \psi_a)] \quad (2.101)$$

where

$$\left.\begin{aligned} \underline{N} &= \psi_b \nabla_t \psi_a - \psi_a \nabla_t \psi_b \\ \underline{Q} &= \phi_b \nabla_t \phi_a - \phi_a \nabla_t \phi_b \end{aligned}\right\} \quad (2.102)$$

The derivation of equation (2.101) from equation (2.100) is given in Appendix A2.4. By proper use of Stokes' and Gauss's Theorems, equation (2.99) can be written as

$$I = \int_S (\theta_b^T L \theta_a - \theta_a^T L \theta_b)\, dS = \oint_C P N_n \, dl + \oint_C R Q_n \, dl + \oint_C W \frac{\partial}{\partial l} (\psi_b \phi_a - \psi_a \phi_b)\, dl \quad (2.103)$$

where N_n and Q_n are the normal components of the vectors $\underline{N}$ and $\underline{Q}$ over the contour C surrounding the surface S. These are given by

$$N_n = \psi_b \frac{\partial \psi_a}{\partial n} - \psi_a \frac{\partial \psi_b}{\partial n}$$

$$Q_n = \phi_b \frac{\partial \phi_a}{\partial n} - \phi_a \frac{\partial \phi_b}{\partial n} \tag{2.104}$$

The functions ψ_a and ϕ_a are proportional to the longitudinal components of the electric and the magnetic fields inside the waveguide. Since the waveguide is assumed to be bounded by perfect conductors, these field components satisfy the following relations:

$$\left.\begin{aligned} \psi_a &= 0; \qquad \frac{\partial \psi_a}{\partial \ell} = 0; \\ \frac{\partial \phi_a}{\partial n} &= 0 \end{aligned}\right\} \tag{2.105}$$

on the guide walls. Substitution of the above boundary conditions in equation (2.103) gives:

$$I = \oint_c \psi_b \frac{\partial \psi_a}{\partial n}\, dl - \oint_c \phi_a \frac{\partial \phi_b}{\partial n} + \oint_c W \frac{\partial}{\partial \ell}(\psi_b \phi_a)\, dl \tag{2.106}$$

The right-hand side of equation (2.106) will be zero when the adjoint functions ψ_b and ϕ_b satisfy the following boundary conditions:

$$\left.\begin{aligned} \psi_b &= 0; \qquad \frac{\partial \psi_b}{\partial \ell} = 0; \\ \text{and} \qquad \frac{\partial \phi_b}{\partial n} &= 0 . \end{aligned}\right\} \tag{2.107}$$

on the waveguide walls. But these adjoint boundary conditions are similar to the boundary conditions satisfied by the original fields ψ_a and ϕ_a. Therefore, the operator $\underline{L}$ is a self-adjoint operator.

Appendix A2

A2.1. Green's Theorem:

Green's Theorem (the divergence theorem) is defined as follows: Let 'v' be a closed region bounded by a surface 's' and let $\underline{A}$ be a vector field which is continuous and has continuous first derivative in v. Then

$$\int_v \nabla \cdot \underline{A}\, dv = \int_s \underline{A} \cdot \underline{n}\, ds \qquad (A2.1)$$

where $\underline{n}$ is the unit outward normal vector to s.

For a vector field $\underline{A}$ in a plane, the two dimensional form of this theorem is given by (1).

$$\int_s \nabla_t \cdot A\, ds = \oint_c \underline{A} \cdot \underline{n}\, dl \qquad (A2.2)$$

where the contour c encloses the surface's.

Now any vector field can be written as the gradient of a scalar field, thus

$$\underline{A} = \nabla_t \phi \qquad (A2.3)$$

where ϕ is a scalar field defined over the surface s. Green's theorem for a scalar field is, therefore,

$$\int_s \nabla_t^2 \phi\, ds = \oint_c \frac{\partial \phi}{\partial n}\, dl \qquad (A2.4)$$

where $\frac{\partial}{\partial n}$ is the outward normal derivative of ϕ on c.

If ϕ and ψ are any two scalar functions, then the symmetric form of Green's Theorem or Green's Identity is obtained by setting

$$\left.\begin{aligned} \underline{A} &= \psi \nabla_t \phi \\ \text{and } \underline{B} &= \phi \nabla_t \psi \end{aligned}\right\} \qquad \text{(A2.5)}$$

Since

$$\nabla_t \cdot (\psi \nabla_t \phi) = \psi \nabla_t^2 \phi + \nabla_t \psi \cdot \nabla_t \phi \qquad \text{(A2.6)}$$

So

$$\int_s (\phi \nabla_t^2 \psi + \nabla_t \psi \cdot \nabla_t \phi)\, ds = \oint_c \phi \frac{\partial \psi}{\partial n}\, dl \qquad \text{(A2.7)}$$

and

$$\int_s (\psi \nabla_t^2 \phi + \nabla_t \phi \cdot \nabla_t \psi)\, ds = \oint_c \psi \frac{\partial \phi}{\partial n}\, dl \qquad \text{(A2.8)}$$

Subtracting equation (A1.7) from equation (A1.8), we obtain

$$\int_s (\psi \nabla_t^2 \phi - \phi \nabla_t^2 \psi)\, ds = \oint_c \left(\psi \frac{\partial \phi}{\partial n} - \phi \frac{\partial \psi}{\partial n}\right) dl \qquad \text{(A2.9)}$$

A2.2 Stokes' Theorem:

Let s be a closed region on a surface, the boundary of s being a closed curve c. We choose a positive side for s and let $\underline{n}$ be the unit vector normal to s on the positive side. The positive direction on c is defined to be that on which an observer would travel to have the interior of s on his left. Let $\underline{c}$ be the unit tangent to the boundary c

in the positive direction and let $\underline{A}$ be a vector field with continuous first derivative in the closed regions. Then Stokes' Theorem states that

$$\int_S \underline{n} \cdot (\nabla \times \underline{A})\, ds = \oint_C \underline{A} \cdot \underline{c}\, dl \qquad (A2.10)$$

Two scalar field form of this theorem is much used in this thesis. For scalar fields ϕ and ψ write

$$\underline{A} = \nabla(\phi\psi) \qquad (A2.11)$$

Then

$$\int_S n.\nabla \times \nabla(\phi\psi)\, ds = \oint_C \nabla(\phi\psi).\underline{c}\, dl = 0 \qquad (A2.12a)$$

i.e.

$$\oint_C \left(\phi \frac{\partial\psi}{\partial c} + \psi\frac{\partial\phi}{\partial c}\right) dl = 0 \qquad (A2.12b)$$

where $\frac{\partial}{\partial c}$ is the tangential derivative on c.

Alternately, set

$$\underline{A} = \psi\nabla\phi \qquad (A2.13)$$

Then

$$\int_S n.\ \nabla \times (\psi\nabla\phi)\, ds = \oint_C \psi \frac{\partial\phi}{\partial c}.\underline{c}\, dl \qquad (A2.14)$$

but $\nabla \times (\psi\nabla\phi) = \psi(\nabla \times \nabla\phi) + \nabla\psi \times \nabla\phi$. (A2.15)

Therefore,

$$\oint_C \psi \frac{\partial\phi}{\partial c} \cdot \underline{c}\, dl = \int_S (\nabla\psi \times \nabla\phi).n\, ds \qquad (A2.16)$$

Since $\nabla \times \nabla\phi \equiv 0$. (A2.17)

Similarly,

$$\oint_c \phi \frac{\partial \psi}{\partial c} . \underline{c} \, dl = \int_s (\nabla \phi \times \nabla \psi) . n ds$$

Hence

$$\oint_c \left(\phi \frac{\partial \psi}{\partial c} - \psi \frac{\partial \phi}{\partial c} \right) . \underline{c} \, dl = 2 \int_s \underline{n} . (\nabla \phi \times \nabla \psi) ds \tag{A2.18}$$

A2.3 Derivation of Equation (2.53).

(a) $\nabla_t . (P \psi \nabla_t \psi) \equiv \psi P \nabla_t^2 \psi + \psi \nabla_t P . \nabla_t \psi + P |\nabla_t \psi|^2$

(b) $\nabla_t . (R\phi \nabla_t \phi) \equiv \phi R \nabla_t^2 \phi + \phi \nabla_t \phi . \nabla_t R + R |\nabla_t \phi|^2$

(c) $\nabla_t \times (W \psi \nabla_t \phi) \equiv \psi \nabla_t W \times \nabla_t \phi + W \nabla_t \psi \times \nabla_t \phi + W \psi \nabla_t \times \nabla_t \phi$

(d) $\nabla_t \times (W\phi \nabla_t \psi) \equiv \phi \nabla_t W \times \nabla_t \psi + W \nabla_t \phi \times \nabla_t \psi + W\phi \nabla_t \times \nabla_t \psi$

(e) $\nabla_t \times \nabla_t \phi \equiv 0$

(f) $\nabla_t \times \nabla_t \psi \equiv 0$

Using the results of the identities (a) (b) (c) and (d) in equation (2.52) we get

$$|k_o^2| = - \left[\int_s \nabla_t . (P \psi \nabla_t \psi) ds - \int_s P |\nabla_t \psi|^2 ds + \int_s \nabla_t . (R\phi \nabla_t \phi) ds \right.$$

$$- \int_S R\,|\nabla_t \phi|^2\, ds + \int_S \nabla_t \times (W\psi\, \nabla_t \phi - W\phi\, \nabla_t \psi)\cdot \underline{a}_z\, ds$$

$$2\int_S a_z \cdot W\,(\nabla_t \phi \times \nabla_t \psi)\, ds\Big] \Big/ \int\Big[\Big(\frac{P}{t}\psi^2 + \frac{R}{t}\phi^2\Big) ds\Big] \qquad \text{(A2.19)}$$

From Green's and Stokes' Theorems, we obtain

$$\int_S \nabla_t \cdot (P\psi \nabla_t \psi)\, ds = \oint_c P\psi \frac{\partial \psi}{\partial n}\, dl \qquad \text{(A2.20)}$$

$$\int_S \nabla_t \cdot (R\phi\, \nabla_t \phi)\, ds = \oint_c R\phi\, \frac{\partial \phi}{\partial n}\, dl \qquad \text{(A2.21)}$$

$$\int_S \underline{a}_z \cdot \nabla_t \times (W\phi\, \nabla_t \psi - W\psi\, \nabla_t \phi)\, ds = \oint \Big(W\phi \frac{\partial \psi}{\partial c} - W\psi \frac{\partial \phi}{\partial c}\Big)\, dl \qquad \text{(A2.22)}$$

Boundary conditions are

$$\left.\begin{aligned} &\psi = 0, \qquad \frac{\partial \psi}{\partial c} = 0 \\ &\text{and} \qquad \frac{\partial \phi}{\partial n} = 0. \end{aligned}\right\} \qquad \text{(A2.23)}$$

on the contour c at the waveguide wall. These boundary conditions when inserted into equations (A2.20), (A2.21) and (A2.22), all reduce to zero. Substituting the results of equations (A2.20) to (A2.22) into equation (A2.19) and after further simplification, we get

$$|k_o^2| = \Big[\int_S P\,|\nabla_t \psi|^2 ds + \int_S R\,|\nabla_t \phi|^2 ds + 2\int_S a_z \cdot W(\nabla_t \psi \times \nabla_t \phi)\cdot ds\Big] \Big/ \Big[\int_S \frac{P}{t}\psi^2\, ds + \int_S \frac{R}{t}\phi^2\, ds\Big] \qquad \text{(A2.24)}$$

A2.4 Derivation of Equation (2.101)

$$\Psi_b \, P \nabla_t^2 \Psi_a + \Psi_b \, \nabla_t P \cdot \nabla_t \Psi_a \equiv \nabla_t \cdot (P \Psi_b \nabla_t \Psi_a) - P \nabla_t \Psi_b \cdot \nabla_t \Psi_a \tag{A2.25}$$

$$\Psi_a \, P \nabla_t^2 \Psi_b + \Psi_a \, \nabla_t P \cdot \nabla_t \Psi_b = \nabla_t (P \Psi_a \nabla_t \Psi_b) - P \nabla_t \Psi_b \cdot \nabla_t \Psi_a \tag{A2.26}$$

On subtracting equation (A2.26) from equation (A2.25), we get

$$\Psi_b P \nabla_t^2 \Psi_a + \Psi_b \nabla_t P \cdot \nabla_t \Psi_a - \Psi_a P \nabla_t^2 \Psi_b - \Psi_a \nabla_t P \cdot \nabla_t \Psi_b$$

$$= \nabla_t \cdot (P \Psi_b \nabla_t \Psi_a - P \Psi_a \nabla_t \Psi_b)$$

$$= \nabla_t \cdot (P \, \underline{N}) \tag{A2.27}$$

Similarly,

$$\phi_b R \nabla_t^2 \phi_a + \phi_b \nabla_t R \cdot \nabla_t \phi_a - \phi_a R \nabla_t^2 \phi_b - \phi_a \nabla_t R \cdot \nabla_t \phi_b$$

$$= \nabla_t \cdot (R \, \underline{S}) \tag{A2.28}$$

and

$$\phi_b \, \underline{a}_z \cdot \nabla_t W \times \nabla_t \Psi_a + \Psi_a \nabla_t W \times \nabla_t \phi_b \cdot \underline{a}_z$$

$$\equiv \left[\nabla_t \times \left\{ W \nabla_t (\Psi_a \phi_b) \right\} - W \nabla_t \times \nabla_t (\phi_b \Psi_a) \right] \cdot \underline{a}_z$$

$$\equiv \underline{a}_z \cdot \nabla_t \times \left\{ W \nabla_t (\Psi_a \phi_b) \right\} \tag{A2.29}$$

Also

$$\psi_b \nabla_t W \times \nabla_t \phi_a + \phi_a \nabla_t W \times \nabla_t \psi_b$$

$$\equiv \nabla_t \times \left\{ W \nabla_t (\psi_b \phi_a) \right\} \qquad \text{(A2.30)}$$

Substitution of the results of equations (A2.27), (A2.28), (A2.29) and (A2.30) into equation (2.100) results in equation (2.101).

Chapter 2 - References

1. Collin, R.E.: "Field Theory of Guided Waves", McGraw-Hill Book Company, New York, 1960.

2. Morse, P. and Feschbach, H.: "Methods of Theoretical Physics", McGraw-Hill, 1953, Chapter 6.

3. Hannaford, C.D.: "Finite-difference/Variational Method for Inhomogeneous Isotropic or Anisotropic Wave-guides", Ph.D. Thesis, Leeds University, February, 1967.

4. Lanczos, C.: "Linear Differential Operators", D.Van Nostrand Co. Ltd., Chapter 4.

Chapter 3

THE FINITE-ELEMENT FORMULATION FOR WAVEGUIDE PROBLEMS

3.1 Formulation of a Problem Suitable for the Finite-element Method

The basic requirement of the development of finite-element equations for approximating continuous operator eigen value equations is to find an extremum functional which can be written in Euler density form. Electromagnetic waves propagating through waveguides is not the only field where the finite-element method can be applied, on the other hand, for many physical problems in the field of applied science it is always possible to derive a variational expression, and, therefore, this method may be usefully applied to those fields also.

As a first step in the development of the finite-element method, we consider a waveguide which is completely filled with a homogeneous, lossless, isotropic dielectric. Also assume that the waveguide is infinitely long and uniform along the axis of propagation. The shape of the transverse cross-section may be arbitrary. By assuming a time variation exp (jwt) where w is the angular frequency and z-dependence exp $(-j\beta z)$, the following wave equation is obtained from Maxwell's equation.[1]

$$\nabla_t^2 \phi + k_o^2 \phi = 0 \tag{3.1}$$

where ∇_t^2 is the transverse Laplacian, ϕ is either the longitudinal component of electric field $\underline{E}$ or the longitudinal component of magnetic field $\underline{H}$ and $k_o^2 = \omega^2 \mu\epsilon - \beta^2$ is the wavenumber for the waveguide. The field quantities E_z and H_z as represented by ϕ must satisfy the following boundary conditions.

a) $\phi = 0$ on the boundary walls (Dirichelet type boundary) (3.2)

b) $\frac{\partial \phi}{\partial n} = 0$ on the boundary walls (Neumann type boundary) (3.3)

where $\frac{\partial}{\partial n}$ is the normal derivative of ϕ at the boundary walls of the waveguide.

A-39550

One form of scalar variational expression for the electromagnetic wave propagating through a homogeneous waveguide can be obtained by premultiplying equations (3.1) by ϕ and integrating over the waveguide cross-section, and is given by (2).

$$\int_S \phi \nabla_t^2 \phi \, ds + k_o^2 \int_S \phi^2 \, ds = F(\phi) \tag{3.4}$$

The expression in equation (2.4) is a variational expression for k_o^2 for all trial functions which satisfy the same boundary conditions as satisfied by the true eigenfunction. The variational expression given above can be

rewritten in Euler density form which is suitable for the development of the finite-element formulation and is given by

$$2J(\phi) = \int_s |\nabla_t \phi|^2 \, ds - k_o^2 \int_s \phi^2 \, ds \tag{3.5}$$

where

$$|\nabla_t \phi|^2 = \left|\frac{\partial \phi}{\partial x}\right|^2 + \left|\frac{\partial \phi}{\partial y}\right|^2 \tag{3.6}$$

The variational principle states that

$$\delta J(\phi) = 0 \quad \text{for} \quad \delta k_o^2 = 0.$$

since $\delta k_o^2 = 0$ at a solution to the wave equations, the field which satisfied the equation (3.5) will, therefore, constitute the eigenfunction of the problem.

3.2 Development of the Finite-element Equations for Triangular Elements.

Instead of approximating the true ϕ by a set of normal mode functions -- in many cases we have incomplete knowledge of these functions -- the finite-element method employs a set of algebraic functions defined over a sub-section of the whole waveguide cross-section. These sub-sections may be polygonal in shape and are called elements. Thus, in the finite-element method, the entire domain over which the operator eigenvalue equation is defined, is divided into a finite number of elements on each of which the actual mode function is approximated by a set of continuous algebraic functions which are only defined over the

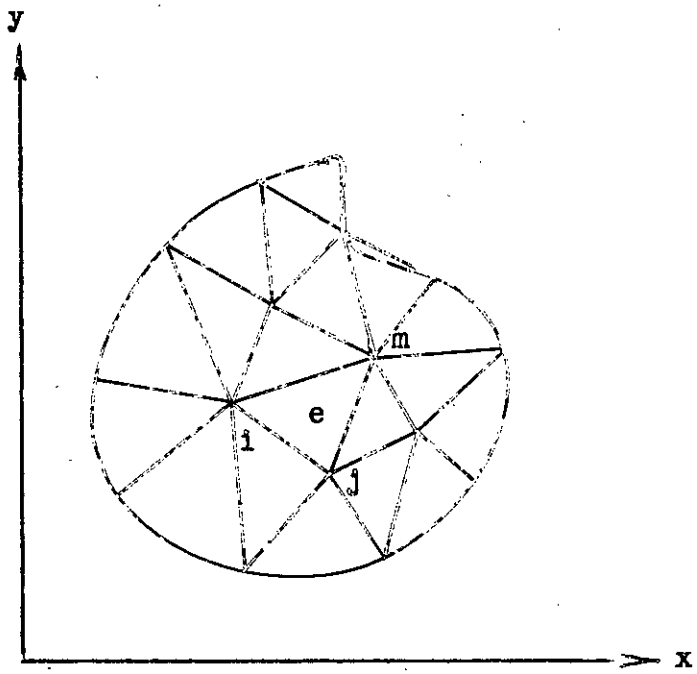

Figure (3.1)
Divisions of an Arbitrary Waveguide
cross-section into Triangular Elements

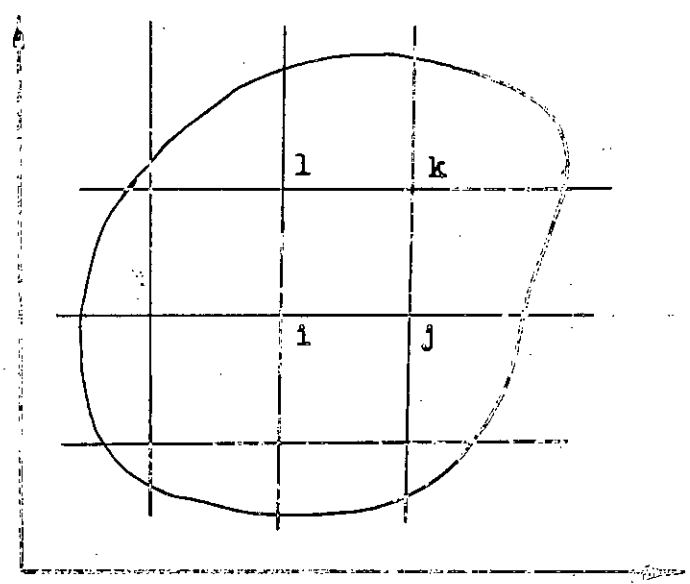

Figure (3.2)
Divisions of an Arbitrary Waveguide
cross-section into square elements.

particular element under consideration, and are linearly dependent on the values of ϕ at the vertices of the element. Hence, if an element has n vertices (for a triangular element n = 3) the potential ϕ within it may be approximated by

$$\phi\ (x,y) = \sum_{k=1}^{n} f_k(x,y)\ \phi_k \tag{3.7}$$

where $f_k(x,y)$ is a predetermined algebraic function which is uniquely defined and differentiable over the element and which reduces to zero outside the element and ϕ_k is the value of ϕ at the vertex k.

Consider an arbitrary shaped waveguide cross-section with the scheme of grading into elements as shown in Figure (3.1). In Fig.(3.1) the transverse cross-sectional area is divided into a set of P triangular subregions or elements. A typical element (the e th) is described by the vertices i, j, and m in cyclic order. Let ϕ_i, ϕ_j, ϕ_m be the values of ϕ at these vertices. Over the element 'e' the functional dependence of $\phi(x,y)$ can be written as

$$\phi^e(x\,y) = \alpha_0 + \alpha_1 x + \alpha_2 y \tag{3.8}$$

where α_0, α_1 and α_2 are to be determined.

If (x_i,y_i), (x_j,y_j) and (x_m,y_m) are the co-ordinates of the vertices i, j, and m, then the coefficients α_0, α_1, and α_2 can be determined from the following set of equations.

$$\phi_i = \alpha_o + \alpha_1 x_i + \alpha_2 y_i$$

$$\phi_j = \alpha_o + \alpha_1 x_j + \alpha_2 y_j \qquad (3.9)$$

$$\phi_m = \alpha_o + \alpha_1 x_m + \alpha_2 y_m$$

Now solving for α_o, α_1 and α_2 in terms of ϕ_i, ϕ_j and ϕ_m and substituting their values in equation (3.8), we obtain

$$\phi^e(x,y) = \frac{1}{2\Delta_e}\Big[(a_i + b_i x + c_i y)\,\phi_i^e + (a_j + b_j x + c_j y)\,\phi_j^e + (a_m + b_m x + c_m y)\,\phi_m^e\Big] \qquad (3.10)$$

where,

$$a_i = x_j y_m - y_j x_m$$

$$b_i = y_j - y_m \qquad (3.11)$$

$$c_i = x_m - x_j$$

and Δ_e is the area of the triangular element, which is given by

$$2\Delta_e = \mathrm{Det}\begin{bmatrix} 1 & x_i & y_i \\ 1 & x_j & y_j \\ 1 & x_m & y_m \end{bmatrix} \qquad (3.12)$$

The values of other parameters can be obtained by considering a cyclic rotation of the suffixes i, j, and m.

Equation (3.10) can be written in compact form by using matrix notation as:

$$\phi^e(x,y) = [N^e]\,[\phi^e] \tag{3.13}$$

where $[N]$ is a (1×3) row matrix and $[\phi]$ is a (3×1) column matrix. They are given by

$$N^e = \frac{1}{2\Delta_e}\left[a_i + b_i x + c_i y \quad a_j + b_j x + c_j y \quad a_m + b_m x + c_m y\right] \tag{3.14}$$

and

$$\phi^e = \left\{\phi_i^e \quad \phi_j^e \quad \phi_m^e\right\} \tag{3.15}$$

The suffix e indicates that the element 'e' is under consideration.

It is important to note that the functional form of the potential $\phi^e(x,y)$ as described in equation (3.10) for all elements of the entire domain satisfied the continuity relation of ϕ throughout the whole region. The values of ϕ along the line joining two adjacent elements do not depend on the values of ϕ at the three vertices describing the elements but only on the values of ϕ at the vertices which are common to two adjacent elements.

This continuity relation of ϕ is essential for the validity of the variational expression. The derivative normal

to the line joining two elements is not, however, continuous for the above type of functional relation, but still finite in magnitude. The finite jump in the normal derivative will not introduce any error in the variational formulation, because the contribution of this type of discontinuity in the normal derivative to the net integrated functional is always zero.

When the form of ϕ as given above is substituted into the right hand side of equation (3.5) and the corresponding integrations are carried out, the extremum functional $J(\phi)$ will be a function of the variables ϕ_k. If there are in all M vertices then

$$J(\phi) = F(\phi_1 \quad \phi_2 \ldots\ldots \phi_M) \tag{3.16}$$

The optimum value of a set of ϕ_k for a certain functional form of $f_k(x,y)$ may be obtained by minimising the functional given in equation (3.16) with respect to each of ϕ_k i.e. equating

$$\frac{\partial J}{\partial \phi_k} = 0 \quad \text{for } k = 1, 2 \ldots\ldots M \tag{3.17}$$

In view of the form of $\phi^e(x,y)$ as given in equation (3.7), equation (3.5) can be written as

$$2J(\phi) = 2\sum_{e=1}^{P} J^e(\phi_i, \phi_j, \phi_m)$$

$$= 2\sum_{e=1}^{P} \left[\int_{\Delta e} |\nabla_t \phi|^2 \, dxdy - k_o^2 \int_{\Delta e} \phi^2 \, dxdy \right] \quad (3.18)$$

In the formulation of the problem as shown above, the extremisation of J over the entire cross-section is equivalent to the extremisation of J over each of the elements individually. Each element contains only three values of ϕ_i and each ϕ_i is common to those elements for which the vertex i is common. If we minimise the functional $J(\phi)$ with respect to each ϕ_i, we obtain the following relation:

$$2\frac{\partial J}{\partial \phi_i} = 2\sum_{e=1}^{P} \frac{\partial J^e}{\partial \phi_i} \quad (3.19)$$

Using the relation for J^e as given in equation (3.18), the above equation can be rewritten as

$$\frac{\partial J^e}{\partial \phi_i} = \int_{\Delta e} \left\{ \frac{\partial \phi}{\partial x} \frac{\partial}{\partial \phi_i}\left(\frac{\partial \phi}{\partial x}\right) + \frac{\partial \phi}{\partial y} \frac{\partial}{\partial \phi_i}\left(\frac{\partial \phi}{\partial y}\right) \right\} dxdy$$

$$- k_o^2 \int_{\Delta e} \phi \frac{\partial \phi}{\partial \phi_i} \, dxdy \quad (3.20)$$

On substituting the values of $\phi(x,y)$ in terms of matrix parameters $[N^e]$ and $[\phi^e]$ in equation (3.20), we get

$$\frac{\partial J^e}{\partial \phi_i} = \int_{\Delta_e} \left[\frac{\partial N^e}{\partial x}\right] \cdot \left[\phi^e\right] \frac{\partial}{\partial \phi_i}\left(\left[\frac{\partial N^e}{\partial x}\right]\left[\phi^e\right]\right) dxdy +$$

$$\int_{\Delta_e} \left[\frac{\partial N^e}{\partial y}\right]\left[\phi^e\right] \frac{\partial}{\partial \phi_i}\left(\left[\frac{\partial N^e}{\partial y}\right]\left[\phi^e\right]\right) dxdy$$

$$- k_o^2 \int_{\Delta_e} \left[N^e\right] \cdot \left[\phi^e\right] \cdot \frac{\partial}{\partial \phi_i}\left(\left[N\right] \cdot \left[\phi^e\right]\right) dxdy \qquad (3.21)$$

After further simplification equation (3.21) reduces to

$$\frac{\partial J^e}{\partial \phi_i} = \int_{\Delta_e} \left\{\left[\frac{\partial N^e}{\partial x}\right]\left[\phi^e\right] \cdot \frac{\partial N_i^e}{\partial x} + \left[\frac{\partial N^e}{\partial y}\right]\left[\phi^e\right] \frac{\partial N_i^e}{\partial y}\right\} dxdy$$

$$- k_o^2 \int_{\Delta_e} \left[N^e\right]\left[\phi^e\right] N_i \quad dxdx \qquad (3.22)$$

where N_i is the i th component of the row matrix $\left[N\right]$ and is given by

$$N_i = (a_i + b_i x + c_i y)/2\Delta_e$$

Therefore, on minimisation of J with respect to ϕ_i (considering the contribution by all the elements), we get

$$\frac{\partial J}{\partial \phi_i} = \sum_{e=1}^{P} \int_{\Delta_e} \left(\left[\frac{\partial N^e}{\partial x}\right]\left[\phi^e\right] \frac{\partial N_i}{\partial x} + \left[\frac{\partial N^e}{\partial y}\right]\left[\phi^e\right] \frac{\partial N_i}{\partial y}\right) dxdy$$

$$- k_o^2 \int_{\Delta_e} \left[N^e\right]\left[\phi^e\right] N_i \quad dxdy \qquad (3.23)$$

Considering the fact that the vertex 'i' is common, only to the R elements associated with it, we can rewrite equation (3.23) as follows:

$$\frac{\partial J}{\partial \phi_i} = \sum_{e=1}^{R} \left\{ \int_{\Delta_e} \left(\left[\frac{\partial N^e}{\partial x}\right] \left[\phi^e\right] \frac{\partial N_i}{\partial x} + \left[\frac{\partial N^e}{\partial y}\right] \left[\phi^e\right] \frac{\partial N_i}{\partial y} \right) dxdy \right.$$

$$\left. - k_o^2 \int_{\Delta_e} \left(\left[N^e\right] \left[\phi^e\right] N_i \right) dxdy \right\} \qquad (3.24)$$

If we consider the minimisation of the functional J with respect to every ϕ_i, we obtain a set of linear algebraic eigenvalue equations which in matrix notation can be written as follows:

$$\underline{A}\ \Phi = k_o^2\ \underline{B}\ \Phi \qquad (3.25)$$

In equation (3.25) **A** and **B** are square matrices of order M and $\underline{\Phi}$ is a (M x 1) column matrix whose components are the values of ϕ_k at the M vertices. Thus we see that the solution of the above matrix eigenvalue problem will give an approximate solution to all waveguide problems for which equation (3.5) is the appropriate variational functional.

3.3 Evaluation of the Components of the Matrices A and B.

Consider the partial contribution to the different components of the matrix **A** subscribed by a typical element 'e'. This can be obtained from equation (3.24) as follows

$$\left.\frac{\partial J^e}{\partial \phi_i}\right|_{\underline{A}} = \int_{\Delta e}\left\{\left[\frac{\partial N^e}{\partial x}\right]\left[\phi^e\right]\frac{\partial N_i^e}{\partial x} + \left[\frac{\partial N^e}{\partial y}\right]\left[\phi^e\right]\frac{\partial N_i^e}{\partial y}\right\} dxdy \qquad (3.26)$$

where $\left.\frac{\partial J^e}{\partial \phi_i}\right|_{A}$ indicates that part of $\frac{\partial J^e}{\partial \phi_i}$ which contributes to the generation of matrix **A**.

Substituting the values of the components of the row matrix $[N]$ and the column matrix $[\phi^e]$ in equation (3.26), and after further simplification, we obtain

$$\left.\frac{\partial J^e}{\partial \phi_i}\right|_{\underline{A}} = \left\{ s_{ii}^e \quad s_{ij}^e \quad s_{im}^e \right\} \begin{bmatrix} \phi_i^e \\ \phi_j^e \\ \phi_m^e \end{bmatrix} \qquad (3.27)$$

where s_{ij}^e indicates the partial contribution to the (i,j)th component of the matrix **A** by the element 'e'.

Now $$S_{ij} = \int_{\Delta_e} \left\{ \frac{\partial N_i^e}{\partial x} \cdot \frac{\partial N_j^e}{\partial x} + \frac{\partial N_i^e}{\partial y} \cdot \frac{\partial N_j^e}{\partial y} \right\} dxdy \tag{3.28}$$

$$\begin{aligned} \text{but,} \quad N_i^e &= (a_i + b_i x + c_i y)/2\Delta_e \\ \text{and} \quad N_j^e &= (a_j + b_j x + c_j y)/2\Delta_e \end{aligned} \tag{3.29}$$

Therefore,

$$\begin{aligned} \frac{\partial N_i^e}{\partial x} &= b_i/2\Delta_e, \quad \frac{\partial N_j^e}{\partial x} = b_j/2\Delta_e \\ \frac{\partial N_i^e}{\partial y} &= c_i/2\Delta_e \quad \frac{\partial N_j^e}{\partial y} = c_j/2\Delta_e \end{aligned} \tag{3.30}$$

Substituting the values of $\frac{\partial N_i^e}{\partial x}$, $\frac{\partial N_j^e}{\partial x}$, $\frac{\partial N_i^e}{\partial y}$, and $\frac{\partial N_j^e}{\partial y}$ in equation (3.28) we obtain

$$S_{ij} = \frac{1}{4\Delta_e} (b_i b_j + c_i c_j) \tag{3.31}$$

Similarly, S_{ii} and S_{im} can be obtained by changing the suffixes appropriately.

In the same way, if J is minimised with respect to ϕ_j^e and ϕ_m^e, we obtain

$$\begin{bmatrix} \frac{\partial J^e}{\partial \phi_i} \\ \frac{\partial J^e}{\partial \phi_j} \\ \frac{\partial J^e}{\partial \phi_m} \end{bmatrix}_{\underline{A}} = \begin{bmatrix} S_{ii}^e & S_{ij}^e & S_{im}^e \\ S_{ji}^e & S_{jj}^e & S_{jm}^e \\ S_{mi}^e & S_{mj}^e & S_{mm}^e \end{bmatrix} \begin{bmatrix} \phi_i^e \\ \phi_j^e \\ \phi_m^e \end{bmatrix} \tag{3.32}$$

or

$$\left.\frac{\partial J^e}{\partial \phi_i^e}\right|_A = \underline{S}^e \cdot \underline{\phi}^e \tag{3.32a}$$

where $\left.\frac{\partial J^e}{\phi_i^e}\right|_A$ is a column matrix given by the left hand side of equation (3.31)

If the elements are all right triangles with vertex 'i' on the corner of the right angle then element submatrix $\underline{S}^e$ would become

$$S^e = \begin{bmatrix} 1 & -\frac{1}{2} & -\frac{1}{2} \\ -\frac{1}{2} & \frac{1}{2} & 0 \\ -\frac{1}{2} & 0 & \frac{1}{2} \end{bmatrix} \tag{3.33}$$

Similarly we can derive an expression for the partial contribution to the components of the matrix $\underline{B}$ subscribed by the element 'e'. This will be

$$\begin{bmatrix} \frac{\partial J^e}{\partial \phi_i^e} \\ \frac{\partial J^e}{\partial \phi_j^e} \\ \frac{\partial J^e}{\partial \phi_m^e} \end{bmatrix}_{\underline{B}} = \begin{bmatrix} F_{ii} & F_{ij} & F_{im} \\ F_{ji} & F_{jj} & F_{jm} \\ F_{mi} & F_{mj} & F_{mm} \end{bmatrix} \begin{bmatrix} \phi_i^e \\ \phi_j^e \\ \phi_m^e \end{bmatrix} \tag{3.34}$$

or

$$\left.\frac{\partial J^e}{\partial \phi^e}\right|_{\underline{B}} = \underline{F}^e \, \underline{\phi}^e \tag{3.35}$$

where

$$F_{ij}^{e} = \frac{1}{4\Delta_e^2}\left\{\int_{\Delta_e} a_i a_j \, dxdy + \int_{\Delta_e} (a_i b_j + a_j b_i) x \, dxdy \right.$$

$$\int_{\Delta_e} (a_i c_j + a_j c_i) y \, dxdy + \int_{\Delta_e} (b_i b_j x^2 \, dxdy)$$

$$\left. \int_{\Delta_e} c_i c_j \, y^2 dxdy + \int_{\Delta_e} (b_i c_j + c_i b_j) xy \, dxdy \right\}. \qquad (3.36)$$

and on simplification element submatrix $\underline{F}^e$ becomes

$$\underline{F}^e = \frac{\Delta_e}{6} \begin{bmatrix} 1 & \frac{1}{2} & \frac{1}{2} \\ \frac{1}{2} & 1 & \frac{1}{2} \\ \frac{1}{2} & \frac{1}{2} & 1 \end{bmatrix} \qquad (3.37)$$

irrespective of the shapes of the triangular elements.

Now combining equations (3.32) and (3.35), we get the partial contribution to the minimisation of $J(\phi)$ subscribed by the approximated function over the element 'e' as

$$\left[\frac{\partial J^e}{\partial \underline{\phi}^e}\right] = \underline{S}^e \cdot \underline{\phi}^e - k_0^2 \; \underline{F}^e \cdot \underline{\phi}^e \qquad (3.38)$$

The matrices $\underline{S}^e$ and $\underline{F}^e$ as obtained above may be called the element submatrices of matrices $\underline{A}$ and $\underline{B}$ respectively. Though they are written for simplicity as (3 x 3) square matrices, each of them is a (M x M) square matrix with at most nine non-zero components. The matrices $\underline{A}$ and $\underline{B}$ are the sum of all the element submatrices generated by all the elements.

3.4 Properties of the Matrix Operators A and B

The properties of the matrices A and B will depend on the nature of the P element submatrices as discussed above. Referring back to section (3) we find

$$S_{ij}^{e} = S_{ji}^{e} \tag{3.39}$$

and $F_{ij}^{e} = F_{ji}^{e}$

Therefore, each of the element submatrices is a symmetric matrix. The matrices A and B are the matrix sum of P element submatrices and thus they are also symmetric. Since each of the vertices is common to a certain number 'R' of the elements which is much less than the total number P, the generated matrices A and B will be sparse band matrices.

We now show that the matrix B as given above is always a positive definite and diagonally dominant matrix. The former condition is necessary for a successful inversion of matrix B in case of direct solution by the matrix inversion method and the latter condition is also necessary for the successful convergence when successive over relaxation type of iterative solution is used to matrix eigenvalue problems.

Equation (3.37) shows that the components of the element submatrix F^{e} are all positive and the algebraic sum of the off-diagonal components of any row is equal to the

diagonal component . For those vertices which are adjacent to the electric or the magnetic wall in waveguide problems, the boundary conditions on the corresponding potential will generate some rows for which the sum of the off-diagonal terms will be less than the diagonal terms. Therefore, the matrix is always diagonally dominant.

Finally, let us consider the quadratic form $\underline{\Phi}^T \underline{F} \underline{\Phi}$ for an element 'e'.

$$\underline{\Phi}^T \underline{F} \underline{\Phi} = F_{ii}\phi_i^2 + F_{jj}\phi_j^2 + F_{mm}\phi_m^2 + 2F_{ij}\phi_i\phi_j + 2F_{im}\phi_i\phi_m + 2F_{jm}\phi_i\phi_m \qquad (3.40)$$

Substituting the value of F_{ij} as given in equation (3.37) into equation (3.40), we obtain

$$\underline{\Phi}^T \underline{F} \underline{\Phi} = \frac{\Delta e}{12}\left[(\phi_i + \phi_j + \phi_m)^2 + \phi_i^2 + \phi_j^2 + \phi_m^2\right] > 0 \qquad (3.41)$$

for all values of non-zero ϕ_i. Therefore the element submatrix $\underline{B}$ is always positive definite.

Similarly, it can be shown that the diagonal components of all the element submatrices $\underline{S}^e$ are positive and the algebraic sum of the off-diagonal terms of any row is exactly equal in magnitude to the diagonal term. Also it can be shown that for triangular elements with interior angles not exceeding 90° , the off-diagonal terms are all negative. This property of triangular elements in the formulation of

the element submatrices $\underline{S}^2$ is shown in Appendix A3.3. Again the boundary conditions on the appropriate potential make the resultant matrix A diagonally dominant.

If we now consider the quadratic form $\underline{\phi}^T \underline{S} \underline{\phi}$ for an element submatrix $\underline{S}^e$, we obtain

$$\underline{\phi}^T \underline{S} \underline{\phi} = S_{ii}\phi_i^2 + S_{jj}\phi_j^2 + S_{mm}\phi_m^2 + 2S_{ij}\phi_i\phi_j$$

$$+ 2S_{im}\phi_i\phi_m + 2S_{jm}\phi_j\phi_m \qquad (3.42)$$

But,

$$S_{ii} \geq -(S_{ij} \quad S_{im})$$

$$S_{jj} \geq -(S_{ij} \quad S_{jm})$$

$$S_{mm} \geq -(S_{im} \quad S_{jm})$$

Substituting the above inequalities into equation (3.42), we obtain

$$\underline{\phi}^T \underline{S} \underline{\phi} \geq -S_{ij}(\phi_i-\phi_j)^2 - S_{im}(\phi_i-\phi_m)^2 - S_{jm}(\phi_j-\phi_m)^2 \qquad (3.43)$$

Since S_{ij}, S_{im} and S_{jm} are negative,

$\underline{\phi}^T \underline{S} \underline{\phi} > 0$ for all non-zero column vector $\underline{\phi}$.

Hence, the element submatrices $\underline{S}^e$ and matrix $\underline{A}$ are also positive definite.

3.5 Development of the Finite-Element Equations for Rectangular Elements.

In this section finite-element discretised equations are developed for grading a waveguide cross-section into rectangular elements. Division of a waveguide into rectangular elements is shown in Figure (3.2). The general approach outlined in section (3.3) remains the same except that the triangular elements are replaced by the rectangular elements and that instead of approximating the true field function over an element by a set of linear algebraic functions, it is approximated by a set of quadratic functions defined over the rectangular element under consideration.

If we consider a typical element 'e' bounded by the vertices i, j, k and ℓ as shown in Fig.(3.2), then over this element the field value $\phi(x,y)$ can be approximated as

$$\phi^e(x,y) = \sum_{\gamma=i,j,k,\ell} N_\gamma(x,y)\,\phi_\gamma \qquad (3.44)$$

where $N_\gamma(x,y) = a_\gamma + b_\gamma x + c_\gamma y + d_\gamma xy$ (3.45)

and ϕ_γ is the value of ϕ at the vertex γ. The quadratic function $N_\gamma(x,y)$ also satisfies the condition that

$$N_\gamma(x_j, y_j) = \delta_{j\gamma}$$

where (x_j, y_j) refers to the co-ordinate of the jth vertex of the element e.

It is now required to solve sixteen unknown coefficients a_γ, b_γ, c_γ and d_γ. These can be obtained

from equation (3.46) and they are given below:

$$
\begin{aligned}
a_i &= 1 + x_i/h_1 + y_i/h_2 + x_i y_i/h_1 h_2 \\
b_i &= -1/h_1 - y_i/h_1 h_2 \\
c_i &= -1/h_2 - x_i/h_1 h_2 \\
d_i &= 1/h_1 h_2
\end{aligned}
\tag{3.47}
$$

$$
\begin{aligned}
a_j &= -(x_i/h_1 + x_i y_i/h_1 h_2) \\
b_j &= 1/h_1 + y_i/h_1 h_2 \\
c_j &= x_i/h_1 h_2 \\
d_j &= -1/h_1 h_2
\end{aligned}
\tag{3.48}
$$

$$
\begin{aligned}
a_k &= x_i y_i/h_1 h_2 \\
b_k &= -y_i/h_1 h_2 \\
c_k &= -x_i/h_1 h_2 \\
d_k &= -1/h_1 h_2
\end{aligned}
\tag{3.49}
$$

$$
\begin{aligned}
a_\ell &= -1_i/h_2 - x_i y_i/h_1 h_2 \\
b_\ell &= y_i/h_1 h_2
\end{aligned}
$$

$$c_\ell = 1/h_2 + x_i/h_1h_2 \qquad (3.50)$$

$$d_\ell = -1/h_1h_2$$

In order that any polynomial approximation N(x,y) to the actual field function may be useful to derive discretised equations in finite element method, it must satisfy the continuity condition of the scalar field ϕ at the interface between any two adjacent elements. In the case of rectangular elements, the field at any point on the common side between two elements shall be uniquely defined in terms of potentials at the two common vertices. It can be easily shown that the functional relation N(x,y) assumed in this section satisfies the above requirement.

If the above quadratic form of $\phi(xy)$ is substituted into the appropriate extremisation functional $J(\phi)$ and the minimisation of $J(\phi)$ with respect to each i is considered, we will get, like triangular elements grading, a set of linear algebraic eigenvalue equations. In matrix notation these can also be written as

$$\underline{A}' \, \underline{\phi} = \underline{B}' \, \underline{\phi} \qquad (3.51)$$

where the form of $\underline{A}'$ and $\underline{B}'$ is slightly different from that of $\underline{A}$ and $\underline{B}$ given in equation (3.25).

It may be mentioned at this stage that the nature of subdivision of the entire domain into triangular and

rectangular elements and the corresponding approximation of linear and quadratic form of the fields inside each element as given in equations (3.8) and (3.44) are not the only possibilities for which this method is valid. It is perfectly valid to take the element subregions other than triangles and rectangles. Subdivision into regular polygons other than triangles and rectangles would require more involved algebraic calculations.

3.6 Evaluation of the Components of the Matrices $\underline{A}'$ and $\underline{B}'$

Components of the matrices $\underline{A}'$ and $\underline{B}'$ can be obtained in a similar way as obtained for triangular subdivisions. If there are P rectangular elements into which the entire domain is divided, the matrices $\underline{A}'$ and $\underline{B}'$ will be the matrix sum of P element submatrices. Each of these element submatrices is a (4 x 4) square matrix, whose components can be determined in the same way as discussed in section (3.3). If $\underline{S}^e$ and $\underline{F}^e$ are element submatrices constituting the matrices $\underline{A}'$ and $\underline{B}'$ respectively then their typical components S^e_{ij} and F^e_{ij} become:

$$S^e_{ij} = (b_i b_j + c_i c_j)\,\square_e + \int_{\square_e} (b_i d_j + d_i b_j)\,y\,dxdy$$
$$+ \int_{\square_e} (c_i d_j + d_i c_j)\,x\,dxdy + \int_{\square_e} d_i d_j (x^2 + y^2)\,dxdy. \qquad (3.52)$$

and

$$F^e_{ij} = a_i a_j \square_e + \int_{\square_e}(a_i b_j + a_j b_i)x \, dxdy + \int_{\square_e}(a_i c_j + c_i a_j)y \, dxdy$$
$$+ \int_{\square_e}(a_i d_j + d_i a_j + b_i c_j + c_i b_j)xy \, dxdy +$$
$$\int_{\square_e} b_i b_j x^2 dxdy + \int_{\square_e} c_i c_j y^2 dxdy +$$
$$\int_{\square_e}(c_i d_j + d_i c_j)x \, y^2 dxdy + \int_{\square_e}(b_i d_j + d_i b_j)x^2 y \, dxdy +$$
$$\int_{\square e} d_i d_j \, x^2 y^2 \, dxdy \qquad (3.53)$$

where $\square_e$ is the area of the rectangular element defined by the suffixes i, j, k and l.

Equation (3.52) and (3.53) are obtained in terms of a common reference co-ordinate system as in Figure (3.2). It is shown in Appendix A3.2 that the components of the element submatrices $\underline{S}^e$ and F^e remain invariant to any change of the origin of the frame of reference. This is also true for the triangularisation scheme. If we now take the origin of co-ordinate system at the centroid of the rectangular element, we obtain

$$S^e_{ij} = (b'_i b'_j \quad c'_i c'_j)\square_e + \frac{d'_i d'_j}{12}\square_e \, (h_1^2 + h_2^2) \qquad (3.53)$$

and

$$F^e_{ij} = a'_i a'_j \square_e + \frac{b'_i b'_j}{12} h_1^2 \square_e + \frac{c'_i c'_j}{12} h_2^2 \square_e +$$
$$\frac{d'_i d'_j}{144} h_1^2 h_2^2 \square_e \qquad (3.54)$$

where a_i', b_i', c_i' d_i' etc. can be obtained by setting $x_i = -h_1/2$, and $y_i = -h_2/2$ in the set of equations (3.47), (3.48) (3.49) and (3.50) and are given by

$$
\begin{aligned}
a_i' &= a_j' = a_k' = a_\ell' = 1/4 \\
b_i' &= -b_j' = -b_k' = b_\ell' = -1/2h_1 \\
c_i' &= -c_j' = -c_k' = c_\ell' = -1/2h_2 \\
d_i' &= -d_j' = d_k' = -d_\ell' = 1/h_1h_2
\end{aligned}
\tag{3.55}
$$

For square mesh grading $h_1 = h_2 = h$(say) and the co-efficients S_{ij}^e and F_{ij}^e become more simple and given by

$$
\begin{aligned}
S_{ij}^e &= -1/6 \text{ if } i \neq j \text{ but they are adjacent vertices} \\
&= \frac{2}{3} \text{ if } i = j \\
&= -\frac{1}{3} \text{ if } i \neq j \text{ but they are diagonally opposite vertices}
\end{aligned}
\tag{3.56}
$$

and

$$
\begin{aligned}
F_{ij}^e &= \frac{h^2}{18} \text{ if } i \neq j \text{ but they are adjacent vertices} \\
&= \frac{h^2}{36} \text{ if } i \neq j \text{ but they are diagonally opposite vertices} \\
&= \frac{h^2}{9} \text{ if } i = j
\end{aligned}
\tag{3.57}
$$

Therefore, the element submatrices S^e and F^e for square mesh become

$$\underline{S}^e = \frac{1}{6}\begin{bmatrix} 4 & -1 & -2 & -1 \\ -1 & 4 & -1 & -2 \\ -2 & -1 & 4 & -1 \\ -1 & -2 & -1 & 4 \end{bmatrix} \tag{3.58}$$

and

$$\underline{F}^e = \frac{1}{36}\begin{bmatrix} 4 & 2 & 1 & 2 \\ 2 & 4 & 2 & 1 \\ 1 & 2 & 4 & 2 \\ 2 & 1 & 2 & 4 \end{bmatrix} \tag{3.58}$$

It can be shown that the matrices $\underline{A}'$ and $\underline{B}'$ which are the matrix sum of P element submatrices $\underline{S}^e$ and $\underline{F}^e$ are symmetric sparse, positive definite and band type matrices.

Appendix A3

A3.1 Evaluation of some important surface integrals for Triangular Elements.

Consider the triangular element as shown in Fig.A3.1. Three important integrals which are associated with the derivation of finite-element equations are:

1) $\int x^2 dxdy$ (A3.1)

2) $\int y^2 dxdy$ (A3.2)

3) $\int xy\, dxdy$ (A3.3)

If we functionally relate y with x or x with y, we get

a) For line AB

$$y = \frac{y_i - y_m}{x_i - y_m} x + \frac{y_i x_m - x_i y_m}{x_i - x_m} \tag{A3.4}$$

$$x = \frac{x_i - x_m}{y_i - y_m} y + \frac{x_i y_m - x_m y_i}{y_i - y_m} \tag{A3.5}$$

b) For line AC

$$y = \frac{y_i - y_j}{x_i - x_j} x + \frac{y_i x_j - x_i y_j}{x_i - x_j} \tag{A3.6}$$

$$x = \frac{x_i - x_j}{y_i - y_j} y + \frac{x_i y_i - y_i x_j}{y_i - y_j} \tag{A3.7}$$

c) For line BC

$$y = \frac{y_j - y_m}{x_j - x_m} y + \frac{y_j x_m - x_j y_m}{x_j - x_m} \tag{A3.8}$$

$$x = \frac{x_j - x_m}{y_j - y_m} y + \frac{x_j y_m - y_j x_m}{y_j - y_m} \qquad \text{(A3.9)}$$

Substituting the appropriate values of x and y and evaluating the integral within the proper limit, we get:

$$\int_A x^2 dxdy = \frac{x_i^4}{4}\left[(y_i-y_j)/(x_i-x_j)\right] + \frac{x_i^3}{3}\left[(y_i x_j - x_i y_j)/(x_i-x_j) - (y_i x_m - x_i y_m)/(x_i-x_m)\right] + \frac{x_j^4}{4}\left[\frac{y_j-y_m}{x_j-x_m} - \frac{y_j-y_i}{x_j-x_i}\right] + \frac{x_j^3}{3}\left[\frac{y_j x_m - x_j y_m}{x_j-x_m} - \frac{y_j x_i - x_j y_i}{x_j-x_i}\right] + \frac{x_m^4}{4}\left[\frac{y_m-y_i}{x_m-x_i} - \frac{y_m-y_j}{x_m-x_j}\right] + \frac{x_m^3}{3}\left[\frac{y_m x_i - x_m y_i}{x_m-x_i} - \frac{y_m x_i - x_m y_j}{x_m-x_j}\right] \qquad \text{(A3.10)}$$

$$\int_A y^2 dxdy = \frac{y_i^4}{4}\left[\frac{x_i-x_j}{y_i-y_j} - \frac{x_i-x_m}{y_i-y_m}\right] + \frac{y_i^3}{3}\left[\frac{x_i y_j - x_j y_i}{y_i-y_j} - \frac{x_i y_m - y_i x_m}{y_i-y_m}\right] + \frac{y_j^4}{4}\left[\frac{x_j-x_m}{y_i-y_m} - \frac{x_j-x_i}{y_j-y_i}\right] + \frac{y_j^3}{3}\left[\frac{x_j y_m - x_m y_j}{x_j-x_m} - \frac{x_j y_i - y_j x_i}{x_j-x_m}\right] + \frac{y_m^4}{4}\left[\frac{x_m-x_i}{y_m-y_i} - \frac{x_m-x_j}{y_m-y_j}\right] + \frac{y_m^3}{3}\left[\frac{x_m y_i - y_m x_i}{y_m-y_i} - \frac{x_m y_j - y_m x_j}{y_m-y_i}\right] \qquad \text{(A3.11)}$$

and

$$\int_{\Delta} xydxdy = \frac{1}{4}(x_m^4-x_i^4)\left[\left(\frac{y_i-y_m}{x_i-x_m}\right)^2-\left(\frac{y_i-y_j}{x_i-x_j}\right)^2\right]+$$

$$\frac{1}{2}(x_m^2-x_i^2)\left[\left(\frac{y_ix_m-x_iy_m}{x_i-x_m}\right)^2-\left(\frac{y_ix_j-x_iy_j}{x_i-x_j}\right)^2\right]+$$

$$\frac{2}{3}(x_m^3-x_i^3)\left[\frac{y_i-y_m}{x_i-x_m}\cdot\frac{y_ix_m-x_iy_m}{x_i-x_m}-\frac{y_i-y_j}{x_i-x_j}\cdot\right.$$

$$\left.\frac{x_jy_i-y_jx_i}{x_i-x_j}\right]+\frac{1}{4}(x_j^4-x_m^4)\cdot\left[\left(\frac{y_j-y_m}{x_j-x_m}\right)^2-\left(\frac{y_j-y_i}{x_j-x_i}\right)^2\right]+$$

$$\frac{1}{2}(x_j^2-x_m^2)\left[\left(\frac{y_jx_m-x_jy_m}{x_j-x_m}\right)^2-\left(\frac{y_jx_i-x_jy_i}{x_j-x_i}\right)^2\right]+$$

$$\frac{2}{3}(x_j^3-x_m^3)\left[\frac{y_j-y_m}{x_j-x_m}\times\frac{y_jx_m-x_jy_m}{x_j-x_m}-\frac{y_j-y_i}{x_j-x_i}\cdot\right.$$

$$\left.\frac{x_iy_j-x_jy_i}{x_j-x_i}\right] \qquad \text{(A3.12)}$$

A3.2 Effects of the change of the origin of the reference co-ordinates on the components of the element submatrices.

It will be shown here that the components of the element submatrices $\underline{S}^e$ and $\underline{F}^e$ remain invariant to any change of the origin of the frame of reference. This is true both for triangular and square mesh grading. We give below a proof for the triangular mesh and the same would follow for square mesh.

Let (x_i, y_i), (x_j, y_j), and (x_m, y_m) be the co-ordinates of the vertices of a triangular element as shown in Fig.(A3.1) with respect to common reference frame, and let (x_i', y_i'),

(x_j', y_j') and (x_m', y_m') be the co-ordinates of the same vertices with respect to a local reference co-ordinates we take the centroid of the triangle as the origin of the local co-ordinates.

Let us consider the following notation in common reference frame:

$$\left.\begin{aligned} a_i &= x_j x_m - y_j x_m \\ a_j &= x_m y_i - y_m x_i \\ a_m &= x_i y_j - y_i x_j \end{aligned}\right\} \qquad \text{(A3.13)}$$

$$\left.\begin{aligned} b_i &= y_j - y_m, \quad b_j = y_m - y_i, \quad b_m = y_i - y_j \\ c_i &= x_m - x_j, \quad c_j = x_i - x_m, \quad c_m = x_j - x_m \end{aligned}\right\} \qquad \text{(A3.14)}$$

The co-ordinates of the vertices i, j, and m in common reference frame can be written in terms of local reference frame as follows:

$$\begin{aligned} x_i &= x_o + x_i', \qquad y_i = y_o + y_i' \\ x_j &= x_o + x_j', \qquad y_j = y_o + y_j' \\ x_m &= x_o + x_m', \qquad y_m = y_o + y_m' \end{aligned} \qquad \text{(A3.15)}$$

where $(x_o\ y_o)$ is the co-ordinate of the centroid of the triangle in common reference system.

If we substitute the values of x_i, x_j, x_m and y_i, y_j and y_m as given in equation (A3.15) in equation (A3.14) and denote the corresponding parameters in the local reference system by primed letters, we get

$$a_i = a_i' - x_o b_i' - y_o c_i'$$

$$a_j = a_j' - x_o b_j' - y_o c_j' \qquad \text{(A3.16)}$$

$$a_m = a_m' - x_o b_m' - y_o c_m'$$

$$b_i = b_i', \quad b_j = b_j', \quad b_m = b_m', \quad c_i = c_i', \quad c_j = c_j'$$

and $c_m = c_m'$

and
$$\left.\begin{aligned} \int x\,dx\,dy &= x_o \Delta_e + \int x'\,dx'\,dy' = x_o \Delta_e \\ \int y\,dx\,dy &= y_o \Delta_e + \int y'\,dx'\,dy' = y_o \Delta_e \end{aligned}\right\} \qquad \text{(A3.17)}$$

Since moment about the centroid is zero,

$$\int x^2\,dx\,dy = x_o^2 \Delta_e + \int x'^2\,dx'\,dy' \qquad \text{(A3.18)}$$

$$\int y^2\,dx\,dy = y_o^2 \Delta_e + \int y'^2\,dx'\,dy' \qquad \text{(A3.19)}$$

$$xy\,dx\,dy = x_o y_o \Delta_e + \int x'y'\,dx'\,dy' \qquad \text{(A3.20)}$$

If we now consider any component S_{ij} of the element submatrix $\underline{S}^e$ we get

$$S_{ij} = (b_i b_j + c_i c_j)/\,4\Delta_e \qquad \text{(A3.21)}$$

But b_i, b_j, c_i and c_j are invariant to a change of co-ordinates therefore components of the element submatrices S^e will also be invariant to the change of reference frame.

Let us now consider a typical component of the element submatrix $\underline{F}^e$, say F_{ij}^e. Then

$$F_{ij}^e = a_i a_j \Delta_e + (a_i b_j + a_j b_i) \int x dx dy + (a_i c_j + a_j c_i) \int y dx dy + b_i b_j \int x^2 dx dy + c_i c_j \int y^2 dx dy + (b_i c_j + c_i b_j) \int xy dx dy \qquad (A3.22)$$

If we substitute the relations given in equations (A3.16) through (A3.20) into equation (A3.22) we get

$$F_{ij} = \left[a_j' a_j' \Delta_e + \frac{b_i' b_j'}{12} \Delta_e \sum_{k=i\,j\,m} x_k'^2 + \frac{c_i' c_j'}{12} \Delta_e \sum_{k=i\,j\,m} y_k'^2 + \frac{b_i' c_j' + c_i' b_j'}{12} \Delta_e \sum_{k=i,j\,m} x_k' y_k' \right] \Big/ 4 \Delta_e^2$$

which is the expression for F_{ij}'. This proves that the change of the origin of the co-ordinates will not affect the components of the matrix F^e.

A3.3 Effect of the shape of the triangular element on the components of element submatrices $\underline{S}^e$

Let us consider a triangular element and the associated co-ordinates as shown in Fig. (A3.2). Let the co-ordinates of the vertices i, j and m be (0,0), (a,0) and (c,b) respectively. The parameters $b^{(s)}$ and $c^{(s)}$ for the

particular element in Fig. A3.2 are:

$$b_i = -b, \qquad b_j = b, \qquad b_m = 0$$
$$c_i = c-a, \qquad c_j = -c, \qquad c_m = a \tag{A3.24}$$

If we now consider the components of the i th row of the element submatrix $\underline{S}^e$, we get,

$$S^e_{ii} = b^2 + (c-a)^2 > 0$$
$$S^e_{ij} = -b^2 - c^2 + ac \tag{A3.25}$$
$$S_{im} = ac - a^2$$

If S_{im} is to be less than zero then a c should be less than a^2, i.e. $c < a$. The inequality $c < a$ implies that the interior angle at the vertex 'j' is less than 90°.

To find the effect of the interior angle at the vertex 'm', let us denote the interior angle at the vertex m by θ and also assume that the lengths of the lines joining the vertex m with the vertices i and j are α and β respectively, then for the triangle ABC we get the following relations:

$$\alpha^2 + \beta^2 - 2\alpha\beta\cos\theta = a^2 \tag{A3.26}$$

$$\left.\begin{aligned} c^2 + b^2 &= \alpha^2 \\ b^2 + (a-c)^2 &= \beta^2 \end{aligned}\right] \tag{A3.27}$$

Substituting the values of α^2 and β^2 from equation (A3.27) into (A3.26) we get

$$2(b^2 + c^2) - 2ac - 2\alpha\beta\cos\theta = 0 \qquad \text{(A3.28)}$$

or $\quad -b^2 - c^2 + ac = -\alpha\beta\cos\theta$

The left hand side of equation (A3.28) will always be less than zero for all values of a, b and c if θ is less than 90°. Therefore, all the off-diagonal terms of any row of the matrix $\underline{S}^e$ will be negative when the interior angles do not exceed 90°.

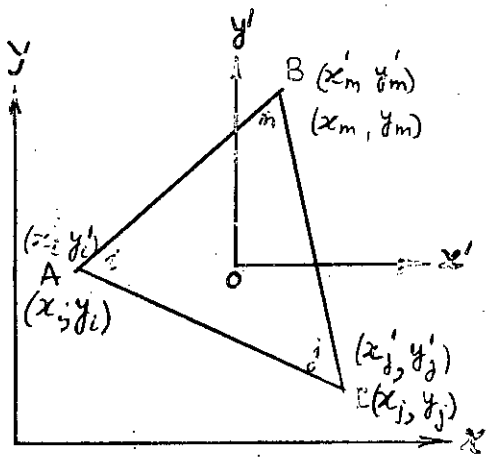

Figure A3.1

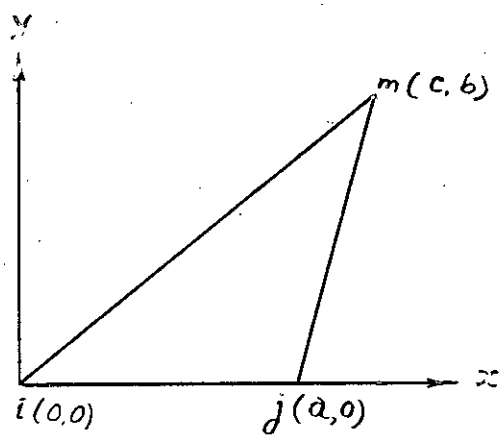

Figure A3.2

Chapter 3 - References

1. Collin, R.E.: "Field Theory of Guided Waves", McGraw-Hill Book Company, 1960.

2. Morse, P.M. and Feshback, H.: "Methods of Theoretical Physics", McGraw-Hill Book Company Inc.

CHAPTER 4

APPLICATIONS OF FINITE-ELEMENT METHOD TO HOMOGENEOUS WAVEGUIDE PROBLEMS

4.1 Description of Problems

In this chapter we consider a few cases of typical homogeneous waveguide problems which have already been solved either analytically or by finite-difference method. The main reason for this analysis is to demonstrate the relative merit of the finite-element method for the following aspects:

a) Its rate of convergence.

b) Its ability to handle awkward boundary shapes.

c) Its ability to treat singular points in boundary value problems.

For all uniform lossless homogeneous waveguides, it is always possible to divide the general propagating mode into two uncoupled modes, namely, the TM or E mode and the TE or H mode. All components of the electric and magnetic field vectors in H-mode propagation can be obtained from the longitudinal component of the magnetic field vector. Similarly, a knowledge of the longitudinal component of the electric field vector is sufficient to determine all other field components in E-mode.

Numerical solutions of the equivalent discretised eigenvalue problem for homogeneous waveguides are obtained by using "Successive Over Relaxation" abbreviated as the SOR technique of iterative methods. A brief description of the SOR technique is given in section (4.2).

Since the main purpose of this thesis is to demonstrate the usefulness of the finite-element method, no effort was made to obtain a generalised computer program which could be used for all types of waveguide boundaries.

To ascertain the rate of convergence, numerical computations are made for cut-off wavenumber k_o^2 in a rectangular waveguide sustaining TE_{10} mode and TM_{01} mode for various mesh sizes in triangular and square element grading and are given in Tables (4.1), (4.2), and (4.3). In section (4.5) results of the computations of the wave number for TM_{01}, TE_{11} and TM_{11} modes in a circular waveguide are given. In section (4.6) a circular waveguide is analysed in rectangular co-ordinates in order to illustrate the scope of treating awkwardly shaped boundaries by the finite-element method. It is found that a slight arbitrary perturbation of the boundary does not affect the wavenumber for TM_{01} mode in a circular waveguide very much and this is shown in Table (4.10). In section (4.7) numerical computations are presented for the dominant mode wavenumber in waveguides possessing one or more

singularities or re-entrant corners. Re-entrant corners are mathematical singularities in waveguides. They create special difficulties in presenting analytic as well as the finite-difference solutions to such a problem. Numerical results for fields and wavenumbers for singular problems such as klystron cavity resonators, L-shaped waveguide, ridged waveguide, and channel waveguide as given in section (4.7) when compared with the results already published by other methods show a good agreement. It is shown that in finite-element method singular points in a waveguide or in a transmission line can be treated in the same way as an ordinary point.)

4.2 Solving the Matrix Eigenvalue Problem

There are many methods by means of which a matrix eigenvalue equation may be solved for its eigenvalues and eigenvectors, but they fall, broadly, into two categories: direct and indirect methods.

Direct methods have the advantage that exact solutions are obtained in a known number of steps determined by the order of the matrix considered. Their disadvantage is that most of the elements of the relevant matrices $\underline{A}$ and $\underline{B}$ must be stored in the computer and since the number of elements in $\underline{A}$ and $\underline{B}$ is equal to the square of the number of vertices generated in grading the domain into triangular or square elements, a considerable amount of storage must be

reserved for problems of modest proportions. In addition, much of the storage space is wasted, since all the rows of the matrices $\underline{A}$ and $\underline{B}$ contain only a few non zero elements, ie. $\underline{A}$ and $\underline{B}$ are sparse.

Indirect methods make use of the fact that there are usually only a few different type of rows present in $\underline{A}$ and $\underline{B}$ which enable one to generate these rows inside the computer by writing specific instructions. For example, consider the solutions of a set of linear equations given by the matrix relation

$$\underline{A}\,\underline{\phi} = \underline{b} \tag{4.1}$$

where $\underline{A}$ for simplicity is assumed to have the form shown below

$$\underline{A} = \begin{bmatrix} 1 & 4 & 1 & - & - & - & - \\ - & 1 & 4 & 1 & - & - & - \\ - & - & 1 & 4 & 1 & - & - \\ - & - & - & 1 & 4 & 1 & - \\ - & - & - & - & 1 & 4 & 1 \end{bmatrix} \tag{4.2}$$

and $\underline{\phi}$ is a column vector with components ϕ_1, ϕ_2, ϕ_3, ϕ_4, ϕ_5 etc. The computer can be instructed to perform the operation

$$b_1 = \phi_1 + 4\phi_2 + \phi_3 \tag{4.3}$$

and then to increase all subscripts by 1 and repeat the operation. This iteration continues until the last row of the matrix is reached. In general, indirect methods require

much less storage than the direct methods.

4.2.1 Description of the Successive Over-Relaxation Technique

Of the several indirect methods which could be applied to the solutions of a matrix eigenvalue problem

$$\underline{A}\,\underline{\Phi} = \underline{B}\,\underline{\Phi} \tag{4.4}$$

the most suitable one, is known as the method of successive over-relaxation. To illustrate its implementation, consider the solutions of equation (4.4) for the eigenvector corresponding to the dominant mode propagation when the eigenvalue is known. Later on, in this section, the means of determining the eigenvalue will be described. We require to solve the system:

$$(\underline{A} - \lambda \underline{B})\,\underline{\Phi} = 0 \tag{4.5}$$

First an approximation to the required $\underline{\Phi}$ is stored in the computer, then for each component of $\underline{\Phi}$, the following process is carried out. For the i th row

$$R_i = (A_i - \lambda B_i)\phi_i \tag{4.6}$$

is computed, where A_i and B_i denote the i th row of matrices $\underline{A}$ and $\underline{B}$ and are, therefore, submatrices of one row only. The quantity R_i is called the error vector. The error vector R should have zero components at each point at a solution. The i th component of $\underline{\Phi}$ i.e. ϕ_i is then replaced by $\phi_i + \alpha R_i$, where α is such that R_i in ϕ_i is

over-compensated. The vector $\bar{\phi}$ is then scanned continually in this way until the residuals i.e. the error components which result at each point are sufficiently small to be neglected. In the above process, the term α is the over-relaxation factor and it affects the rate of convergence to a great extent. There is an optimum value of α for which the system converges most rapidly and this may be obtained during computation (1).

One disadvantage of the SOR method is that it cannot be used with guarantee for an arbitrary matrix, because, for this process, convergence is only guaranteed when the matrices $\underline{A}$ and $\underline{B}$ are symmetric and positive definite, i.e. when the singular matrix $(A - \lambda B)$ is semidefinite. In mathematical notation this implies that:

$$\bar{\phi}^T (A - \lambda_o B)\bar{\phi} \geq 0 \qquad (4.7)$$

This latter requirement is always satisfied for homogeneous waveguide problems, because, for any arbitrary set of eigenvectors $\bar{\phi}$, the computed eigenvalue obtained by the Rayleigh quotient

$$\lambda_{computed} = \frac{\bar{\phi}^T A \bar{\phi}}{\bar{\phi}^T B \bar{\phi}} \qquad (4.8)$$

is always greater than the actual eigenvalue; so the quadratic form $\bar{\phi}^T A \bar{\phi}$ is greater than $\lambda_o \bar{\phi}^T B \bar{\phi}$ for the least eigenvalue. This is not true for the eigenvalue other than the smallest, which means that convergence cannot always be

expected when trying for other modes.

4.2.2 Determination of the Least Eigenvalues

Consider now the case of evaluating the least eigenvalue and its eigenvector simultaneously. This is usually done by starting with as good an estimate as possible of the required solution from physical consideration. Let $\lambda^{(0)}$ and $\underline{\phi}^{(0)}$ be the starting eigenvalue and the eigenvector. An attempt is then made to solve

$$(\underline{A} - \lambda^{(0)}\underline{B})\,\underline{\Phi}^{(0)} = 0 \qquad (4.9)$$

This, clearly, cannot be solved, because $\lambda^{(0)}$ is not the correct eigenvalue. If an initial guess to λ is uncertain then an estimate of λ can be made by evaluating the Rayleigh quotient from equation (4.8) which because of its stationary nature at a solution, produces a better estimate of λ from a poor estimate of the eigenvector. This estimate of λ is then substituted in equation (4.9) and the SOR technique is applied for obtaining better $\underline{\Phi}$.

These two iterative processes, i.e. the determination of the Rayleigh quotient to find the latest estimate of the eigenvalue and the improvement of the eigenvector $\underline{\Phi}$ are continued alternately, until two successive estimates agree to some specified degree and successive increments in the field values become sufficiently small. For the best result it is

of course desirable to use the latest estimate of eigenvalue at every iteration. In practice this demands more computational time and an interval of 3 to 4 iterations before re-estimating the eigenvalue is found necessary to produce satisfactory results. A computer program for evaluating the dominant mode wavenumber and the corresponding eigenvector is given in Appendix (A4.1) which will demonstrate the use of the method described in this section.

4.3 Eigenvalue Extrapolation

When errors in computed eigenvalues in three successive mesh halvings are in geometric progression, an extrapolation known as Aitkin δ^2 process produces a correct result. If λ_1, λ_2 and λ_3 are three successive approximations to the correct eigenvalue λ_i and if

$$\lambda_1 = \lambda_i + \alpha\epsilon$$

$$\lambda_2 = \lambda_i + \alpha\epsilon^2 \quad .$$

and $$\lambda_3 = \lambda_i + \alpha\epsilon^3$$

then it can be shown[2] that

$$_i = \lambda_1 - \frac{(\lambda_1 - \lambda_2)^2}{(\lambda_1 - 2\lambda_2 + \lambda_3)} \tag{4.10}$$

It is found that, even if the errors on mesh halving are not in geometric progression, it is still possible to obtain an improved result with this extrapolation. To

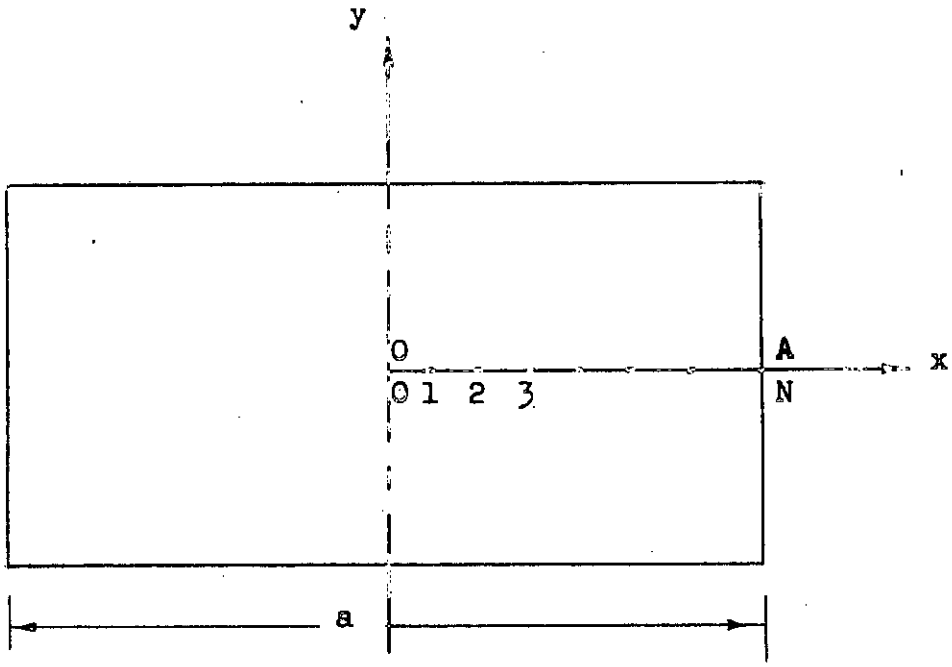

Figure (4.1)
Cross-section of
a
Rectangular Waveguide

solve any given waveguide problem, we, therefore, may start with a reasonable coarse mesh and continue mesh halving either until sufficient accuracy has been achieved or until a prescribed number of storage location within the computer have been occupied. Thus the accuracy which may eventually be obtained is limited to the floating-point round off error and the available computer storage size.

4.4 Particular Solutions

4.4.1 TE_{10}-Mode in a Rectangular Waveguide

This will illustrate the form of finite-element discretised equations for one dimensional problems. For TE_{10}-mode in a rectangular waveguide, there is no variation of field quantities with respect to one of the transverse co-ordinates. A cross-section of a rectangular waveguide together with the reference frame of co-cordinates is shown in Figure (4.1). For TE_{10}-mode, variation of fields with respect to y axis is zero. The extremisation function for this problem is given by (3)

$$J(\phi) = \int_s \left(\frac{\partial \phi}{\partial x}\right)^2 dx - k_o^2 \int \phi^2 dx \qquad (4.11)$$

where ϕ is a scalar potential representing the longitudinal component of the magentic field. If the half width OA is divided into 'n' equal parts marked by 0, 1, 2, 3....n res-

pectively, and $\phi_1, \phi_2, \phi_3 \ldots\ldots \phi_n$ are the values of ϕ at the points 1, 2, 3.....etc. then assuming a linear dependence of ϕ between two successive points and inserting this functional form of ϕ in equation (4.11) and following the general formulation of finite-element method, we obtain a discretised equation for the p th node point in terms of potentials at the $(P-1)^{th}$ and $(P+1)^{th}$ points as follows:

$$-\phi_{(P-1)} + 2\phi_P - \phi_{(P+1)} = \frac{k_o^2 h^2}{6} \left(\phi_{(P-1)} + 4\phi_P + \phi_{(P+1)} \right) \quad (4.12)$$

where h = length of an element, i.e. distance between two subsequent points.

If the same problem is treated by the finite-difference method, the corresponding discretised equation would be

$$-\phi_{(P-1)} + 2\phi_P - \phi_{(P+1)} = k_o^2 h^2 \phi_P \quad (4.13)$$

Comparing equation (4.12) with equation (4.13) we find that in finite-difference method only the potential at the p th node is weighted by the wavenumber k_o^2 but in the case of the finite-element method all the associated potentials for the discretised equation at the p th point are properly weighted by the wavenumber k_o^2. In this respect, the finite-element method may be a more natural approximation to a physical problem than the finite-difference method. Furthermore, in both the methods, the resultant discretised set of equations can be written in compact form as

$$\underline{A}\,\underline{\Phi} = \underline{B}\,\underline{\Phi} \tag{4.14}$$

where $\underline{A}$ is a square, symmetric, positive definite, band matrix of bandwidth 3 and is the same in both the methods but matrix $\underline{B}$ is a diagonal matrix for finite-difference method and square, symmetric, positive definite and diagonally dominant band matrix for finite-element method. Bandwidth of $\underline{B}$ is the same as that of $\underline{A}$.

4.4.2 Characteristics of F.E. and F.D. Representations for one Dimensional Wave Equation

In a heuristic way, we will show in this subsection that the finite-difference formulation of one dimensional wave equation for propagation in waveguides will generate a matrix eigenvalue problem whose solution would be a lower bound to the true eigenvalue. On the other hand the variational expression used for the finite-element formulation always gives an upper bound to the wavenumber. To show this property, let us expand the potential at (P+1) th node and (P-1) th node in terms of their values and derivatives at the P th node by Taylor series. This gives

$$\phi_{P+1} = \phi_P + h\frac{\partial\phi}{\partial x}\Big|_P + \frac{h^2}{2!}\frac{\partial^2\phi}{\partial x^2}\Big|_P + \frac{h^3}{3!}\frac{\partial^3\phi}{\partial x^3}\Big|_P + \frac{h^4}{4!}\frac{\partial^4\phi}{\partial x^4}\Big|_P \ldots \tag{4.15}$$

and

$$\phi_{(P-1)} = \phi_P - h\frac{\partial\phi}{\partial x}\Big|_P + \frac{h^2}{2!}\frac{\partial^2\phi}{\partial x^2}\Big|_P - \frac{h^3}{3!}\frac{\partial^3\phi}{\partial x^3}\Big|_P + \frac{h^4}{4!}\frac{\partial^4\phi}{\partial x^4}\Big|_P \cdots \tag{4.16}$$

If equations (4.15) and (4.16) are added together, we obtain

$$-\phi_{(P+1)} + 2\phi_P - \phi_{(P-1)} = -h^2\frac{\partial^2\phi}{\partial x^2}\Big|_P - \frac{2h^4}{4!}\frac{\partial^4\phi}{\partial x^4}\Big|_P - \frac{2h^6}{6!}\frac{\partial^6\phi}{\partial x^6}\Big|_P \tag{4.17}$$

If we use the following relations for the partial differentials:

$$\frac{\partial^2\phi}{\partial x^2}\Big|_P = -k_o^2\,\phi_P$$

$$\frac{\partial^4\phi}{x^4}\Big|_P = \frac{\partial^2}{\partial x^2}\left(\frac{\partial^2\phi}{\partial x^2}\right)\Big|_P = -k_o^2\frac{\partial^2\phi}{\partial x^2}\Big|_P = k_o^4\,\phi_P$$

$$\frac{\partial^6\phi}{\partial x^6}\Big|_P = -k_o^6\,\phi_P$$

and so on and insert them in equation (4.17), we get

$$k_o^2 h^2\,\phi_P = -\phi_{(P-1)} + 2\phi_P - \phi_{(P+1)} + \frac{2h^4k_o^4\phi_P}{4!} - \frac{2h^6k_o^6}{6!}\phi_P + \frac{2h^8k_o^8}{8!}\phi_P + \cdots \tag{4.18}$$

If we denote $h^2k_o^2$ by λ_o then in terms of λ_o equation (4.18) can be re-written as

$$-\phi_{(P-1)} + 2\phi_P - \phi_{(P+1)} = \phi_P\left(\lambda_o - \frac{2}{4!}\lambda_o^2 + \frac{2}{6!}\lambda_o^3 - \frac{2}{8!}\lambda_o^4 \cdots\cdots\right) \quad (4.19)$$

Equation (4.19) gives the exact representation of the difference relation. In finite-difference method, the entire right hand side of equation (4.19) is replaced by a single term of the form $\lambda\phi_P$. This then gives a relation between the true eigenvalue λ_o and the approximated eigenvalue λ as follows:

$$\lambda = \lambda_o\left(1 - \frac{2}{4!}\lambda_o + \frac{2}{6!}\lambda_o^2 - \frac{2}{8!}\lambda_o^3 + \frac{2}{10!}\lambda_o^5 \cdots\right) \quad (4.20)$$

In the case of TE_{10}-mode in a rectangular waveguide, the maximum value of λ_o is $\left(\frac{\pi}{4}\right)^2$ (for dominant mode) and this is the condition for $h = \frac{a}{2}$. If we insert the above value of λ_o in the expression for equation (4.20) we find that the expression within the round bracket becomes less than unity. Thus the eigenvalue λ evaluated by the discretised equation obtained by finite-element method would be less than the true eigenvalue λ_o.

4.4.3 Numerical Results for TE_{10}-Mode

It is expected that when the element length decreases linear approximation to field variation between two adjacent nodes would give fairly good results. Table (4.1) shows the effect of the element length on the numerical computations of the wavenumber k_o^2 in a rectangular waveguide. The same

Table also shows the corresponding results obtained by the finite-difference method. Comparing the results obtained by two methods with that of exact solution, we find that on successive element halving, the finite-difference solution approaches the true eigenvalue from below and the finite-element solution approaches the true eigenvalue from above and their accuracy is of the same order.

Table (4.1) TE_{10}-Mode in a Rectangular Waveguide

$\frac{h}{a}$	Finite-Element		Finite-Difference		Analytic
	$(k_o a)^2$	% Error(k_o)	$(k_o a)^2$	% Error$(k_o a)$	$(k_o a)^2$
1/2	12.0000	9.800	8.0000	9.8	
1/4	10.3666	2.840	9.3720	2.54	
1/6	10.0970	1.080	9.6462	1.136	
1/8	9.9970	0.600	9.7434	0.640	
1/10	9.9510	0.410	9.7887	0.410	9.8696
1/12	9.9261	0.286	9.8134	0.286	
1/14	9.9110	0.210	9.8284	0.210	
1/16	9.9013	0.159	9.8380	0.159	
1/18	9.8946	0.127	9.8446	0.127	
1/36	9.8759	<0.03	9.8634	<0.03	
1/72	9.8714	<0.008	9.8681	<0.008	
1/144	9.8703	<0.005	9.8693	<0.005	

4.4.4 TM_{11}-Mode in a Rectangular Waveguide

Theoretical analysis shows that the wavenumber k_o^2 for TM_{11}-mode in a rectangular waveguide is related with the guide dimensions as follows:

$$k_o^2 = \left(\frac{\pi}{a}\right)^2 + \left(\frac{\pi}{b}\right)^2 \tag{4.21}$$

The ratio $\frac{b}{a}$ is normally called the aspect ratio for the guide. Numerical computations of k_o^2 using both square mesh and triangular mesh are performed for waveguides with aspect ratios 1 and 4/9. For demonstrating the relative accuracy, results of k_o^2 computed by standard 5-point and 9-point finite-difference methods along with finite-element computations are tabulated in Tables (4.2) and (4.3).

The schemes of grading the waveguide cross-section into triangular and square elements are shown in Figures (4.2) and (4.3). For TM_{11}-mode extremisation functional can be formulated in terms of the longitudinal components of electric field which goes to zero on the waveguide walls. Therefore, only the interior vertices will be the effective vertices for generating the discretised equations. If ϕ_o is the value of ϕ at a typical vertex, say '0' and ϕ_1, ϕ_2, $\phi_3 \ldots \phi_8$ are the values of ϕ at the eight adjacent vertices to the vertex '0' as shown in Figures (4.2) and (4.3) then the discretised equations for ϕ_o would be

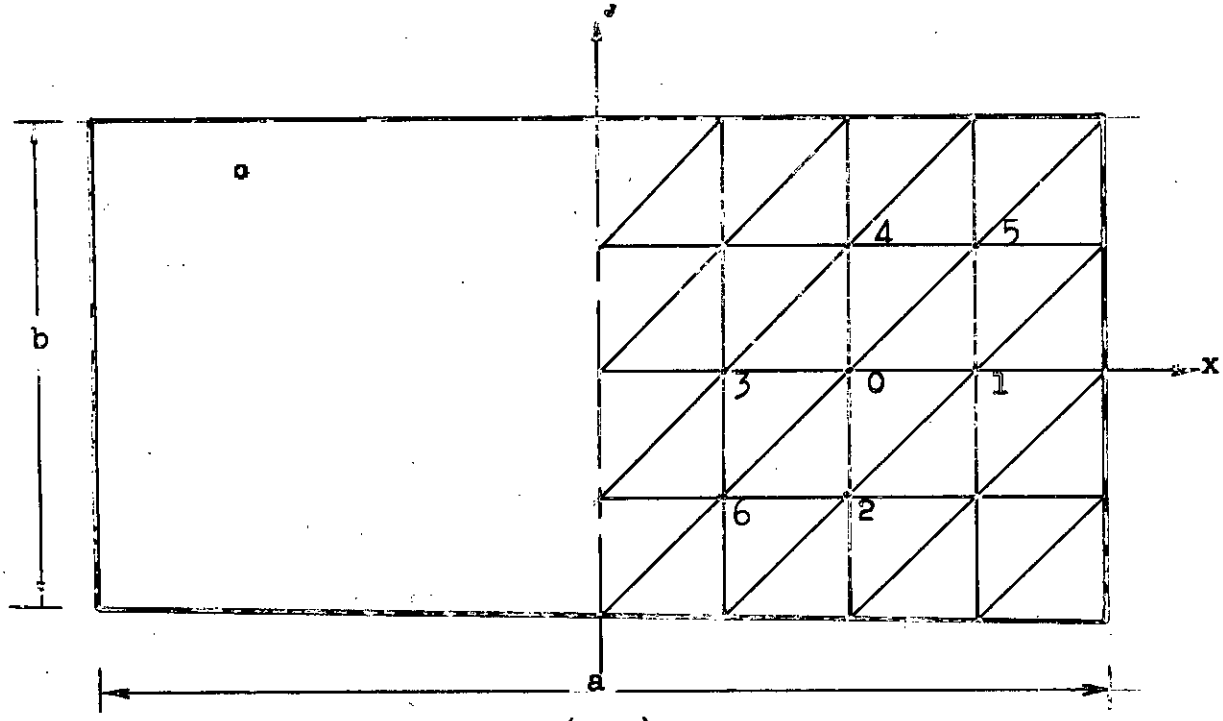

Figure (4.2)
Triangular mesh grading of
a
Rectangular Waveguide.

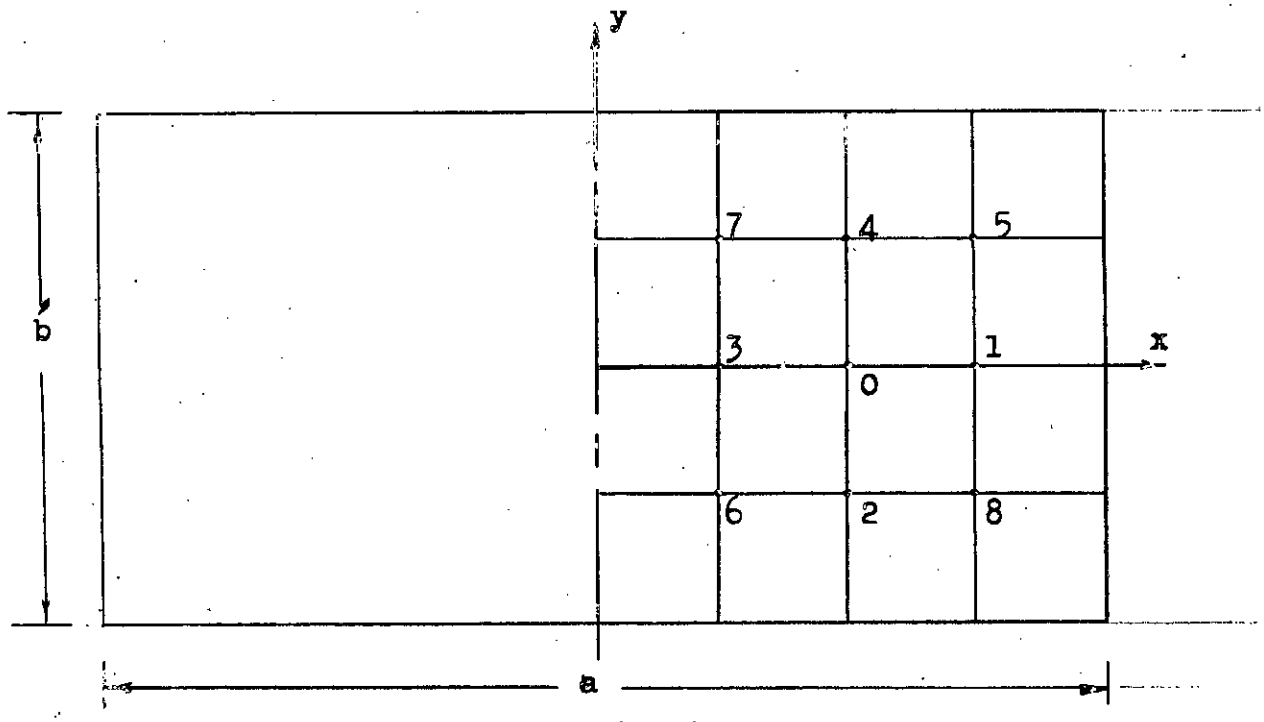

Figure (4.3)
Grading of a rectangular
waveguide into square meshes.

$$4\phi_o - \sum_{i=1}^{4} \phi_i = \frac{k_o^2 h^2}{12} \left(6\phi_o + \sum_{i=1}^{6} \phi_i \right) \tag{4.22}$$

for triangular element,

$$4\phi_o - \sum_{i=1}^{4} \phi_i = k_o^2 h^2 \phi_o \tag{4.23}$$

for 5-point finite-difference,

$$8\phi_o - \sum_{i=1}^{8} \phi_i = \frac{k_o^2 h^2}{6} \left(8\phi_o + 2 \sum_{i=1}^{4} \phi_i + \tfrac{1}{2} \sum_{i=5}^{8} \phi_i \right) \tag{4.24}$$

for square mesh finite-element, and

$$8\phi_o - \sum_{i=1}^{8} \phi_i = 3\, k_o^2 h^2 \phi_o \tag{4.24a}$$

for 9-point finite-difference.

Results of the numerical computations for $(k_o a)^2$ as given in Tables (4.2) and (4.3) show that for square waveguide, the order of accuracy obtained by the finite-element method with square mesh is almost the same as the 5-point finite-difference method for the same number of discretised equations, but for aspect ratio 4/9, finite-element computations (both square and triangular elements) produce better approximation than the finite-difference approximation. For both waveguides, in finite-element method, square mesh grading produces consistently better results than the triangular mesh grading and this is not so in the case of the finite-difference method.

Table 4.2 TM_{11}-Mode in a Rectangular Waveguide

Aspect ratio $\frac{b}{a} = 1.00.$

$\frac{h}{a}$	$(k_0a)^2$ Finite-Element		$(k_0a)^2$ Finite-Difference	
	□-element	◿-right triangular element	5-point	9-point
$\frac{1}{2}$	24.000	32.000	16.000	10.667
$\frac{1}{4}$	20.773	22.848	18.745	16.915
$\frac{1}{18}$	19.789	19.876	19.689	19.589
$\frac{1}{36}$	19.752	19.772	19.727	19.702

Analytic $(k_0a)^2 = 19.739$

Table 4.3 Same Waveguide as in Table (4.2) with

Aspect ratio $\frac{b}{a} = 4/9$

$\frac{h}{a}$	$(k_0a)^2$ Finite-Element		$(k_0a)^2$ Finite-Difference	
	□- element	◿-element	5-point	9-point
$\frac{1}{18}$	60.505	60.903	57.219	58.671
$\frac{1}{36}$	60.001	60.156	59.171	59.542
$\frac{1}{72}$	59.877	59.905	59.668	59.764

Analytic $(k_0a)^2 = 59.834.$

4.5 Circular Waveguide

If in a two dimensional boundary value problem, the functional variation of the fields with respect to any one of the dimensions is known, then the corresponding extremum functional can be written in terms of only one variable. For a circular waveguide, the extremum functional is given by

$$J(\phi) = \int_S \left(\frac{\partial \phi}{\partial r}\right)^2 r\,dr\,d\theta + \int_S \frac{1}{r}\left(\frac{\partial \phi}{\partial \theta}\right)^2 dr\,d\theta - k_o^2 \int_S \phi^2\, r\,dr\,d\theta \tag{4.24}$$

where ϕ is the longitudinal component of the appropriate field vector. In a circular waveguide, the azimuthal variation of ϕ takes the form $\cos n\theta/\sin n\theta$. If we insert the above form of θ dependence for ϕ into equation (4.24) and integrate with respect to θ, then the resultant integrals will be functions of r only. We now divide the radius 'a' into a number of line segments as shown in Figure (4.4), each of these segments becoming the element in a one-dimensional problem. We assume a linear variation of the field over each element and following the procedure discussed earlier, we obtain a set of linear algebraic equations. The solutions of the lowest eigenvalue of this set of equations will correspond to the wavenumber for TE_{n1} or TM_{n1} mode. To illustrate this, a few of the typical discretised equations for TM_{01}, TM_{11} and TE_{11} modes corresponding to the scheme of grading as shown in Figure (4.4) are given below:

(a) TM_{01}-Mode:

If 'P' is an interior vertex, then

$$-(2P-1)\phi_{(P-1)} + 4P\phi_P - (2P+1)\phi_{(P+1)} = \frac{(k_o h)^2}{6}\left\{(2P-1)\phi_{P-1} + 8P\phi_P \quad (2P+1)\phi_{(P+1)}\right\} \tag{4.25}$$

and for the vertex at the centre of the guide

$$\phi_o - \phi_1 = \frac{(k_o h)^2}{6}(\phi_o + \phi_1) \tag{4.26}$$

where h is the length of each element.

(b) TM_{11}-Mode:

For TM_{11}-mode, all effective vertices are interior vertices and for any vertex 'P', we obtain:

$$-\left[P(P-1)\ln\left(\frac{P}{P-1}\right)\right]\phi_{P-1} + \left[(P-1)^2\ln\left(\frac{P}{P-1}\right) + (P+1)^2\ln\left(\frac{P+1}{P}\right)\right]\phi_P$$

$$-\left[P(P+1)\ln\left(\frac{P+1}{P}\right)\right]\phi_{(P+1)} = \frac{(k_o h)^2}{12}\left[(2P-1)\phi_{(P-1)} + 8P\phi_P + (2P+1)\phi_{(P+1)}\right] \tag{4.27}$$

(c) TE_{11}-Mode:

For all interior vertices the discretised equations will be the same as equation (4.27) but for the vertex N at the guide wall. This becomes:

$$-\left[N(N-1)\ln\left(\frac{N}{N-1}\right)\right]\phi_{N-1} + \left[1 + (N-1)^2\ln\left(\frac{N}{N-1}\right)\right]\phi_N$$

$$= \frac{(k_o h)^2}{12}\left[(2N-1)\phi_{N-1} + (4N-1)\phi_N\right] \tag{4.28}$$

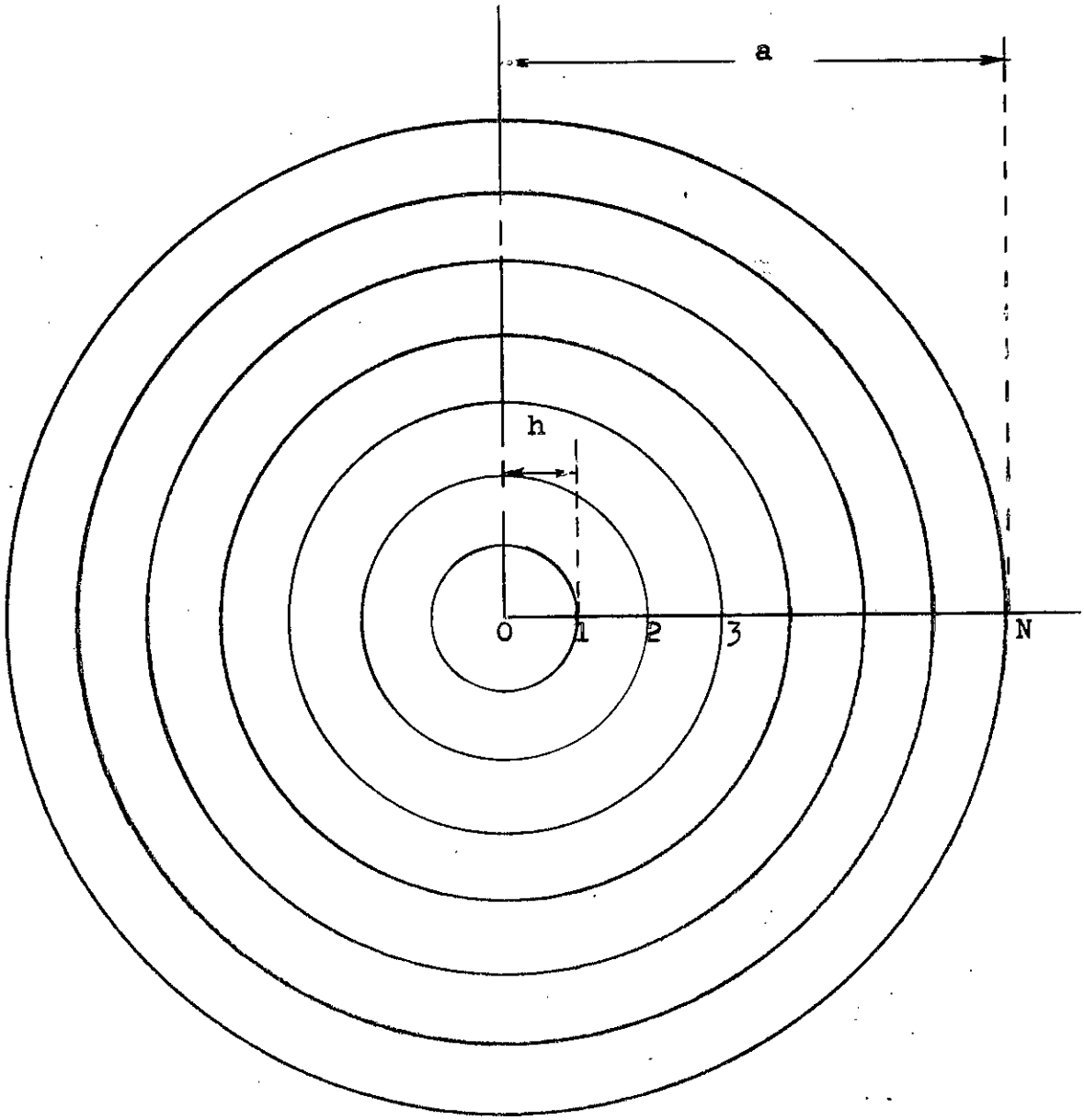

Figure (4.4)
Cross-section of a
Circular Waveguide

Numerical computations of wavenumber $(k_o a)^2$ for a circular waveguide sustaining TM_{01}, TM_{11} and TE_{11} modes are given in Tables (4.4), (4.5) and (4.6). To show the relative advantage of the finite-element method for this type of problem over the finite-difference method, results of numerical computations of the above waveguide as reported by Muilwyk[4] are given in Tables (4.7), (4.8) and (4.9).

A comparative study shows that the errors in $(k_o a)^2$ is significantly larger in finite-difference method. This is partly because of the imperfect fittings of the mesh to the boundary and partly because of the lack of using the azimuthal symmetry that exists in a circular waveguide sustaining TM_{01} mode and also because of the lack of using the known azimuthal variations for TE_{11} and TM_{11} modes.

4.6 Boundary Matching

The theory developed in this thesis can be suitably applied to problems with arbitrary boundaries. In the finite-element method, an arbitrary boundary is approximated by a set of piece wise linear boundaries. The common points between successive linear boundaries are considered as boundary vertices. The resultant eigenvalue operators still remain symmetric. As an illustration a circular waveguide is analysed numerically in cartesian co-ordinates for TM_{01}-mode, and the curved boundary is discretised as shown in Figures (4.5),

Table 4.4 A Circular Waveguide sustaining E_{01} Mode

Finite-Element Method

h/a	$(k_o a)^2$	$k_o a$	% Error	Extrap. $(k_o a)$	Extrap. % Error
1	6.000	2.450	1.860		
$\frac{1}{2}$	5.858	2.420	0.620		
$\frac{1}{3}$	5.827	2.414	0.372	2.405	0.0005
$\frac{1}{4}$	5.810	2.410	0.206	2.395	-0.415
$\frac{1}{5}$	5.802	2.409	0.145	2.406	0.042
$\frac{1}{6}$	5.796	2.408	0.104	2.404	-0.063
$\frac{1}{7}$	5.793	2.407	0.075	2.405	0.025
$\frac{1}{8}$	5.791	2.406	0.058	2.406	0.037
$\frac{1}{9}$	5.789	2.406	0.041		
$\frac{1}{20}$	5.784	2.405	0.0005		

First root of J_o (K_a), $K_a = 2.405$

Table 4.5 TM_{11}-Mode in a Circular Waveguide

Finite-Element Approximation

$\frac{h}{a}$	$(k_o a)^2$	$k_o a$	% Error	Extrap. $k_o a$	Extrap. % Error
$\frac{1}{2}$	16.636	4.079	6.40		
$\frac{1}{3}$	15.546	3.942	2.86		
$\frac{1}{4}$	15.168	3.894	1.59		
$\frac{1}{5}$	14.994	3.872	1.04		
$\frac{1}{6}$	14.899	3.859	0.71		
$\frac{1}{7}$	14.842	3.852	0.52		
$\frac{1}{8}$	14.805	3.847	0.39	3.840	0.208
$\frac{1}{9}$	14.779	3.844	0.31	3.841	0.235
$\frac{1}{10}$	14.760	3.841	0.23		

First root of $J_o'(K_a)$, $K_a = 3.832$

Table 4.6 H_{11}-Mode in a Circular Waveguide

Finite-Element Approximation

$\frac{h}{a}$	$(k_o a)^2$	$(k_o a)$	% Error	Extrap. $k_o a$
1	4.000	2.000	8.70	
$\frac{1}{2}$	3.518	1.875	0.84	
$\frac{1}{3}$	3.446	1.856	0.81	
$\frac{1}{4}$	3.421	1.850	0.45	1.844
$\frac{1}{5}$	3.410	1.848	0.37	
$\frac{1}{6}$	3.404	1.845	0.21	
$\frac{1}{7}$	3.400	1.844	0.15	
$\frac{1}{8}$	3.398	1.843	0.11	1.842
$\frac{1}{9}$	3.396	1.842	0.08	1.841

First root of $J_1(K_a)$ $K_a = 1.841$

Table 4.7 Circular Waveguide E_{01}-Mode

Finite-Difference Method (outside approx.)

$\frac{h}{a}$	$(k_o a)^2$	$k_o a$	% Error	Extrap. $k_o a$	% Error Extrap.
$\frac{1}{4}$	5.133	2.266	-5.80		
$\frac{1}{8}$	5.440	2.332	-3.0		
$\frac{1}{16}$	5.582	2.363	-1.80	2.389	-0.70
$\frac{1}{32}$	5.669	2.381	-1.00	2.411	0.25
$\frac{1}{64}$	5.725	2.393	-0.50	2.412	0.30
$\frac{1}{128}$	5.756	2.399	-0.25	2.407	0.10

Table 4.8 Circular Waveguide E_{01} Mode

Finite-Difference Method (Inside approximation)

$\frac{h}{a}$	$(k_o a)^2$	$k_o a$	% Error	Extrap. $k_o a$	% Error
$\frac{1}{4}$	8.027	2.833	17.80		
$\frac{1}{8}$	6.883	2.624	9.10		
$\frac{1}{16}$	6.249	2.499	3.90	2.337	-2.80
$\frac{1}{32}$	6.001	2.449	1.90	2.417	0.50
$\frac{1}{64}$	5.840	2.427	0.90	2.408	0.10
$\frac{1}{128}$	5.838	2.416	0.50	2.408	0.10

Table 4.9 Circular Waveguide H_{11} Mode

Finite-Difference Method (Outside Approx.)

h/a	$(k_0a)^2$	k_0a	% Error	Extrap. k_0a	%Error Extrap.
$\frac{1}{4}$	2.956	1.719	-6.60		
$\frac{1}{8}$	3.109	1.763	-4.20		
$\frac{1}{16}$	3.236	1.799	-2.30	1.956	6.20
$\frac{1}{32}$	3.299	1.808	-1.30	1.834	-0.40
$\frac{1}{9}$	3.121	1.767	-4.10		
$\frac{1}{18}$	3.251	1.803	-2.10		
$\frac{1}{36}$	3.518	1.821	-1.10	1.840	-0.30
$\frac{1}{72}$	3.354	1.831	-0.50	1.843	0.10

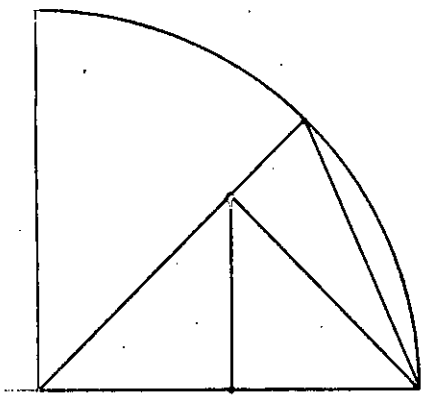

Figure (4.5)

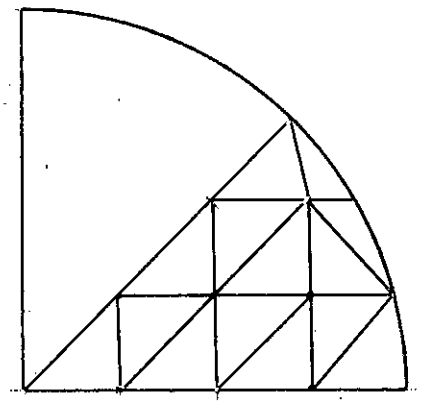

Figure (4.6)

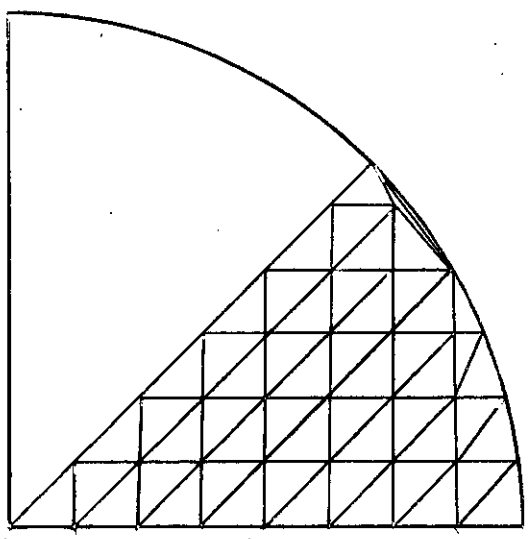

Figure (4.7)

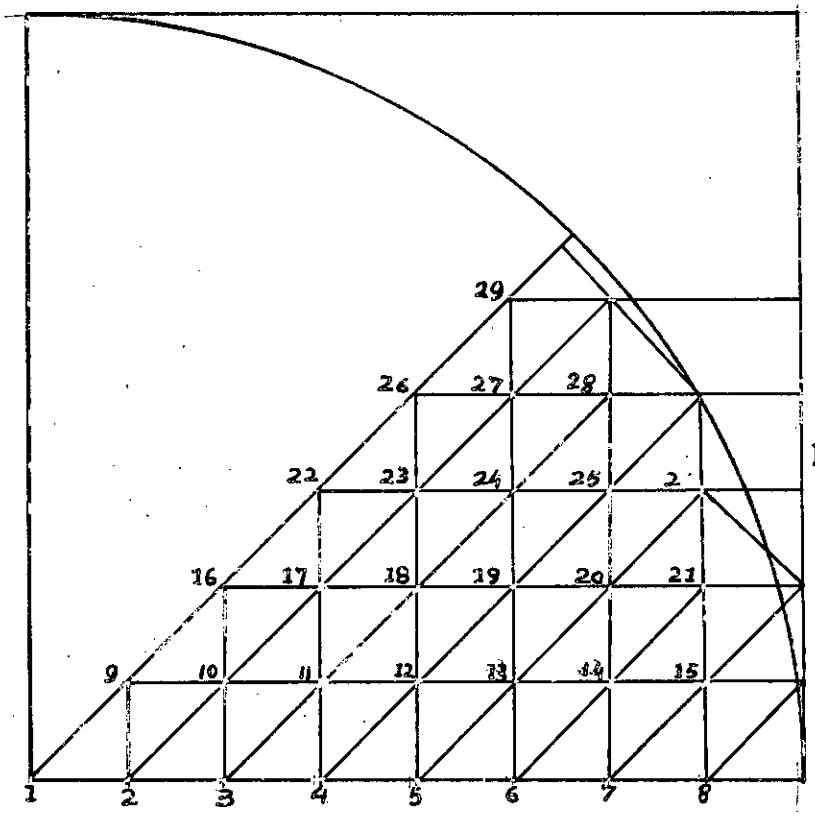

Figure (4.8)

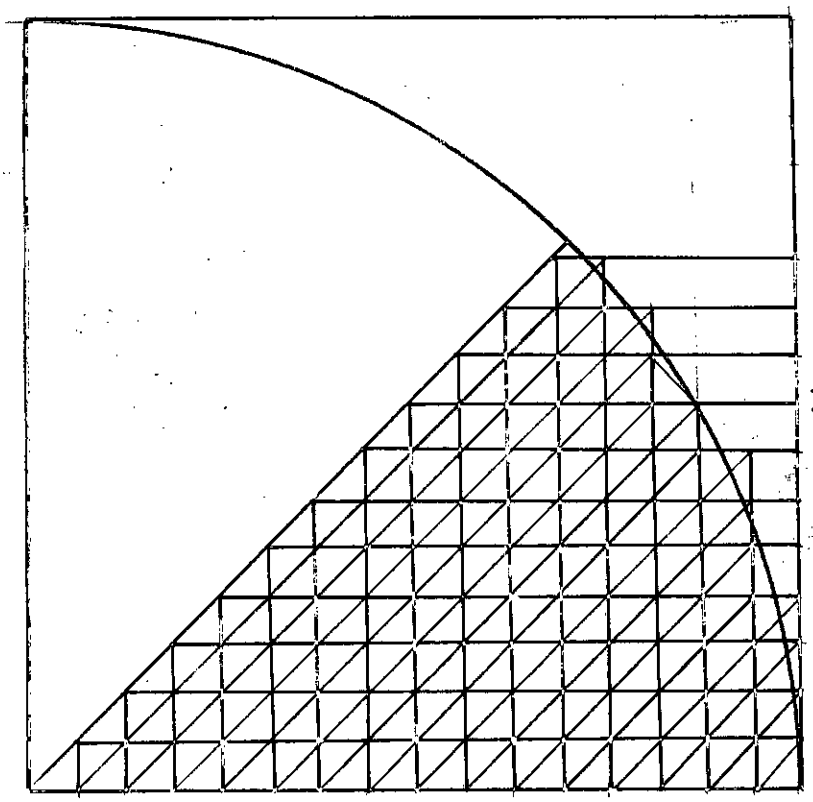

Figure (4.9)

(4.6) and (4.7). Also, to see the effect of the perturbation of the boundary on TM_{01} mode, a circular waveguide is divided into a number of elements as shown in Figures (4.8) and (4.9). Numerical results are tabulated in Table (4.10). Comparing the computed results with the exact result, we find that the rate of convergence is fairly rapid and the wavenumber is not very sensitive for a slight change of the physical boundary.

Table 4.10 TM_{01}-Mode in a Circular Waveguide in Cartesian Co-ordinates

$\frac{h}{a}$	Fig. No.	Number of Effective Nodes	$(k_0a)^2$	k_0a	Analytical k_0a
1/2	4 - 5	3	6.90	2.63	
1/4	4 - 6	9	6.30	2.51	
1/8	4 - 7	31	6.07	2.46	2.405
1/8	4 - 8	29	6.01	2.45	
1/16	4 - 9	107	5.96	2.44	

4.7 Singularities in Waveguides

4.7.1 Mathematical Approach to Singular Points in Waveguide Problems

In a homogeneous waveguide when the guide wall changes direction through an interior angle greater than π, a mathematical singular point is created. This type of corner in a waveguide system is, normally, referred to as a re-entrant corner. Re-entrant corners exist in L-shaped

waveguide, ridged waveguide, channel waveguide, etc. Near the sharp corner the scalar potential ϕ as appropriate to a particular mode of propagation, varies rapidly. This can be verified by expanding the transverse Laplacian in polar co-ordinates near the re-entrant corner and keeping the origin of the co-ordinates at the corner. This becomes

$$\nabla_t^2 \phi = \frac{\partial^2 \phi}{\partial r^2} + \frac{1}{r}\frac{\partial \phi}{\partial r} + \frac{1}{r^2}\frac{\partial^2 \phi}{\partial \theta^2} \tag{4.28}$$

If the radius of curvature of the re-entrant corner is small compared with the wave length inside the waveguide, then near the close vacinity of the corner, we can approximate the wave equation by Laplace's equation. Now for the Laplace's equation $\nabla_t^2 \phi = 0$, the general form of solution in polar co-ordinates can be written as

$$\left.\begin{aligned} \phi(r,\theta) &= A_m r^m \sin m\theta \\ \text{or} \quad & B_m r^m \cos m\theta \end{aligned}\right\} \text{ for any } m \tag{4.29}$$

If ϕ represents the magnetic field then $\frac{\partial \phi}{\partial n} = 0$ on the guide wall; where $\frac{\partial}{\partial n}$ indicates the derivative normal to the wave-guide wall. An appropriate form of the solution for ϕ near the corner will be

$$\phi(r,\theta) = \sum_{m=0} B_m \cos\left(\frac{m\pi\theta}{\alpha}\right) r^{(m\pi/\alpha)} \tag{4.30}$$

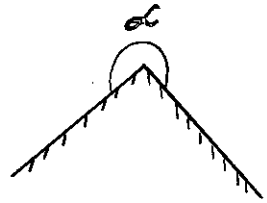

Figure (4.10)

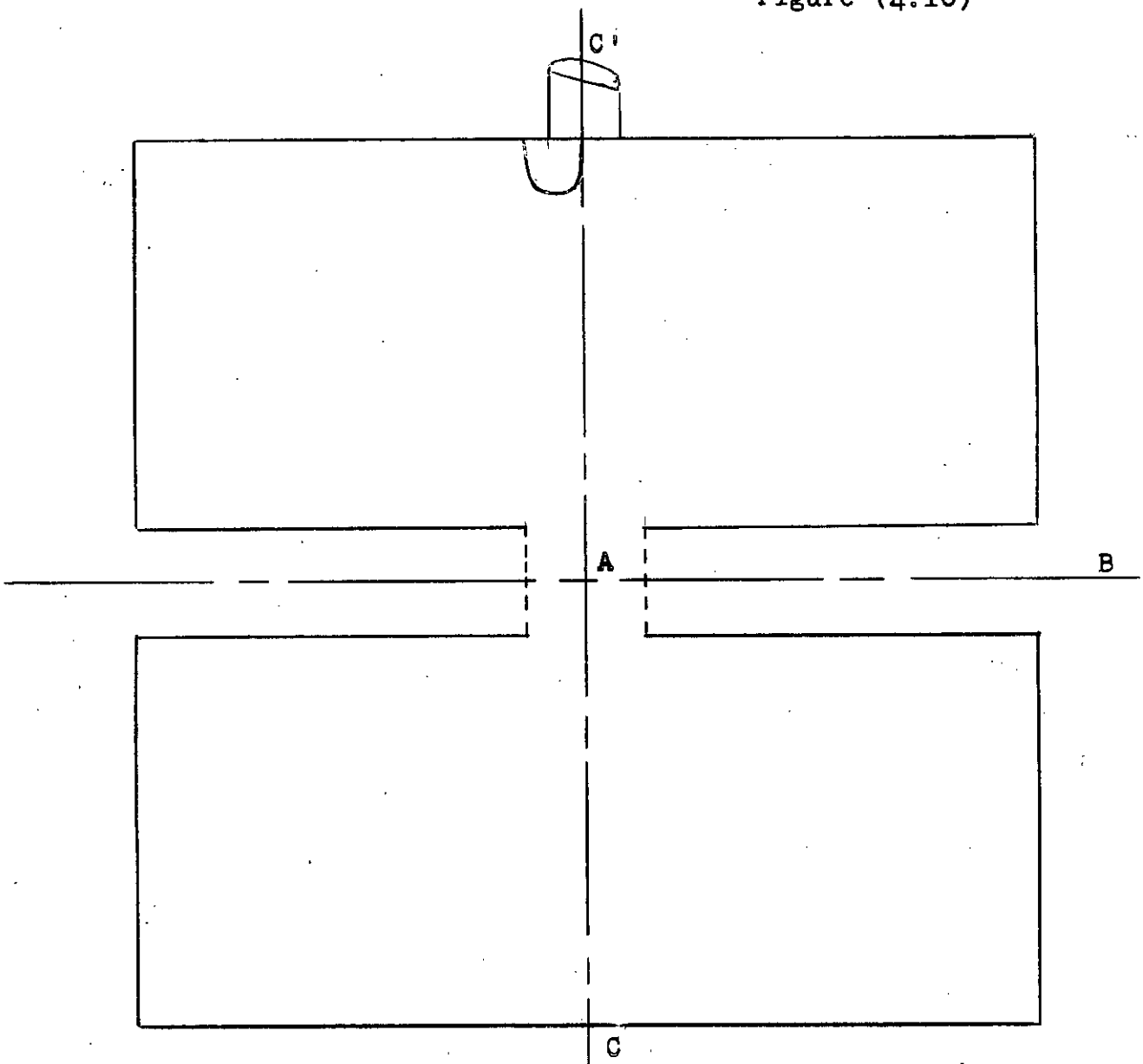

Figure (4.11)
Cross-section of a klystron oscillator

where α is the angle in radians of the re-entrant corner shown in Figure (4.10).

If ϕ represents the longitudinal component of electric field inside the waveguide, i.e. TM-mode propagation then $\phi = 0$ on the guide wall including the re-entrant corner and the solution for ϕ will be

$$\phi\ (r,\theta) = \sum_{k=1} A_k \sin\left(\frac{k\pi\theta}{\alpha}\right) r^{(k\pi/\alpha)} \tag{4.31}$$

In either case, it can be seen that for $\alpha > \pi$ the exponent of r is less than unity for k=1 and normal derivative $\frac{\partial\phi}{\partial n}$ does not exist at the origin. In this respect re-entrant corner in waveguide raises severe theoretical problems.

4.7.2 Practical Treatment of Singular Points

Exact analytic solution in compact form cannot be obtained for singular problems. So far, the finite difference formulation of the waveguide problems treated this type of singular points in two different ways. The first method consists of subtracting the singular point from the finite-difference field and this is done by considering a finer mesh near the singular point and ignoring the existence of the singular point. This type of formulation cannot be justified mathematically. In the other method which was proposed by Motz[5] (1946) and Woods[6] (1953), fields at nodes near the singular point are approximated by a few

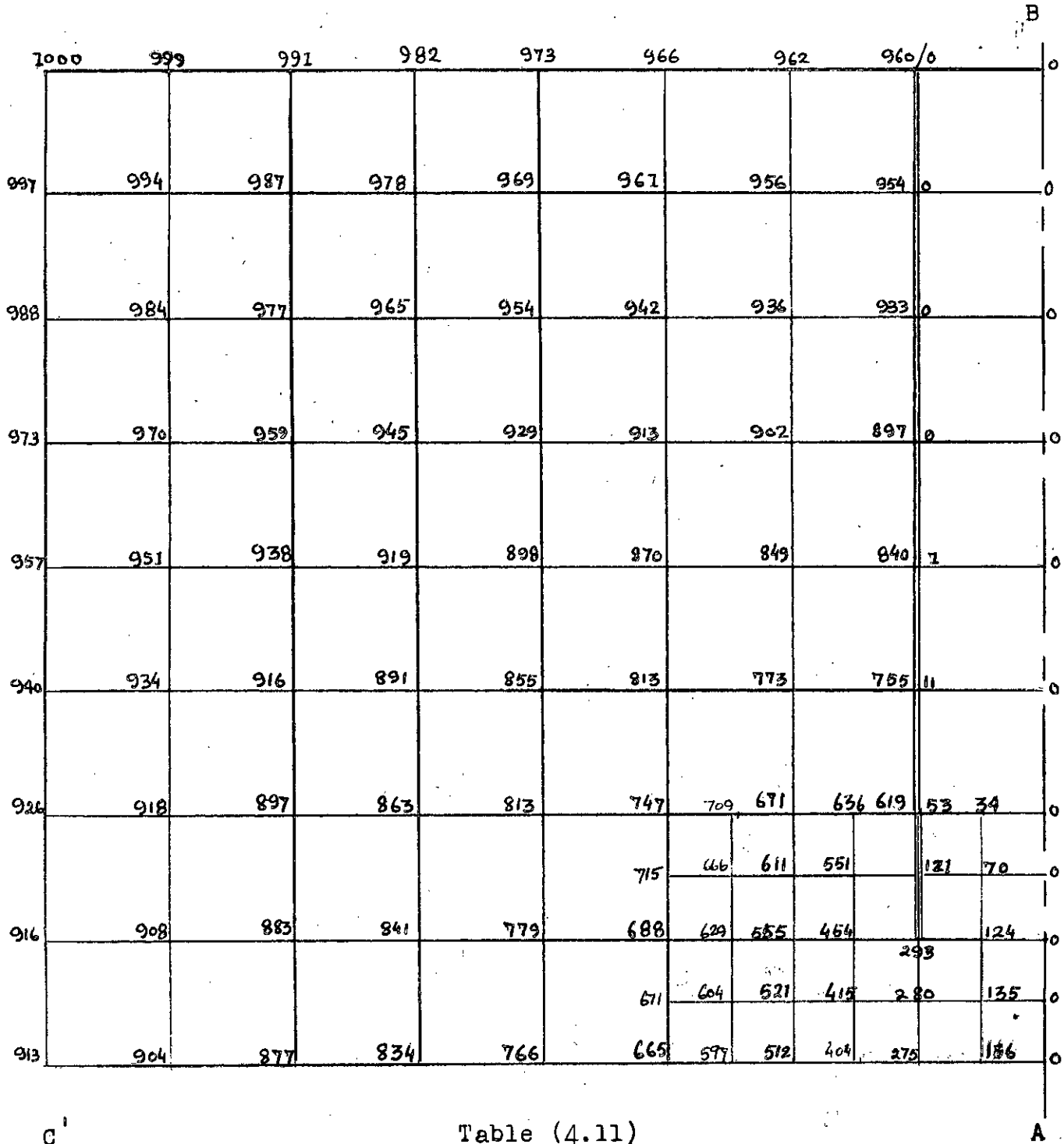

Table (4.11)
Finite-Difference Solution to Fields
in a Klystron Cavity Oscillator (Fig. 4.11)

	1000	999	993	987	977	969	963	961/0				0
997	995	990	982	972	963	957	954	0				0
989	987	980	962	957	945	937	933	0				0
977	973	964	950	932	916	902	897	0				0
961	957	944	925	900	873	857	842	2.6				0
945	939	923	896	860	818	778	759	12				0
930	923	904	869	819	754	716	677	642	624	55	36	0
					723	673	617	557	509	123	71	0
921	913	890	849	787	696	636	560	459	296		126	0
					679	612	528	420	283		137	0
917	909	885	841	774	673	604	517	409	278		138	0
C												A'

Table (4.12)
Finite-element Solution to the same
Problems as in Table (4.11)

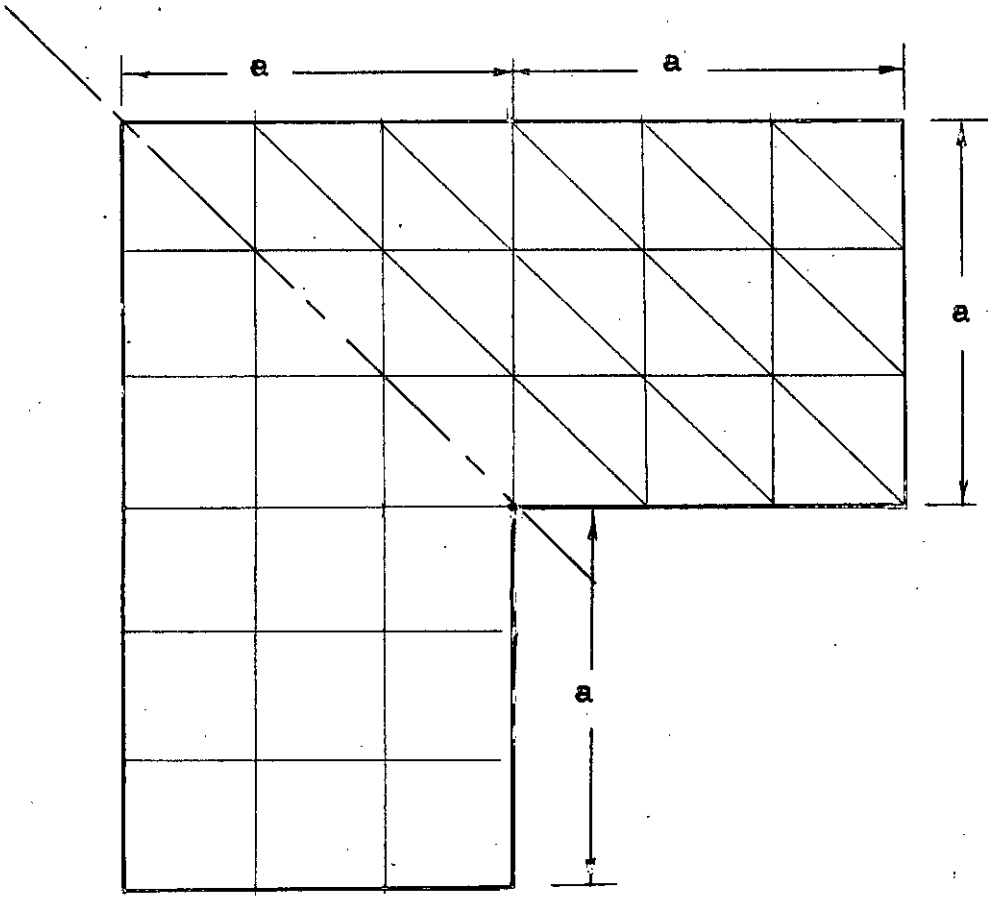

Figure (4.12)
Cross-section of a
L-Shaped Waveguide

terms of a relevant series. In particular, Motz considered a case for $\alpha = 2\pi$, and this is shown in Figure (4.11) and the finite-difference approximation of the fields is shown in Table (4.11).

In the finite-element method no special treatment is required for singular point and it can be treated in the same way as any other ordinary point. This is physically conceivable, because, singularity is a local effect and indeed in any physical problem of wave propagation, all field components will have continuous derivatives of all order at all points inside the waveguide. Finite-element computations of the field for the same problem as in Figure (4.11) is tabulated in Table (4.12). For comparison, the number of nodes in the finite-element method kept to the same value as that of the finite-difference calculation reported by Motz and Southwell[7].

4.7.3 L-Shaped Waveguide

The geometry of a L-shaped waveguide is shown in Figure (4.12). A wave propagating through such a guide has strong similarity to the dominant mode vibration in an L-shaped membrane. Results of the numerical computations of the dominant mode wavenumber by the finite-element and finite-difference methods are presented in Tables (4.13) and (4.14) respectively. For the symmetric mode, in which

Table 4.13 Fundamental TM-Mode in a L-Shaped Waveguide

Finite-element Method Δ-mesh.

$\frac{h}{a}$	$(k_o a)^2$	$k_o a$	% Error	Extrap. $k_o a$	Extrap. % Error
$\frac{1}{2}$	14.079	3.752	20.08		
$\frac{1}{4}$	10.774	3.282	5.72		
$\frac{1}{6}$	10.181	3.190	2.76	3.170	2.08
$\frac{1}{8}$	9.965	3.156	1.67	3.150	1.45
$\frac{1}{9}$	9.905	3.147	1.38		
$\frac{1}{18}$	9.723	3.118	0.45		
$\frac{1}{36}$	9.667	3.109	0.16	3.105	0.006

Ref. (10) $k_o a = 3.105$

Table 4.14 Same Waveguide as in Table 4.13

* Finite-difference Method

$\frac{h}{a}$	$(k_0a)^2$	k_0a	Error %	Extrap.	Extrap. % Error
$\frac{1}{4}$	9.641	3.105	$\angle$0.007		
$\frac{1}{8}$	9.693	3.113	+0.30		
$\frac{1}{9}$	9.691	3.113	+0.30		
$\frac{1}{18}$	9.670	3.110	+0.20		
$\frac{1}{36}$	9.654	3.107	+0.06	3.099	-0.20
$\frac{1}{72}$	9.646	3.106	0.03	3.105	.009

* The above table is reproduced from Reference 4.

the corner is truly a re-entrant type, the behaviour of the eigenvalue on successive mesh halving is rather remarkable in finite-difference method, in the sense that it is not monotonic on mesh halving. A refinement of interval $\frac{h}{a}$ between $\frac{1}{4}$ to $\frac{1}{8}$ actually gives poorer results (8).

In the finite-element method, for triangular mesh, the difference between the true eigenvalue and the computed one is relatively large for a coarse mesh size but the rate of convergence on successive mesh halving is comparatively rapid. For square mesh, results would be more accurate for the same mesh size. The calculated wavenumber by the finite-element method is always a monotonically decreasing function of mesh halving and extrapolation produces results very close to that given in reference (9).

4.7.4 Ridged Waveguide

It is shown by Cohn[10] and other authors that an introduction of a ridge into a rectangular waveguide decreases the cut-off frequency of the dominant mode while having little effect on the cut-off frequencies of other higher order modes. This property of the ridged waveguide finds its use in the microwave mode isolator, because, in the case of dielectric loaded waveguide isolator, propagation of unwanted mode at higher frequencies is difficult to avoid. The band-width of the dominant mode propagation is larger in ridged

waveguide than the corresponding unridged waveguide.

Exact analytic solutions for a single ridged or a double ridged waveguide are very difficult to obtain and approximate analytic solutions for the cut-off wavelength λ_c for TE_{no}-mode in such a waveguide have been given by Cohn[10], Hopfer[11], and Daly[12]. Hopfer[11] made the analysis of a single ridged waveguide of usual aspect ratio 0.45 and for other aspect ratios he provided correction curves which are essentially a first order correction on the value of the cut-off wavelength at the aspect ratio 0.45. The theoretical basis of Cohn's and Hopfer's analysis is the consideration of the existence of a transverse resonance in a waveguide for propagating mode. The effect of other higher order modes excited by the presence of the discontinuity at the ridge is taken into account by an equivalent discontinuity capacitance.

The transmission of TE_{10} mode in a rectangular waveguide may be represented by two converging TEM waves of free space wavelength λ_o and an angle 2θ between the wave fronts such that

$$\cos 2\theta = \frac{\lambda_o}{2a} \tag{4.32}$$

where a is the broad side width of the waveguide. For the dominant mode in a ridged rectangular waveguide, Pyle[13], using the above principle, approximated a ridged waveguide by two parallel plate transmission lines of different heights

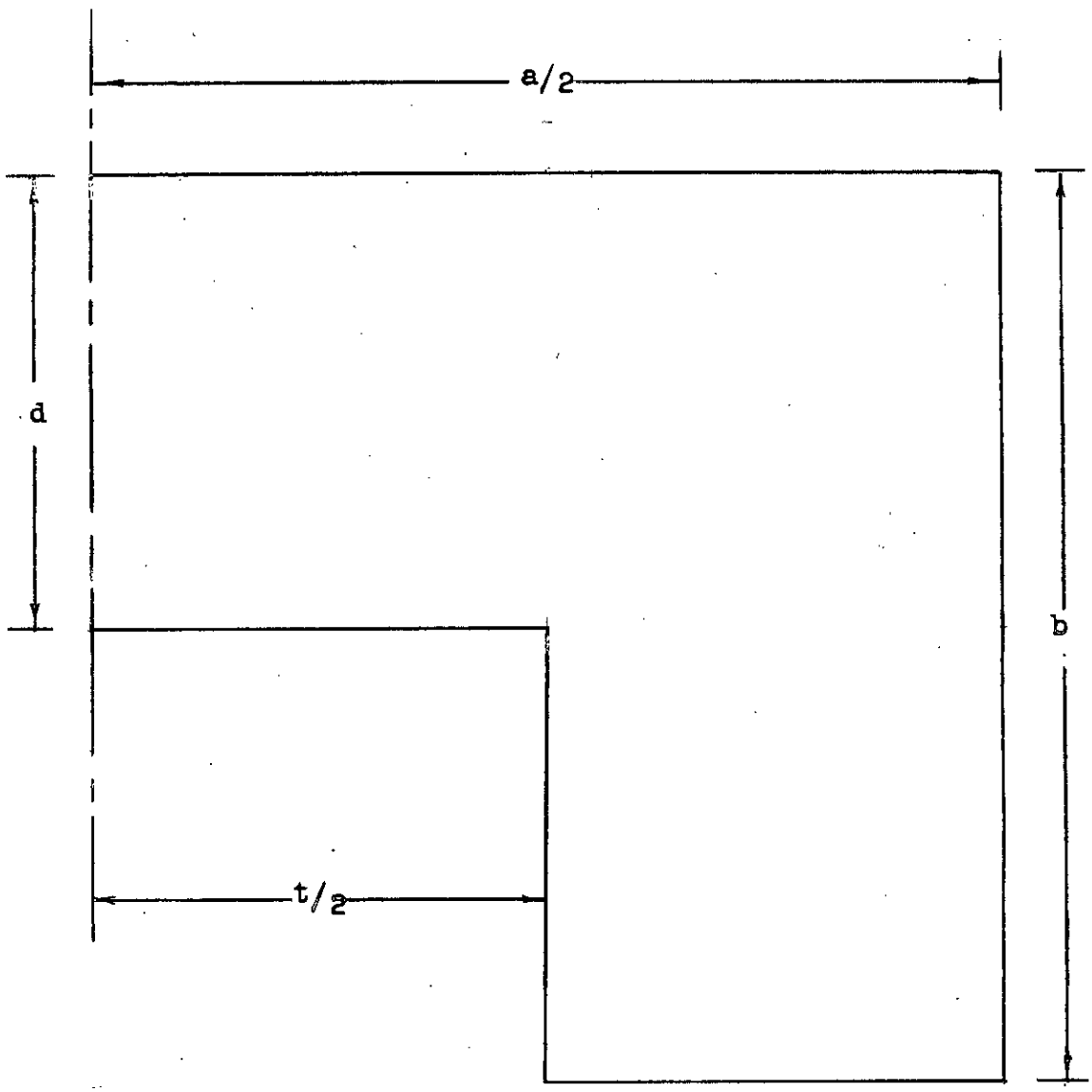

Figure (4.13)
Half cross-section of a
Ridged Rectangular Waveguide

propagating in the transverse direction. The outer parallel plate X-line is shorted at one end and the other end is connected to the inner parallel plate-transmission line; and then considered the case of resonance from transmission line equations. Pyle also modified the first order correction curves given by Hopfer to get more accurate curves. He considered the effect of the proximity of the outer walls on the discontinuity capacitance. Pyle states that the design tables and graphs published by him for worst configuration of the ridge may be in error by a few percent.

Daly[12] gave an approximate theoretical solution for the cut-off relation and for the fields by considering orthogonal mode approach. In this method, a general solution of wave equation in rectangular co-ordinates can be written for each region of the ridged waveguide in the form of an infinite series whose co-efficients are determined by applying the appropriate boundary conditions on the guide walls, on the axis of symmetry as well as on the line of discontinuity between two regions.

The geometry of a single ridged waveguide is shown in Figure (4.13). The existence of singular points in such a waveguide makes the problem complicated for treating by the standard finite-difference method. This problem when treated by the finite-element method for evaluating the wavenumber

as well as for finding the normalised axial component of magnetic field for the dominant mode propagation gives an upper bound to the wavenumber and the wavenumber smoothly approaches the true value as the mesh size decreases, irrespective of the value of the ratios $\frac{t}{a}$ and $\frac{d}{b}$. The results of the wavenumber computed for $\frac{t}{a} = 0.5$, $\frac{b}{a} = 0.45$ and $\frac{d}{b} = 0.5$ are tabulated in Table (4.15). The same table also shows the approximate analytic results given by Cohn[10] (transverse resonance), Daly[12] (normal mode approximation) and the experimental results reported by Daly[12]. Table (4.16) shows the comparative results of the finite-element computations (Triangular mesh and square mesh) and the finite-difference computations.

4.7.5 Channel Waveguide

The configuration of a channel waveguide is shown in Figure (4.14). The use of this type of waveguide was proposed to have increasing power handling capacity. In 1962, Vilmur and Ishii[14] reported the result of an investigation to determine the cut-off wavelength for a range of channel depths and widths. They made the analysis by using the field matching technique of Iashkin[15] and also by the transverse resonance method of Cohn[10]. They found that two approaches produced appreciably different results.

Table 4.15 Dominant Mode Wavenumber in a Single Ridged Waveguide as shown in Figure (4.13)

$\frac{h}{a} = 0.45, \quad \frac{d}{b} = 0.5, \quad \frac{t}{a} = 0.5$

$\frac{h}{a}$	$(2a/\lambda_c)^2$ Finite-element Δ	$(2a/\lambda_c)^2$ Cohn	$(2a/\lambda_c)^2$ Daly	$(2a/\lambda_c)^2$ Experimental - Daly
$\frac{1}{36}$	0.52907	0.585	0.535	0.527
$\frac{1}{72}$	0.52680			

Table 4.16 Dominant Mode Wavenumber in a Single Ridged Rectangular Waveguide as shown in Figure (4.13) with

$\frac{b}{a} = 0.5, \qquad \frac{d}{b} = 0.5, \qquad \frac{t}{a} = 0.5$

Methods used	$\frac{h}{a}$	$(k_o a)^2$	$(k_o a)$	% Error $k_o a$ *	Extrap. $k_o a$
□ mesh F.E	$\frac{1}{8}$	5.226	2.286	1.60	
◿ mesh F.E		5.290	2.300	2.22	
5-point F.D		5.596	2.366	5.20	
□ mesh F.E	$\frac{1}{16}$	5.118	2.262	0.53	
◿ mesh F.E		5.153	2.270	0.89	
5-point F.D		5.275	2.297	2.10	
□ mesh F.E	$\frac{1}{32}$	5.081	2.254	0.17	2.250
◿ mesh F.E		5.097	2.257	0.31	2.247
5-point F.D		5.147	2.269	0.80	2.250
□ mesh F.E	$\frac{1}{64}$	5.070	2.252	0.08	2.251
◿ mesh F.E		5.075	2.253	0.13	2.251
5-point F.D		5.095	2.257	0.30	2.249
□ mesh F.E	$\frac{1}{128}$	5.064	2.250	.01	
◿ mesh F.E		5.067	2.251	0.04	2.250
5-point F.D		5.074	2.253	0.10	2.249
5-point F.D	$\frac{1}{256}$	5.066	2.251	0.04	2.250

* % Error is calculated with respect to results given by Pyle (13), ie. $k_o a = 2.250$

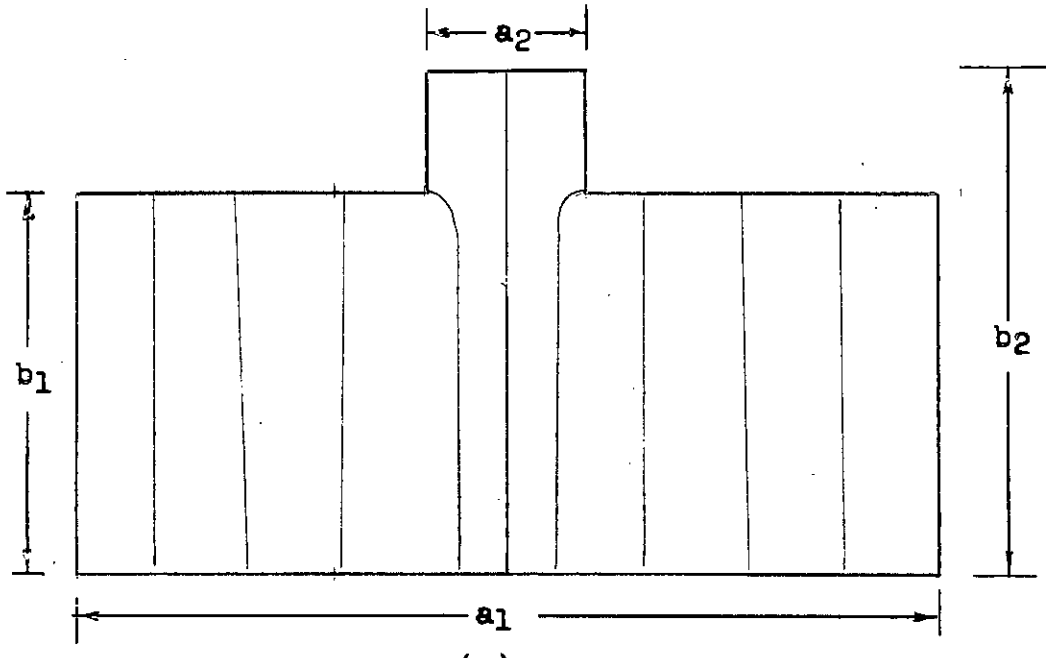

(a)

Figure (4.14)
Channel Waveguide Field Configuration
a) TE_{10} Mode b) TE_{01} Mode

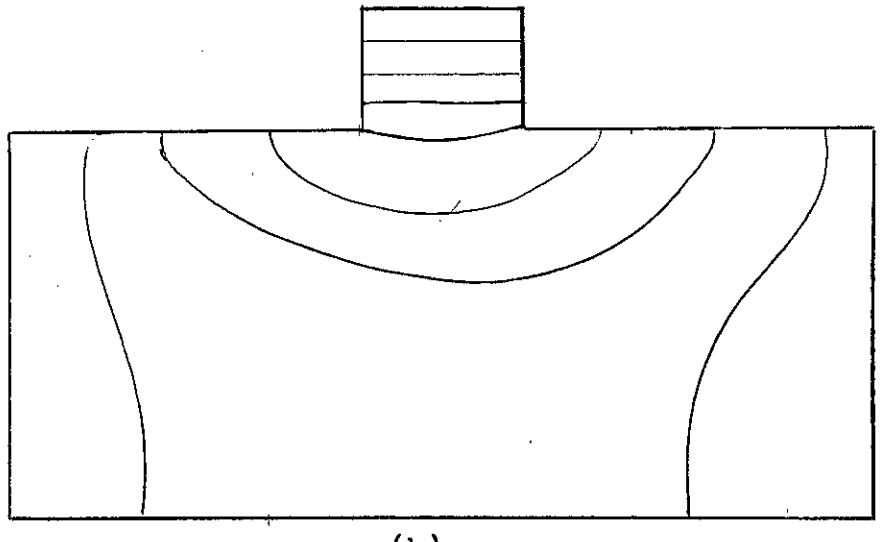

(b)

Later on, Roth and Ishii[16] made some practical experiments to verify this discrepancy. Their observations seemed to indicate that there were indeed two modes of propagation, one following Iashkin's method and the other following Cohn's method. The existence of two propagating modes can be considered by assuming the transverse electric field distribution for the dominant mode as shown in Figures (4.14a) and (4.14b).

Numerical computations of the dominant mode wavenumber corresponding to the transverse electric field distribution as in Figure (4.14a) are performed by the finite-element method and the results are given in Table (4.17).

Table 4.17 TE_{10} type mode in a Channel Waveguide with dimensions as in Figure (4.14a).

$$\frac{a_2}{a_1} = \frac{2}{9}\ ; \quad \frac{b_1}{b_2} = 0.5; \quad \frac{b_1}{a_1} = \frac{4}{9}\ .$$

$\frac{h}{a_1}$	$(k_o a_1)^2$	$k_o a_1$	$\frac{\lambda c}{\lambda cH}$	Experimental Ref. 16
$\frac{1}{18}$	10.3225	3.2120	1.030	
$\frac{1}{36}$	10.2391	3.2014	1.025	1.065
$\frac{1}{72}$	10.2244	3.1975	1.020	

In Table (4.17) λ_c/λ_{cH} is the ratio of the cut-off wavelength of a regular rectangular waveguide to that of the corresponding channel waveguide.

Analyses of a few examples considered in this section show that for all types of homogeneous waveguide problems, the finite-element method can be profitably used in determining the eigenvalues without involving any extra difficulties in treating awkwardly shaped boundaries or singular points.

4.8 Transmission Lines with Singularities

In this section finite-element is used in determining the field distribution and the characteristic impedance of a few transmission lines possessing singular points. For such a problem analytic solution of the distribution of potential and the characteristic impedance sometimes requires involved calculations. A few examples treated in this section will demonstrate the suitability of the finite-element method for striplines.

Transmission lines including the striplines can support TEM wave if the medium is homogeneous. The solution of TEM wave reduces the general wave equation to that of a 2-dimensional Laplace's equation with boundaries determined by the line cross-section. The propagation characteristics for TEM wave depends only on the medium[17,18]. Based on this, the characteristic impedance Z_o is given by

$$Z_o = \sqrt{\frac{L}{C}} = \frac{\sqrt{\mu\epsilon}}{C} \tag{4.33}$$

where C is the capacitance and L is the inductance per unit length of the line.

The capacitance C is related with the supply voltage V, the potential distribution ϕ over the cross-section and the stored energy as follows:

Total electric energy stored/unit length

$$= \frac{1}{2} CV^2 = \frac{\epsilon}{2}\int_s |\nabla_t \phi|^2 \, ds \tag{4.34}$$

where ϕ is a solution of $\nabla_t^2 \phi = 0$ with the given boundary conditions.

It can be shown that for V equal to unity, the expression

$$C = \epsilon\int_s |\nabla_t \phi|^2 \, ds \tag{4.35}$$

is a variational functional for C and is an upper bound to C. The discretised finite-element equations for ϕ will be of the form

$$\underline{A}\,\underline{\Phi} = \underline{b} \tag{4.36}$$

where $\underline{A}$ and $\underline{\Phi}$ convey the same meaning as described earlier and $\underline{b}$ is a column vector whose components are given by the boundary condition on the potential ϕ. Solution of the matrix equation (4.36) gives the distribution of ϕ over the discrete set of points within the transmission line as generated by the finite-element discretisation.

4.8.1 Determination of Capacitance

In order to determine C approximate methods (for complicated line structure—normally strip lines) based on the estimates for the fringing capacitance were first introduced[19,20]. Later a number of workers used conformal mappings[21-29], but few cases usually assuming infinitely thin conductors can be calculated in closed form, even they lead to rather complicated expressions in elliptic functions; otherwise an approximation must be made to obtain usable results.

In the finite-difference method, C is, usually, determined by numerically evaluating the following integrals:

$$C = \epsilon_0 \oint_c \phi \frac{\partial \phi}{\partial n} \, dl \tag{4.37}$$

where $\frac{\partial \phi}{\partial n}$ is the normal derivative of ϕ on a closed path c surrounding the live conductor. The presence of singular points requires to make certain approximation to $\frac{\partial \phi}{\partial n}$ at points near the singularities. In the finite-element method we do not require any such approximation and we can calculate the capacitance by evaluating the total stored electric energy as follows:

$$\frac{C}{\epsilon} = \int_s |\nabla_t \phi|^2 \, dxdy = \int_s \left\{ \left(\frac{\partial \phi}{\partial x}\right)^2 + \left(\frac{\partial \phi}{\partial y}\right)^2 \right\} dxdy \tag{4.38}$$

Now over an element, ϕ is approximated by

$$\phi^e(x,y) = \sum_k N_k(x,y)\ \phi_k \tag{4.39}$$

where $N_k(x,y)$ is an algebraic polynomial in x,y and its nature depends on the shape of the elements under consideration.

Therefore over the element 'e', we obtain

$$\left.\frac{\partial \phi}{\partial x}\right|_e = \sum_k \frac{\partial N_k}{\partial x}\ \phi_k \tag{4.40}$$

and

$$\left.\frac{\partial \phi}{\partial y}\right|_e = \sum_k \frac{\partial N_k}{\partial y}\ \phi_k \tag{4.41}$$

Therefore, contribution to C by an element 'e' is given by

$$\left.\frac{C}{\epsilon}\right|_e = \sum_k \sum_r \int_e \left[\frac{\partial N_k}{\partial x}\cdot\frac{\partial N_r}{\partial x} + \frac{\partial N_k}{\partial y}\cdot\frac{\partial N_r}{\partial y}\right]\phi_k\phi_r\ dxdy$$

$$= \sum_r \sum_k S^e_{rk}\ \phi_r\phi_k \tag{4.42}$$

Hence, $\left.\frac{C}{\epsilon}\right|_e$ can be written in matrix notation as

$$\left.\frac{C}{\epsilon}\right|_e = \underline{\Phi}^{eT}\ \underline{S}^e\ \underline{\Phi}^e \tag{4.43}$$

where $\underline{S}^e$ is an element submatrix whose components depend on the nature of N(x,y) and $\underline{\Phi}$ is a column matrix whose components are the values of ϕ at the vertices of element 'e'.

If there are in all R elements into which the entire cross-section is subdivided then the total capacitance C_T would be

$$\frac{C_T}{\epsilon_o} = \sum_{e=1}^{R} \underline{\phi}^{eT} \; \underline{S}^e \; \underline{\phi}^e$$

$$= \underline{\phi}^T \; \underline{D} \; \underline{\phi} \qquad (4.44)$$

where the matrix $\underline{D}$ differs from the matrix $\underline{A}$ in that the order of the matrix D is determined by the sum total of the interior vertices and the vertices on the live conductor but the order of the matrix $\underline{A}$ is determined by the number of interior vertices only.

4.8.2 Numerical Results

4.8.2a Square Transmission Line

This problem has been worked out by Gilles[30], Jeffreys[31] and Woods.[6] Jeffreys and Woods made allowances for the singular points. Figure (4.15) shows a portion of the cross-section of a square cable. The inner conductor is considered to be at 10,000 volts. AB and CD are lines of symmetry. Elements are considered to be right triangular in shape and the corresponding N(x,y) is assumed to be linear in form, i.e.

$$N(x,y) = \alpha_0 + \alpha_1 x + \alpha_2 y$$

over the element. Numbers at positions (a),(b) and (c) in Figure (4.15) correspond to the values of potential given by the finite-elements, Jeffrey's, and Wood's methods respectively.

A comparative study of the potential distribution given in Fig.(4.15) shows that near singular point results given by Jeffrey's method are closer to that obtained by the finite-element method and at other regular points F.E. and F.D. results agree quite favourably. Jeffrey[31] obtained

(a)= Finite-element
(b)= Jeffrey's
(c)= Woods(FD)

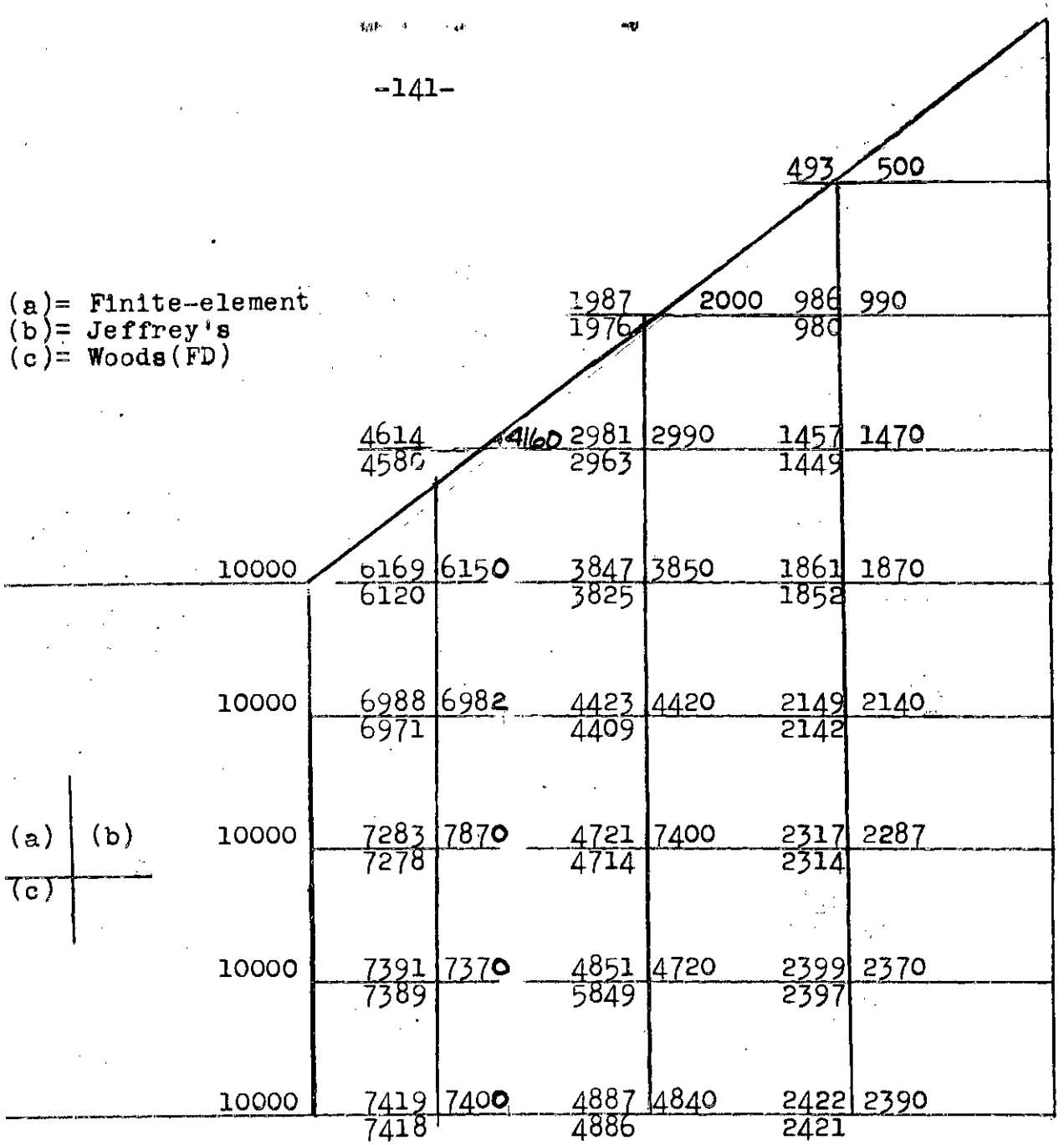

Figure (4.15)

C = 0.821 e.s.u., while Gilles, ingnoring singularity, found C = 0.832 e.s.u. An analytic result which is presumably quite accurate was given by Bowman[32]. He found C = 0.8144. We calculated capacitance for three different mesh sizes and they are as follows:

$\frac{h}{a} = \frac{1}{6}$, C = 0.8230 e.s.u.,

$\frac{h}{a} = \frac{1}{10}$, C = 0.8192 e.s.u.,

$\frac{h}{a} = \frac{1}{16}$, C = 0.8170 e.s.u.

4.8.2b Homogeneous Strip Line

A homogeneous strip line with two inner strips placed between two parallel ground planes is shown in Figure (4.16). It is apparent from symmetry that capacitance of such a line is four times that of the reduced line shown in Figure (4.17). For numerical analysis we assumed that the two outer ground planes are shorted at the ends. It is shown[22] that for a fixed separation of the ground planes, if the ratio of the width of the ground plane to the width of the inner strip exceeds a certain value, then the exact impedance and the approximate value obtained by assuming infinite width ground planes agree within less than one percent. Potential distribution and the characteristic impedance of

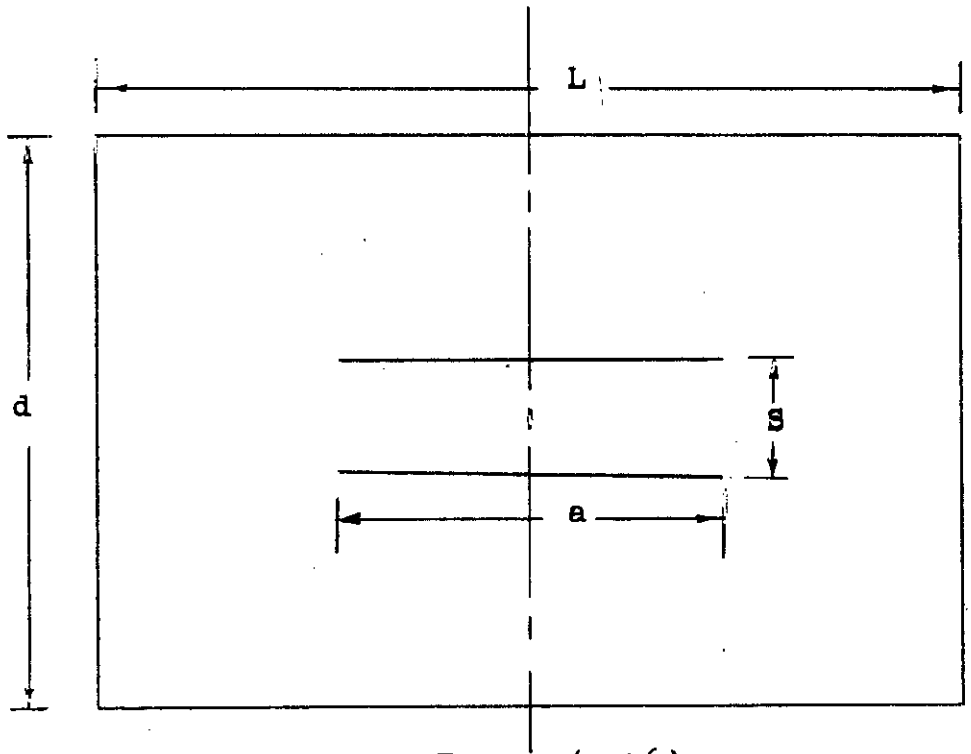

Figure (4.16)
The Basic Triplate Line

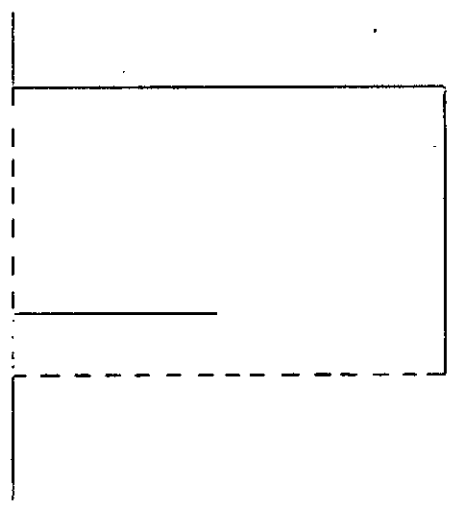

Figure (4.17)
Reduced Triplate Line
Solid lines indicate electric walls and broken lines indicate magnetic walls.

Table (4-18). Potential Distribution of a Strip Line as in Fig. (4-16)

Top figures $\frac{L}{d} = 2.50$, Bottom figures $\frac{L}{d} = 3.5$, $\frac{h}{b} = \frac{1}{40}$

$Z_0 = 49.277934$ for $\frac{L}{d} = 3.5$,

$= 49.036271$ for $\frac{L}{d} = 2.5$.

246 246	245 245	242 242	234 234	218 216	192 193	158 160	123 127	91 96	64 73	42 68
495 495	493 493	488 490	475 475	446 447	393 396	319 323	242 249	176 186	124 137	91 100
747 747	745 745	741 741	730 730	701 702	621 623	479 483	349 358	249 262	172 192	112 140
1000 	1000 	1000 	1000 	1000 	1000 	605 611	425 435	298 314	205 228	138 165
1000 	999 999	998 999	992 993	967 967	858 860	630 634	451 462	316 332	213 240	140 174
1000 	1000 	1000 	1000 	1000 	1000 	605 611	425 435	298 314	205 228	138 165

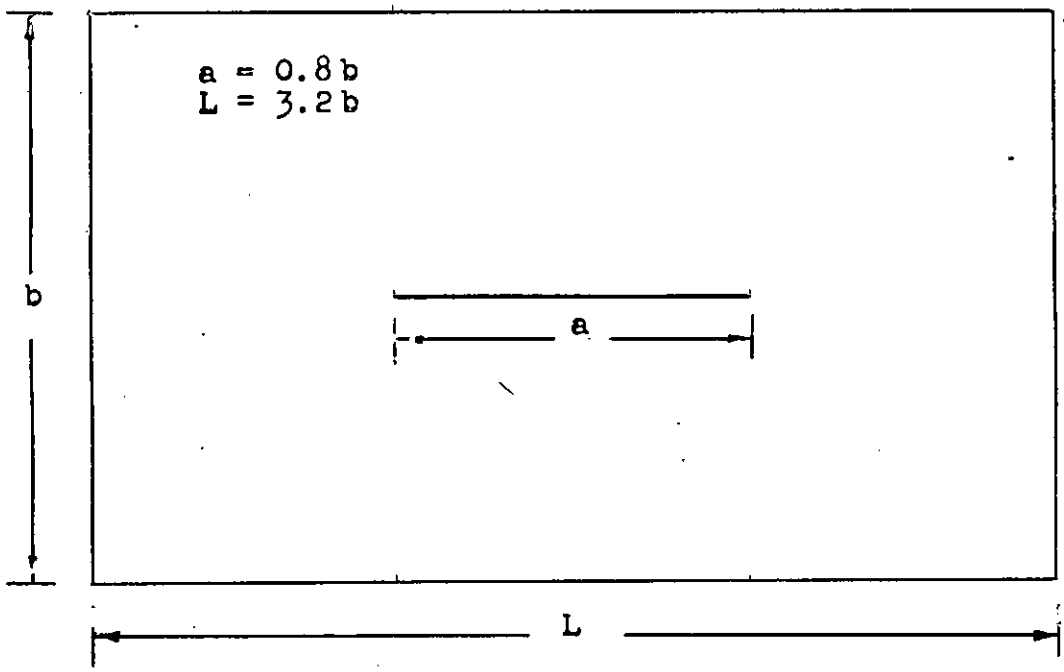

Figure (4.18)
Cross-section of
a
Homogeneous Symmetric Strip Line

Table 4.19 Characteristic Impedance of a Strip-line as shown in Figure (4.18)

No. of Vertices	Characteristic Impedance (Ω)			
	Square Mesh grading	Extrap. Impedance	Triangular Mesh Grading	Extrap. Impedance
17 x 6	73.5112 Ω		71.6898 Ω	
33 x 11	74.7069 Ω		73.7922 Ω	
65 x 21	75.3193 Ω	75.9624 Ω	74.8614 Ω	75.9679 Ω

Exact Impedance Ref.(33) Z = 75.9079 Ω

such a line are computed by the finite-element method with triangular mesh grading for $\frac{s}{d} = 0.2$, $\frac{L}{d} = 2.5$ and 3.5 and $\frac{a}{d} = 1.0$, and results are tabulated in Table (4.18). In Table (4.19) numerical results for the characteristic impedance of a strip line as shown in Figure (4.18) are tabulated for various mesh sizes in square and triangular mesh discretisations which also clearly demonstrates the advantage of square mesh over the triangular mesh.

4.9 Conclusions:

A study of the results presented in this chapter for a few homogeneous waveguide and transmission line problems shows that in all cases the finite-element method with square mesh discretisation gives a better approximation than the corresponding triangular element discretisation or the finite-difference solutions. This is particularly true for problems with re-entrant corner as shown for the ridged rectangular waveguide. Similar results may be expected for the L-shaped and the channel waveguide. For the transmission line with singularities, if the degree of sharpness of the re-entrant corner becomes very high for an example $\alpha = 2\pi$ in the problem of Figure (4.17), the relative error in the calculation of the capacitance would be more. This is due to the fact that near the 2π corner potential gradient

calculated even on the bilinear assumption of potential distribution over an element near such a point becomes relatively a crude approximation for the actual stiff variation of the potential gradient exists at such a region. However, even for a coarse mesh grading, it is possible to keep the relative error in the computation of the characteristic impedance within a few percent. Since the finite-element method gives an upper bound to the capacitance, the corresponding characteristic impedance becomes a lower bound and one may use the results of three successive mesh halvings for relatively coarse mesh to obtain a finer result by using a suitable extrapolation technique.

The fact that good accuracy may be obtained with a relatively small mesh is most important in consideration of maximum economy of computer facilities. The computational time spent in solving a p'th order equation increases rapidly as p increases. It is, therefore, most essential to achieve as high an accuracy as possible with the smallest size of the matrix. This is most conveniently brought about by the use of FE methods. For an arbitrary cross-section, it would be appropriate to use a square mesh at interior points and a triangular mesh at the boundary. The symmetry of the generated matrix eigenvalue problem will not be destroyed by such a mixed grading.

Chapter 4 - References

1. Carre, B.A.: "The Determination of the Optimum Accelerating Factor for Successive Over Relaxation", Computer Journal Vol. 14, No. 1. pp 73-78, April 1961.

2. Abramowitz and Slign: "Handbook of Mathematical Functions", Dover, p. 18.

3. Morse, P.M. and Feshbach, H.: "Methods of Theoretical Physics", part II, McGraw-Hill, Chapter 9.

4. Muilwyk, C.A.: "The Finite-Difference Solution of Arbitrary Shaped Waveguide with Arbitrary Fillings", Ph.D. Thesis (1967), Department of Electrical and Electronic Engineering, University of Sheffield.

5. Motz, H.: "Calculation of Electromagnetic Field Frequency and Circuit Parameters of High Frequency Resonator Cavities", Proc. IEE, Vol. 93, Part II, pp 335, 1946.

6. Woods, L.C. "Relaxation Treatment of Singular Points in Poission's Equations", Quart. Journal of Mech. and Appl. Math., Vol. VI, Part 2, 1953.

7. Allen, D.N., Fox, L., Motz, H. and Southwell, R.V.: "Relaxation method applied to Engineering Problems VIIC Free Transverse Vibrations of Membranes with Application to Two-dimensional Oscillation in

Electromagnetic System", Philosophical Transactions of Royal Society, Sec. A, 1945, Vol. 239, p. 488.

8. Fox, L.: "Numerical solution of Ordinary and Partial Differential Equations", Pergam 1962. p. 301.

9. Reid, J.K. and Walsh, J.E.: "An Elliptic Eigenvalue Problem for a re-entrant region", J. Soc. Indust. Appl. Math, Vol. 13, pp. 837-850, September 1965.

10. Cohn, S.B.: "Properties of Ridged Waveguides", Proc. IRE, Vol. 35, pp. 783-788, August 1947.

11. Hopfer, S.: "The Design of Ridged Waveguide", IRE Trans. on Microwave Theory and Techniques, Vol. MTT-3, pp. 20-29, October 1955.

12. Daly, P.: "Investigation of Magnetic Field Polarisation in Waveguides", Ph.D. Thesis (1962), Department of Electrical Engineering, University of Glasgow.

13. Pyle, J.R.: "The cut-off Wavelength of TE_{10} Mode in Ridged Rectangular Waveguides of any Aspect Ratios", IEEE Trans. on Microwave Theory and Techniques, Vol. MTT-14, No. 4, pp. 175-183, April 1966.

14. Ishii, R. and Vilmur, R.J.: "The Channel Waveguide", IRE Trans. on Microwave Theory and Techniques, Vol. MTT-10, pp. 220-221, May 1962.

15. Ishkin, A.I.: "The Calculation of Fundamental Critical Wavelength for a Rectangular Waveguide with Longitudinal Rectangular channels and Ridges", Radio Engineering, Vol. 13, pp. 220-221, May 1962.

16. Roth, J.P. and Ishii, R.: "The cut-off Characteristics of the Channel Waveguide", IEEE Trans. on Microwave Theory and Techniques, Vol. MTT-12, pp. 245-247, March 1964.

17. Schelkunoff, S.A.: "Electromagnetic Waves", D.Van Nostrand Co. Ltd., Chapters 8-9, pp. 1955.

18. Assadourian, F. and Rimai, E.: "Simplified Theory of Micro-strip transmission system", Proc. IRE, Vol. 40, pp. 1651-1657, December 1952.

19. Cohn, S.B.: "Characteristic Impedance of Shielded Strip Transmission Line", IRE Trans. on Microwave Theory and Techniques, Vol. MTT-2, pp.52-65, July 1954.

20. Bates, R.H.: "The Characteristics Impedance of the Shielded Slab Lines", IRE Trans. on Microwave Theory and Techniques, Vol. MTT-4, pp. 28-33, January 1956.

21. Hayt, W.A.: "Potential Solution of a Homogeneous Strip-line of finite-width", IRE Trans. on Microwave Theory and Techniques, Vol. MTT-3, pp. 16-18, July 1955.

23. Buda, R.G.: "Method of Calculating the Characteristic Impedance of a Strip Transmission Line to a Given Degree of Accuracy", IRE. Trans. on Microwave Theory and Techniques, October 1958, pp. 440-446.

24. Foster, K. "The Characteristic Impedance and Phase Velocity of High-2 Triplate Line", Journal of British IRE, December 1958, pp. 715-724.

25. Collin, R.E.: "The Characteristic Impedance of a Slotted co-axial Line", IRE Trans. on Microwave Theory and Techniques, January 1956, pp. 4-8.

26. Horgan, J.D.: "Coupled Strip Transmission Line with Rectangular Inner Conductors", IRE Transaction on Microwave Theory and Techniques, Vol. MTT-5, pp. 92-98, April 1957.

27. Park, D.: "Planer Transmission Lines", IRE Trans. on Microwave Theory and Techniques, April 1955, pp. 8-12.

28. Dahlman, B.A.: "A Double-Ground plane Strip-Line System for Microwaves", IRE Trans. on Microweve Theory and Techniques, October 1955, pp. 52-57.

29. Wheeler, H.A.: "Transmission Line Properties of Parallel Strips Separated by a Dielectric Sheet", IEEE Trans. on Microwave Theory and Techniques, March 1965, pp. 174-185.

30. Gilles, D.C.: Proc. Roy. Soc. A 193 (1948), p. 428.

31. Jeffreys, H. and Jeffreys, B.: "Methods of Mathematical Physics", Cambridge, 1950.

32. Bowman, F. Proc. London Math. Soc., Vol. 41. (1936) p. 271.

33. Whiting, K.B.: "A Treatment of Boundary Singularities in Finite Difference Solutions of Laplace's Equation", IEEE Trans. on Microwave Theory and Techniques, October 1968, pp. 889-891.

APPENDIX A-4.

A SAMPLE PROGRAM TO ILLUSTRATE THE USE OF THE SOR TECHNIQUE IN WAVEGUIDE PROBLEMS.

```
COMMENT  This program illustrates the use of the
         SOR technique for the solution of a single ridged
         waveguideas shown in figure 4-13).
         (p-1)=number of subdivisions of (a/2);
         (q-1)=    ,,          ,,        of(b-d);
           a  =    ,,          ,,        of(a-c);
           c  =    ,,          ,,        of c;

begin   library A0,A6;
integer p,q,n,r1,r2,r3,r4,r5,r6,r7,r8,a,b,c;
real K;
open(20); open(70);
p:=read(20); q:=read(20);    a:=read(20);
b:=read(20); c:=read(20);
n:=(b+1)×p+c×q;
begin
      real gamma,alpha;
      array H[1:n];

procedure Aconstant(i);
value i;  integer i;
begin
        r1:=i-1;    r2:=i+1;    r3:=i-p;    r4:=i+p;
        r5:=i-1+p;  r6:=i-1-p;  r7:=i+1-p;  r8:=i+1+p;
end;
procedure Bconstant(i);
value i; integer i;
```

```
begin
        r1:=i-1;    r2:=i+1;     r3:=i-q;     r4:=i+q;
        r5:=i-1+q; r6:=i-1-q; r7:=i+1-q;  r8:=i+1+q;
end;
procedure Iteration;
begin

        real Rh;  integer i,r;
        i:=1;
        Rh:=((2-2×K)×H[i]-(K+1/2)×(H[i+1]+H[i+p])-(1+K/2
                )×H[2+p])×alpha/(2-2×K);
        H[i]:=H[i]+Rh;
        for i:= 2 step 1 until p-1 do
        begin
                Aconstant(i);

        Rh:=((4-4×K)×H[i]-(K+1/2)×(H[r1]+H[r2])-(1+2×K)
           ×H[r4]-
                                        (1+K/2)×(H[r5]+H[r8]))×alpha
                /(4-4×K);
H[i]:=H[i]+Rh;
end;
i:=p;
Rh:=((2-2×K)×H[i]-(K+1/2)×(H[i-1]+H[i+p])-(1+K/2)×H[i+p-1]
                )×alpha/(2-2×K);
        H[i]:=H[i]+Rh;
        for r:=1 step 1 until b-1 do
begin
        i:=r×p+1;   Aconstant(i);
        Rh:=((4-4×K)×H[i]-(1+2×K)×H[r2]-(1/2+K)×(H[r3]+
                H[r4])
                -(1+K/2)×(H[r7]+H[r8]))×alpha/(4-4×K);
        H[i]:=H[i]+Rh;
```

```
for i:=r×p+2 step 1 until (r+1)×p-1 do
begin
        Aconstant(i);
Rh:=((8-8×K)×H[i]-(1+2×K)×(H[r1]+H[r2]+H[r3]+H[r4])-(1+1/2×
        K)×
                                (H[r5]+H[r6]+H[r7]+H[r8]))×alpha/(8-8×K);
H[i]:=H[i]+Rh;
end;
i:=(r+1)×p;
Aconstant(i);
Rh:=((4-4×K)×H[i]-(1+2×K)×H[r1]-(1/2+K)×(H[r3]+H[r4])-(1+K/2
        )×
                (H[r5]+H[r6]))×alpha/(4-4×K);
H[i]:=H[i]+Rh;
endr;
        i:=b×p+1;
        Rh:=((4-4×K)×H[i]-(1+2×K)×H[i+1]-(1/2+K)×(H[i-p]
                +H[i+p])
        -(1+1/2×K)×(H[i-p+1]+H[i+1+p]))×alpha/(4-4×K);
        H[i]:=H[i]+Rh;
for i:=b×p+2 step 1 until b×p+a-1 do
begin
        Rh:=((8-8×K)×H[i]-(1+2×K)×(H[i-1]+H[i+1]+H[i-p]+H[
                i+p])-
 (1 K/2) ×(H[i-1+p]+H[i-1-p]+H[i+1-p]+H[i+1+p]))×alpha/(8-8×K);
        H[i]:=H[i]+Rh;
end;
i:=b×p+a;

Rh:=((6-6×K)×H[i]-(1+2×K)×(H[i-1]+H[i-p])-(1+1/2×K)×(H[i+1-p]

        +H[i-1+p]+H[i-1-p])-(1/2+K)×(H[i+p]+H[i+1]))×
                alpha/(6-6×K);
```

```
H[i]:=H[i]+Rh;
for i:=i+1 step 1 until b×p+(p-1) do
begin
Aconstant(i);
Rh:=((4-4×K)×H[i]-(K+1/2)×(H[r1]+H[r2])-(1+2×K)×H[r3]-(1+K/
2)×(                          H[r6]+H[r7]))×alpha/(4-4×K);
H[i]:=H[i]+Rh;
end;
        i:=(b+1)×p;
Rh:=((2-2×K)×H[i]-(K+1/2)×(H[i-1]+H[i-p])-(1+K/2)×H[i-
                 i-p])×alpha/(2-2×K);
H[i]:=H[i]+Rh;
i:=(b+1)×p+1;
Rh:=((4-4×K)×H[i]-(K+1/2)×(H[i-p]+H[i+q])-(1+2×K)×H[i+1]-
   (1+K/2)×(H[i+1-p]+H[i+1+q]))×alpha/(4-4×K);
H[i]:=H[i]+Rh;
for i:=i+1 step 1 until (b+1)×p+q-1 do
begin
Rh:=((8-8×K)×H[i]-(1+2×K)×(H[i-1]+H[i+1]+H[i-p]+H[i+q])
        -(1+K/2)×(H[i+1-p]+H[i+1+q]+H[i-1-p]+H[i-1+q]))×
        alpha/(8-8×K);
H[i]:=H[i]+Rh;
end;
i:=(b+1)×p+q;
Rh:=((4-4×K)×H[i]-(1+2×K)×H[i-1]-(1+K/2)×(H[i-1+q]+H[i-1-p])-
        (K+1/2)×(H[i+q]+H[i-p]))×alpha/(4-4×K);
H[i]:=H[i]+Rh;
if c<3 then goto L1;
for r:=2 step 1 until c-1 do
begin
        i:=(b+1)×p+1+(r-1)×q;      Bconstant(i);
Rh:=((4-4×K)×H[i]-(K+1/2)×(H[r3]+H[r4])-(1+2×K)×H[r2]-
                (1+K/2)×(H[r7]+H[r8]))×alpha/(4-4×K);
H[i]:=H[i]+Rh;
for i:= (r-1)×q+(b+1)×p+2 step 1 until r×q+(b+1)×p-1 do
```

```
begin
        Bconstant(i);
        Rh:=-((8-8×K)×H[i]-(1+2×K)×(H[r1]+H[r2]+H[r3]+H[r4])-
        (1+K/2)×(H[r5]+H[r6]+H[r7]+H[r8]))×alpha/(8-8×K);
        H[i]:=H[i]+Rh;
end;
        i:= (b+1)×p+r×q;     Bconstant(i);
        Rh:=-((4-4×K)×H[i]-(K+1/2)×(H[r3]+H[r4])-(1+2×K)×
                H[r1]-(1+K/2)×(H[r5]+H[r6]))×alpha/(4-4×K);
                H[i]:=H[i]+Rh;
endr;
L1:
end Iteraion;


procedure Variation;
begin    real Num,Denom;    integer i,r;
Num:=Denom:=0;
i:=1;
Num:=Num+H[i]×(2×H[i]-H[i+1]/2-H[i+p]/2-H[i+p+1]);
Denom:=Denom+H[i]×(2×H[i]+H[i+1]+H[i+1+p]/2+H[i+p]);
for i:=2 step 1 until p-1 do
begin
Aconstant(i);
Num:=Num+H[i]×(4×H[i]-(H[r1]+H[r2])/2-H[r4]-H[r5]-H[r8]);
Denom:=Denom+H[i]×(4×H[i]+H[r1]+H[r2]+H[r4]×2+(H[r5]+H[r8])/2);
end;
i:=p;
Num:=Num+H[i]×(2×H[i]-(H[i-1]+H[i+p])/2-H[i-1+p]);
Denom:=Denom+H[i]×(2×H[i]+H[i-1]+H[i+p]+H[i+p-1]/2);

for r:=1 step 1 until b-1 do
begin
```

```
i:=r×p+1;          Aconstant(i);
Num:=Num+H[i]×(4×H[i]-(H[r3]+H[r4])/2-H[r2]-H[r7]-H[r8]);
Denom:=Denom+H[i]×(4×H[i]+H[r3]+H[r4]+2×H[r2]+H[r7]/2+H[r8]/2);
for i:=r×p+2 step 1 until (r+1)×p-1 do
begin
        Aconstant(i);
  Num:=Num+H[i]×(8×H[i]-(H[r1]+H[r2]+H[r3]+H[r4])-H[r5]-H[r6]
                                    -H[r7]-H[r8]);
  Denom:=Denom+H[i]×(8×H[i]+2×(H[r1]+H[r2]+H[r3]+H[r4])+(H[r5]
                                    +H[r6]+H[r7]+H[r8])/2);
end;
i:=(r+1)×p;          Aconstant(i);
  Num:=Num+H[i]×(4×H[i]-(H[r3]+H[r4])/2-H[r1]-H[r5]-H[r6]);
  Denom:=Denom+H[i]×(4×H[i]+H[r1]×2+H[r3]+H[r4]+(H[r5]
                  +H[r6])/2);
endr;


i:=b×p+1;          Aconstant(i);
Num:=Num+H[i]×(4×H[i]-(H[r3]+H[r4])/2-H[r2]-H[r7]-H[r8]);
Denom:=Denom+H[i]×(4×H[i]+H[r3]+H[r4]+2×H[r2]+H[r7]/2+H[r8]/2);
for i:=i+1 step 1 until b×p+a-1 do
begin
        Aconstant(i);
  Num:=Num+H[i]×(8×H[i]-H[r1]-H[r2]-H[r3]-H[r4]-H[r5]-H[r6]
                                    -H[r7]-H[r8]);
  Denom:=Denom+H[i]×(8×H[i]+(H[r1]+H[r2]+H[r3]+H[r4])×2+1/2×(
                    H[r5]+H[r6]+H[r7]+H[r8]));
end;
i:=b×p+a;          Aconstant(i);
  Num:=Num+H[i]×(6×H[i]-H[r1]-H[r3]-H[r5]-H[r6]-H[r7]-(H[r2]+H[
        r4])
        /2);
  Denom:=Denom+H[i]×(6×H[i]+2×(H[r1]+H[r3])+H[r2]+H[r4]+1/2×(
                    H[r5]+H[r6]+H[r7]));
```

```
For i:=i+1  step 1  until (b+1)×p-1 do
begin
        Aconstant(i);

  Num:=Num+H[i]×(4×H[i]-(H[r1]+H[r2])/2-H[r3]-H[r6]-H[r7]);
  Denom:=Denom+H[i]×(4×H[i]+H[r1]+H[r2]+2×H[r3]+(H[r6]+H[r7])/2);
end;
        i:=(b+1)×p;
        Num:=Num+H[i]×(2×H[i]-(H[i-1]+H[i-p])/2-H[i-1-p]);
        Denom:=Denom+H[i]×(2×H[i]+H[i-1]+H[i-p]+H[i-1-p]/2);

i:=(b+1)×p+1;
Num:=Num+H[i]×(4×H[i]-H[i-p]/2-H[i+q]/2-H[i+1]-H[i+1+q]-H[i+
                1-p]);
Denom:=Denom+H[i]×(4×H[i]+H[i-p]+H[i+q]+H[i+1]×2+H[i+1+q]
                /2+H[i+1-p]/2);
for i:=i+1 step 1 until (b+1)×p+q-1 do
begin
  Denom:=Denom+H[i]×(8×H[i]+2×(H[i+1]+H[i-1]+H[i-p]+H[i+q]
        )+1/2×(H[i-1-p]+H[i-1+q]+H[i+1-p]+H[i+1+q]));
Num:=Num+H[i]×(H[i]×8-H[i-1]-H[i+1]-H[i-p]-H[i+q]-H[i-1-p]
        -H[i-1+q]-H[i+1-p]-H[i+1+q]);

end;

i:=(b+1)×p+q;
Num:=Num+H[i]×(4×H[i]-H[i-1]-H[i-1+q]-H[i-1-p]-(H[i-p]+H
                [i+q])/2);
Denom:=Denom+H[i]×(4×H[i]+2×H[i-1]+H[i-p]+H[i+q]+(H[i-1+q]
        +H[i-1-p])/2);
if c<3 then goto L2;
for r:=2 step 1 until c-1 do
begin
        i:=(b+1)×p+1+(r-1)×q;     Bconstant(i);
```

```
Num:=Num+H[i]×(H[i]×4-(H[r3]+H[r4])/2-H[r2]-H[r7]-H[r8]);
Denom:=Denom+H[i]×(4×H[i]+H[r3]+H[r4]+2×H[r2]+(H[r7]+H[r8])/2);

for i:= (r-1)×q+(b+1)×p+2 step 1 until r×q+(b+1)×p-1 do
begin
Beonstant(i);
Num:=Num+H[i]×(8×H[i]-H[r1]-H[r2]-H[r3]-H[r4]-H[r5]-H[r6]-H[r7]
                                                    -H[r8]);
Denom:=Denom+H[i]×(8×H[i]+(H[r1]+H[r2]+H[r3]+H[r4])×2+1/2
                  ×(H[r5]+H[r6]+H[r7]+H[r8]));
end;
i:=(b+1)×p+r×q;        Beonstant(i);
Num:=Num+H[i]×(4×H[i]-(H[r3]+H[r4])/2-H[r1]-H[r5]-H[r6]);
Denom:=Denom+H[i]×(4×H[i]+2×H[r1]+H[r3]+H[r4]+(H[r5]+H[r6])/2);
endr;
L2:        gamma:=Num/Denom;
end V ariation;
procedure Normalisation;
begin
real RH,N;  integer i;
N:=abs(H[1]);
for i:=2 step 1 until n do
begin
        RH:=abs(H[i])
                        ;
        if RH>N then N:=RH;
endi;
for i:=1 step 1 until n do
H[i]:=H[i]/N;
end Normalisation;
```

```
        integer innerit,outerit,startit,i,j,m,r,u,f1,f2,f3,f4,f5;
        f1:=format([14s+nd.dddddddd]);
        f2:=format([ddc]);
        f3:=format[sdddc]);
        f4:=format([sdd.ddddc]);
        f5:=format([6s+dd.ddddddc]);

       for i:=1 step 1 until n-q do H[i]:=1;
        for i:=n-q+1 step 1 until n do H[i]:=0;
        innerit:=read(20);
        outerit:=read(20);
        startit:=read(20);
        gamma:=read(20);
        alpha:=read(20);
        close(20);

        write(70,f3,p); write(70,f3,q); write(70,f2,innerit);
        write(70,f3,outerit); write(70,f2,startit);
        write text(70,[[c10s]gamma[11s]d/lamda[c]]);
        write(70,f1,gamma);
        write(70,f5,((b+c)↑2×24×gamma));
        K:=gamma;
        for i:=1 step 1 until startit do Iteration;
        Normalisation;   Variation;
        write(70,f1,gamma);
        write(70,f5,(p-1)↑2×24×gamma);
Start:  for i:=1 step 1 until outeritdo
        begin
              K:=gamma;
              for u:=1 step 1 until innerit do
```

```
            Iteration; Normalisation; Variation;
            write(70,f1,gamma);
            write(70,f5,(p-1)↑2×24×gamma);
        end i;
        if abs(K-gamma)>0.0000001 then goto Start:
        for i:=1 step 1 until n do
        write(70,format([5s+nd.dddddddc]),H[i]);
        end close(70); close(70);
end
```

Chapter 5

FINITE-ELEMENT METHOD FOR INHOMOGENEOUS WAVE GUIDES

5.1 Description of the Problem

In this chapter we consider the applications of the finite-element method to inhomogeneous waveguide systems. An inhomogeneous waveguide is filled with two or more sectionally constant dielectrics. As in the case of the homogeneous waveguides considered in a previous chapter, the waveguides to be considered extend to $\pm\infty$ in the direction of a cartesian co-ordinate system. Configuration of a waveguide arbitrarily filled with three distinct dielectrics is shown in Figure (5.1). As is usual, for a real propagation, a time dependence of the field quantities of the form $\exp(jwt)$ and a z -dependence of the form $\exp(-j\beta z)$ are assumed.

It is also assumed that the variations of the distribution of dielectrics are confined in the transverse plane and along the axis of propagation the dielectric distribution is assumed to be uniform. Solutions of the wave equations for the longitudinal components of fields are desired for this type of problem, because the longitudinal components of the field vectors are always parallel to the

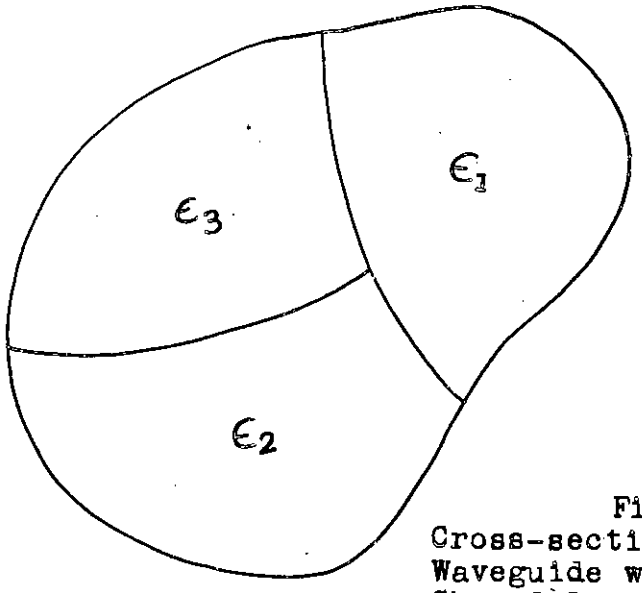

Figure (5.1)
Cross-section of an Arbitrary Waveguide with Arbitrarily Shaped Dielectric Fillings

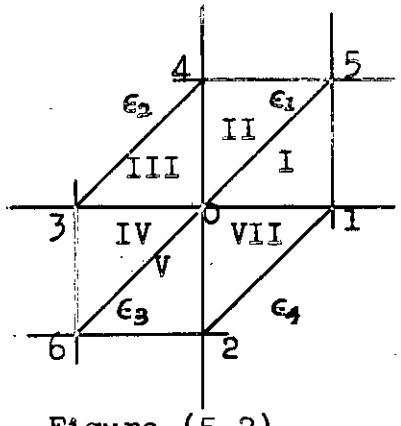

Figure (5.2)
Scheme of triangular mesh grading

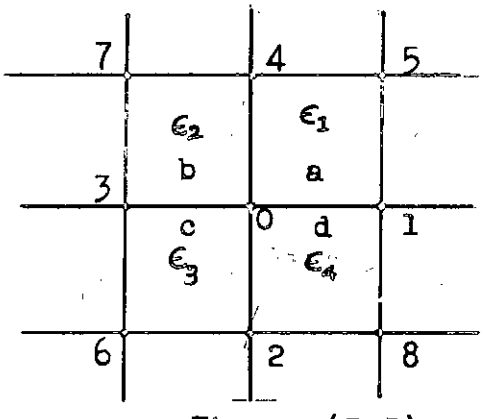

Figure (5.3)
Scheme of square mesh grading

waveguide walls as well as to the interface boundaries between two dielectric regions, irrespective of their orientations in the transverse plane and also because the longitudinal components of the field vectors are continuous and information about the longitudinal components are sufficient to determine all other field components.

In each region S_i, wave equations in E_z and H_z can be written as

$$(\nabla_t^2 + k_i^2)\, E_{zi} \,\Big|\, H_{zi} = 0 \tag{5.1}$$

where,

$$k_i^2 = w^2 \mu_o \epsilon_o \epsilon_{ri} - \beta^2 \tag{5.2}$$

The set of wave equations (5.1) are defined over the region S_i. Simultaneous solutions of E_{zi} and H_{zi} are needed to obtain a complete information regarding the propagation characteristics of such a waveguide. The field component E_{zi} and H_{zi} satisfy the following boundary conditions

$$E_z = 0; \quad \frac{\partial H_z}{\partial n} = 0 \tag{5.3}$$

on the waveguide walls and E_z and H_z are continuous at interface boundaries. At the interface boundaries that part of the transverse components of the field vectors which are tangential to the interface are also continuous. The transverse components of $\underline{E}$ and $\underline{H}$ fields can be determined

from E_z and H_z, the relations being given below:

$$\underline{E}_t = \frac{jw\mu_o}{k_i^2} \underline{a}_z \times \nabla_t H_z - \frac{j\beta}{k_i^2} \nabla_t E_z \tag{5.4}$$

$$\underline{H}_t = \frac{-j\beta}{k_i^2} \nabla_t H_z - \frac{jw\epsilon}{k_i^2} \underline{a}_z \times \nabla_t E_z \tag{5.5}$$

For convenience, one of the regions is considered to be vacuum (air) and the relative permittivities of other regions are considered to be ϵ_{ri}. If we normalise the field component E_z by multiplying it with $\frac{w\epsilon_o}{\beta_o}$ and designate the new expression $\frac{w\epsilon_o}{\beta_o} E_z$ by a scalar function ψ and replace H_z by another scalar function ϕ, then ϕ and ψ will be dimensionally the same. Furthermore, if we define τ_i as a ratio of the wavenumber k_o^2 in the vacuum region to the wavenumber k_i^2 in the region ϵ_{ri}, then we can rewrite the wave equations in each region in terms of the scalar potential ϕ and ψ as follows:

$$(\tau_i \nabla_t^2 + k_o^2)\, \phi / \psi = 0 \tag{5.6}$$

The boundary conditions that ψ and ϕ should satisfy are the same as for E_z and H_z. On a plane boundary between the subregions S_i and S_j, the continuity of the tangential components of the transverse electric field vector yields

$$\tau_i \left[-\left(\frac{\partial\psi}{\partial c}\right)_i + \frac{1}{\beta^2}\left(\frac{\partial\phi}{\partial n}\right)_i \right] = -\tau_j \left[-\left(\frac{\partial\psi}{\partial c}\right)_j + \frac{1}{\beta^2}\left(\frac{\partial\phi}{\partial n}\right)_j \right] \tag{5.7}$$

where $\vec{\beta} = \left(\frac{\beta c}{w}\right)$, and $\frac{\partial}{\partial c}$ and $\frac{\partial}{\partial n}$ indicate the spatial differentiation with respect to the tangential and the outward normal directions to the boundaries of each dielectric subregion. The unit outward normal vector $\underline{n}$ and the unit tangential vector $\underline{c}$ to the boundaries of each region are so defined that the cross-product $\underline{n} \times \underline{c}$ gives a unit vector $\underline{a_z}$ along the z-axis.

Similarly, the continuity of the tangential transverse component of magnetic field yields:

$$\tau_i \left[\epsilon_i \left(\frac{\partial \psi}{\partial n}\right)_i + \left(\frac{\partial \phi}{\partial c}\right)_i \right] = -t_j \left[\epsilon_j \left(\frac{\partial \psi}{\partial n}\right)_j + \left(\frac{\partial \phi}{\partial c}\right)_j \right] \qquad (5.8)$$

Therefore, any solution of the inhomogeneous waveguide problem for ψ and ϕ must satisfy the wave equation (5.1) together with the continuity relations (5.7) and (5.8), in addition to the boundary conditions on the guide walls.

5.2 Finite-Element Equations and the Matrix Formulation

5.2.1a The Matrix Formulation and Properties

It would be shown that the principle underlying the applications of the finite-element technique to homogeneous waveguide systems will remain the same for inhomogeneous waveguides. A variational function for inhomogeneous waveguide problems shall contain both ϕ and ψ fields together and this can be written in Euler density form as

$$\mathcal{J}(\phi,\psi) = \sum_{i} \Big[\tau_i \int_{S_i} |\nabla_t \phi|^2 \, ds + \bar{\beta}^2 \tau_i \epsilon_i \int_{S_i} |\nabla_t \psi|^2 \, ds +$$

$$2\bar{\beta}^2 \tau_i \int_{S_i} \underline{a_z} \; (\nabla_t \psi \times \nabla_t \phi) ds - k_o^2 \Big(\int_{S_i} \phi^2 ds +$$

$$\bar{\beta}^2 \epsilon_i \int_{S_i} \psi^2 ds \Big) \Big] \qquad (5.9)$$

The first step in the development of the finite-element equations for an inhomogeneous waveguide problem is to divide the entire cross-section into a number of subregions such that each of these subregions is filled with one dielectric. This type of subdivision will generate a few boundary lines common between two different dielectric regions. The second step is to subdivide each of the above-mentioned subregions into a number of regular polygonal meshes as in the case of homogeneous waveguides. Like the homogeneous waveguides, we shall consider only the triangular and the square meshes. Let there be R elements (may be triangular or square) into which the entire cross-section be divided. The extremum functional $J(\phi,\psi)$ can now be discretised into R functionals as given below

$$J(\phi,\psi) = \sum_{e=1}^{R} J^e(\phi,\psi) \qquad (5.10)$$

where $J^e(\phi,\psi)$ is the contribution to $J(\phi,\psi)$ by the element 'e' and is given by

$$J^e(\phi,\psi) = \tau_1 \int_e |\nabla_t \phi|^2 \, ds + \bar{\beta}^2 \tau_1 \epsilon_1 \int_e |\nabla_t \psi|^2 \, ds +$$

$$2\bar{\beta}^2 \tau_1 \int_e \underline{a_z} \cdot (\nabla_t \psi \times \nabla_t \phi) ds - k_o^2 \left[\int_e \phi^2 \, ds + \right.$$

$$\left. \bar{\beta}^2 \epsilon_1 \int_e \psi^2 \, ds \right] \qquad (5.11)$$

In equation (5.11) $\int_e$ indicates that the domain of integration is over the element 'e' under consideration.

As the permittivity is constant over each of the elements, there is no discontinuity in the derivatives of ϕ and ψ over an element. Therefore, any polynomial approximation to ϕ and ψ shall uniquely determine their values within the element in terms of their values at the vertices of the element. Like homogeneous waveguides discussed previously, we consider the same type of functional relations for ϕ and ψ over each element, i.e. over an element 'e'

$$\phi^e(x,y)/\psi^e(x,y) = \sum_{k=i,j,m} N_k(x,y)\phi_k/\psi_k \qquad (5.12)$$

for the triangular grading where

$$N_k(x,y) = \alpha_k + \beta_k x + \gamma_k y \qquad (5.13)$$

and

$$\phi^e(x,y)/\psi^e(x,y) = \sum_{r=i,jkl} M_r(x,y)\,\phi_r/\psi_r \qquad (5.14)$$

for the square mesh grading where

$$M_r(x,y) = a_r + b_r x + c_r y + d_r xy \tag{5.15}$$

The values of α_k, β_k and γ_k as well as a_r, b_r, c_r and d_r are given in Chapter 3.

If the functional forms of ϕ and ψ as given in equation (5.12) and (5.14) are substituted into the right-hand side of the extremum functional $J^e(\phi,\psi)$ and the relevant integrations are carried out, then J will be functions of a set of variables ϕ_k and ψ_k at the vertices of the elements, i.e. if there are in all N vertices

$$J(\phi,\psi) = F(\phi_1, \phi_2, \phi_3 \ldots\ldots \phi_N, \psi_1, \psi_2 \ldots\ldots \psi_N) \tag{5.16}$$

The optimum set of ϕ_k and ψ_k for a certain functional form of N(x,y) and M(x,y) may be obtained by minimising the function J given in equation (5.16) with respect to each ϕ_m and ψ_m, i.e. by solving the set of equations:

$$\frac{\partial}{\partial\phi_m/\partial m}\left[J(\phi,\psi)\right] = 0 \tag{5.17}$$

for m = 1,2.....N.

This way of minimisation of J results in a matrix eigenvalue problem of the form

$$\underline{A}\,\underline{\theta} = \lambda \underline{B}\,\underline{\theta} \tag{5.18}$$

where $\underline{\theta}$ is a column matrix whose components are the N values of ϕ_k and ψ_k at the vertices generated and $\underline{A}$ and $\underline{B}$ are square, symmetric, sparse band type matrices. For in all N vertices, the order of matrices $\underline{A}$ and $\underline{B}$ will be 2N instead of N as in the case of the homogeneous waveguide problems. This is because of the simultaneous existence of ϕ and ψ at each vertex.

5.2.1b Properties of Matrices $\underline{A}$ and $\underline{B}$

The properties of matrices $\underline{A}$ and $\underline{B}$ would follow the properties of the component parts of the extremum function from which they are generated. If we write these component parts in operator form 'say' D_A and D_B then

$$D_A = \sum_{e=1}^{R} \left[\tau_i \int_e |\nabla_t \phi|^2 ds + \bar{\beta}^2 \tau_i \epsilon_i \int_e |\nabla_t \psi|^2 ds + 2\bar{\beta}^2 \tau_i \int_e \underline{a_z} \cdot (\nabla_t \psi \times \nabla_t \phi) ds \right] \tag{5.19}$$

$$D_B = \sum_{e=1}^{R} \left[\int_e \phi^2 ds + \bar{\beta}^2 \epsilon_i \int_e \psi^2 ds \right] \tag{5.20}$$

From equation (5.20), it is obvious that D_B would be always positive. Therefore, the corresponding matrix $\underline{B}$ will be always positive definite. The value of D_A will be greatly influenced by the values of τ_i. For propagating mode $\bar{\beta}^2$ can take values varying for 0 to ϵ_i, and the corresponding range of τ_i is $\frac{1}{\epsilon_i}$ to $-\infty$ with $\tau_i = 0$ when $\bar{\beta}^2 = 1$ and $\tau_i = -\infty$ when $\bar{\beta}^2 = \epsilon_i$. It is therefore useful to consider the behaviour of D_A in two parts: first with τ_i positive and

then with τ_i negative.

With τ_i positive $\tau_i \int_e |\nabla_t \phi|^2 ds + \bar{\beta}^2 \tau_i \epsilon_i \int |\nabla_t \psi|^2 ds$ is always positive but $2\bar{\beta}^2 \tau_i \int_e \underline{a_z} . (\nabla_t \psi \times \nabla_t \phi) ds$ can take either positive or negative values. The maximum negative value can be

$$-2\bar{\beta}^2 \tau_i \int_e |\nabla_t \psi| |\nabla_t \phi| \, ds$$

and for this worst condition we can rewrite D_A as follows

$$D_A = \sum_{e=1}^{R} \int_e \tau_i \left\{ |\nabla_t \phi|^2 + \bar{\beta}^2 \epsilon_i |\nabla_t \psi|^2 - 2\bar{\beta}^2 (|\nabla_t \phi| \, |\nabla_t \psi|) \right\} ds$$

$$= \sum_{e=1}^{R} \tau_i \int_e \left\{ (|\nabla_t \phi| - |\nabla_t \psi| \bar{\beta})^2 + (\epsilon_i - 1) \bar{\beta}^2 |\nabla_t \psi|^2 + 2\bar{\beta}(1-\bar{\beta}) |\nabla_t \phi| \cdot |\nabla_t \psi| \right\} ds \qquad (5.21)$$

Since $\bar{\beta}$ is less than unity for the range of $\tau_i > 0$ and ϵ_i is greater than unity, the integrand in equation (5.21) is always positive. Therefore, for τ positive D_A is also positive and the corresponding discretised matrix $\underline{A}$ will also be positive definite.

For $\bar{\beta} > 1$, i.e. for $\tau < 0$, two cases may arise:

a) Contribution to D_A by the elements inside the dielectric zone may be less in magnitude than the contribution to D_A by the elements inside the air region, i.e. in the range where

$$\sum_{\text{'e' over diel.}} |\tau_1| \int \Big[(|\nabla_t \phi| - \bar{\beta}|\nabla_t \psi|)^2 + (\epsilon_1 - 1)\bar{\beta}^2 |\nabla_t \psi|^2 +$$

$$2\bar{\beta}(1-\bar{\beta})|\nabla_t \phi| \cdot |\nabla_t \psi| \Big] ds <$$

$$\sum_{\text{'e' over air}} \int \Big[(|\nabla_t \phi| - \bar{\beta}|\nabla_t \psi|)^2 + 2\bar{\beta}(1-\bar{\beta})|\nabla_t \phi| \cdot |\nabla_t \psi| \Big] ds \qquad (5.22)$$

If both the integrands in the above inequality are positive, which may be the case for $(1-\bar{\beta})$ very small, then in this zone of $\bar{\beta}$ the associated matrix may have both positive and negative eigenvalues. The eigenvalues of most interest, i.e. the one corresponding to the dominant mode propagation, is the least (in magnitude) negative one and has a negative sign associated with it because

$$k_o^2 = w^2 \mu_o \epsilon_o (1-\bar{\beta}^2)$$

is negative for $\bar{\beta} > 1$.

b) Contribution to D_A by the element in dielectric region may exceed in magnitude than the respective contribution by the elements in the air region, i.e.

$$\sum_{\text{'e' diel.}} |\tau_1| \int_e \Big[(|\nabla_t \phi| - \bar{\beta}|\nabla_t \psi|)^2 + (\epsilon_1 - 1)\bar{\beta}^2 |\nabla_t \psi|^2 + 2(\bar{\beta} - \epsilon_1 + \tfrac{1}{\tau_1})|\nabla_t \phi| \cdot$$

$$|\nabla_t \psi| \Big] ds > \sum_{\text{'e' air}} \Big[\int_e |\nabla_t \phi|^2 ds + \bar{\beta}^2 \int_e |\nabla_t \psi|^2 ds \Big] \qquad (5.23)$$

In this zone of $\bar{\beta}$ the associated matrix **A** will have negative eigenvalues. Thus we conclude that for the range of $\bar{\beta}$ less than unity both the matrices **A** and **B** will be positive definite and for $\bar{\beta} > 1$, the matrix **B** will still be positive definite and the properties of the matrix **A** will be determined by the conditions (a) and (b) as discussed above.

5.2.2 Derivation of Discretised Equation for a General Point

The derivation of the finite-element equations for the general case of a point at a junction of four dielectric quadrants is discussed in detail, and the equations for special cases are deduced therefrom. The configurations in question are shown in Figures (5.2) and (5.3). The vertex 'o' is surrounded by six triangular elements I-VI in Figure (5.2), and by four square elements in Figure (5.3). There are six adjacent vertices to the vertex 'o' in Figure (5.2) and eight vertices adjacent to vertex 'o' in Figure (5.3). Potentials ϕ and ψ at these vertices are labelled by ϕ_1-ϕ_8 and ψ_1-ψ_8. If we now consider the minimisation of $J(\phi,\psi)$ as given in equation (5.16) with respect to ϕ_o and ψ_o, we obtain:

$$\frac{\partial J}{\partial \phi_o} = 0 = \sum_{e=I}^{VI} \frac{\partial J}{\partial \phi_o}\Big|_e \tag{5.24}$$

$$\frac{\partial J}{\partial \psi_o} = 0 = \sum_{e=I}^{VI} \frac{\partial J}{\partial \psi_o}\Big|_e \tag{5.25}$$

for the triangular element discretisation and

$$\frac{\partial J}{\partial \phi_o} = 0 = \sum_{e=a,b,c,d} \frac{\partial J}{\partial \phi_o}\Big|_e \tag{5.26}$$

$$\frac{\partial J}{\partial \psi_o} = 0 = \sum_{e=a,b,c,d} \frac{\partial J}{\partial \psi_o}\Big|_e \tag{5.27}$$

for discretisation into square elements, where the subscript $|_e$ refers to a particular element 'e'.

5.2.2a Subregions in 1st and 3rd Quadrants

In the first quadrant with permittivity ϵ_1, we have two triangular elements I and II bounded by vertices (0,1,5) and (0,5,4) and one square element bounded by vertices (0,1,5,4). Using the appropriate approximation to ϕ and ψ over each element and following the standard procedure described for the finite-element method as in a previous chapter, we obtain the partial contribution to $\frac{\partial J}{\partial \phi_o}$ and $\frac{\partial J}{\partial \psi_o}$ by elements in the first quadrant:

$$\frac{\partial J}{\partial \phi_o}\Big|_{\epsilon_1} = \frac{\tau_1}{2}(-\phi_1 + 2\phi_o - \phi_4) + \frac{\tau_1 \bar{\beta}^2}{2}(\psi_1 - \psi_4) - \frac{(k_o h)^2}{24}(\phi_1 + 4\phi_o + \phi_4 + 2\phi_5) \tag{5.28}$$

$$\frac{\partial J}{\partial \psi_o}\Big|_{\epsilon_1} = \frac{\tau_1 \bar{\beta}^2 \epsilon_1}{2}(-\psi_1 + 2\psi_o - \psi_4) + \frac{\tau_1 \bar{\beta}^2}{2}(\phi_4 - \phi_1) - \frac{(k_o h)^2 \bar{\beta}^2 \epsilon_1}{24}(\psi_1 + 4\psi_o + \psi_4 + 2\psi_5) \tag{5.29}$$

for the triangular elements, and

$$\left.\frac{\partial J}{\partial \phi_o}\right|_{\epsilon_1} = \frac{\tau_1}{6}(-\phi_1 + 4\phi_o - 2\phi_5 - \phi_4) + \frac{\tau_1 \bar{\beta}^2}{4}(\psi_1 - \psi_4)$$

$$- \frac{(k_o h)^2}{36}(4\phi_o + 2\phi_1 + \phi_5 + 2\phi_4) \tag{5.30}$$

$$\left.\frac{\partial J}{\partial \psi_o}\right|_{\epsilon_1} = \frac{\tau_1 \bar{\beta}^2 \epsilon_1}{6}(-\psi_1 + 4\psi_o - 2\psi_5 - \psi_4) + \frac{\tau_1 \bar{\beta}^2}{4}(\phi_4 - \phi_1)$$

$$- \frac{(k_o h)^2 \quad {}^2 \quad 1}{36}(4\psi_o + 2\psi_1 + \psi_5 + 2\psi_4) \tag{5.31}$$

for the square elements.

Using the symmetry of the configuration, we obtain the contribution from the elements in the third quadrant:

$$\left.\frac{\partial J}{\partial \phi_o}\right|_{\epsilon_3} = \frac{\tau_3}{2}(-\phi_3 + 2\phi_o - \phi_2) + \frac{\bar{\beta}^2 \tau_3}{2}(\psi_3 - \psi_2)$$

$$- \frac{(k_o h)^2}{24}(\phi_2 + 4\phi_o + 2\phi_6 + \phi_3) \tag{5.32}$$

$$\left.\frac{\partial J}{\partial \psi_o}\right|_{\epsilon_3} = \frac{\tau_3 \bar{\beta}^2 \epsilon_3}{2}(-\psi_3 + 2\psi_o - \psi_2) + \frac{\bar{\beta}^2 \tau_3}{2}(\phi_2 - \phi_3)$$

$$- \frac{(k_o h)^2 \bar{\beta}^2 \epsilon_3}{24}(4\psi_o + \psi_2 + \psi_3 + 2\psi_6) \tag{5.33}$$

for the triangular elements, and

$$\left.\frac{\partial J}{\partial \phi_0}\right|_{\epsilon_3} = \frac{t_3}{6}\,(4\phi_0 - \phi_2 - \phi_3 - 2\phi_6) + \frac{\bar{\beta}^2 t_3}{4}\,(\psi_3 - \psi_2)$$

$$- \frac{(k_0 h)^2}{36}\,(4\phi_0 + 2\phi_2 + 2\phi_3 + \phi_6) \qquad (5.34)$$

$$\left.\frac{\partial J}{\partial \psi_0}\right|_{\epsilon_3} = \frac{t_3 \bar{\beta}^2 \epsilon_3}{6}\,(4\psi_0 - \psi_2 - \psi_3 - 2\psi_6) + \frac{\bar{\beta}^2 t_3}{4}\,(\phi_2 - \phi_3)$$

$$- \frac{(k_0 h)^2 \bar{\beta}^2 \epsilon_3}{36}\,(4\psi_0 + 2\psi_2 + 2\psi_3 + \psi_6) \qquad (5.35)$$

for the square element grading.

5.2.2b Subregions in 2nd and 4th Quadrants

Only one triangular element or one square element is associated with each of the 2nd and 4th quadrants. The contributions from each region are found as discussed above and are given by:

$$\left.\frac{\partial J}{\partial \phi_0}\right|_{\epsilon_2} = \frac{t_2}{2}\,(-\phi_3 + 2\phi_0 - \phi_4) + \frac{\bar{\beta}^2 t_2}{2}\,(\psi_4 - \psi_3)$$

$$- \frac{(k_0 h)^2}{24}\,(\phi_3 + 2\phi_0 + \phi_4) \qquad (5.36)$$

$$\frac{\partial J}{\partial \psi_o}\Big|_{\epsilon_2} = \frac{\tau_2 \bar{\beta}^2 \epsilon_2}{2}(-\psi_3 + 2\psi_o - \psi_4) + \frac{\bar{\beta}^2 \tau_2}{2}(\phi_3 - \phi_4)$$

$$- \frac{(k_o h)^2 \bar{\beta}^2 \epsilon_2}{24}(2\psi_o + \psi_3 + \psi_4) \tag{5.37}$$

$$\frac{\partial J}{\partial \phi_o}\Big|_{\epsilon_4} = \frac{\tau_4}{2}(-\phi_1 + 2\phi_o - \phi_2) + \frac{2\tau_4}{2}(\psi_2 - \psi_1)$$

$$- \frac{(k_o h)^2}{24}(2\phi_o + \phi_1 + \phi_2) \tag{5.38}$$

$$\frac{\partial J}{\partial \psi_o}\Big|_{\epsilon_4} = \frac{\tau_4 \bar{\beta}^2 \epsilon_4}{2}(-\psi_1 + 2\psi_o - \psi_2) + \frac{\bar{\beta}^2 \tau_4}{2}(\phi_1 - \phi_2)$$

$$- \frac{(k_o h)^2 \bar{\beta}^2 \epsilon_4}{24}(2\psi_o + \psi_1 + \psi_2) \tag{5.39}$$

for the triangular element discretisations and

$$\frac{\partial J}{\partial \phi_o}\Big|_{\epsilon_2} = \frac{\tau_2}{6}(4\phi_o - \phi_4 - \phi_3 - 2\phi_7) + \frac{\tau_2 \bar{\beta}^2}{2}(\psi_4 - \psi_3)$$

$$- \frac{(k_o h)^2}{36}(4\phi_o + 2\phi_4 + 2\phi_3 + \phi_7) \tag{5.40}$$

$$\frac{\partial J}{\partial \psi_o}\Big|_{\epsilon_2} = \frac{\tau_2 \epsilon_2 \bar{\beta}^2}{6}(4\psi_o - \psi_4 - \psi_3 - 2\psi_7) + \frac{\tau_2 \bar{\beta}^2}{2}(\phi_3 - \phi_4)$$

$$- \frac{{}^2(k_o h)^2}{36}\ {}_2(4\psi_o + 2\psi_4 + 2\psi_3 + \psi_7) \tag{5.41}$$

$$\frac{\partial J}{\partial \phi_o}\bigg|_{\epsilon_4} = \frac{\tau_4}{6}(4\phi_o - \phi_1 - \phi_2 - 2\phi_8) + \frac{\tau_4\bar{\beta}^2}{2}(\psi_2 - \psi_1)$$

$$- \frac{(k_o h)^2}{36}(4\phi_o + 2\phi_1 + 2\phi_2 + \phi_8) \qquad (5.42)$$

$$\frac{\partial J}{\partial \psi_o}\bigg|_{\epsilon_4} = \frac{\tau_4\bar{\beta}^2\epsilon_4}{2}(4\psi_o - \psi_1 - \psi_2 - 2\psi_8) + \frac{\tau_4\bar{\beta}^2}{2}(\phi_1 - \phi_2)$$

$$- \frac{(k_o h)^2\bar{\beta}^2\epsilon_4}{36}(4\psi_o + 2\psi_1 + 2\psi_2 + \psi_8) \qquad (5.43)$$

for the square element grading.

5.2.2c General Discretised Equations

Adding equations (5.28), (5.32), (5.36) and (5.38) and using the relations given in equation (5.24) we obtain the finite-element equation for ϕ_o in triangular mesh grading

$$\sum_{i=1}^{4}\tau_i\phi_o - \frac{(\tau_1+\tau_2)}{2}\phi_4 - \frac{(\tau_2+\tau_3)}{2}\phi_3 - \frac{(\tau_3+\tau_4)}{2}\phi_2$$

$$- \frac{(\tau_1+\tau_4)}{2}\phi_1 + \frac{\bar{\beta}^2\tau_1}{2}(\psi_1 - \psi_4) + \frac{\bar{\beta}^2\tau_2}{2}(\psi_4 - \psi_3)$$

$$\frac{\bar{\beta}^2\tau_3}{2}(\psi_3 - \psi_2) + \frac{\bar{\beta}^2\tau_4}{2}(\psi_2 - \psi_1)$$

$$= \frac{(k_o h)^2}{12}\left(6\phi_o + \sum_{i=1}^{6}\phi_i\right) \qquad (5.44)$$

Similarly, adding equations (5.29), (5.33), (5.37) and (5.39), we get the finite-element equation for ψ_o as follows:

$$\sum_{i=1}^{4} \tau_i \epsilon_i \bar{\beta}^2 \psi_o - \bar{\beta}^2 \left[\frac{(\tau_1\epsilon_1 + \tau_2\epsilon_2)}{2} \psi_4 + \frac{(\tau_3\epsilon_3 + \tau_4\epsilon_4)}{2} \psi_2 \right.$$

$$\left. \frac{(\tau_2\epsilon_2 + \tau_3\epsilon_3)}{2} \psi_3 + \frac{(\tau_4\epsilon_4 + \tau_1\epsilon_1)}{2} \psi_1 \right] +$$

$$\bar{\beta}^2 \left[\frac{\tau_1}{2} (\phi_4 - \phi_1) + \frac{\tau_2}{2} (\phi_3 - \phi_4) + \frac{\tau_3}{2} (\phi_2 - \phi_3) + \right.$$

$$\left. \frac{\tau_4}{2} (\phi_1 - \phi_2) \right] = \frac{(k_o h \bar{\beta})^2}{12} \left[(2\epsilon_1 + 2\epsilon_3 + \epsilon_2 + \epsilon_4) \cdot \right.$$

$$\psi_o + \epsilon_1 \psi_5 + \epsilon_3 \psi_6 + \frac{(\epsilon_1 + \epsilon_4)}{2} \psi_1 + \frac{(\epsilon_4 + \epsilon_3)}{2} \psi_2 +$$

$$\left. \frac{(\epsilon_3 + \epsilon_2)}{2} \psi_3 + \frac{(\epsilon_1 + \epsilon_2)}{2} \psi_4 \right] \qquad (5.45)$$

In the same way, adding equations (5.30), (5.34), (5.40) and (5.42) as well as equations (5.31), (5.35), (5.41) and (5.43), we obtain the finite-element equations for the potentials ϕ_o and ψ_o at the vertex 'o' in square mesh grading as follows:

$$\sum_{i=1}^{4} 2\tau_i\phi_o - \tau_1\phi_5 - \tfrac{1}{2}(\tau_1+\tau_2)\phi_4 - \tfrac{1}{2}(\tau_2+\tau_3)\phi_3 - \tfrac{1}{2}(\tau_3+\tau_4)\phi_2$$

$$- \tfrac{1}{2}(\tau_4+\tau_1)\phi_1 + \tfrac{3}{2}\bar{\beta}^2\tau_1(\psi_1-\psi_4) + \tfrac{3}{2}\bar{\beta}^2\tau_2(\psi_4-\psi_3) +$$

$$\tfrac{3}{2}\bar{\beta}^2\tau_3(\psi_3-\psi_2) + \tfrac{3}{2}\bar{\beta}^2\tau_4(\psi_2-\psi_1)$$

$$= \frac{(k_oh)^2}{6}\left[8\phi_o + 2\sum_{i=1}^{4}\phi_i + \tfrac{1}{2}\sum_{i=5}^{8}\phi_i\right] \tag{5.46}$$

and

$$2\bar{\beta}^2\sum_{i=1}^{4}\tau_i\epsilon_i\psi_o - \frac{\bar{\beta}^2}{2}\Big[(\tau_1\epsilon_1+\tau_2\epsilon_2)\psi_4 + (\tau_2\epsilon_2+\tau_3\epsilon_3)\psi_3 +$$

$$(\tau_3\epsilon_3+\tau_4\epsilon_4)\psi_2 + (\tau_4\epsilon_4+\tau_1\epsilon_1)\psi_1\Big] + \tfrac{3}{2}\bar{\beta}^2\Big[\tau_1(\phi_4-\phi_1) +$$

$$\tau_2(\phi_3-\phi_4) + \tau_3(\phi_2-\phi_3) + \tau_4(\phi_1-\phi_2)\Big]$$

$$= \frac{(k_oh)^2}{6}\Big[\sum_{i=1}^{4} 2\epsilon_i\psi_o + \tfrac{1}{2}(\epsilon_1\psi_5 + \epsilon_2\psi_7 + \epsilon_3\psi_6 + \epsilon_4\psi_8) +$$

$$(\epsilon_1+\epsilon_4)\psi_1 + (\epsilon_4+\epsilon_3)\psi_2 + (\epsilon_3+\epsilon_2)\psi_3 + (\epsilon_2+\epsilon_1)\psi_4\Big] \tag{5.47}$$

If there are n vertices the resulting finite-element equations can be written in matrix form as follows:

$$\underline{A}\,\underline{\Theta} = \lambda\,\underline{B}\,\underline{\Theta} \tag{5.48}$$

where $\lambda = \frac{(k_o h)^2}{12}$ or $\frac{(k_o h)^2}{6}$ as appropriate for the type of discretisation under consideration and $\underline{A}$ and $\underline{B}$ are $2n \times 2n$ square symmetric band matrices.

5.3 Special Cases

5.3.1 Interior Vertices

Interior vertices are those contained within a uniform subregion and make up the great majority of points in most problems. For such points τ_i and ϵ_i have single values and the equations (43), (44), (45) and (46) reduce to

$$\tau(4\phi_o - \sum_{i=1}^{4} \phi_i) = \frac{(k_o h)^2}{12} (6\phi_o + \sum_{i=1}^{6} \phi_i) \tag{5.49}$$

and

$$\tau\bar{\beta}^2 (4\psi_o - \sum_{i=1}^{4} \psi_i) = \frac{(k_o h)^2}{12} \bar{\beta}^2 (6\psi_o + \sum_{i=1}^{6} \psi_i) \tag{5.50}$$

for triangular mesh grading, and

$$\tau (8\phi_o - \sum_{i=1}^{8} \phi_i) = \frac{(k_o h)^2}{6} (8\phi_o + 2\sum_{i=1}^{4} \phi_i + \tfrac{1}{2}\sum_{i=5}^{8} \phi_i \tag{5.51}$$

and

$$\bar{\beta}^2\tau(8\psi_o - \sum_{i=1}^{8} \psi_i) = \frac{(k_o h)^2}{6} \bar{\beta}^2 \left\{ 8\psi_o + 2\sum_{i=1}^{4} \psi_i + \tfrac{1}{2}\sum_{i=5}^{8} \psi_i \right\} \tag{5.52}$$

for square mesh grading.

5.3.2 Plane Boundary Vertices

Those vertices lying on a plane boundary between two dielectrics are called plane boundary vertices. Such a vertex may be generated if we consider $\epsilon_1 = \epsilon_2$, $\epsilon_3 = \epsilon_4$, $\tau_1 = \tau_2$ and $\tau_3 = \tau_4$. Of most interest is the case where one of the dielectrics is a vacuum. Accordingly, we present the equations for the case of $\epsilon_1 = 1$ and $\epsilon_3 = \epsilon_r$.

$$\tfrac{1}{2}(1+\tau)\,(4\phi_0-\phi_1-\phi_3) - \phi_4 - \tau\phi_2 + \frac{\bar{\beta}^2}{2}\,(1-\tau)(\psi_1-\psi_3)$$

$$= \frac{k_0\,h^2}{12}\,(6\phi_0 + \sum_{i=1}^{6}\phi_i) \qquad (5.53)$$

and

$$\tfrac{1}{2}(1+\tau\epsilon_r)(4\,\psi_0-\psi_1-\psi_3) - \psi_4 - \tau\epsilon_r\psi_2 + \tfrac{1}{2}(1-\tau)(\phi_3-\phi_1)$$

$$= \frac{k_0\,h^2}{12}\Big[(1+\epsilon_r)3\,\psi_0 + \tfrac{1}{2}(1+\epsilon_r)(\psi_1+\psi_3) + \psi_4 + \psi_5 + \epsilon_r(\psi_2+\psi_6)\Big] \qquad (5.54)$$

for grading into triangular meshes, and

$$\tfrac{1}{2}(1+\tau)(8\phi_0-\phi_1-\phi_3) - \phi_4 - \phi_5 - \phi_7 - \tau(\phi_2+\phi_6+\phi_8)$$

$$\frac{3}{2}\bar{\beta}^2\,(1-\tau)(\psi_1-\psi_3) = \frac{k_0\,h^2}{6}\,\Big(8\phi_0 + 2\sum_{i=1}^{4}\phi_i + \tfrac{1}{2}\sum_{i=5}^{8}\phi_i\Big) \qquad (5.55)$$

and

$$\tfrac{1}{2}(1+\epsilon_r\tau)(8\,\psi_o-\psi_1-\psi_3)-\psi_4-\psi_5-\psi_7-\tau\,\epsilon_r\,(\psi_2+\psi_6+\psi_8)$$

$$\tfrac{3}{2}(1-\tau)(\phi_3-\phi_1) = \frac{(k_o\,h)^2}{6}\Big[4(1+\epsilon_r)\,\psi_o+$$

$$2\,\psi_4+2\,\epsilon_r\,\psi_2+(1+\epsilon_r)(\psi_3+\psi_1)+\tfrac{1}{2}\,\psi_5+\tfrac{1}{2}\,\psi_7+$$

$$\frac{\epsilon_r}{2}\,\psi_6+\frac{\epsilon_r}{2}\,\psi_8\Big] \tag{5.56}$$

for grading into square meshes.

5.3.3 $\frac{\pi}{2}$ dielectric corner

A special case occurs when a point lies at a $\pi/2$ edge between two dielectrics. Here, for example, $\epsilon_1 = \epsilon_2 = \epsilon_4$, $\tau_1 = \tau_2 = \tau_4$. If one of the dielectrics is vacuum, say $\epsilon_1 = 1$, then writing $\epsilon_3 = \epsilon_r$, we obtain

$$(3+\tau)\phi_o-\tfrac{1}{2}(1+\tau)(\phi_2+\phi_3)-\phi_1-\phi_4+\frac{\bar{\beta}^2}{2}(\tau-1)(\psi_3-\psi_2)$$

$$=\frac{(k_oh)^2}{12}\Big(6\phi_o+\sum_{i=1}^{6}\phi_i\Big) \tag{5.57}$$

and

$$(3+\tau\,\epsilon_r)\,\psi_o-\tfrac{1}{2}(1+\tau\,\epsilon_r)(\psi_2+\psi_3)-\psi_1-\psi_4+\tfrac{1}{2}(\tau-1)(\phi_2-\phi_3)$$

$$=\frac{(k_oh)^2}{12}\Big[(4+2\,\epsilon_r)\,\psi_o+\psi_1+\psi_4+\psi_5+\frac{(1+\epsilon_r)}{2}(\psi_3+\psi_2)+\epsilon_r\psi_6\Big] \tag{5.58}$$

for triangular mesh grading, and

$$(6+2\tau)\phi_o - \tfrac{1}{2}(1+\tau)(\phi_2+\phi_3) - \phi_1 - \phi_4 - \phi_5 - \phi_7 - \phi_8 - \tau\phi_6 +$$

$$\frac{3}{2}\bar{\beta}^2(\tau-1)(\psi_3-\psi_2) = \frac{(k_o h)^2}{6}\left(3\phi_o + 2\sum_{i=1}^{4}\phi_i + \tfrac{1}{2}\sum_{i=5}^{8}\phi_i\right) \tag{5.59}$$

and

$$(6+2\tau\epsilon_r)\psi_o - \tfrac{1}{2}(1+\tau\epsilon_r)(\psi_2+\psi_3) - \psi_1 - \psi_4 - \psi_5 - \psi_7 - \psi_8 - \tau\epsilon_r\psi_6$$

$$+\frac{3}{2}(\tau-1)(\phi_2-\phi_1) = \frac{(k_o h)^2}{6}\Big[(6+2\epsilon_r)\psi_o + (1+\epsilon_r)(\psi_2+\psi_3) +$$

$$2(\psi_1+\psi_4) + \tfrac{1}{2}(\psi_5+\psi_7+\psi_8) + \frac{\epsilon_r}{2}\psi_6\Big] \tag{5.60}$$

for square mesh grading of the waveguide cross-section.

5.5 Applications

A number of standard slab loaded waveguides are analysed in some detail to demonstrate the usefulness of the finite-element formulation and to estimate the relative accuracy on successive decrease of element sizes. These results are compared with the exact analytic results as well as the results obtained from the finite-difference method wherever possible.

5.5.1 A Rectangular Waveguide partially filled with a Full-Height-Dielectric Slab

The geometry of a rectangular waveguide with a full-height-dielectric slab placed symmetrically at the centre of the broad side is illustrated in Figure (5.4). Electromagnetically, the dielectric slab is mounted in the E-plane at the centre of the rectangular waveguide. Analytic solutions in compact form can be obtained for this type of dielectric loading. The two appropriate type of modes corresponding to TE and TM-modes that can be sustained by the above waveguide are called the longitudinal section electric mode (LSE) and the longitudinal section magnetic mode (LSM). The LSE mode is characterised by $E_x = 0$, and the LSM mode is characterised by $H_x = 0$.

The dominant mode propagating through the above slab loaded waveguide would be odd TE mode, and field vector would be independent of y co-ordinates. A detailed discussion of this type of waveguide is given by Vartanian, Ayres and Helgesson[1]. Exact relation between the propagation constant $\bar{\beta}$ and the frequency w can be obtained by solving the following transcendental equation:

$$\frac{\tan(m)}{m} = \eta \frac{\tan(q)}{q} \qquad (5.61)$$

where $\eta = \frac{s}{d}$;

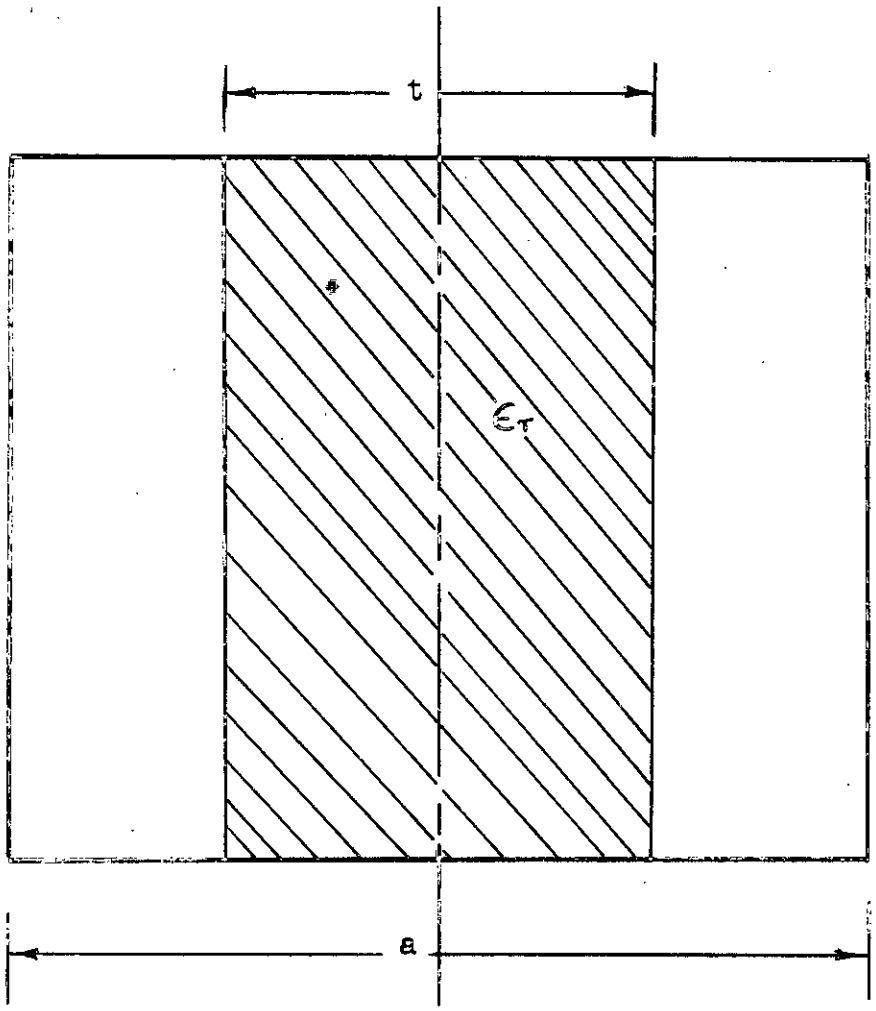

Figure (5.4)

Rectangular Waveguide Loaded
with
a Full-height Dielectric Slab

and m and q are given by

$$\left(\frac{m}{d}\right)^2 = \left(\frac{w}{c}\right)^2 - \bar{\beta}^2 \tag{5.62}$$

$$\left(\frac{q}{s}\right)^2 = \epsilon_r \left(\frac{w}{c}\right)^2 - \bar{\beta}^2 \tag{5.63}$$

Numerical analysis of the above waveguide by the finite-difference method is reported by Collins and Daly(2) and also by Muilwyk(3). We have analysed a problem with $\frac{d}{s}$ = 1.0 and ϵ_r = 1.50 and 2.45, by the finite-element method and also by the finite-difference method. The computational values of the cut-off wavenumber for various values of τ obtained by both the methods together with that obtained by solving the transcendental equation are tabulated in Tables (5.1) and (5.2). Comparing the computed results with that of the exact analytic solution, we find that the finite-element method gives comparatively accurate results for the same number of mesh points.

The dispersion characteristics for the above waveguide system for ϵ_r = 1.50 and 2.45 are shown in Figure (5.5). In Table (5.3) we present the computed values of normalised H_z for various values of $\bar{\beta}$ and Figure (5.6) gives a corresponding graphical plot of H_z as a function of x.

Table (1) A rectangular waveguide partially filled with a dielectric slab as in Figure (5.4)

$\epsilon_r = 1.500$

$\bar{\beta}$	t	$(W\ a/c)^2$				% Error	
		h/a	F.E	F.D	Exact	F.E	F.D
0.00	0.667	1/8	7.0624	6.8799	6.9923	1.001	-1.610
		1/16	7.0098	6.9641		0.107	-0.400
		1/32	6.9967	6.9853		0.063	-0.100
0.20	0.666	1/8	7.2674	7.0795	7.1958	1.000	-1.635
		1/16	7.2138	7.1667		0.250	-0.405
		1/32	7.2004	7.1886		0.064	-0.102
0.40	0.627	1/8	7.9607	7.7540	7.8845	0.954	-1.655
		1/16	7.9035	7.8517		0.241	-0.416
		1/32	7.8892	7.8763		0.060	-0.101
0.60	0.561	1/8	9.4646	9.2166	9.3789	0.913	-1.730
		1/16	9.4007	9.3385		0.232	-0.434
		1/32	9.3847	9.3691		0.060	-0.105
0.70	0.505	1/8	10.7883	10.5031	10.6961	0.7685	-1.804
		1/16	10.7196	10.6479		0.219	-0.451
		1/32	10.7023	10.6843		0.021	-0.110
0.80	0.419	1/8	12.8617	12.5162	12.7611	0.788	-1.919
		1/16	12.7872	12.7003		0.204	-0.476
		1/32	12.7684	12.7466		0.057	-0.114

Table (1) continued

β	τ	$(\omega a/c)^2$				% Error	
		h/a	F.E	F.D	Exact	F.E	F.D
		1/8	16.4338	15.9779		0.658	-2.134
0.90	0.275	1/16	16.3547	16.2397	16.3263	0.174	-0.530
		1/32	16.3345	16.3057		0.052	-0.126
		1/8	19.3493	18.7964		0.535	-2.311
0.95	0.196	1/16	19.2710	19.1312	19.2410	0.156	-0.570
		1/32	19.2509	19.2159		0.052	-0.130
		1/8	31.2463	30.2179		0.148	-3.182
1.05	-0.258	1/16	31.2109	30.9469	31.2000	0.035	0.812
		1/32	31.2005	31.1341		<0.002	0.212
		1/8	38.7482			0.019	
1.08	-0.499	1/16	38.7682	38.4042	38.7681	<0.0011	0.940
		1/32	38.7708	38.6791		0.007	0.226
		1/8	46.2252			-0.252	
1.10	-0.724	1/16	46.3189		46.3429	-0.052	
		1/32	46.3391	46.2170		-0.019	- .270
		1/8	57.2924			-0.523	
1.12	-1.036	1/16	57.5239		57.5943	-0.122	
		1/32	57.5770			-0.03	

Table (1) continued

β	τ	$(\omega\, a/c)^2$				% Error	
		h/a	F.E	F.D	Exact	F.E	F.D
1.14	-1.495	1/8	75.0657		75.7409	-0.218	
		1/16	75.5757			-0.060	
		1/32	75.6959				
1.16	-2.238	1/8	107.1481		108.6574	-1.390	
		1/16	108.2888			-0.300	
		1/32	108.5631			-0.087	
1.20	-7.333	1/8			395.5500		
		1/16	391.2899			-0.949	
		1/32	428.2916			+8.000	

Table (2) Same Waveguide as in Table (1) with $\epsilon_r = 2.45$

$\bar{\beta}$	t	$\frac{h}{a}$	$(\omega a/c)^2$			% Error	
			F.E	F.D	Exact	F.E	F.D
0.00	0.408	1/8	4.5229	4.4012	4.4880	0.778	-1.925
		1/16	4.4970	4.4664		0.200	-0.481
		1/32	4.4905	4.4828		0.056	-0.116
0.20	0.398	1/8	4.6058	4.4816	4.5708	0.767	-1.951
		1/16	4.5798	4.5485		0.197	-0.498
		1/32	4.5732	4.5654		0.053	-0.118
0.40	0.367	1/8	4.8738	4.7414	4.8381	0.740	-2.000
		1/16	4.8472	4.8140		0.189	-0.498
		1/32	4.8405	4.8322		0.049	-0.122
0.60	0.312	1/8	5.3965	5.2480	5.3609	0.663	-2.080
		1/16	5.3695	5.3320		0.160	-0.540
		1/32	5.3626	5.3532		0.032	-0.145
0.80	0.199	1/8	6.3482	6.1686	6.3111	0.589	-2.260
		1/16	6.3209	6.2755		0.156	-0.565
		1/32	6.3139	6.3026		0.044	-0.135
0.90	0.116	1/8	7.1072	6.9013	7.0731	0.480	-2.420
		1/16	7.0808	7.0286		0.109	-0.630
		1/32	7.0739	7.0609		0.011	-0.173
0.95	0.063	1/8	7.6007	7.3770	7.5679	0.432	-2.520
		1/16	7.5752	7.5184		0.097	-0.655
		1/32	7.5685	7.5543		0.008	-0.180

Table (2) continued

β	τ	$\frac{h}{a}$	$(\omega\, a/c)^2$			% Error	
			F.E	F.D	Exact	F.E	F.D
		1/8	9.8683	9.5541		0.252	-2.940
1.10	-0.169	1/16	9.8512	9.7708	9.8433	0.080	-0.735
		1/32	9.8463	9.8262		0.032	-0.174
		1/8	10.8012	10.4454		0.156	-3.178
1.14	-0.260	1/16	10.7892	10.6978	10.7844	0.045	-0.828
		1/32	10.7855	10.7627		0.010	-0.202
		1/8	12.6663			<0.002	
1.20	-0.436	1/16	12.6675	12.5518	12.6661	<0.020	-0.900
		1/32	12.6669	12.6378		<0.010	-0.222
		1/8	14.8877				
1.25	-0.634	1/16	14.9089	14.7602	14.6627		
		1/32	14.9132	14.8756			
		1/8	18.1549			-0.415	
1.30	-0.932	1/16	18.2135		18.2306	-0.093	
		1/32	18.2267			-0.021	
		1/8	23.3554			-0.722	
1.35	-1.311	1/16	23.4891		23.5282	-0.166	
		1/32	23.5203			-0.033	
		1/8	32.6419			-1.220	
1.40	-1.959	1/16	32.9451		33.0438	-0.300	
		1/32	33.0174			-0.080	
		1/8					
1.45	-3.173	1/16	53.1911		53.2007		
		1/32	53.3847				

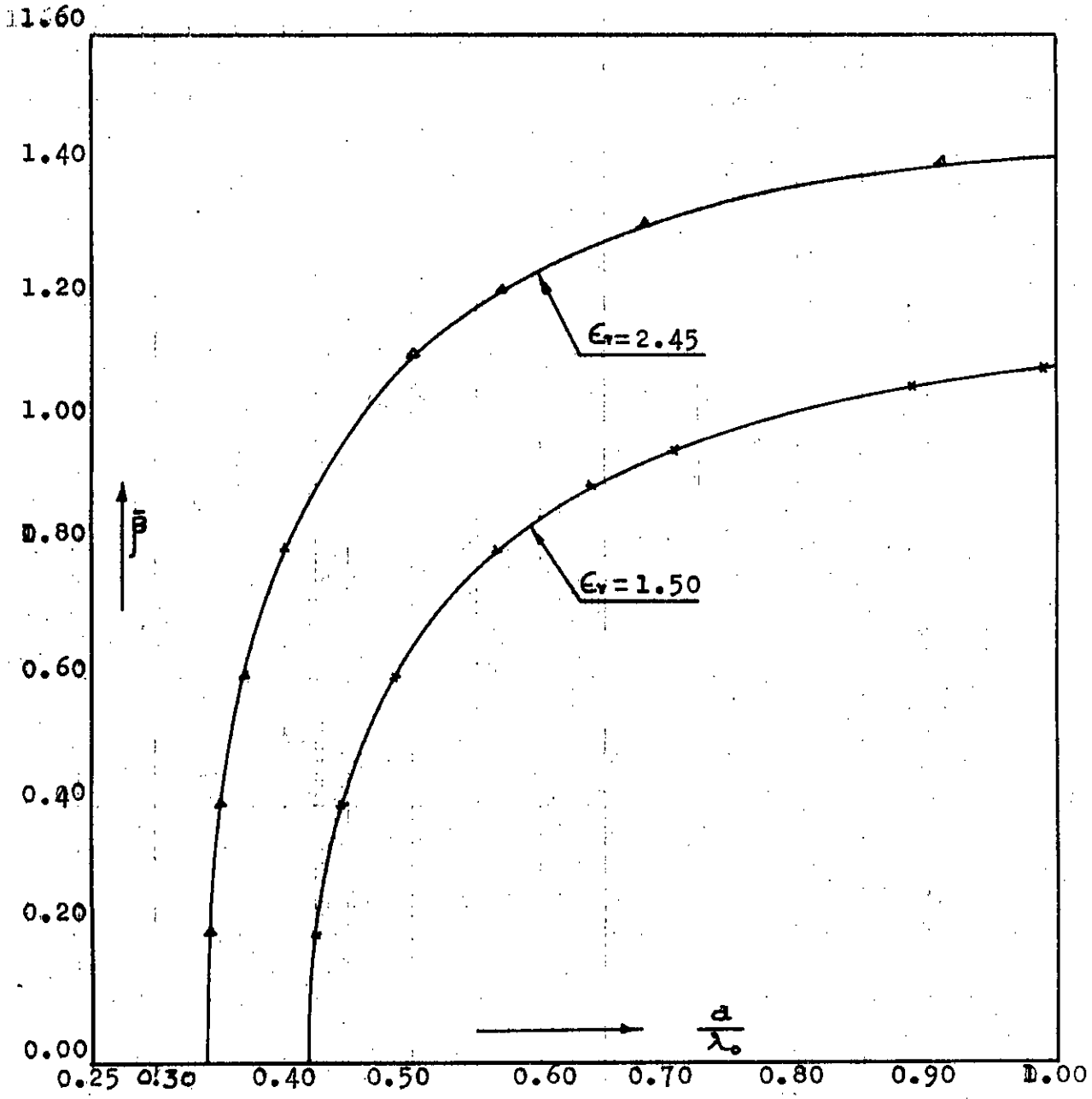

Fig.(5.5): Dispersion Curves for two Dielectrics for the Probleb in Fig.(5.4).

Table (3) Normalised H_z for dominant mode in the Waveguide of Figure (5.4)

a) $\epsilon_r = 1.500$

$\frac{2x}{a}$	H_z			
	$\bar{\beta} = 0.5$	$\bar{\beta} = 0.95$	$\bar{\beta} = 1.10$	$\bar{\beta} = 1.20$
0.000	0	0	0	0
0.125	222	264	286	317
0.250	435	517	557	607
0.375	631	746	800	842
0.500	800	942	1000	1000
0.625	886	967	891	432
0.750	948	986	816	191
0.875	987	999	772	93
1.000	1000	1000	758	67

Table (3) Normalised H_z for dominant mode in the Waveguide of Figure (5.4)

b) $\varepsilon_r = 2.45$

$\frac{2x}{a}$	H_z			
	$\bar{\beta} = 0.50$	$\bar{\beta} = 0.95$	$\bar{\beta} = 1.20$	$\bar{\beta} = 1.40$
0.000	0	0	0	0
0.125	247	275	284	295
0.250	483	537	554	570
0.375	699	775	797	811
0.500	884	977	1000	1000
0.625	934	987	932	744
0.750	970	991	885	581
0.875	992	999	857	491
1.000	1000	1000	849	462

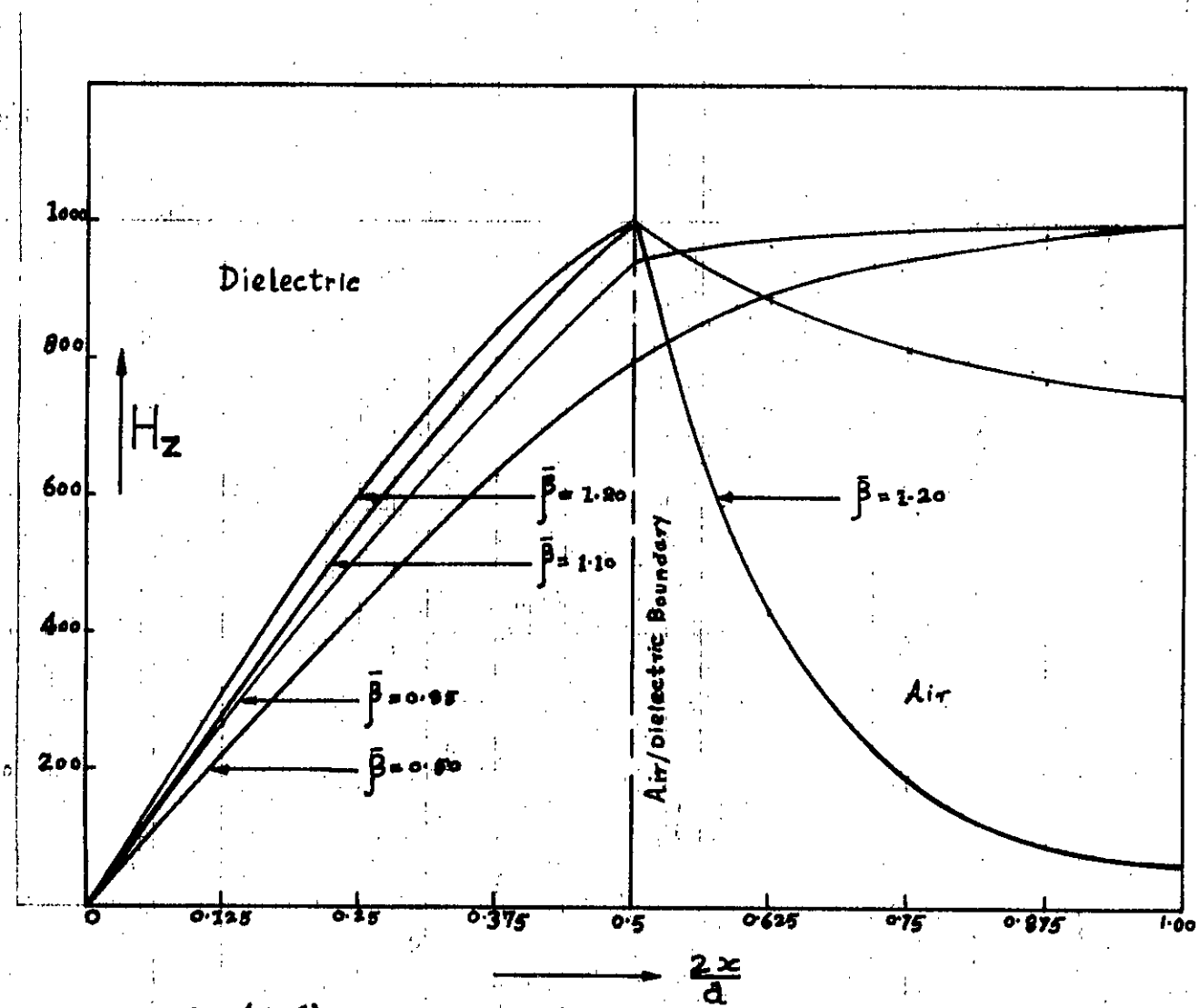

Fig.(5.6): Normalised H_z as a Function of x for TE_{10} Mode in the Problem of Fig.(5.4). $\epsilon_r = 1.500$

5.4.2 A Slab Loaded Rectangular Waveguide with Slab Perpendicular to E at cut-off

The configuration of Figure (5.7) shows the cross-section of a rectangular waveguide with a dielectric slab placed at one side of the guide. This is a somewhat more interesting example. In the preceding case (Section 5.4.1) was involved a mode of transmission that was transverse electric both to the direction of propagation and to the direction normal to the dielectric interface. In the present case, if the interface normal is chosen as the reference direction, the field configuration may be considered to be that of E-mode. The field has components E_x, E_y, E_z and H_y and H_z. Hence, with respect to the axis of propagation, the LSM mode is a hybrid one and provides a suitable test for the finite-element method. Exact theoretical analysis for the propagation characteristic involves a transcendental equation and this is given by Marcuvitz (P. 392, ref.(4)) which may be written in terms of ϵ_r, τ and k_o^2 as follows:

$$\epsilon_r \sqrt{(k_o a)^2 - \pi^2} \tan\left(\frac{b-d}{a}\sqrt{(k_o a)^2 - \pi^2}\right) = -\sqrt{\frac{(k_o a)^2}{\tau} - \pi^2}$$

$$\tan\left(\frac{d}{a}\sqrt{\frac{(k_o a)^2}{\tau} - \pi^2}\right) \qquad (5.64)$$

Using the symmetry of the problem and applying the relevant finite-element equations at each point for ϕ and ψ

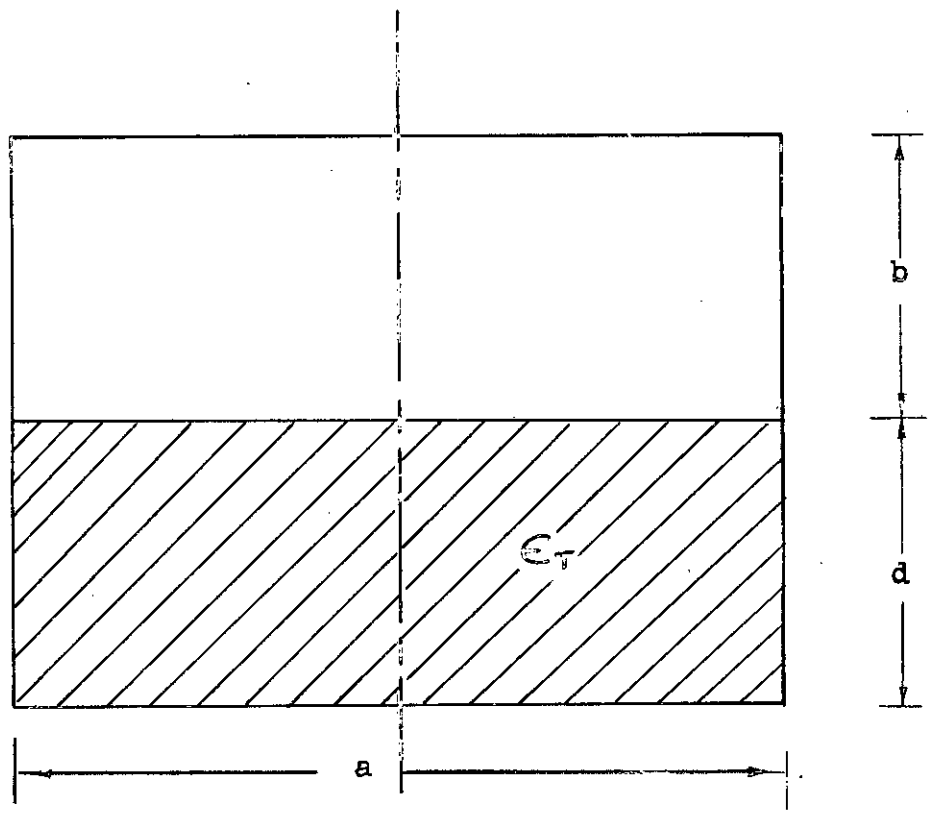

Figure (5.7)

A Rectangular Waveguide
with
Dielectric at Bottom of the Guide

(for triangular elements), we arrive at a matrix equation whose eigenvalues for various meshes are compared in Tables (5.4), (5.5) and (5.6) with those of Marcuvitz[4]. In Figure (5.8) dispersion curves are presented from the results of Tables (5.4), (5.5) and (5.6). With the maximum value of ϕ normalised to 1000 field values of ϕ and ψ are shown at a particular frequency in Table (5.7) and their contours in Figure (5.9). By means of numerical differentiation, it is possible to calculate the values of the transverse fields. In Table (5.8) calculated values of $\sqrt{\frac{\varepsilon_0}{\mu_0}}\, E_y$ and H_x are presented and in Figure (5.10) their contours are drawn. By the same process the values of H_y can be shown to be zero at each point within a small error. It is to be expected that large errors occur in the transverse fields since the calculations involve differentiation of eigenvectors.

Table (5.4) A Rectangular Waveguide with a Dielectric Slab Perpendicular to E at cut-off (with dimensions as in Figure (5.7)

$\epsilon_r = 1.50$

$\bar{\beta}$	h/a	$(wa/c)^2$		$\bar{\beta}$	h/a	$(wa/c)^2$	
		F-Element	Marcu-vitz			F.E.	Marcuvitz
	1/8	8.0417			1/8	20.6629	
0.00	1/10	8.0085	7.9482	0.90	1/10	20.4623	20.0942
	1/12	7.9902			1/12	20.3515	
	1/8	8.6485			1/8	24.9336	
0.30	1/10	8.6120	8.5457	0.95	1/10	24.5576	23.8540
	1/12	8.5919			1/12	24.3476	
	1/8	9.9775			1/8	37.9711	
0.50	1/10	9.9323	9.8515	1.05	1/10	38.1277	38.3463
	1/12	9.9082			1/12	38.1617	
	1/8				1/8		
0.60	1/10	11.0890	10.9929	1.07	1/10	43,6915	43.5963
	1/12	11.0604			1/12	43.6117	
	1/8	12.9017			1/8	50.9835	
0.70	1/10	12.8332	12.7084	1.09	1/10	50.8465	50.4524
	1/12	12.7955			1/12	50.7026	
	1/8	15.7078			1/8	55.4688	
0.80	1/10	15.6063	15.4208	1.10	1/10	55.2133	54.7281
	1/12	15.5504			1/12	55.0571	

Table (5.4) continued

$\bar{\beta}$	h/a	wa/c		$\bar{\beta}$	h/a	wa/c	
		F-Element	Marcu-vitz			F.E.	Marcuvitz
	1/8	66.9999			1/8	111.7533	
1.12	1/10	66.6015	65.7952	1.16	1/10	110.7804	109.0891
	1/12	66.3791			1/12	110.2718	
	1/8	83.9966			1/8	164.7526	
1.14	1/10	83.3693	82.2270	1.18	1/10	163.2288	160.6095
	1/12	83.0173			1/12	162.5000	

Table (5.5) Same Waveguide as in Figure (5.7) with $\varepsilon_r = 2.45$

$\bar{\beta}$	h/a	$(\omega a/c)^2$ F-Element	$(\omega a/c)^2$ Marcuvitz	$\bar{\beta}$	h/a	$(\omega a/c)^2$ F-Element	$(\omega a/c)^2$ Marcuvitz
	1/8	5.9364			1/8	11.9227	
0.00	1/10	5.9067	5.8520	1.06	1/10	12.0345	12.1982
	1/12	5.8903			1/12	12.0638	
	1/8	6.0615			1/8	13.1799	
0.20	1/10	6.0304	5.9731	1.10	1/10	13.1733	13.1705
	1/12	6.0131			1/12	13.2068	
	1/8	6.4665			1/8	15.2350	
0.40	1/10	6.4302	6.3637	1.16	1/10	15.1503	15.0038
	1/12	6.4102			1/12	15.1061	
	1/8	7.2588			1/8	16.9067	
0.60	1/10	7.2102	7.1216	1.20	1/10	16.7846	16.5716
	1/12	7.1835			1/12	16.7115	
	1/8	7.8725			1/8	18.9848	
0.70	1/10	7.8121	7.7014	1.24	1/10	18.8263	18.5350
	1/12	7.7788			1/12	18.7335	
	1/8	8.7120			1/8	25.1459	
0.80	1/10	8.6295	8.4778	1.32	1/10	24.8979	24.3000
	1/12	8.5838			1/12	24.7495	
	1/8	9.9291			1/8	30.0417	
0.90	1/10	9.7914	9.5337	1.36	1/10	29.7158	
	1/12	9.7146			1/12	29.5293	
	1/8	10.8649			1/8	37.3572	
0.95	1/10	10.6451	10.2534	1.40	1/10	36.9195	
	1/12	10.5181			1/12	36.6842	

Table (5.6) Same Waveguide as in Figure (5.7) with $\epsilon_r = 8.85$

$\bar{\beta}$	h/a	$(\omega a/c)^2$ F-Element	$(\omega a/c)^2$ Marcuvitz	$\bar{\beta}$	h/a	$(\omega a/c)^2$ F-Element	$(\omega a/c)^2$ Marcuvitz
0.00	1/8	2.100	2.053	1.30	1/8	2.666	2.581
	1/10	2.083			1/10	2.642	
	1/12	2.074			1/12	2.625	
0.20	1/8	2.111	2.063	1.50	1/8	2.922	2.814
	1/10	2.094			1/10	2.882	
	1/12	2.085			1/12	2.860	
0.40	1/8	2.145	2.094	1.70	1/8	3.263	3.133
	1/10	2.127			1/10	3.217	
	1/12	2.117			1/12	3.192	
0.60	1/8	2.204	2.148	1.90	1/8	3.734	3.583
	1/10	2.185			1/10	3.679	
	1/12	2.174			1/12	3.649	
0.80	1/8	2.297	2.228	2.10	1/8	4.436	4.253
	1/10	2.273			1/10	4.369	
	1/12	2.259			1/12	4.333	
0.90	1/8	2.368	2.279	2.30	1/8	5.572	5.337
	1/10	2.338			1/10	5.488	
	1/12	2.321			1/12	5.443	
1.05	1/8	2.250	2.373	2.50	1/8	7.684	7.357
	1/10	2.333			1/10	7.566	
	1/12	2.352			1/12	7.503	
1.10	1/8	2.420	2.408	2.60	1/8	9.598	9.187
	1/10	2.448			1/10	9.446	
	1/12	2.338			1/12	9.370	

Table (5.7) Computed Values of normalised H_z and $\frac{w\epsilon_o}{\beta} E_z$ for the Waveguide as in Figure (5.7) with $\epsilon_r = 1.50$, $\bar{\beta} = 1.10$, and $h/a = 1/12$

0	19	36	50	62	68	70
0	0	0	0	0	0	0
0	20	38	54	66	73	75
41	39	35	29	20	10	0
0	24	46	66	81	90	93
88	85	75	62	44	22	0
0	32	62	88	107	119	123
148	142	128	104	73	38	0
0	45	87	122	150	167	173
230	222	198	162	114	59	0
0	64	124	175	215	240	248
345	334	299	244	173	90	0
0	91	180	254	313	348	361
510	497	443	365	257	135	0
0	139	271	383	470	525	545
464	448	402	329	232	120	0
0	181	350	497	609	680	705
397	383	343	280	198	102	0
0	215	417	590	723	807	836
313	302	271	221	156	80	0
0	242	467	660	808	900	932
217	209	187	152	107	55	0
0	258	498	703	860	957	989
111	107	95	77	54	28	0
0	265	510	719	878	975	1000
0	0	0	0	0	0	0

axis of symmetry

x

y

Top figures – $H_z = \phi$

Bottom figures $\frac{\omega\epsilon_o}{\beta} E_z = \psi$

Table (5.8) Calculated Values of $\sqrt{\frac{\epsilon_0}{\mu_0}}\,E_y$ and H_x for the Dominant modes in the Waveguide shown in Figure (5.7) for $\epsilon_r = 1.5$, $\bar{\beta} = 1.1$, and $\frac{h}{a} = 1/12$.

	200		192		172		141		100		54
	234		225		202		165		116		63
	215		206		185		151		107		56
	252		243		217		177		125		65
	260		251		225		184		131		69
	305		295		264		215		153		80
	345		334		299		245		174		92
	406		391		351		288		204		106
	480		467		417		344		244		129
	564		548		489		402		286		151
	680		674		594		498		346		189
	799		789		696		583		409		221
1063	970	1060	945	981	880	797	745	575	510	298	290
	709		702		661		529		393		204
	1462		1440		1285		1065		750		402
	1131		1112		992		823		579		309
	1921		1865		1674		1375		973		510
	1484		1439		1292		1060		752		394
	2292		2217		1990		1626		1151		598
	1772		1713		1536		1255		890		462
	2570		2482		2224		1814		1280		662
	1985		1918		1719		1401		988		511
	2748		2649		2368		1926		1353		691
	2122		2044		1829		1487		1044		531
	2817		2709		2416		1960		1370		674
	2178		2094		1866		1514		920		518

Axis of symmetry

x → Top figures → H_x

Bottom figures → $\sqrt{\frac{\epsilon_0}{\mu_0}}\,E_y$

y

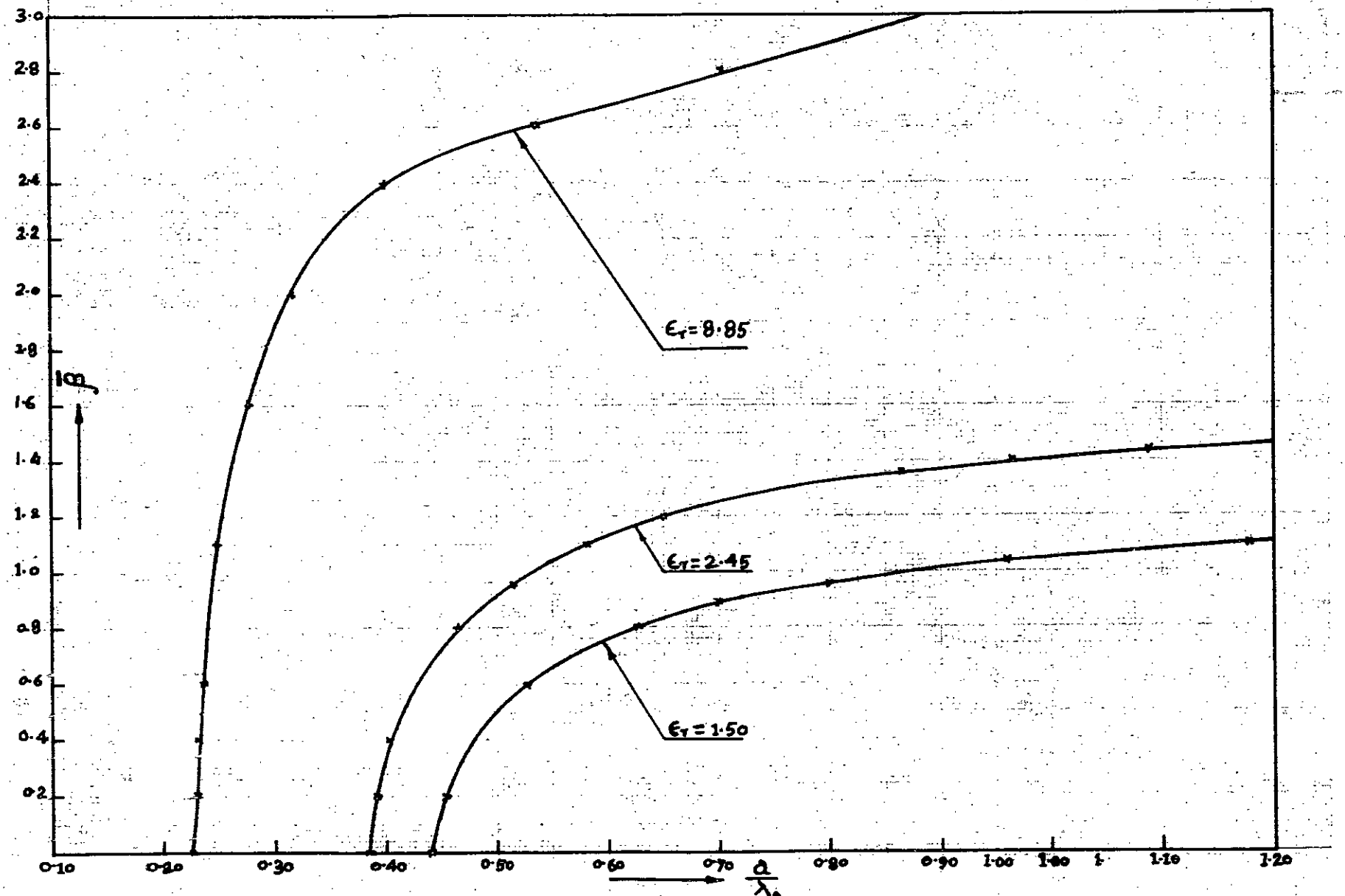

Fig. (5-8): Variations of $\bar{\beta}$ with a/λ_0 for three Dielectrics in Fig. (5-7).

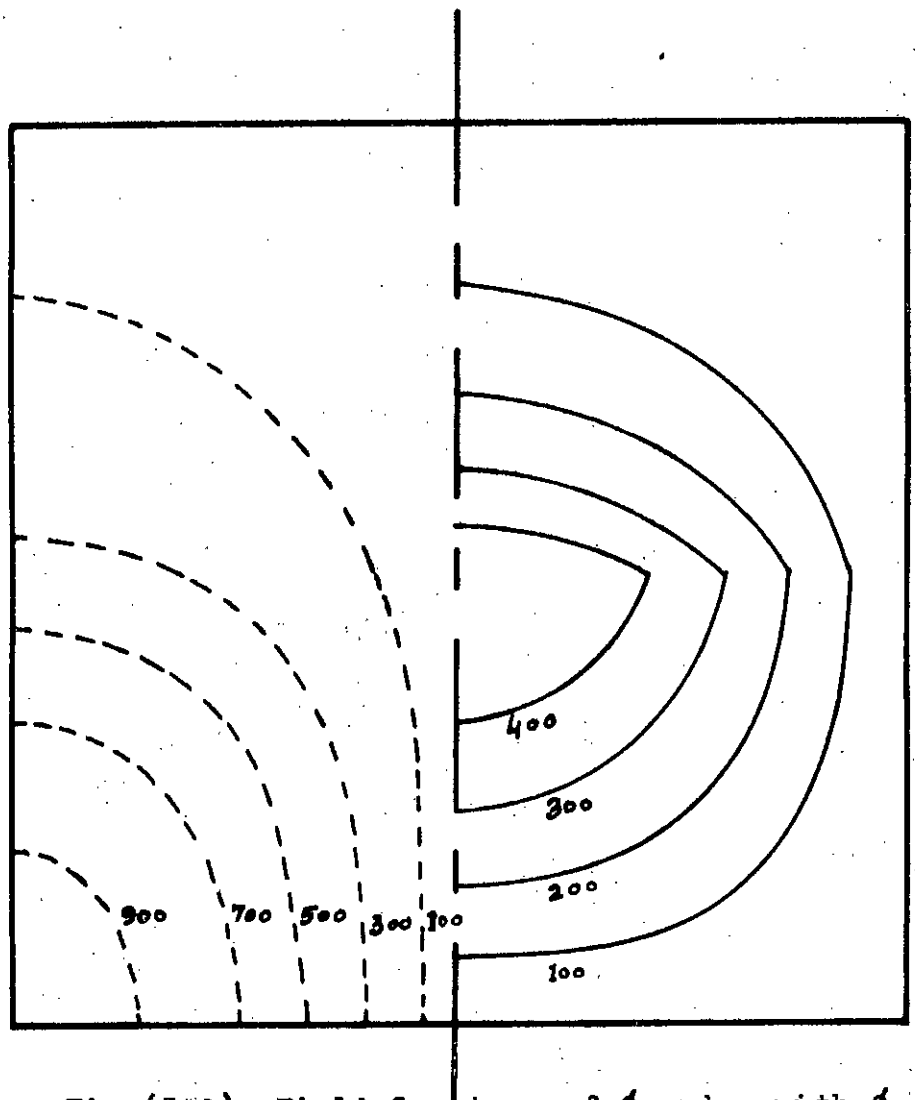

Fig.(5.9): Field Countour of ϕ and with ϕ Normalised to 1000.

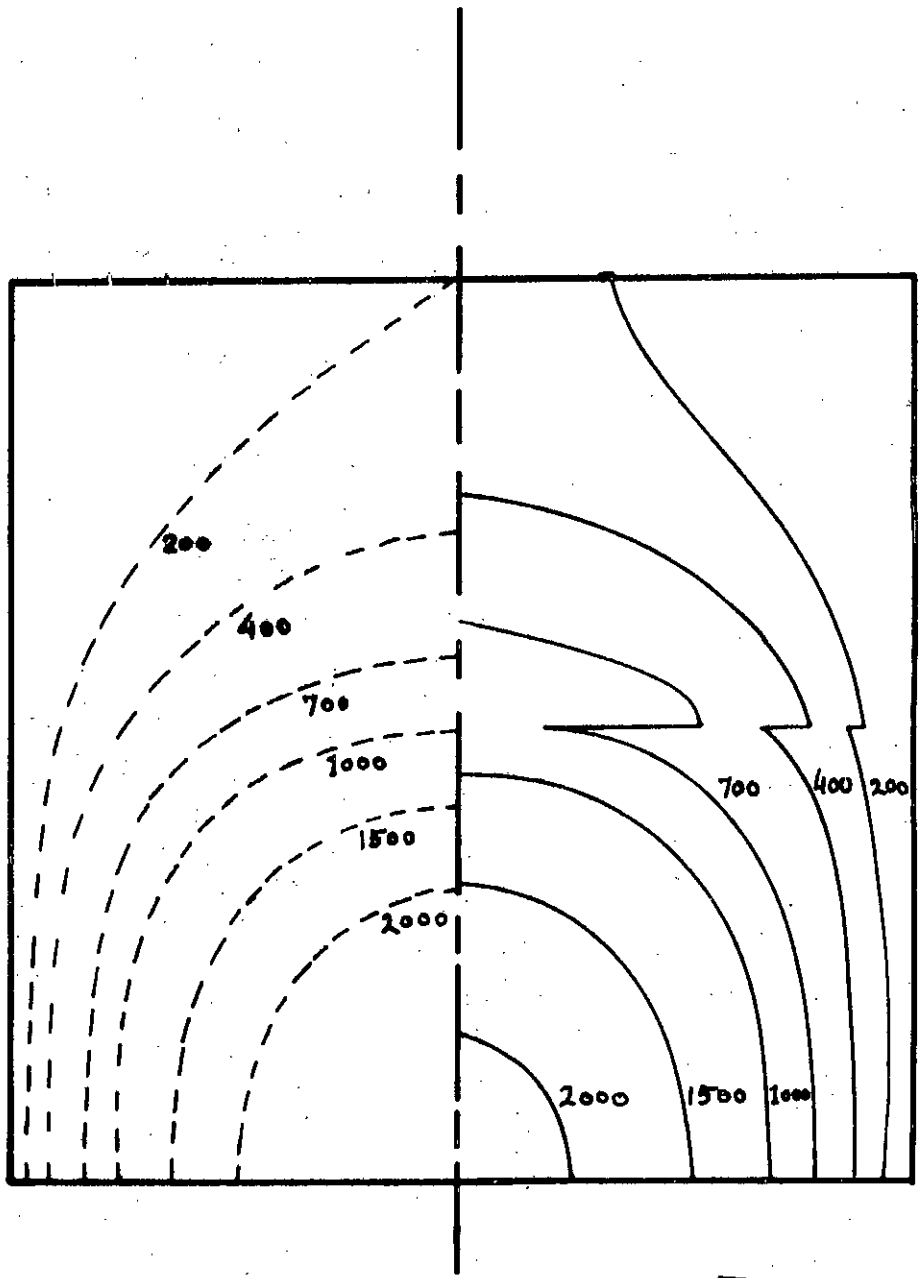

Fig.(5.10): Field Countour of H_x and $\sqrt{\frac{\epsilon_0}{\mu_0}}E_y$ with ϕ Normalised to 1000. ---------- H_x

———————— $\sqrt{\frac{\epsilon_0}{\mu_0}}E_y$

5.4.3 A Rectangular Waveguide Partially Filled with a Rectangular Dielectric Insert

The general configuration of a rectangular waveguide with a rectangular dielectric insert is illustrated in Figure (5.11). Exact analytic solution in compact form is not possible for this type of dielectric filling. An approximate analytic solution based on the principle of transverse resonance is given by Lavik and Unger[5]. Numerical solutions by the finite-difference method are reported by Hannaford[6] and Muilwyk[3]. We present in this section two sets of results obtained by the finite-element method. The first set corresponds to one of the waveguides considered in reference (5) and is shown in Figure (5.12) and the second set of results corresponds to the waveguide considered in reference (3); this is shown in Figure (5.13). These results demonstrate the relative accuracy and convergence of the finite-element method. No attempt is made to present comprehensive dispersion curves for a large number of permittivities over the working range, because the main purpose of this thesis is to verify the application of the finite-element method for waveguide problems.

For the range of $\bar{\beta}$ less than unity and for triangular mesh discretisation, numerical computations of the

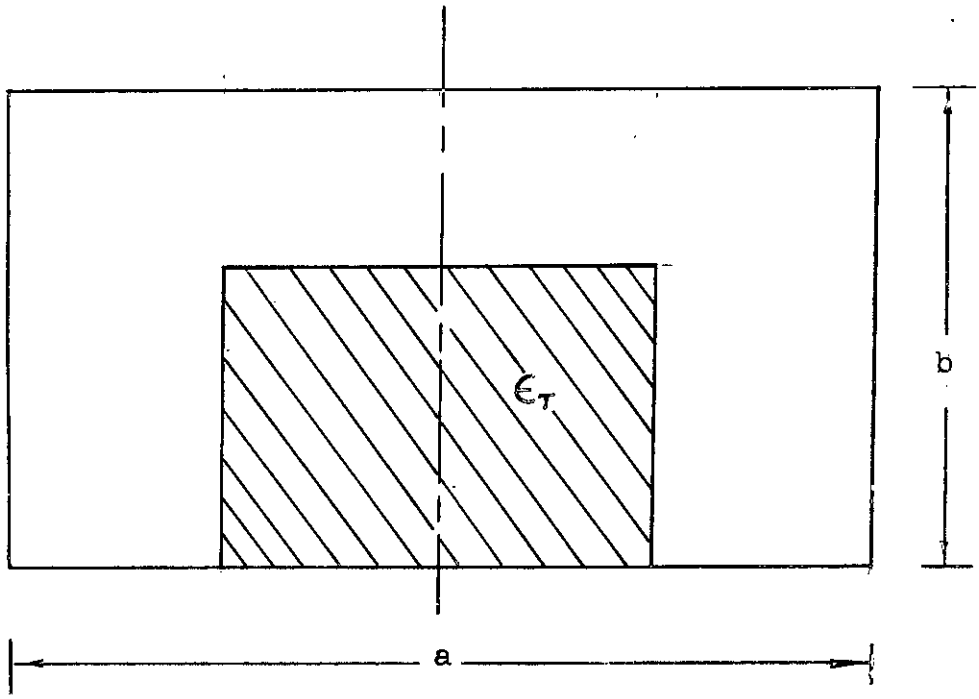

Figure (5.11)
Dielectric Insert in Rectangular Waveguide

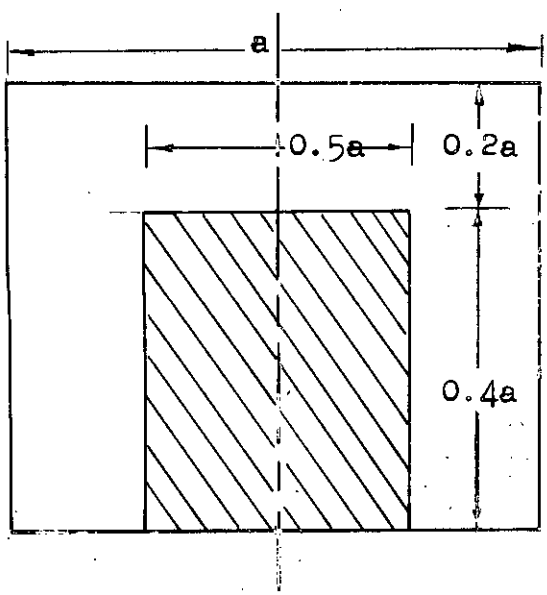

Figure (5.12)
Dielectric Loaded Waveguide solved by Successive over-relaxation method

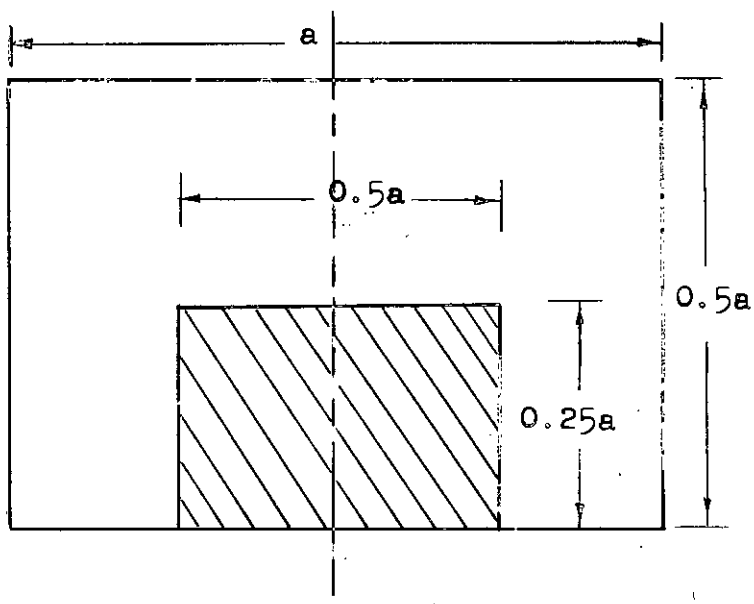

Figure (5.13)
Dielectric Loaded Waveguide solved by NPL Procedure PROC 2929

wavenumber for the dielectric loaded waveguide as shown in Figure (5.12) are performed by the SOR type iteration technique. Results of $\omega a/c$ against $\bar{\beta}a$ for $\epsilon_r = 3, 6, 15$ are shown in the form of dispersion curves in Figures (5.14), (5.15) and (5.16). In figures (5.14), (5.15) and (5.16) we also reproduce for comparison the results given by Lavik and Unger and Figure (5.16) also shows the results of the corresponding finite-difference solutions as reported in reference (6).

The SOR technique becomes uncertain in solving the dominant mode wavenumber for the range of $\bar{\beta}$ greater than unity. For this range of $\bar{\beta}$ we used a semi-iterative method developed at NPL, namely, NPL Procedure Proc 2929 which works on the property of Sturm sequence. For this range of $\bar{\beta}$, the particular geometry of the waveguide as in Figure (5.13) is considered, because, the finite-difference solutions of this problem are also available (3).

To demonstrate the relative accuracy between the square mesh and triangular mesh discretisations, the problem in Figure (5.13) is analysed for both the type of elements. It is found that for the same size of matrices, i.e. for the same number of vertices, square mesh produces better results than triangular mesh. This can be seen from the results presented in Table (5.9). It is also found that on decreasing

the dimensions of the successive elements, errors in the computed values of the wavenumber and the eigenfunction decrease monotonically. In Tables (5.10) and (5.11), we present the computed values of the longitudinal component of the magnetic field ϕ normalised to 1000 and the corresponding electric field ψ at two particular frequencies.

Dispersion curves for $\epsilon_r = 3, 6$ and 15 for the waveguide in Figure (5.13) are given in Figure (5.17). To demonstrate the relative rate of convergence on decreasing the element dimensions, results of the computed values of $(\omega a/c)^2$ for $\frac{h}{a} = \frac{1}{8}, \frac{1}{12}, \frac{1}{16}$ are presented in Table (5.12) and their corresponding graphical representations are given in Figure (5.18). The same figure also shows the results reported in Reference (3). It is interesting to note that for the waveguide as considered above, it is possible to sustain backward wave propagation[5] and this could be seen from the dispersion characteristics shown in Figure (5.18)

Table (5.9) Rectangular Waveguide Partially filled with a Dielectric Insert as in Figure (5.13).

$\epsilon_r = 6.00$

$\bar{\beta}$	h/a	$(\omega a/c)^2$ Square Mesh	$(\omega a/c)^2$ Triangular Mesh	$\bar{\beta}$	h/a	$(\omega a/c)^2$ Square Mesh	$(\omega a/c)^2$ Triangular Mesh
	1/8	5 6281	5 6793		1/8	9.2540	8.3154
0.00	1/12	5 5662	5 5968	1.20	1/12	9.6874	9.3775
	1/16	5 5444	5 5640		1/16	9.6899	10.2775
	1/8	5.7304	5.7894		1/8	10.6106	9.8725
0.20	1/12	5.6652	5.6951	1.30	1/12	10.7103	10.4444
	1/16	5.6408	5.6553		1/16	10.7489	10.4350
	1/8	6.0537	6.1611		1/8	11.2728	9.1575
0.40	1/12	5.9731	6.0429	1.40	1/12	11.6225	10.9911
	1/16	5.9430	6.0034		1/16	11.7345	11.4380
	1/8	6.6588	6.8764		1/8	14.6884	14.3246
0.60	1/12	6.5379	6.6420	1.60	1/12	14.7557	14.6098
	1/16	6.4925	6.5823		1/16	14.7762	14.6973
	1/8	7.7229	8.3338		1/8	19.5095	19.5157
0.80	1/12	7.4682	7.7574	1.80	1/12	19.5151	19.5197
	1/16	7.3700	7.5704		1/16	19.5132	19.5168
	1/8	8.7440	10.1352		1/8	23.2320	23.4826
0.90	1/12	8.2265	8.9136	1.90	1/12	23.2180	23.3292
	1/16	8.0326	8.4161		1/16	23.2091	23.2748
	1/8	9.9772	12.9111		1/8	28.6625	29.2599
0.95	1/12	8.9566	10.5129	2.00	1/12	28.6331	28.9449
	1/16	8.5883	9.2742		1/16	28.6228	28.7576
	1/8	7.9504	7.6231				
1.10	1/12	8.6280					
	1/16	8.8343	8.1253				

Table (5.10a) Computed values of H_z normalised to 1000 for the problem in Figure (5.13), for $\epsilon_r = 3.0$ and $\bar{\beta} = 0.9$

	141	277	274	395	502	497	577	642	633	667	689	678
	144		280	403	498	506	586		642	675	680	686
	143		280	403		506	586		642	675		685
	146		286	411		515	595		650	682		693
	152	303	297	427	538	534	614	678	668	698	718	707
	155		303	435		544	623		675	704		713
	166		325	471		586	665		710	734		741
	170		332	479		598	671		715	740		747
a	c 185	377	364	533	693	686	738	770	764	778	788	782
	190		374	545	688	693	742		769	784	783	788
b	d 235		459	662		832	820		822	824		825
	238		465	666		830	826		828	831		832
	270	533	525	750	924	929	890	868	871	864	860	862
	273		529	752		925	893		878	871		869
	291		564	800		982	934		905	891		887
	294		567	802		981	937		911	898		894
	298	583	576	816	1000	1000	948	913	917	900	890	895
	302		582	820	1000	1000	957		923	908	894	903

a	c
b	d

a - square element h/a = 1/8

b - square element h/a = 1/12

c - square element h/a = 1/16

d - triangular element h/a = 1/16

Table (5.10b) Computed Values of normalised $E_z(\psi)$ for max. H_z = 1000 for the problem in Figure (5.13).

$\bar{\beta} = 0.9$ and $\epsilon_r = 3.00$

	113		110		101		88		70		52		33		16	
	113		110		101		87		70		50		32		15	
234	231		225	207	207		179	142	141		102	67	64		31	
	231		225		207		178		140		99		62		30	
	358		350		323		277		214		148		89		42	
	359		350		322		275		212		143		87		41	
510	500		488	461	454		396	287	293		173	98	101		47	
503	501		489		452		387	290	285		174		101		47	
	405		396		368		322		272		167		97		44	
	408		398		368		321		262		165		96		45	
291	285		279	261	260		231	199	196		128	74	75		34	
	288		281		261		230		192		125		74		34	
	147		144		135		120		102		68		41		19	
	150		145		135		120		101		67		40		19	

(a)	(c)
(b)	(d)

a - square mesh h/a = 1/8

b - square mesh h/a = 1/12

c - square mesh h/a = 1/16

d - triangular mesh h/a = 1/16

Table (5.11a) Computed values of H_z normalised to 1000 for Problem in Figure (5.13) with $\bar{\beta} = 1.3$, $\epsilon_r = 3.00$, n = 128.

0	43	82	115	139	155	164	167	168
	42	80	113	138	154	161	163	162
	46	89	124	150	166	174	176	176
	45	86	121	149	164	170	172	171
	58	111	155	186	201	204	202	200
	55	106	149	185	199	200	197	195
	80	151	218	256	270	257	243	237
	71	145	196	259	264	251	238	233
	106	235	282	418	383	328	295	284
	93	217	249	413	372	325	293	282
	198	380	546	721	507	407	350	332
	187	371	532	728	522	411	353	334
	262	506	717	839	625	476	399	375
	253	492	696	844	622	481	405	381
	303	582	812	998	692	524	433	404
	295	569	802	980	698	530	441	413
	317	608	851	1000	722	540	445	415
	311	597	835	1000	720	547	454	428

Top Figures for □ mesh.

Bottom Figures for ◿ mesh.

Table (5.11b) Computed values of normalised E_z (ψ) with max. H_z = 1000 for problem in Figure (5.13)

0	0	0	0	0	0	0	0	0
108 107	105 104	96 95	82 82	65 66	47 47	29 29	13 14	0
233 230	226 223	207 204	176 174	137 140	96 97	59 58	27 27	0
390 384	382 372	346 343	297 287	223 236	151 151	83 86	37 39	0
622 594	579 572	557 539	435 421	372 387	179 199	97 104	43 45	0
524 509	512 493	464 451	396 370	281 270	177 170	93 95	41 42	0
385 373	374 361	341 329	288 279	234 227	131 132	73 73	32 33	0
203 198	198 191	180 173	154 146	111 109	71 68	39 39	17 17	0
0	0	0	0	0	0	0	0	0

ψ at different nodes ϵ_r = 3.00

Top figures for □ mesh β = 1.3

Bottom figures for ⊿ mesh n = 128

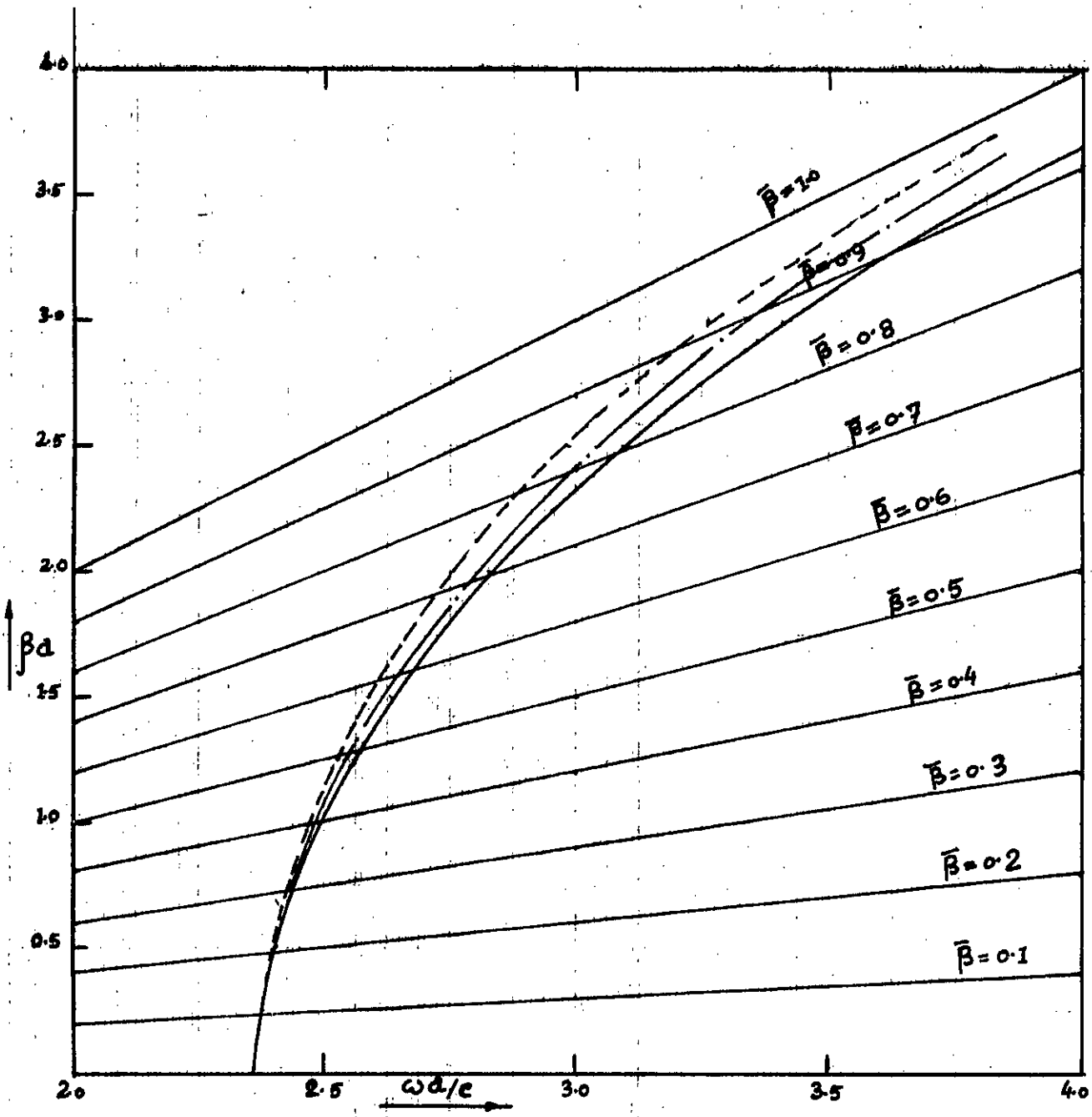

Fig.(5.14): Dispertion Curves for ϵ_r=3.00 in Waveguide of Fig.(5.13).

- - - - - Lavik and Unger
—·— FE Method(525 nodes)
——— FE Method(143 nodes)

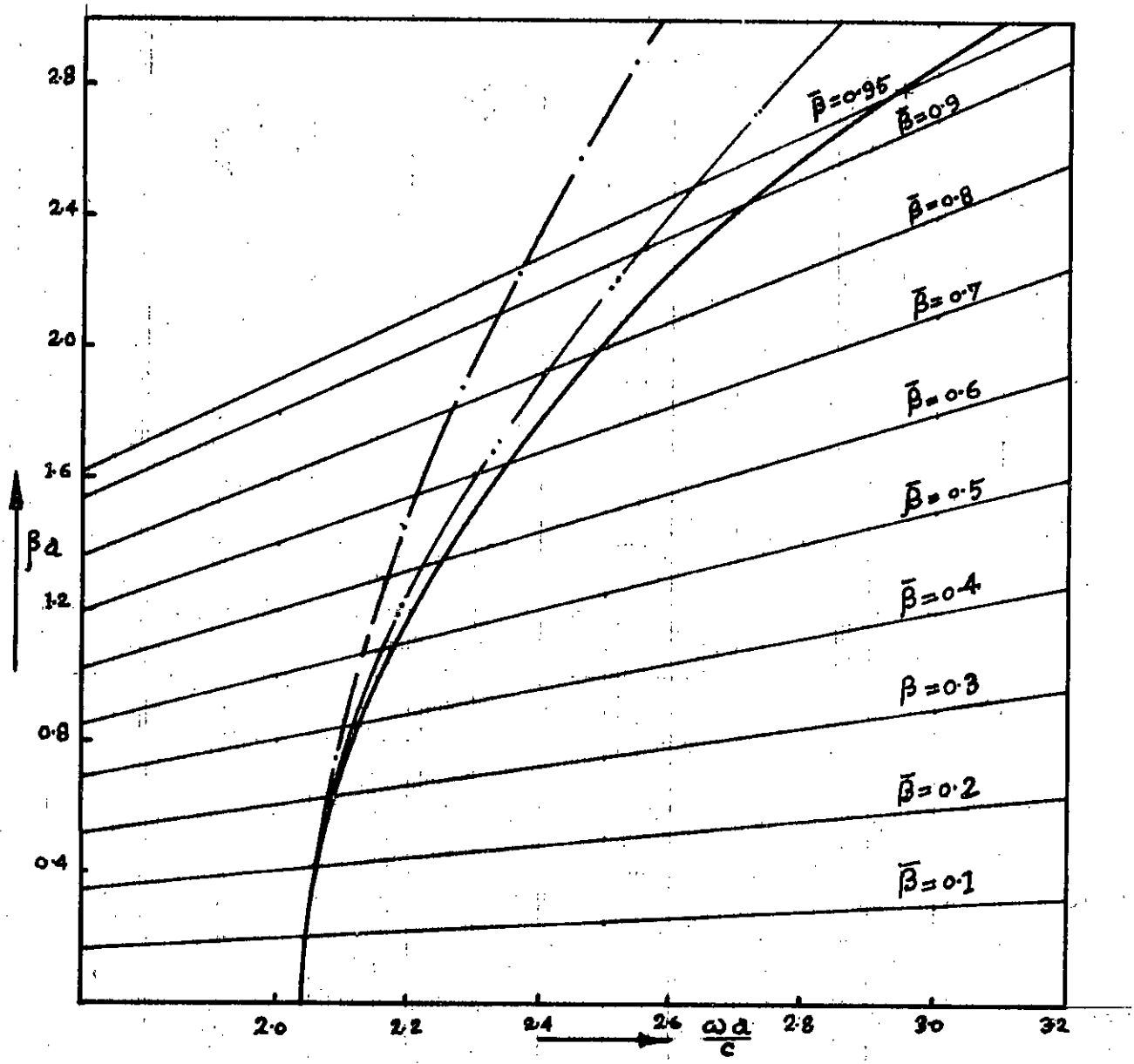

Fig.(5.15): Dispersion Curves for ϵ_r=6.00 in Waveguide of Fig.(5.13).

——·——Lavik and Unger

——··——FE Method(525 nodes)

————FE Method(143 nodes)

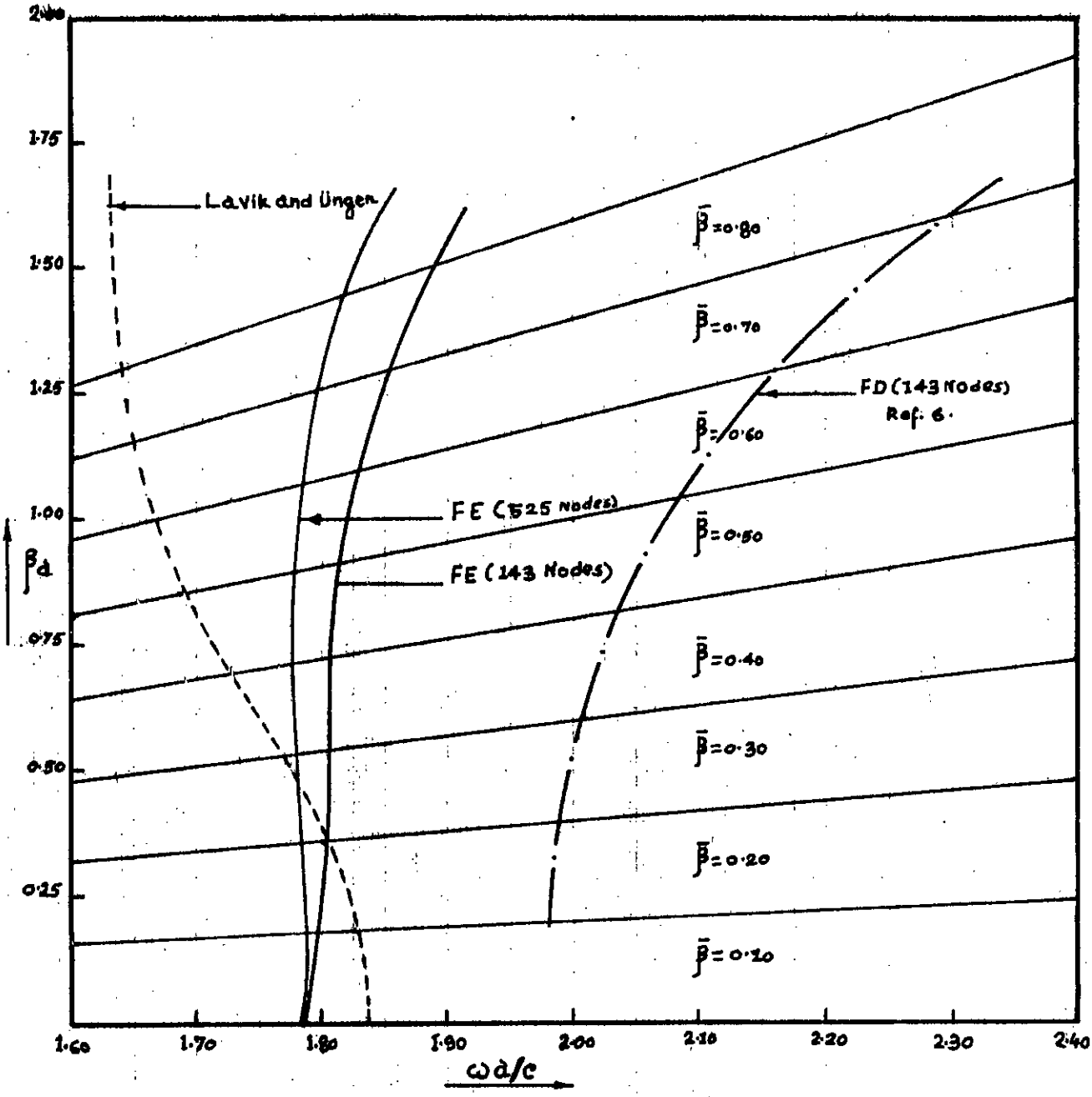

Fig.(5.16): Dispersion Curves for $\epsilon_r = 15.00$ in Waveguide of Fig.(5.13).

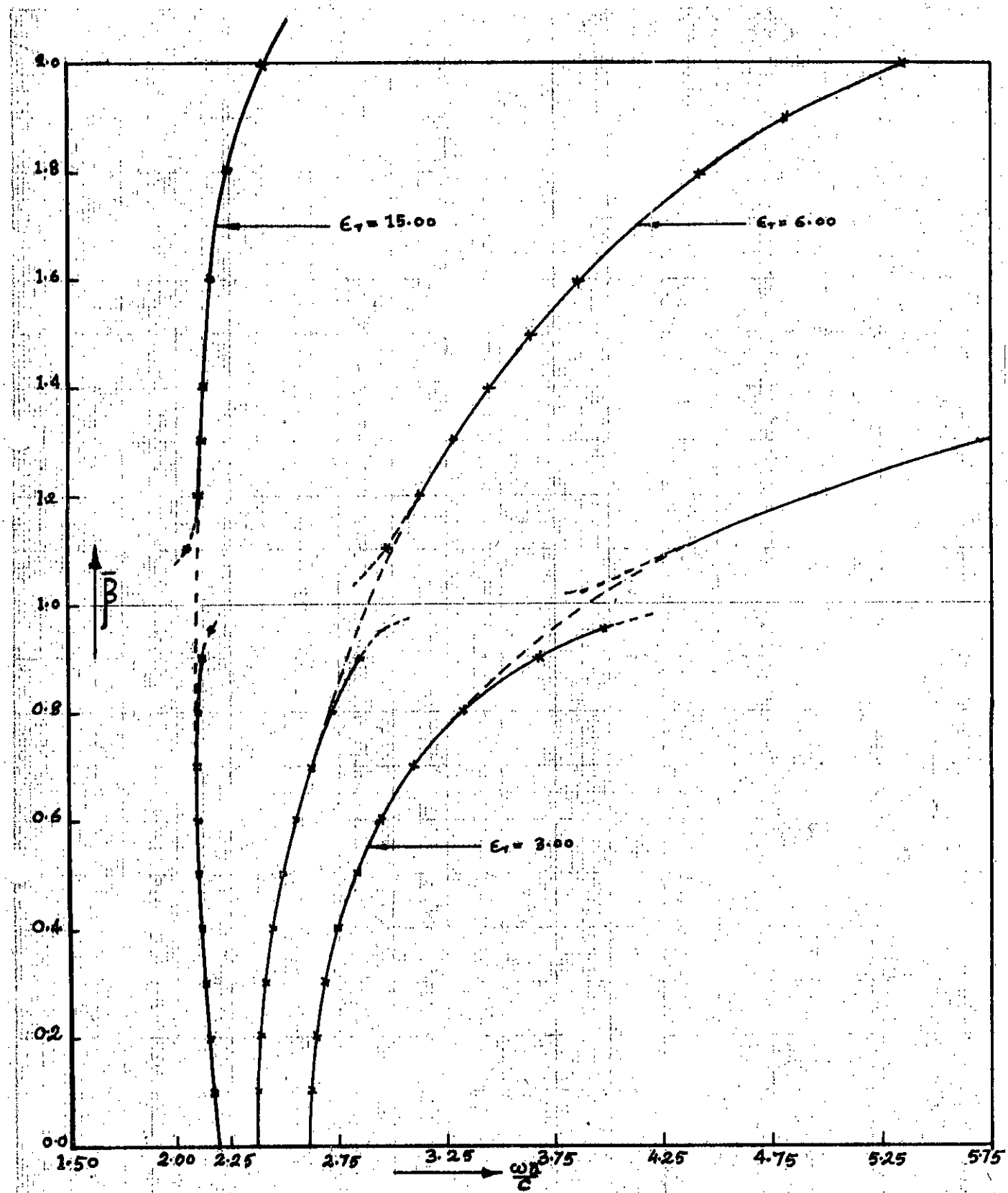

Fig.(5.17): Variations of $\bar{\beta}$ with $\omega a/c$ for Three Dielectrics in Fig.(5.12).

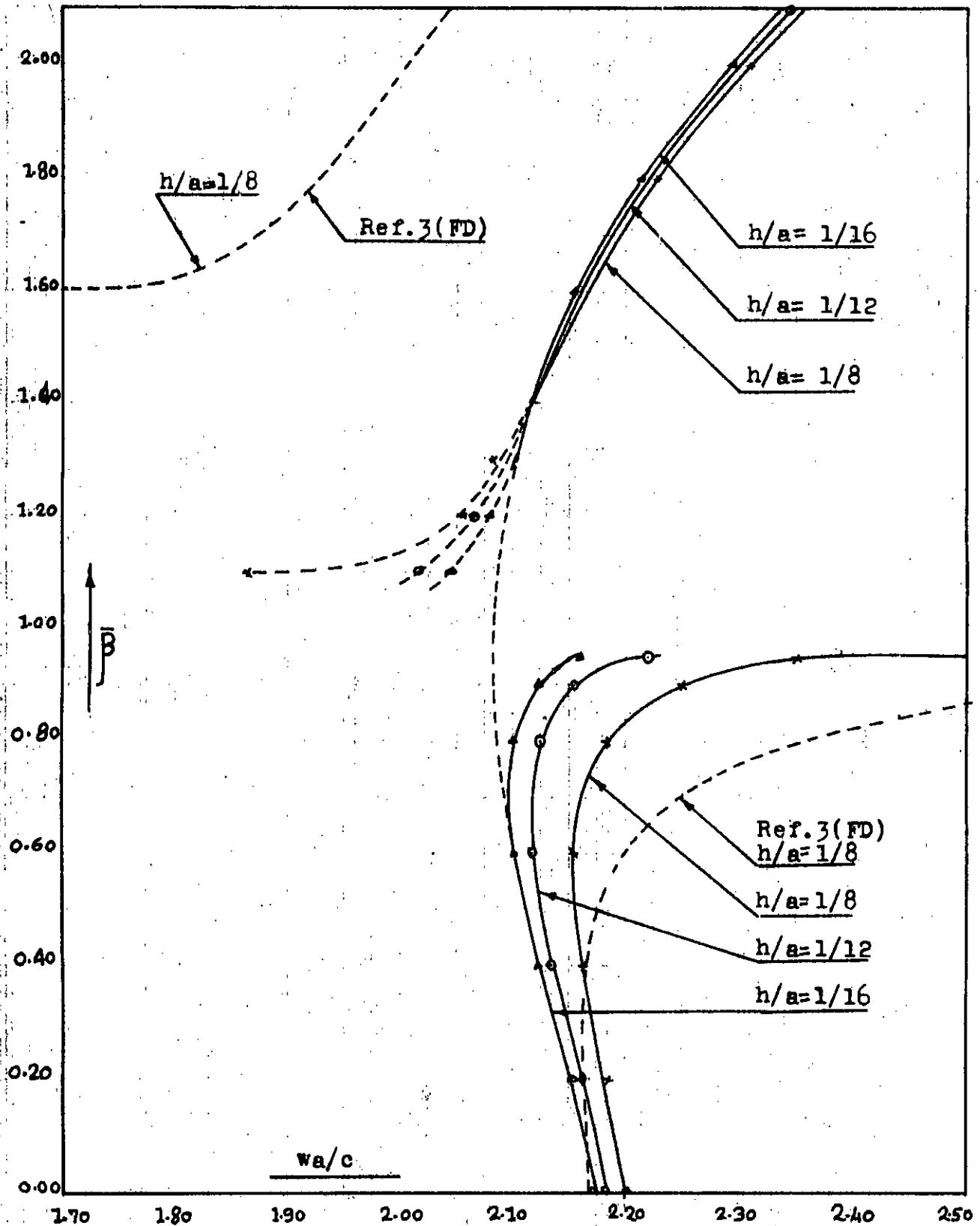

Fig.(5.18) Variations of $\bar{\beta}$ with $\omega a/c$ for three Successive Mesh Subdivisions in Fig(5.12).

5.5 Conclusions

For the range of $\bar{\beta}$ less than unity, the matrix operators $\underline{A}$ and $\underline{B}$ for inhomogeneously loaded waveguides remain positive definite and the 'SOR' technique when applied to the discretised finite-element equations converges almost at the same speed as when applied to the corresponding finite-difference equations, and always gives an upper bound to the true solutions. In the case of a one dimensional problem, the 'SOR' technique can also be used for obtaining converging solutions for $\bar{\beta} > 1$ in both the finite-element and the finite-difference methods. But the relative stability of the 'SOR' solution is greater for the finite-element method than the finite difference method. This can be seen from a study of the results given in Tables (5.1) and (5.2), where the blank spaces under the column $(\omega a/c)^2$ show that the SOR method does not converge to the dominant mode eigenvalues for those particular values of $\bar{\beta}$. The FE and the FD results in Tables (5.1) and (5.2) are computed under identical conditions.

For hybrid mode problems, the 'SOR' method becomes uncertain for the range of $\bar{\beta}$ greater than unity. In this range of frequencies there is a range of $\bar{\beta}$ for which the matrix operator $\underline{A}$ becomes indefinite and the 'SOR' method

often fails to converge to the dominant mode solutions. Unfortunately, this range of $\bar{\beta}$ starts from $\bar{\beta} = 1$. If $\bar{\beta}$ is sufficiently greater than unity, i.e. the range of frequencies for which condition (b) in section (5.2.1) is satisfied, the matrix operator $\underline{A}$ again becomes definite in character and the 'SOR' technique may give converging solution provided we could start with a suitable set of initial eigenvectors. In the case of hybrid mode problems as considered in sections (5.4.2) and (5.4.3), we used a standard Library procedure borrowed from the NPL as mentioned earlier. A combination of the SOR method and the NPL Procedure PROC 2929 may be found useful for calculating the eigenvalues for the whole range of $\bar{\beta}$.

A comparative study of the computations for the dominant mode eigenvalues in inhomogeneous waveguides obtained by the finite-element and the finite-difference methods shows that the finite-element results are relatively more accurate than the finite-difference results for the same size of the equivalent matrix operators. The matrix operator $\underline{A}$ is exactly the same in both the methods. The matrix operator $\underline{B}$ in the finite-element method is replaced by a unit matrix operator in the corresponding finite-difference method. One is thus led to the unexpected conclusion that the weakness of the usual finite-difference method lies

not in its relatively coarse modelling of the Laplacian operator, as is sometimes thought, but rather in its inaccurate discretisation of the identity operator. This is substantiated by the numerical results reported in this thesis.

For the range of $\bar{\beta} > 1$, the computations of $\left(\frac{\omega a}{c}\right)^2$ for various mesh sizes show that for $\bar{\beta}$ close to unity computed $\frac{\omega a}{c}$ approaches the true value from below and for $\bar{\beta}$ sufficiently away from unity but less than $\sqrt{\epsilon_r}$, computed $\frac{\omega a}{c}$ approaches the true value from above. This supports the hypothesis drawn about the character of the matrix operator $\underline{A}$ in section (5.2).

Finally, it may be mentioned that the field singularities in dielectric loaded waveguide can be treated in the same way as the re-entrant corners in homogeneous waveguides are treated. Also for an arbitrary type of dielectric loading, the dielectric/vacuum interface can be treated in the same way as arbitrary shaped boundaries are considered for homogeneous waveguide problems.

Chapter 5

References

1. Varlanian, P.H., Ayres, W.P. and Helgesson, A.L.: "Propagation in Dielectric Slab Loaded Rectangular Waveguides", IRE Trans. on Microwave Theory and Techniques, pp.215-222, April, 1958.

2. Collins, J.H. and Daly, P.: "Calculations for Guided Electromagnetic Waves Using Finite-Difference Methods", J. Electronics and Control, Vol. 14, p.361, 1963.

3. Muilwyk, C.A.: "The finite-difference solutions of Arbitrarily Shaped Waveguide with Arbitrary Filling", Ph.D. Thesis, University of Sheffield, 1967.

4. Marcuvitz, N.: Waveguide Handbook, McGraw-Hill Book Co., 1951.

5. Lavik, A. and Unger, H.: "Der Rechteckhohlleiler mit Rechteckigen Stoffeinsatz", Archiv der Electrischen Ubertragung, 18 Heft, 1, p.25, 1964.

6. Hannaford, C.D.: "Finite-difference/variational Method for inhomogeneous isotropic or anisotropic Waveguides", Ph.D. Thesis, University of Leeds, 1967.

Chapter 6

WAVEGUIDE LOADED WITH GENERALISED ISOTROPIC DIELECTRIC

6.1 Introduction

In the previous chapter we considered the problem of inhomogeneously filled waveguide systems where the variation of permittivity was sectionally constant. In this penultimate chapter, this restriction on permittivity is relaxed. Here we consider a continuous variation of the relative permittivity as a function of the transverse coordinates, otherwise, uniform along the axis of propagation. This type of dielectric variation may occur in a plasma filled waveguide, where the density of electron beam may vary as a function of the radius of the beam. The equivalent permittivity in such a case can be shown[1] to be

$$\epsilon_r = 1 - \frac{N e^2}{m \epsilon_0 \omega^2} \qquad (6.1)$$

where N = density of electron.

Analytic treatment of the above type of problem involves the simultaneous solutions of the differential wave equations (2.29) and (2.30); and solutions of these equations cannot be obtained in a simple form. This type of waveguide problem could be profitably analysed by numerical techniques. Although there are various types of numerical

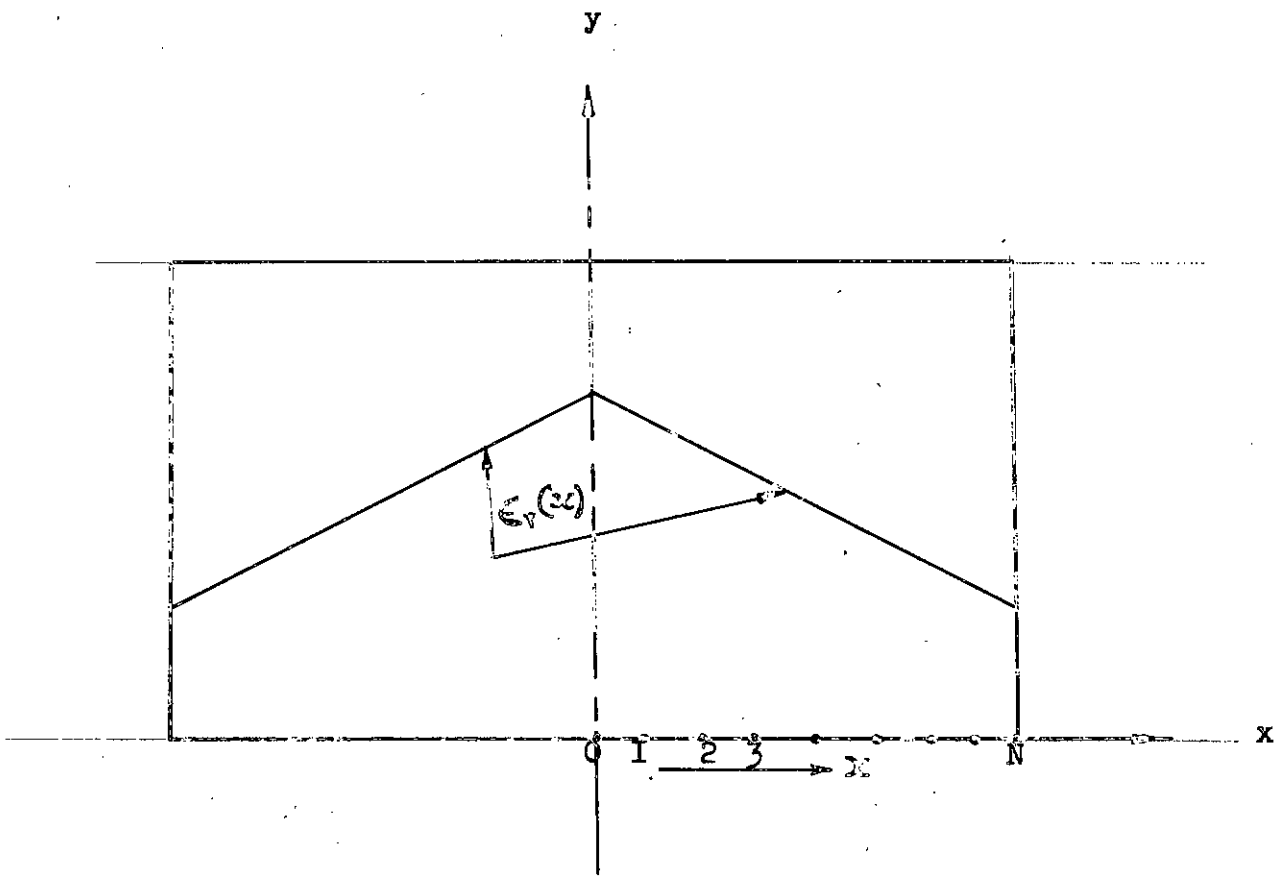

Figure (6.1)
A Rectangular Waveguide filled
with
Linearly Varying Dielectric

approaches which could be applied to this problem, we will describe here only the finite-element and the Rayleigh Ritz methods. These two methods have much similarity in their formulation. Both start with the same variational expression. It is shown that for those problems where the variation of the dielectric is such that the following two functions:

$$F_1(x,y) = (ax^2 + by^2 + cxy + dx + ey + f)\ \epsilon_r(x\,y) \tag{6.2}$$

and

$$F_2(x,y) = \frac{1}{\epsilon_r(x,y) - \bar{\beta}^2} \tag{6.3}$$

where a, b, c, d, e, and f are constants, are integrable, the finite-element method would be relatively easier to program than the Rayleigh Ritz method.

A rectangular waveguide filled with a linearly varying dielectric is analysed by the finite-element method and results are tabulated in Tables (6.1) and (6.2)

6.2 Finite-Element Approach to Generalised Medium

A variational expression for a waveguide filled with a generalised isotropic dielectric is developed in Chapter 2, and we rewrite that here for completeness.

$$J(\phi,\ ) = \int_s \tau(x,y)\,|\nabla_t\phi|^2\,ds + \bar{\beta}^2 \int_s \tau(x,y)\,\epsilon_r(x,y)\,|\nabla_t\psi|^2\,ds +$$

$$2\bar{\beta}^2 \int_s \tau(x,y)\ \underline{a_z}\cdot(\nabla_t\psi \times \nabla_t\phi)\,ds - k_o^2 \int_s \phi^2\,ds$$

$$- \beta^2 k_o^2 \int_s \psi^2 \epsilon_r(x,y)\, ds \tag{6.4}$$

To illustrate the use of the finite-element technique we consider a rectangular waveguide filled with an isotropic dielectric whose relative permittivity varies linearly along the x-co-ordinate and uniform along the y and z co-ordinates. This is shown in figure (6.1). Mathematically, $\epsilon_r(x)$ can be written as

$$\epsilon_r(x) = \epsilon_o\left(\epsilon_{r1} - \frac{\epsilon_{r1} - \epsilon_{r2}}{a} x\right) \tag{6.5}$$

where a is the half width of the broad side of the guide.

The wave-equations for the generalised medium in waveguide is given by

$$\epsilon_r \bar{\beta}^2 \tau \nabla_t^2 \psi + \beta^2 \epsilon_r k_o^2 \psi + \beta^2 \nabla_t(\tau \epsilon_r) . \nabla_t \psi + \bar{\beta}^2 \underline{a}_z . \nabla_t \tau \times \nabla_t \phi = 0 \tag{6.6}$$

and

$$\tau \nabla_t^2 \phi + k_o^2 \phi + \nabla_t \tau . \nabla_t \phi - \beta^2 \underline{a}_z . (\nabla_t \tau \times \nabla_t \psi) = 0 \tag{6.7}$$

Expanding the cross-product components of equations (6.6) and (6.7) which are the coupling terms between ϕ and ψ we obtain

$$\bar{\beta}^2 \tau \epsilon_r \nabla_t^2 \psi + \bar{\beta}^2 \epsilon_r k_o^2 \psi + \bar{\beta}^2 \nabla_t(\tau \epsilon_r) . \nabla_t \psi + \bar{\beta}^2 . (\tau_x \phi_y - \phi_x \tau_y) = 0 \tag{6.8}$$

$$\tau \nabla_t^2 \phi + k_o^2 \phi + \nabla_t \tau . \nabla_t \phi - \bar{\beta}^2 (\tau_x \Psi_y - \tau_y \Psi_x) = 0 \qquad (6.9)$$

The dominant mode propagation through such a waveguide would be TE_{10} type in nature. The corresponding variational expression becomes

$$J(\phi) = \int_o^a \tau \nabla_t \phi^2 dx - k_o^2 \int_o^a \phi^2 dx \qquad (6.10)$$

where $$\tau = \frac{1 - \bar{\beta}^2}{\epsilon_r(x) - \bar{\beta}^2} = \frac{E}{D - x/L} \qquad (6.11)$$

$$E = 1 - \bar{\beta}^2$$
$$D = \epsilon_{r1} - \bar{\beta}^2$$
$$L = \frac{a}{\epsilon_{r1} - \epsilon_{r2}} \qquad (6.12)$$

In Equation (6.10) ϕ represents the longitudinal component of the magnetic field vector. Let us now divide the half width OL (Fig.6.1) into N equal parts and call them as elements. If we consider a linear variation of ϕ over each of these elements then the potential ϕ (x) over an element 'e' described by the i th and (i-1)th nodes is given by

$$\phi^e(x) = \frac{\phi_{(i-1)} x_i - \phi_i x_{(i-1)}}{x_i - x_{(i-1)}} + \frac{\phi_i - \phi_{(i-1)}}{x_i - x_{(i-1)}} x \qquad (6.13)$$

If the above functional form of $\phi(x)$ and $\epsilon_r(x)$ are substituted into equation (6.10) and the partial con-

tribution of each element is taken into consideration then $J(\phi)$ will be a functional of $\phi_1, \phi_2 \ldots\ldots \phi_N$, i.e. the values of ϕ at the vertices so generated. Finally, minimisation of $J(\phi_1, \phi_2 \ldots\ldots \phi_N)$ with respect to each ϕ_i will generate a set of linear algebraic eigenvalue equations. For illustration, let us consider an element (say 'e' th) described by i th and (i-1)th vertices. Then

$$\left.\frac{\partial J}{\partial \phi_i}\right|_e = \frac{E\left[\phi_i - \phi_{(i-1)}\right]}{h^2} \int_e \frac{dx}{D-x/\ell} - \frac{k_o^2 \phi_i}{h^2} \int_e (x-x_i)^2 dx$$

$$- \frac{k_o^2}{h^2} \phi_{(i-1)} \int_e \left(x - x_{(i-1)}\right)\left(x_i - x\right) dx \qquad (6.14)$$

Equation (6.14) can be easily solved. We give below the final results in the form of element submatrices. Let $S^1, S^2 \ldots\ldots S^N$ be the element submatrices corresponding to the matrix $\underline{A}$, then

$$S^1 = \frac{E\ell}{h^2}\left\{\ln D - \ln(D - h/\ell)\right\}\begin{bmatrix} 1 & -1 \\ -1 & 1 \end{bmatrix} \qquad (6.15)$$

and

$$S^P = \frac{E\ell}{h^2}\left\{\ln D - \frac{(P-1)h}{\ell} - \ln(D - Ph/\ell\right\}\begin{bmatrix} 1 & -1 \\ -1 & 1 \end{bmatrix} \qquad (6.16)$$

for $P = 1, 2 \ldots\ldots N$.

where h = length of each element, i.e. $|x_i - x_{i-1}|$.

The element submatrices of the matrix $\underline{B}$ will be of the same form as obtained previously for TE_{10}-mode in a rectangular waveguide. Combining the partial contribution to $\frac{\partial J}{\partial \phi_1}$ by the adjacent elements to the vertex 'i' and setting $\frac{\partial J}{\partial \phi_1} = 0$ we obtain a finite-element equation for ϕ_1. We give below a few typical finite-element equations for the above problem.

(a) 1st vertex

$$\frac{E\ell}{h^2}\left[\ell n D - \ell n(D-2h/\ell)\right]\phi_1 - \frac{E\ell}{h^2}\left[\ell n(D-h/\ell) - \ell n(D-2h/\ell)\right]\phi_2$$

$$= \frac{k_o^2 h}{6}(4\phi_1 + \phi_2) \qquad (4.17)$$

(b) P th vertex

$$-\frac{E\ell}{h^2}\left[\ell n\left\{D-(P-1)h/\ell\right\} - \ell n\,(D-Ph/\ell)\right]\phi_{(P-1)}$$

$$\frac{E\ell}{h^2}\left[\ell n\left\{D-(P-1)h/\ell\right\} - \ell n\left\{D-(P+1)h/\ell\right\}\right]\phi_P - \frac{E\ell}{h^2}.$$

$$\left[\ell n(D-Ph/\ell) - \ell n\left\{D-(P+1)h/\ell\right\}\right]\phi_{(P+1)}$$

$$= \frac{k_o^2 h}{6}\left[\phi_{(P-1)} + 4\phi_P + \phi_{(P+1)}\right] \qquad (4.18)$$

(c) N th vertex

$$-\frac{E\ell}{h^2}\left[\ell n\{D-(N-1)h/\ell\}-\ell n(D-a/\ell)\right]\phi_{(N-1)}$$

$$\frac{E\ell}{h^2}\left[\ell n\{D-(N-1)h/\ell\}-\ell n(D-a/\ell)\right]\phi_N=\frac{k_o^2 h}{6}(\phi_{(N-1)}+2\phi_N) \tag{4.19}$$

Numerical solutions of $(\omega a/c)$ for two different values of $\epsilon_r(x,y)$ and for various values of $\bar{\beta}$ are given in Tables (6.1) and (6.2).

Table (6.1) A rectangular waveguide completely filled with a linearly varying Dielectric as in Fig.(6.1)

$$\epsilon_r(x) = 3 - \frac{2x}{a}$$

$\bar{\beta}$	No. of Elements	$\frac{2\omega a}{c}$	$\bar{\beta}$	No. of Elements	$\frac{2\omega a}{c}$
0.000	5	2.036	0.800	5	2.377
	7	2.029		7	2.367
	10	2.025		10	2.362
	15	2.023		15	2.360
0.300	5	2.075	0.900	5	2.501
	7	2.068		7	2.489
	10	2.064		10	2.483
	15	2.062		15	2.480
0.600	5	2.208	0.950	5	2.577
	7	2.200		7	2.564
	10	2.196		10	2.558
	15	2.193		15	2.555

Table (6.2) Same Waveguide as in Table (6.1) with $\epsilon_r(x) = (4 - \frac{2x}{a})$

$\bar{\beta}$	No. of Elements	$\frac{2\omega a}{c}$
0.00	5	1.710
	7	1.705
	10	1.703
	15	1.702
0.10	5	1.714
	7	1.709
	10	1.706
	15	1.704
0.30	5	1.734
	7	1.729
	10	1.726
	15	1.725
0.50	5	1.778
	7	1.772
	10	1.769
	15	1.768
0.70	5	1.850
	7	1.844
	10	1.840
	15	1.839
0.90	5	1.961
	7	1.954
	10	1.949
	15	1.948
0.95	5	1.996
	7	1.989
	10	1.986
	15	1.984

$\bar{\beta}$	No. of Elements	$\frac{2\omega a}{c}$
1.05	5	2.086
	7	2.074
	10	2.070
	15	2.068
1.10	5	2.130
	7	2.124
	10	2.120
	15	2.118
1.15	5	2.188
	7	2.180
	10	2.176
	15	2.174
1.20	5	2.254
	7	2.244
	10	2.240
	15	2.237
1.25	5	2.328
	7	2.317
	10	2.312
	15	2.310
1.30	5	2.413
	7	2.401
	10	2.396
	15	2.393

6.2.1 Extension to two-dimensional variations

Although computational results are presented in the previous section for a simple one dimensional problem, the method can be extended to problems having 2-dimensional variations of the relative permittivity. For such a problem an appropriate variational functional is given by equation (6.4). Equation (6.4) differs from equation (5.9) which is formulated for inhomogeneous waveguide in that τ and ϵ_r are no longer constants and therefore, cannot be taken outside the integral signs. Following the line of approach as described for inhomogeneous systems, we can write the partial contribution to the minimisation of $J(\phi, \Psi)$ with respect to ϕ_i and Ψ_i by an element 'e' associated with the vertex 'i' as follows:

$$\left.\frac{\partial J^e}{\partial \phi_i}\right|_e = \int_e \tau(x,y) \left\{ \left[\frac{\partial N}{\partial x}\right]\left[\Phi^e\right] \frac{\partial N_i}{\partial x} + \left[\frac{\partial N}{\partial y}\right]\left[\Phi^e\right] \frac{\partial N_i}{\partial y} \right\} dxdy +$$

$$\bar{\beta}^2 \int_e \tau(x,y) \left\{ \left[\frac{\partial N}{\partial x}\right]\left[\Psi^e\right] \frac{\partial N_i}{\partial y} - \left[\frac{\partial N}{\partial y}\right]\left[\Psi^e\right] \frac{\partial N_i}{\partial x} \right\} dxdy$$

$$- k_o^2 \int_e \left[N\right]\left[\phi^e\right] N_i \, dxdy \qquad (6.20)$$

and

$$\frac{\partial J^e}{\partial \Psi_i}\Big|_e = \bar{\beta}^2 \int_e \tau(x,y)\ \epsilon_r(x,y)\left\{\left[\frac{\partial N}{\partial x}\right]\left[\Psi^e\right]\frac{\partial N_i}{\partial x} + \left[\frac{\partial N}{\partial y}\right]\left[\Psi^e\right]\frac{\partial N_i}{\partial y}\right\} dxdy$$

$$+ \bar{\beta}^2 \int_e \tau(x,y)\left\{\left[\frac{\partial N}{\partial y}\right]\left[\phi^e\right]\frac{\partial N_i}{\partial x} - \left[\frac{\partial N}{\partial x}\right]\left[\phi^e\right]\frac{\partial N_i}{\partial y}\right\} dxdy$$

$$- k_o^2\ \bar{\beta}^2 \int_e \epsilon_r(x,y)\ [N]\ [\Psi^e]\ N_i\ dxdy \qquad (6.21)$$

where $[N]$ is a row matrix and $[\phi^e]$ and $[\Psi^e]$ are column matrices as defined earlier. Since the components of $[N]$ are linear functions of x, and y, $\left[\frac{\partial N}{\partial x}\right]$, $\left[\frac{\partial N}{\partial y}\right]$, $\frac{\partial N_i}{\partial x}$ and $\frac{\partial N_i}{\partial y}$ are constants, equations (6.20) and (6.21) can be rewritten in a more simple form as follows:

$$\frac{\partial J}{\partial \phi_i}\Big|_e = [G][\phi^e] \int_e \tau(x,y)\ dxdy + [V][\Psi^e]\ \bar{\beta}^2 \int_e \tau(x,y)\ dxdy$$

$$- k_o^2 \int [N]\ [\phi^e]\ N_i\ dxdy \qquad (6.20b)$$

and

$$\frac{\partial J}{\partial \Psi_i}\Big|_e = \bar{\beta}^2 [G][\Psi^e] \int_e \tau(x,y)\ \epsilon_r(x,y)\ dxdy - [V]\ [\phi^e]\ \bar{\beta}^2 \int_e \tau(x,y)\ dxdy - k_o^2\ \bar{\beta}^2 \int_e [N]\ [\Psi^e]\ N_i\ dxdy \qquad (6.21b)$$

where $[G]$ and $[V]$ are row matrices and are given by

$$[G] = \left[\frac{\partial N}{\partial x}\right]\frac{\partial N_1}{\partial x} + \left[\frac{\partial N}{\partial y}\right]\frac{\partial N_1}{\partial y} \tag{6.22}$$

$$[V] = \left[\frac{\partial N}{\partial x}\right]\frac{\partial N_1}{\partial y} - \left[\frac{\partial N}{\partial y}\right]\frac{\partial N_1}{\partial x} \tag{6.23}$$

Therefore, evaluation of $\left.\frac{\partial J}{\partial \phi_1}\right|_e$ and $\left.\frac{\partial J}{\partial \psi_1}\right|_e$ over an element 'e' would be relatively easier, if the following integrals

(a) $$\int_e \tau(x,y)\, dxdy \tag{6.24}$$

(b) $$\int_e \epsilon_r(x,y)\, [N]\, N_1\, dxdy \tag{6.25}$$

which are of the same form as equations (6.2) and (6.3), have simple analytic solutions.

A complicated variation of $\epsilon_r(x,y)$ which makes the above set of integrals analytically unsolvable, may be approximated by a set of suitable piece-wise simple functions defined over an element or over an element, $\epsilon_r(x,y)$ may be approximated by some sort of its weighted average so as to make the equations (6.24) and (6.25) analytically solvable. However, it is to be hoped that further research in numerical analysis will extend the use of the finite-element method for treating complex boundary value problems.

6.3 Rayleigh-Ritz Method

The essential theme of the Rayleigh Ritz method consists of approximating the true eigenfunction by a finite set of suitable trial functions (preferably orthogonal functions) with unknown amplitude co-efficients and then adjusting each of these unknown amplitude co-efficients so as to obtain the best possible results for the particular set considered. This is normally done by extremising a functional which is variational for the physical quantity under consideration. Extremisation is performed with respect to each of the unknown amplitude co-efficients. This type of extremisation generates a set of linear algebraic equations which is equivalent to the continuous operator eigenvalue equation and whose solutions give the approximate solutions to the eigenvalues of the physical problem.

For the method to converge successfully with increasing the number of terms in the series approximation of the true eigenfunction, it is generally required that the set of trial functions must form a complete set. The most suitable trial functions to use in the analysis of a waveguide filled with inhomogeneous or generalised media are, therefore, the normal mode functions of the corresponding homogeneous waveguide, because, they form a complete set, they are orthogonal and they also satisfy the boundary con-

ditions at the guide walls. Hence, those types of homogeneous waveguides for which the normal mode functions are known when loaded with piece-wise constant or continuously variable dielectric, can be analysed in principle by the Rayleigh-Ritz method. But for awkwardly shaped waveguides, the normal mode functions are not known, consequently, this type of waveguide would not be suitable for analysis by the Rayleigh-Ritz method. In other words, use of normal mode functions limits the application of the Rayleigh-Ritz method to waveguides with simple boundary shapes such as a rectangular or a circular waveguide. In practice, however, most of the waveguides are either rectangular or circular in shape and other types of waveguides are rarely used.

6.3.1 Practical Difficulties:

In principle, Rayleigh-Ritz method may be applied to rectangular waveguide with all types of rectangular dielectric inserts but numerical computations based on this principle as reported in reference (2) show a poor convergence on successive increase of the number of the normal mode functions used even for a simple problem as in Figure (5.4). This is probably because the normal derivatives of the scalar potential ϕ is discontinuous at the vacuum/dielectric interface but the approximation functions in the Rayleigh-Ritz method have continuous derivatives at

this boundary. Computational results given in reference (2) also show that this method fails to give converging solution, for the normalised propagation constant greater than unity for the problem in Figure (5.4). Another disadvantage of the direct use of this method is that the associated matrices are dense in nature; as a result one cannot take advantage of the SOR technique for obtaining an iterative solution.

The finite-element method considered in this thesis, broadly speaking, is an extension of the Rayleigh-Ritz principle and does not suffer from the above mentioned disadvantages. Rayleigh-Ritz method is used in Reference (2) to obtain the dispersion characteristics of a waveguide partially filled with a full height dielectric slab. For comparison, we reproduce the results of Reference (2) in Tables (6.3) and (6.4) and the corresponding finite-element calculations are given in Table (6.5). A study of these results clearly demonstrates the usefulness of the finite-element method.

Table (6.3) Results of the Least Eigenvalue obtained by the Rayleigh-Ritz method for the Problem in Figure (5.4)

$\epsilon_r = 2.45$

$\frac{b}{a} = 0.5 \qquad \frac{t}{a} = 0.5 \qquad \bar{\beta} = 0.5$

No. of modes	Least Eigen value $(k_o a/\pi)^2$	$(\omega a/c)^2$
1	0.4599	6.0519
2	0.3965	5.2174
3	0.3964	5.2165
4	0.3905	5.1379
5	0.3904	5.1378
6	0.3883	5.1089
7	0.3882	5.1089
8	0.3871	5.0939
9	0.3871	5.0939
10	0.3869	5.0912
Analytic	-	5.0600
Berk's	-	5.1162

Table (6.4) Same Waveguide as in Table (6.3) for $\bar{\beta} = 1.20$

No. of modes	Least Eigenvalue $(k_0 a/\pi)^2$	$(\omega a/c)^2$
1	- 0.1751	3.9276
2	- 0.5928	13.2970
3	- 0.2688	6.0294
4	- 0.5338	13.0966
5	- 0.2904	6.5143
6	- 0.5778	12.9583
7	- 0.2831	6.3490
8	- 0.5742	12.8796
9	- 0.2531	5.6766
10	- 0.5720	12.8304
Analytic	-	12.6661
Berk's[3]	-	13.2347

Table (6.5) Results of the Same Waveguide as in Table (6.3) by Finite-Element Method

	Finite-Element No. of Elements	Finite-Element $(W\ a/c)^2$	Analytic $(W\ a/c)^2$	Rayleigh-Ritz 10 modes	Berk's
0.5	4	5.0960	5.0600	5.0912	5.1162
	8	5.0692			
	16	5.0624			
1.20	4	12.6663	12.6661	Oscillating see Table (6.4)	13.2347
	8	12.6675			
	16	12.6669			

6.3.2 Rayleigh-Ritz Method for Arbitrary Loading

For a generalised medium which is the subject matter of this chapter, direct use of the Rayleigh-Ritz method would involve considerable mathematical difficulties; even for a simple type of one-dimensional variation as considered in Section (6.2), evaluation of the co-efficients of the matrices requires numerical integrations. For a general variation, the extremisation functional involves both ϕ and Ψ fields together. If we now approximate the scalar functions ϕ and Ψ by a set of normal mode functions having both x and y variations, we can write

$$\phi = \sum_{n=1}^{N} \left(a_n \cos \frac{n\pi x}{a} \right) \left(\sum_{m=0}^{M} b_m \cos \frac{m\pi y}{b} \right) \qquad (6.26)$$

$$\psi = \left(\sum_{r=1}^{R} C_r \sin \frac{r\pi x}{a} \right) \left(\sum_{s=1}^{S} ds \sin \frac{s\pi y}{b} \right); \qquad (6.27)$$

when the above functional form of ϕ and ψ are substituted into the variational expression $J(\phi, \psi)$ and integrations are carried out then J becomes a function of the unknown amplitude co-efficients a_n, b_m, c_r and ds and can be written as

$$J(a_n, b_m, c_r, d_s) = \sum_{mnpq} a_n \; a_p \; b_m \; b_q \; Amnpq +$$

$$\sum_{mnrs} a_m \; b_m \; c_r \; d_s \; C_{mnrs} + \sum_{rsij} c_r \; c_i \; d_s \; d_j,$$

$$B_{rsij} - \lambda \left(\sum_{mnpq} a_n \; a_p \; b_m \; b_q \; D_{mnpq} + \sum_{rsij} c_r \; c_i \; d_s \; d_j \; . \right.$$

$$\left. E_{rsij} \right); \qquad (6.28)$$

where

$$A_{mnpq} = \int_s t(x\ y) \left(\nabla_t f_{mn} \cdot \nabla_t f_{pq} \right) dxdy \qquad (6.29)$$

$$B_{sij} = \bar{\beta}^2 \int_s t(x,y) \; \epsilon_r(x\ y) \left(\nabla_t g_{rs} \cdot \nabla_t g_{ij} \right) dxdy \qquad (6.30)$$

$$C_{mnrs} = \bar{\beta}^2 \int_s t(x,y) \left(\nabla_t g_{rs} \times \nabla_t f_{mn} \right) \cdot \underline{a}_z \; dxdy \qquad (6.31)$$

$$D_{mnpq} = \int_s f_{mn} \cdot f_{pq} \; dxdy \qquad (6.32)$$

$$E_{rsij} = \bar{\beta}^2 \int_s \epsilon_r(x,y) \quad g_{rs} \cdot g_{ij} \quad dxdy \tag{6.33}$$

$$f_{mn} = \cos \frac{m\pi x}{a} \quad \cos \frac{m\pi y}{b} \tag{6.34}$$

and

$$g_{rs} = \sin \frac{r\pi x}{a} \quad \sin \frac{s\pi y}{b} \tag{6.35}$$

A typical term of the integrals in equations (6.29) to (6.33) becomes of the form

$$\int_s \frac{1}{\epsilon_r(xy) - \bar{\beta}^2} \left(\cos \frac{n\pi x}{a} \quad \cos \frac{m\pi y}{b} \quad \cos \frac{p\pi x}{a} \quad \cos \frac{q\pi y}{b}\right) dxdy \tag{6.36}$$

For a linear variation of $\epsilon_r(x,y)$ as considered in the problem of Figure (6.1) the co-efficients B_{rsij} and C_{mnrs} and E_{rsij} become zero and A_{mnpq} and D_{mnpq} take the form

$$A_{mn} = \frac{mn\pi^2}{a^2} \int_0^a \frac{E}{D-x/\ell} \left(\sin \frac{m\pi x}{a} \quad \sin \frac{n\pi x}{a}\right) dx \tag{6.37}$$

$$B_{mn} = \int_0^a \cos \frac{m\pi x}{a} \quad \cos \frac{n\pi x}{a} \, dxdy \tag{6.38}$$

Equation (6.37) is a form of sine integral and requires numerical integration.

Chapter 6

References

1. Straton, A.J., "Electromagnetic Theory" McGraw-Hill Book Company, pp.327.

2. Hannaford, C.D., "The Finite Difference/Variational Method for Inhomogeneous Isotropic or Anisotropic Waveguides." Ph.D. Thesis, The University of Leeds, 1967.

3. Berk, A.D. "Variational Principles for Electromagnetic Resonators and Waveguides", Proc. I.R.E. Trans. AP-4, p. 104, 1956.

Chapter 7

CONCLUSIONS AND RECOMMENDATIONS

7.1 Conclusions

It is shown in Chapter 2 that for all types of isotropic dielectric loaded waveguides, it is possible to express the wave equation as an operator eigenvalue problem for the longitudinal component of the field vectors. By means of general operator theory it is also possible to derive a scalar variational expression for the wavenumber $k_o^2 = \omega^2 \mu_o \epsilon_o - \beta^2$ in terms of $\frac{\omega \epsilon_o}{\beta} E_z$ and H_z.

The finite-element method which is developed as an alternative to the finite-difference method has the following advantages:

a) A uniform treatment of the boundary conditions and the differential equations is obtained without any special consideration of the detailed nature of the boundary or its location with respect to the vertices generated in the discretisation of the domain into a finite number of elements. The co-efficients of the finite-element replacement of the boundaries are determined by the areas of the sections of the polygons cutout by the boundary and their moments and are, therefore, not very sensitive to the variations of the local slope of the boundary. In this method no special construction

is needed to treat the boundary nodes. The generated matrix eigenvalue problem always remains symmetric irrespective of the awkwardness of the boundaries of the waveguides.

b) The convergence of the solutions obtained by this method for the wavenumber is ensured by the general theory of the variational calculus and as such requires no special proof.

c) Singular points in waveguide problems can be treated consistently without involving any extra difficulties as is often the case with the finite-difference method.

d) For the inhomogeneous and the generalised mediums, the derivations of the discretised equations for the interior and the interface boundary nodes can be obtained from a general formulation.

e) A few examples treated in Chapter 4 for the homogeneous waveguides and for the transmission lines reveal the following main feature of the finite-element method. The boundedness of the eigenvalues obtained by the finite-element method follows from the property of the original extremum operator. Thus for the variational formulation considered in Chapter 4, the computational values of the eigen solutions give an upper bound to the true wave number or the capacitance. For strip line, if we reformulate a variational functional for the capacitance so as to have a lower bound to the true capacitance then we can obtain fairly accurate results by taking the algebraic mean of the two solutions for the same divisions.

Another feature of the finite-element method is that it is more flexible than the finite-difference method. The finite-difference method is a mathematically oriented technique in which the discretised equations are obtained by using the Taylor Series expansion of the fields at the neighbouring nodes in terms of their values and derivatives at the node under consideration. The finite-element method is a problem oriented technique in the sense that, depending on the physical nature of the problem, one can choose a suitable set of trial functions over an element to approximate the actual fields. Of course, the set of trial fields over two adjacent elements should satisfy the continuity relation at the interface boundaries.

The linear and the bilinear form of approximations of the fields over a triangular and a rectangular element as considered throughout this thesis give us an additional facility of generating the matrix co-efficients inside the computer instead of storing them at the beginning.

In the finite-element method, rate of convergence of the iterative solutions and the closeness of the eigenvalues obtained thereby, will depend largely upon the trial functions. Since this method is based on the principle of minimisation of a functional which is variational, a slight deviation of the trial fields from the true fields will have relatively little effect on the change of the eigenvalues.

For strip lines with infinitely thin strips embedded inside the ground planes or irises in waveguides, the linear or the bilinear approximation of the fields becomes a poorer approximation to the very sharp variation of the fields near the singular points. For such a problem a higher order polynomial approximation will produce a better result. Another advantage of the finite-element method is that the property of the monotonically decreasing error functions could be used to produce a good result by extrapolating from the results of three successive coarse mesh halvings.

7.2 Extension of the FE Method and Recommendation

The theory presented in this thesis may also take into account the consideration of a higher degree polynomial approximation to the fields over a triangular or a rectangular element. This could be done without sacrificing the continuity relation of the field between two adjacent elements, if the degree of the polynomial and the number of vertices describing the element satisfy the following relation[1]:

$$\frac{1}{2}(n+1)(n+2) \geq N\,n$$

where n = degree of the polynomial considered,

N = number of sides of the polygon.

Thus, N = 3 for a triangular element and 4 for a rectangular element. If $N\,n = \frac{1}{2}(n+1)(n+2)$, we need (n-1) additional points on each side of the element. On the other hand, if

$M = \frac{1}{2}(n+1)(n+2) - Nn$, then for a compatible solution, it is needed to consider M extra points anywhere inside the element in addition to (n-1) extra points on each side of the polygon. Thus we see that for a triangular element it is possible to obtain a consistent solution with a polynomial of any degree. It is shown[2] that a higher degree polynomial produces a better result for homogeneous waveguides; the same may be expected for the inhomogeneous waveguides also.

The procedure described in Chapter 6 could be usefully exploited for analysing the propagation behaviour of a "plasma loaded" waveguide with isotropic plasmas. Plasma loaded waveguide differs from inhomogeneous waveguide in that the relative permittivity of the plasma insert varies continuously over the guide cross-section.

Considerable scope remains for the future work in the applications of the finite-element method to propagation problems. In particular, the method will be useful in determining higher order modes in waveguides and strip lines (both homogeneous and inhomogeneous) problems.

References - Chapter 7

1. Dunne, P.C.: "Complete Polynomial Displacement Fields for Finite-element Method", The Aeronautical Journal of the R.A.Soc., pp.245-246, March 1968.

2. Silvester, P.: "A General High-Order Finite-Element Waveguide Analysis Program", IEEE Transactions on Microwave Theory and Techniques, Vol. MTT-17, No. 4, April 1969.

বাংলাদেশ প্রকৌশল বিশ্ববিদ্যালয়
নং 39550
তাং 23.3.77
লাইব্রেরী, ঢাকা